Polyspecific snake antivenom: manufacturing method development and toxicity profiling using an invertebrate model

A thesis submitted in fulfilment of the requirement for the degree of Doctor of Philosophy (PhD)

by

Mender Mohammed Mender

September 2022

School of Bioscience

Cardiff University

Abstract

Snakebite envenoming (SBE) presents unmet challenges particularly in Sub-Saharan Africa (SSA). Almost all SBE in SSA is due to bites by snakes belonging to the Elapidae and Viperidae families. Antivenom is highly effective in treating SBE. However, there is unprecedented shortage of antivenoms in SSA. This requires a significant increase in production of high quality and cost-effective polyspecific antivenoms against the most clinically relevant snake species within the Elapidae and Viperidae families.

A manufacturing process was developed to produce equine-derived whole IgG and $F(ab')_2$ polyvalent antivenoms against ten snake species belonging to the Bitis, Dendroaspis, Echis and Naja genera. Ion exchange chromatography was used to isolate IgG(T) from the rest of the equine IgG subclasses. The binding capacity of the IgG(T)-enriched and IgG(T)-depleted antivenoms was characterised using immunological assays. Galleria mellonella and Vero cell assays were developed to assess snake venom toxicity and antivenom efficacy.

The $F(ab')_2$ antivenom produced in this study demonstrated excellent stability, physicochemical and immunological properties comparable to the original Fav-Afrique™ product which was terminated in 2014.

The IgG(T) subclass accounts for the majority of equine IgG isotype in hyperimmune horse plasma. However, the IgG(T)-depleted antivenom had a higher binding capacity and better venom toxin recognition pattern compared to the IgG(T)-enriched antivenom.

The G. mellonella larval model exhibited a statistically significant difference in toxicity profiles between the viper and elapid snake species. Additionally, the larval model was able to differentiate the antivenom efficacy in protecting toxicity induced by the viper and elapid venoms. This supports the implementation of this model as a strong candidate to reduce or replace the current in vivo preclinical tests for snake venom toxicity and antivenom efficacy. Likewise, a dose-and species-dependent cytotoxicity effect was observed in Vero cells treated with viper and elapid venoms. Thus, the sensitivity of Vero cell cytotoxicity assays supports its inclusion as a quality control assay for antivenom.

Preface

Chapter 1 describes the introductory information about the nature, synthesis, and storage of snake venoms from ten medically relevant snakes belonging to the *Bitis*, *Echis*, *Naja* and *Dendroaspis* genera residing in SSA. This chapter also covers the safety, efficacy and pharmacological characteristics of available antivenoms in SSA. The third part of this chapter covers the current epidemiological background of SBE, burden and management. This chapter is published as a review in "Advanced Protein Chemistry and Structural Biology (APCSB): Immunotherapeutics, 1e Volume 129", under the title "Antivenom: An immunotherapy for the treatment of snakebite envenoming in sub-Saharan Africa". Details for this publication is included in the appendices (Appendix VII).

Chapter 2 details the general methods and materials that were used throughout the experimental chapters, Chapters 3-5.

Chapter 3 outlines the development of a simple and inexpensive manufacturing process, complimented by several physiochemical and immunological studies which quantify and compare the quality of the newly manufactured antivenom to the 'gold standard' Fav-Afrique™ antivenom.

Chapter 4 reports the characterisations of equine IgG subclasses in hyperimmune horse plasma (HHP). Results obtained from this chapter were used to test the hypothesis that IgG(T) is the exclusive venom toxin neutralising subclass. Equine IgG subclasses were separated using two-step chromatography, followed by ELISA, Western blotting and Small-Scale Affinity Purification (SSAP) for quantification.

Chapter 5 presents the development of the *Galleria mellonella* larval model and Vero cell cytotoxicity assays to quantify snake venom toxicity and antivenom efficacy. The Vero cell cytotoxicity assay was used to assess the toxicity of all the snake venoms, except the 3 *Dendroaspis* species, covered in this study. The same snake venoms were also used to assess the suitability of the larval invertebrate model to quantify venom toxicity. Chapter 6 provides a summarised overall discussion for the thesis chapters, future works, limitations and conclusion remarks.

Table of content

List of Figures

List of Tables

Acknowledgment

In the name of Allah, the Most Gracious and the Most Merciful.

This thesis becomes a reality with the kind support of many individuals. I would like to extend my sincere thanks to all of them.

Firstly, I would like to acknowledge both Knowledge Economy Skills Scholarship-II (KESS2) and MicroPharm Limited for their financial support during this project. An immense thank you to Professor John Landon, Dr Ibrahim Al-Abdulla and Ian Cameron for offering me this PhD opportunity. Also, I would like to express my gratitude to all MicroPharm staff, particularly Dr Rossen Donev, Dr Fiona Bolton, Hayley Jakeman, and Matt Aldridge for their continues support and helps during the pandemic and beyond.

Thank you to all the students and academics at Cardiff University particularly Dr Emyr Lloyd-Evans for kindly allowing me to use his laboratory, Gaia, Marika, Emily and Hannah for helping me settling in their labs. Special thanks to Professor Nick Casewell from LTMS for kindly providing me with antivenom samples.

Foremost, I would like to express my sincere gratitude to my supervisors Dr Mark Young and Professor Colin Berry for their invaluable help of constructive comments and suggestions throughout the experimental work and writing the thesis, without their support this PhD thesis wouldn't be possible.

Finally, I am most grateful to my family for constantly encouraging and supporting me. Thank you of course to my friends: your friendship and support have added a lot to my life.

Dedications

I am dedicating this thesis to:

- My mother for her unconditional love and continues support.
- My father, although he has never lived long enough to see this adventure, his advice “continue studying until you achieve a doctoral degree” inspired me to start this PhD journey.
- And my youngest brother Abdelaziz whose life cut short at the tender age of 21, during the final stages of my writing up this thesis.

Abbreviations

%	Percentage
°C	Degree centigrade
$	United states dollar
20WBCT	20 minutes whole blood clotting test
3FTX	Three finger toxin
3Rs	Reduction, Replacement and Refinement
ACE	Angiotensin-converting enzyme
AChE	Acetyl cholinesterase
AEX	Anion exchange chromatography
AMP	Antimicrobial peptide
ANOVA	Analysis of variance
API	Active pharmaceutical ingredients
ASNA-C	Asna Antivenom-C
ASV	African Society of Venimology
AV	Antivenom
BPP	Bradykinin potentiate peptide
BPTI	Bovine pancreatic trypsin inhibitor
Ca^{2+}	Calcium
Ca_v	Calcium voltage gate ion
CCS	Comparative clinical study
$CD4^+$	Cluster of differentiation
cGMP	Cyclase guanosine monophosphate
CL	Clearance
cm	Centimetre
CNBr	Cyanogen bromide
CNG	Cyclic nucleotide gated
CNS	Central nervous system
CO_2	Carbon dioxide
CPP	Critical process parameter

CQA	Critical quality attributes
CRD	Cysteine-rich domain
CRiSP	Cysteine-rich secretary protein
CTA	Cytotoxicity assay
CTL	C-type lectin
DALY	Disability-adjusted life year
DAR	Delayed Adverse Reaction
DEAE	Diethylaminoethyl
DF	Dilution Factor
DIS	Disintegrin
DMEM	Dulbecco's modified Eagle's medium
DMSO	Dimethyl sulfoxide
DPBS	Dulbecco's Phosphate Buffered Saline
DTT	Dithiothreitol
DTX	Dendrotoxin
e.g.	Example
EAR	Early Adverse Reaction
EC_{50}	Half-maximal effective concentration
ECACC	European Collection of Authenticated Cell Cultures
ECL	Enhancer chemiluminescent substrate
ED_{50}	Median Effective Dose
EDTA	Ethylenediaminetetraacetic acid
ELISA	Enzyme-linked immunosorbent assay
F(ab')2	Divalent antigen-binding fragment
Fab	Monovalent antigen-binding fragment
FBS	Foetal Bovine Serum
Fc	Fragment Crystallisable
FDA	Food and Drug Administration
Fig	Figure
FT	Flow through
g	Gram
g/L	Gram per litre
g/mol	gram per mole

GDP	Gross Domestic Product
GF	Glass fibre
GMP	Good manufacturing practice
GPIb	Glycoprotein receptors
HCL	Hydrochloric acid
HCP	Host cell protein
HHP	Hyperimmune Horse Plasma
HMW	High molecular weight
HPLC	High performance (or pressure) liquid chromatography
i.e.	id est “that is”
IC_{50}	Half-maximal inhibitory concentration
ICH	International Conference on Harmonisation
ICP	Instituto Clodomiro Picado
ICTA	Immunocytotoxicity assay
IF λ	Interferon gamma
Ig	Immunoglobulin
IgA	Immunoglobulin A
IgD	Immunoglobulin D
IgE	Immunoglobulin E
IgG	Immunoglobulin – G
IgM	Immunoglobulin M
IgY	Immunoglobulin Y
IL-4	Interleukin-4
kDa	Kilodalton
kg	Kilogram
KTT	Kunitz type toxin
K_v	Voltage gated potassium ion
L	Litre
LAAO	L-amino acid oxidases
LAL	Limulus Amebocyte Lysate
LAR	Late adverse reaction
LD_{50}	Median Lethal Dose
LPS	Lipopolysaccharides

M	Molarity
mAb	Monoclonal antibody
mAU	Milli-absorbance unit
mAU	Milli Absorbance Unit
mg	Milligram
mg/mL	Milligram per millilitre
MHD	Minimum haemorrhage dose
mL	Millilitre
mL/min	Millilitre per minute
MLD	Methionine-leucine- aspartic acid
mm	Millimetre
MND	Minimum Necrotising Dose
Mr	Relative mass
mS/cm	Milliosmole per centimetre
MW	Molecular weight
MWCO	molecular weight cut-off
MWM	Molecular weight marker
nAChR	Nicotinic acetyl cholinesterase receptor
NaCl	Sodium chloride
Na_v	Voltage gated sodium ion
NGF	Nerve growth factor
NHP	Non-Hyperimmune Horse Plasma
nm	Nanometre
nMWCO	Nominal molecular weight cut-off
NP	Natriuretic peptides
NSAID	Nonsteroidal anti-inflammatory drug
NTD	Neglected Tropical Disease
OD	Optical density
PBS	Phosphate buffered saline
PBST	Phosphate buffered saline containing Tween-20
PBW	Wash buffer for Affinity column
PCR	Polymerase chain reaction
PD	Pharmacodynamics

PES	Polyethersulfone
PK	Pharmacokinetics
PLA_2	Phospholipase A_2
PS80	Polysorbate 80
PTD	Posttraumatic stress disorder
QA	Quality Assurance
QC	Quality control
QXL	Q-sepharose XL
RCT	Randomised clinical trial
RFU	Relative Fluorescence Unit
RGD	Arginine- glycine-aspartic acid
Rt	Retention time
RTA	Ready-To-Administer
SAIMR	South African Institute for Medical Research
SAVP	South African Vaccine Production
SBE	Snakebite envenoming
ScNtx	Short-chain α-neurotoxin
SD	Standard deviation
SDS-PAGE	Sodium dodecyl Sulphate-Polyacrylamide Gel Electrophoresis
SEC	size-exclusion chromatography
SIRS	Systemic inflammatory response syndrome
SpAb	Specific antibody
SSA	Sub-Saharan Africa
SSAC	Small-scale Affinity Chromatography
SSAP	Small-scale Affinity Purification
SVDK	Snake venom detection kit
SVMP	Snake venom Metalloproteinase
SVSP	Snake venom serine peptidase
$t_{1/2}$	half-life
TB	tuberculosis
TBS	Tris buffered Saline
TGF-β	Transforming growth factor- beta
Th1	T- helper-1 cells

Th2	T-helper-2 cells
TIgG	Total IgG
TMB	3, 3′, 5, 5′-Tetramethylbenzidine
UK	Unite Kingdom
UN	United Nations
USA	United States of America
USD	United states dollar
UV	Ultraviolet
V	Volt
v/v	Volume to volume
Vd	Volume of distribution
VEGF	Vascular endothelial growth factor
VGD	Valine- glycine- aspartic acid
vWF	von Willebrand factor
W/v	Weight to volume
w/w	Weight to weight
WC	Western C
WFI	Water for Irrigation
WHO	World health organisation
α	Alpha
β	Beta
γ	Gamma
ϰ	Kappa
λ	Lambda
μg	Microgram

Chapter 1: General Introduction

The overall aim of this project was to develop a manufacturing process for an effective and affordable polyspecific antivenom for use in sub-Saharan Africa (SSA). Achievement of this aim required consideration of the manufacturing process as well as characterisation and assay of the efficacy of the product. It is clearly important that this work is viewed in the context of current pharmaceutical technology used to manufacture antivenoms. The purpose of this introduction is to highlight key snake venom toxins, their implication in envenoming and the epidemiology of snakebite envenoming, with a particular emphasis on SSA. The introduction will also provide a comprehensive review on the safety, efficacy and accessibility of antivenoms currently marketed in this region.

1.1 Snakebite envenoming

Snakebite envenoming (SBE) is an endemic and debilitating condition primarily affecting the remote subsistence farming communities of Africa, Asia, and Latin America (Kasturiratne et al. 2008). If untreated, there is significant morbidity and mortality and, depending on venom toxicity, death can occur within 1 to 25 hours after envenoming (Baldé et al. 2013). The World Health Organisation (WHO) finally classified SBE as a category A (i.e., priority) Neglected Tropical Disease (NTD) in 2017 (Chippaux 2017; Williams et al. 2019a). NTDs may be defined as a ‘diverse group of communicable and non-communicable diseases that are common in low-income populations of Africa, Asia, and the Americas (Casewell et al. 2020). Category A is an underrated condition causing significant morbidity and mortality, disproportionately affecting poorer communities, which can potentially be improved using appropriate management schemes.

1.1.1 The burden of snakebite envenoming

Venomous snakes are found throughout the world, with the exception of high altitudes, areas of permafrost and a few islands (Kasturiratne et al. 2008). However, as shown in Figure 1.1, over 95% of SBE occurs in deprived, remote and rural areas of Southern Asia, Southeast Asia, SSA and Latin America (Kasturiratne et al. 2008; Chippaux 2011; Benjamin et al. 2018).

Geographically, “sub-Saharan Africa” is an ambiguous term used to describe 48 of the 54 African countries that are fully or partially located south of the Saharan desert (United Nations (UN) definition). The exceptions being Algeria, Djibouti, Egypt, Morocco, Sudan, and Tunisia. Therefore, throughout this study, and in line with institutions such as UN development programme, the World Bank and other funding organisations, the SSA term will be used to denominate these African countries.

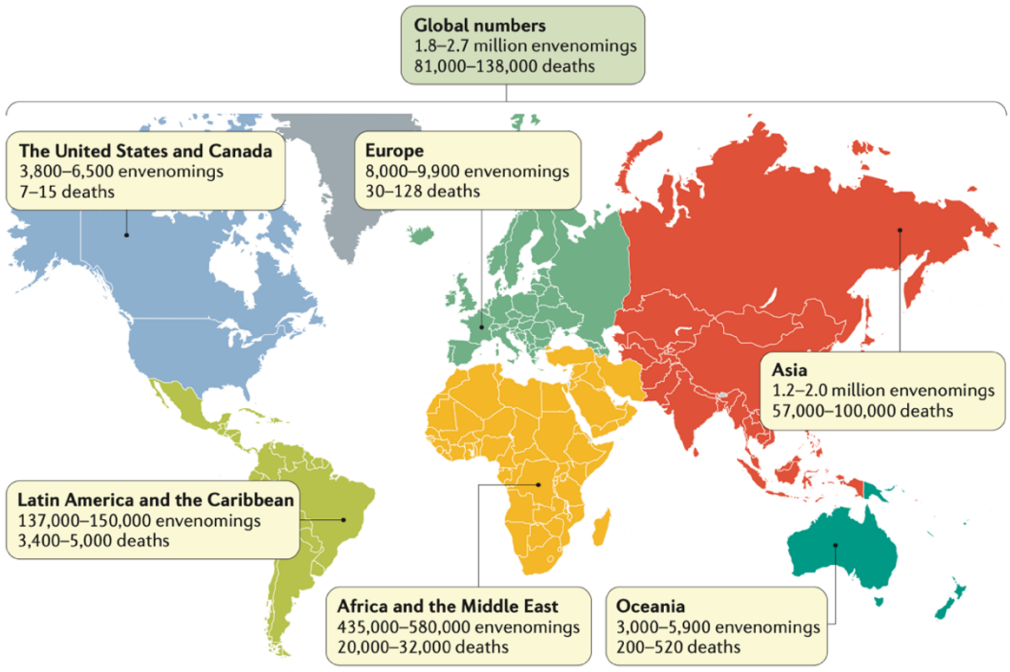

Figure 1.1 Global estimation of annual snakebite envenomings and deaths.

Taken from (Gutierrez, et al. 2017a). Reprinted with permission.

The global incidence of SBE, and its associated mortality is inconsistently reported between publications suggesting that there is a lack of comprehensive global assessment of the disease’s epidemiology. Global incidences of snakebite associated burden was reported at approximately 1.84 million SBE and 93,000 deaths annually (Kasturiratne et al. 2008). Others (Williams et al. 2010; Gutierrez et al. 2017a) suggest that the global incidence of snakebite is far higher, with approx. 5 million SBE leading to about 400,000 life-long disabilities and over 150, 000 deaths, annually. Despite compelling evidence of a higher snakebite incidence in SSA, there is unprecedented lack of epidemiological studies of the SBE burden in this region. The annual burden of SBE in SSA was estimated to be 100,000 cases with 32,000 deaths

(Kasturiratne et al, 2008), but Chippaux (2011) reported 314,078 bites, 7331 deaths and the number of amputations ranging from 5,908 to 14,614. Such discrepancies may have arisen due to the different methodology used in different studies (Kasturiratne et al. 2008; Chippaux 2011). Lower SBE estimations could reflect under-reporting, which mostly relies on records from clinical settings and many incidents out with this setting remain unreported (Kasturiratne et al. 2008) and, in addition, the accuracy of such records is questionable (Calvete et al. 2014).

Interestingly, some studies (Rahman et al. 2010; Mohapatra et al. 2011; Ediriweera et al. 2016) used household surveys to provide a more adequate estimation of SBE burden. However, this is extremely expensive, laborious and time-consuming, discouraging such potential investigations. Furthermore, in some regions 20 to 70% of snakebite victims do not present to clinical centres because they are either unaware treatment is available, cannot afford treatment and/or prefer using traditional and religious healing methods (Brown 2012). Many snakebite victims only go to modern medical centres in cases where further treatment is needed, or if the traditional healing is not effective and their condition worsens (Chippaux 2011).

1.1.2 Vulnerability to snakebites in the SSA region

Although venomous snakes are ubiquitous, snakebite represents a daily hazard for the inhabitants of remote, rural, tropical and sub-tropical regions of Asia and Africa (Chippaux 2011). Understanding snake species' behaviours and geographical distribution, availability of antivenoms and access to suitable clinical centres are key factors for assessing vulnerability of populations to SBE (Longbottom et al. 2018).

As shown in Figure 1.2, populations living in tropical regions such as the Democratic Republic of Congo, are at highest risk. Factors such as non-mechanical and traditional farming, failure of farmers to use protective boots and gloves, heavy rainfall flooding snakes out of their burrows, and attraction of snakes to rodents and poultry found around grain stores in proximity to human habitation, increases potential human-snake interactions. Thus, agricultural workers and nomadic farmers, particularly young males and children (Chippaux 2011; Dalhat 2015), pregnant women (Habib 2015), and

families living in poorly constructed houses are particularly vulnerable. Despite elegant studies which used the household survey to assess incidence of snakebite at a national level (Rahman et al. 2010; Mohapatra et al. 2011; Ediriweera et al. 2016), the global magnitude of snakebite and its clinical ramifications have not been fully elucidated (Longbottom et al. 2018).

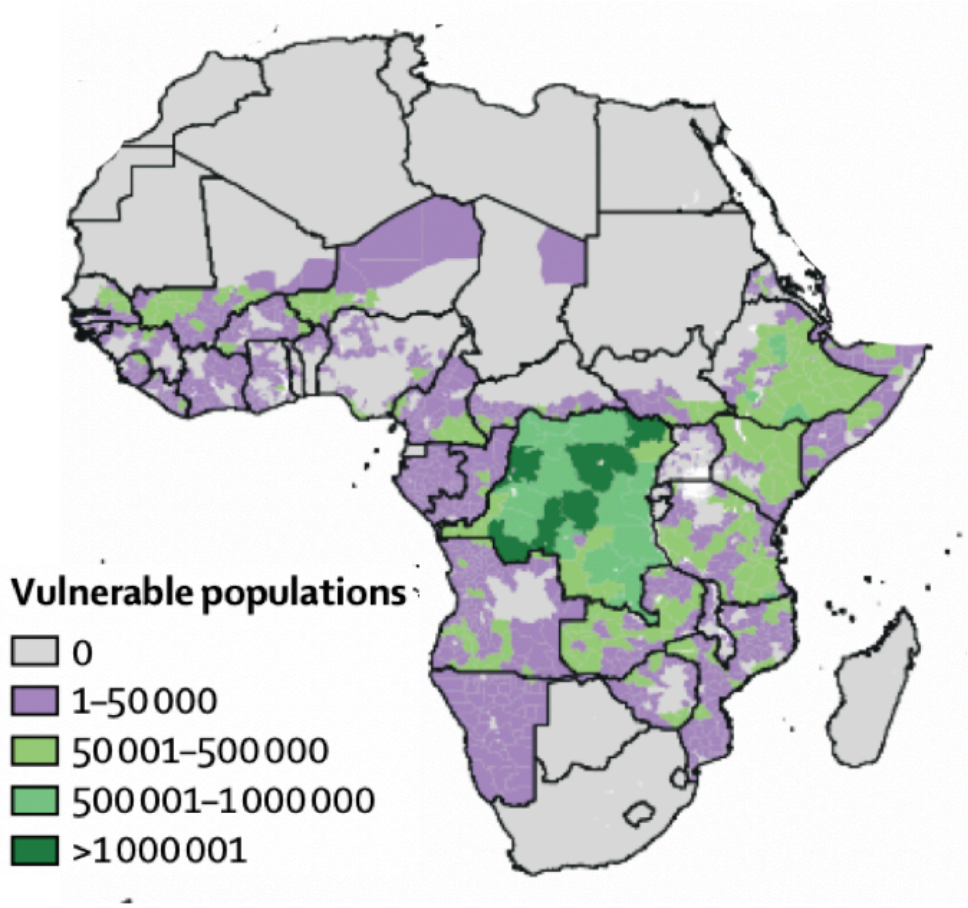

Figure 1.2 Vulnerability to snakebite in the African continent.

Taken from (Mender et al. 2021). Reprinted with permission

1.1.3 Socioeconomic impact of SBE in sub-Saharan Africa

SBE is a significant health problem for rural dwellers in Africa, Asia and Latin America, who already face a dual burden of communicable and non-communicable NTDs. This is strongly linked to low 'per capita Gross Domestic Product' (GDP) and Human Development index, which results from loss of income due to illness and disability, expenditure for treatment and premature death (Habib et al. 2015a). SBE is strongly associated with an increased mortality rate, post-traumatic stress disorder (PTSD), long term injury (Halilu

et al. 2019), mental health disorders, miscarriage in pregnancy and blindness (Dalhat 2015).

It is evident that the global burden of SBE is amongst the highest of identified NTDs occurring in SSA, being ranked fourth in 2012 in West African countries (Habib et al. 2015a). Despite this, SBE is underrated, and it has taken far too long to be recognised and to receive some of the necessary funding from local governments, national and international institutions. It was 2018 before the Wellcome Trust announced a multi-million pound fund available to attain the WHO target to reduce SBE-associated mortality and morbidity by 50% by 2030 (Williams et al. 2019a). Roadmap pathways have been created by the WHO encompassing four fundamental strategies: 1) identification of safe and effective treatments; 2) empowering and engaging local communities; 3) an integrated healthcare system; 4) global internship and coordination (Williams et al. 2019a).

1.1.4 Clinical presentation of SBE

Clinical manifestations of snakebite are species specific and can be broadly grouped as cytotoxic (Warrell et al. 1976b), neurotoxic (Warrell et al. 1976a; Baldé et al. 2013), and haemorrhagic (Warrell et al. 1974; Warrell et al. 1976b; Warrell et al. 1977; Chippaux et al. 2007). Clinical presentation is dependent on the arsenal of venom toxins delivered, each of which may act individually or synergistically. Individual venom composition is not only species specific, but influenced by factors such as geographical location, age and diet (Chippaux et al. 1991; Chippaux and Goyffon 1998). Snakes from the *Bitis, Echis, Naja* and *Dendroaspis* genera are responsible for the majority of medically significant SBEs in SSA.

1.1.4.1 African Adders (*Bitis* species)

Although some species in the *Bitis* genus are present in Saudi Arabia (Paixão-Cavalcante et al. 2015), most of the medically important adders, including the puff adder (*Bitis arietans*), Gabon viper (*Bitis gabonica*), *Bitis gabonica rhinoceros* and *Bitis nasicornis,* are indigenous to Africa (Calvete et al. 2007). Together with the saw-scaled viper and black-necked spitting cobra (see below), the puff adder is responsible for most SBEs in SSA (Currier et al. 2010; Habib 2015). Venoms from the *Bitis* species are rich in highly toxic

components, such as snake venom serine proteinases (SVSPs); C-type lectins (CTLs) and snake venom metalloproteinases (SVMPs) (Calvete et al. 2007). Clinical symptoms of envenoming include: extensive tissue necrosis, cytotoxicity, hypotension, coagulopathy, haemorrhage and cardiotoxicity (Paixão-Cavalcante et al. 2015).

1.1.4.2 Saw-scaled or carpet vipers (*Echis* species)

The majority of publications describing venom composition of *Echis spp.* focus on *E. ocellatus* (Wagstaff and Harrison 2006; Casewell et al. 2009; Wagstaff et al. 2009; Calvete et al. 2010; Hamza et al. 2016; Rogalski et al. 2017) and *E. carinatus* (Patra et al. 2017), whereas those describing *E. leucogaster* (Escoriza et al. 2009; Albulescu et al. 2020) and *E. pyramidum (Conlon et al. 2013)* are limited. SVMPs are the major venom toxin component in venoms from *Echis* species (Wagstaff and Harrison 2006; Calvete et al. 2010). Headache, seizures, vomiting, systemic haemorrhage, incoagulable blood, swelling, blistering and necrosis are the hallmark signs and symptoms associated with *Echis* envenomings (Warrell et al. 1977; Habib et al. 2008; Habib 2015). Extensive tissue necrosis may result in renal failure (Warrell et al. 1977). If treatment is delayed, death occurs most commonly due to intracranial haemorrhage (Habib and Abubakar 2011). This genus of snakes is responsible for more deaths, globally (Casewell et al. 2009) and in Nigeria, *E. ocellatus* accounts for the highest mortality and more life-changing injuries than any other snake species (Habib et al. 2008; Warrell 2008).

1.1.4.3 Mambas (*Dendroaspis* species)

Dendroaspis spp. are medically important snakes, which are present exclusively in SSA (Harvey and Robertson 2004). The black mamba (*D. polylepis*) is highly venomous and very aggressive, envenoming resulting in potentially fatal neurological signs (Laustsen et al. 2015). Mamba venom is highly toxic, dominated by postsynaptic and presynaptic neurotoxins, including Kunitz type toxins (KTTs) and 3-finger toxins (3FTXs) (Ainsworth et al. 2018). Clinical signs include local tissue swelling, ptosis, fasciculation, dizziness, nausea, respiratory paralysis and cardiac arrhythmia that are potentially fatal (Lauridsen et al. 2016; Ainsworth et al. 2018).

1.1.4.4 Cobras (*Naja* species)

The Egyptian cobra (*Naja haje*), the black-necked spitting cobra (*N. nigricollis)* and the forest cobra (*Naja melanoleuca*) are the most medically important cobras in SSA. Proteomic studies (Petras et al. 2011; Malih et al. 2014; Lauridsen et al. 2017) demonstrate that their venoms are dominated by 3FTXs neurotoxins (Warrell et al. 1976a) and phospholipase A_2 (PLA_2) cytotoxins (Warrell et al. 1976b). Clinical signs of envenoming include local tissue swelling and necrosis, vomiting, drowsiness, impaired speech, ptosis and potentially fatal respiratory paralysis (Warrell et al. 1976a; Warrell et al. 1976b). Interestingly, despite the fact that the venom of *N. nigricollis* is made up of over 70% 3FTXs (Petras et al. 2011), associated clinical signs are dominated by extensive tissue necrosis at the bite site (Warrell et al. 1976b; Habib 2015).

1.1.5 Management of snakebite-associated morbidity and mortality

In SSA, integrated medical centres are scarce, often situated many miles from the vulnerable farming communities where snakebites are frequent (Kipanyula and Kimaro 2015). The use of traditional and religious medicine is often the first port of call, despite being considered as time-wasting and potentially harmful treatments (Yates et al. 2010; Hasan et al. 2012; Ghose and White 2016). These treatments include scarification, emetics, snakestones, suction at the bite site, tight arterial bands, and even digit amputation (Yates et al. 2010; Habib 2015; Ghose and White 2016).

Potentially, the most effective methods of preventing and improving treatment of SBE include education, raising awareness within vulnerable communities and improving transportation to appropriate medical centres (Gutierrez et al. 2017a). First Aid should include: seeking advice over the phone; hygiene at the bite site, pressure immobilisation, removal of constrictive items, placing the patient in lateral recumbency, administration of artificial respiration and rapid transfer to the nearest clinic (Warrell 2009; Ghose and White 2016). The use of nonsteroidal anti-inflammatory drugs (NSAID) should be avoided, unless otherwise advised by a medical specialist (Ghose and White 2016). Admission to hospital should ideally occur within 24 hours of the bite for assessment and appropriate treatment, including antivenom. It is estimated

that a delay of 1 hour increases mortality by 1% and 1 day by 23% (Habib and Warrell 2013). Encouraging the financial support of local manufactures of effective antivenoms, from local and global institutions, is key to the control of SBE. This was demonstrated by the reduction in fatality from *E. ocellatus* bites from 11.1% to 1.3% after the introduction of geographically relevant antivenoms in West Africa (Habib and Warrell 2013).

Identification of the snake responsible by bite configuration, evidence from witnesses and victim, geographical location and knowledge of clinical manifestations of species commonly found in the area, allows rapid administration of the correct antivenom (Dhananjaya et al. 2015). Presentation of the killed snake responsible may allow identification, although misidentification is possible unless performed by an experienced herpetologist. Education of healthcare professionals and First Aiders; stocking up with geographically appropriate antivenoms and associated medications must be the primary goal of hospitals providing care for victims of SBE. In this way, mortality may be significantly reduced (Habib and Warrell 2013, Visser et al. 2008 and Ediriweera et al. 2016). Medications such as antihistamine (chlorpheniramine), corticosteroids and adrenaline must be stocked to treat any adverse reactions to antivenom, including anaphylaxis (Habib 2015).

Triage of SBE victims, where clinical presentations are spectra and time-dependent, with a thorough medical and laboratory investigation are key to establishing a prompt and appropriate treatment plan (Gutierrez et al. 2017a). The 20-minute whole blood clotting test (20WBCT) is a simple, inexpensive bedside test which may be performed to identify incoagulable blood of patients envenomed by snakes such as *Echis spp*., which induce a consumptive coagulopathy (Dhananjaya et al. 2015; Habib 2015; Benjamin et al. 2018). Bites by *N. nigricollis* induce haematological abnormalities and complement depletion (Warrell et al. 1976b). Immunological and molecular techniques, such as Enzyme-linked Immunosorbent Assy (ELISA) and Polymerase Chain Reaction (PCR), may be used to identify venom more reliably in tertiary care centres (Habib 2015; Williams et al. 2019b). In Australia, there is a snake venom detection kit (SVDK) available at a cost of 150-200 USD (Valenza et al. 2021), which is both unaffordable and unavailable in SSA.

The major effects of systemic envenoming are generally amenable to antivenom therapy (Habib 2015), but exceptions include PTSD and effects of local envenoming such as amputation (Halilu et al. 2019). Despite these discrepancies, antivenom remains the mainstay of SBE treatment (Chippaux et al. 2007b, Habib and Warrell 2013).

1.1.6 Geographical distribution and dietary acquisition of snakes

Venomous snakes occupy virtually all ecological niches (Vidal et al. 2007). Snakes such as *Bitis arietans, B. gabonica, Echis leucogaster, E. ocellatus, Naja haje, N. nigricollis, N. melanoleuca, Dendroaspis jamesoni, D. polylepis* and *D. viridis* are abundant in tropical and SSA (Tasoulis and Isbister 2017). As shown in Figure 1.3, these snakes occupy different regions of the African continent.

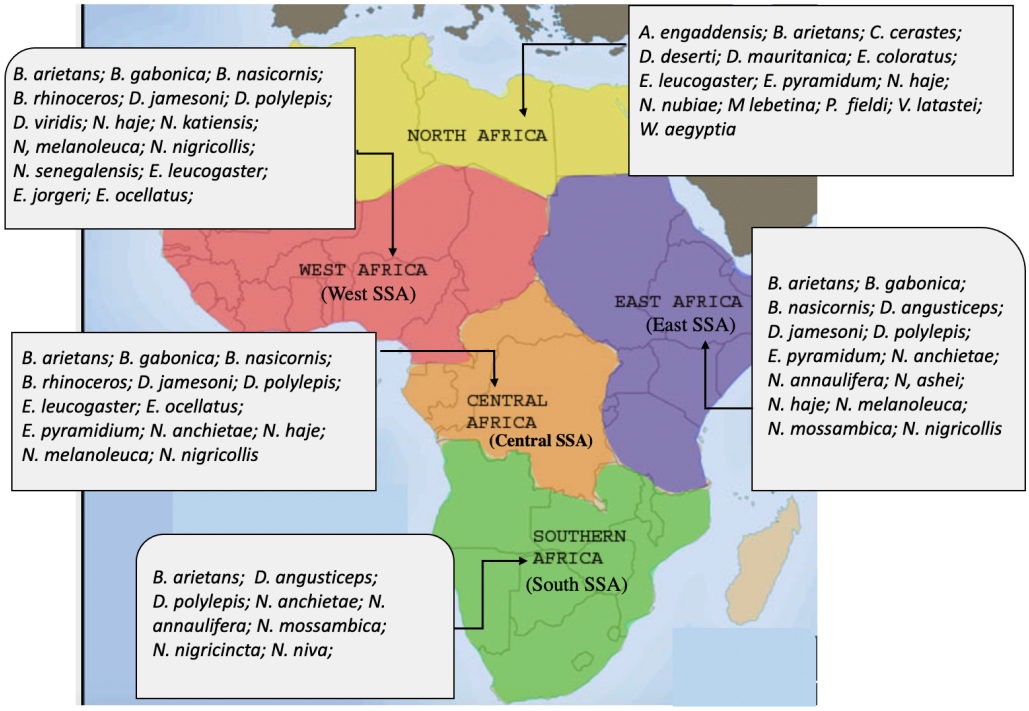

Figure 1.3 Distributions of clinically relevant snakes in Africa.

Descriptions: *Atractaspis engaddensis; Bitis arietans; Bitis gabonica; Bitis nasicornis; Cerates cerastes; Dendroaspis angusticeps; Dendroaspis jamesoni; Dendroaspis polylepis; Dendroaspis viridis; Daboia deserti; Daboia Mauritania; Echis coloratus; Echis jorgeri; Echis leucogaster; Echis ocellatus; Echis pyramidin; Naja annaulifera; Naja ashei; Naja anchietae; Naja haje; Naja melanoleuca; Naja mossamica; Naja nigricincta; Naja nigricollis; Naja niva; Naja nubiae; Naja Senegalensis; Macrovipera lebetina; Pseudocerastes fieldi; Vipera latastei; Walterinnesia aegyptia.*

Taken from (Mender et al. 2021). Reprinted with permission.

Venomous snakes feed on various prey, including small mammals, amphibians, reptiles, birds, snails, fish, chickens, lizards, rats and even other snakes (Kang et al. 2011). The diet of different snakes is largely influenced by environmental factors, predator and prey size, prey vulnerability and adaptive evolution (Barlow et al. 2009).

1.2 Snake venom: overview

Venom can be defined as a toxic substance, or mixture of substances, which is delivered to internal tissues via a wound (e.g., snake bite), and which acts in a dose-dependent manner. In venomous snakes the arsenal of toxins injected via a bite, or sprayed onto victims, is an effective bioweapon used primarily to incapacitate their prey or secondarily to deter predators (Mackessy 2009). Snake venom consists of a mixture of enzymes, non-enzymatic proteins, peptides, and polypeptides, accounting for around 95% dry weight (Carregari et al. 2018), the remainder consists of non-proteinaceous compounds including inorganic salts, amines, carbohydrate, metal ions and lipids (Munawar et al. 2018).

1.2.1 Constituents of snake venom

A single venom may contain more than 100 different proteins (Mackessy 2009), one study has identified over 200 proteins (Petras et al. 2016). Additionally, the complex mix of toxins of a single venom is reflected by the multitude of clinical manifestations observed in envenomed patients. Various venom proteins may present unique biological and pharmacological modes of action; but homologous structures between protein isoforms make classification into a small number of toxin families possible (Kang et al. 2011). Although the biochemical composition of venom is so variable (Chippaux et al. 1991), it is dominated by the major protein families, which are consistent across the taxa (Mackessy 2009). External factors such as diet, age and geographical location may influence production of venom even within a species (Mackessy 2009). Large numbers of protein families have been identified in venom from snakes found in SSA, using genomics and proteomics (Calvete et al. 2007; Casewell et al. 2009; Petras et al. 2011; Malih et al. 2014;

Laustsen et al. 2015; Petras et al. 2016). Major toxin families identified are: PLA_2, SVMPs, SVSPs, cysteine-rich secretory proteins (CRiSPs), 3FTXs, L-amino acid oxidases (LAAOs); disintegrins (DIS), CTLs, KTTs, dendrotoxins, Naturetic peptides (NPs), vascular endothelial growth factors (VEGFs) and nerve growth factors (NGFs). Further studies are required to elucidate the mechanisms governing the pharmacological actions of these proteins in order to achieve the milestone of discovering effective therapeutic strategies. Nevertheless, excellent reviews pertaining to the current understanding of structures and mechanisms of snake venom toxins are available, for example (Doley and Kini 2009; Kang et al. 2011; Mackessy and Saviola 2016; Munawar et al. 2018).

1.2.1.1 Snake venom Metalloproteinase (SVMP)

Snake venom metalloproteinases (SVMPs) are zinc-dependent enzymes which vary in size from 20- 100 kDa. Based on structural domains, SVMPs are classified into three groups; P-I, P-II and P-III (Kang et al. 2011; Takeda et al. 2012) (Figure 1.4.). Although, four groups of SVMPs were reported in previously classifications (Calvete 2005; Fox and Serrano 2005), the heterodimeric P-IV SVMPs are now included in the P-III SVMP group as a subclass P-IIId (Takeda et al. 2012; Chakrabarty and Chanda 2017).

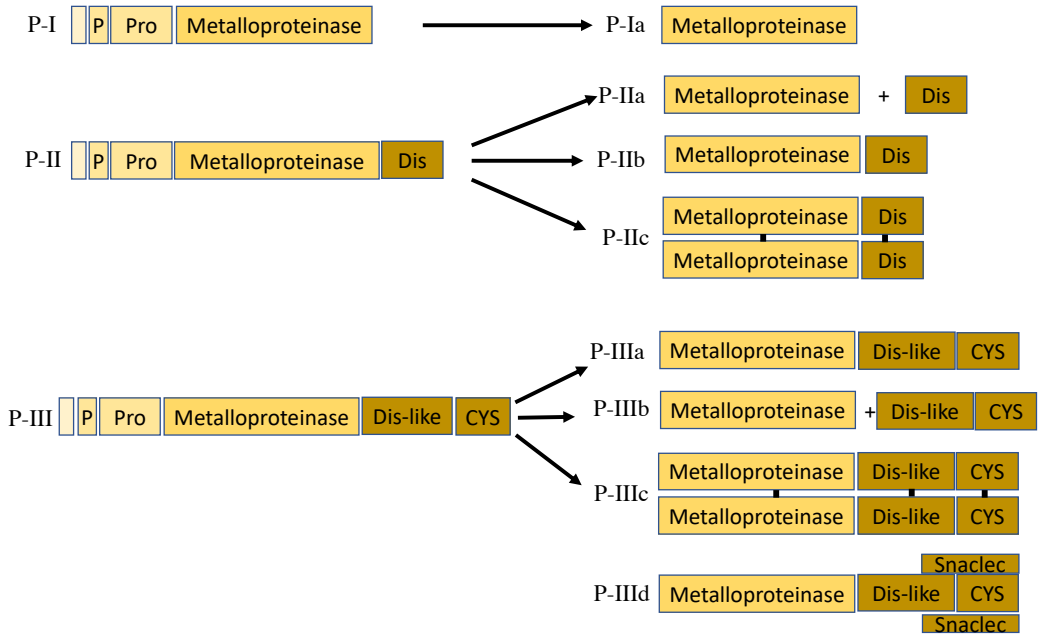

Figure 1.4 Simplified diagram of SVMPs classes and their post-translationally modified forms in snake venoms.

Main features include: intact (P-Ia, P-IIb and P-IIIa); proteolytically processed into multiple products (P-IIa and P-IIIb); dimeric (P-IIc and P-IIIc) and P-IIId which contain C-type lectin like domain (Snaclec). Abbreviations: P, peptides; pro, prodomian; Dis, disintegrin domain; Dis-like, disintegrin-like domains; CYS, cysteine-rich domains.

Adapted from (Casewell et al. 2011).

The smallest P-I SVMPs, molecular mass 20- 30 kDa, contain only the metalloprotease domain (Calvete 2005; Oyama and Takahashi 2017). P-I SVMPs induce less potent haemorrhagic activity, compared to the more biologically complex P-III SVMPs, suggesting that structural complexity is a direct factor associated with lethality (Fox and Serrano 2005).

P-II SVMPs (30- 60 kDa) contain the metalloprotease domain in addition to a canonical disintegrin domain, linked to the carboxyl terminus via a short spacer peptide that acts as an interdomain segment between the metalloprotease and disintegrin domains (Fox and Serrano 2008), also see Figure 1.4. Based on their sequence variations, class P-II SVMPs can be subdivided into five subtypes: P-IIa; P-IIb, P-IIc, P-IId and P-IIe (Fox and Serrano 2008). With the exception of P-IIb, these proteinases undergo post-translational proteolytic processing, resulting in the release of disintegrin domains (Fox and Serrano 2008).

Class P-III SVMPs (60- 100 kDa) are composed of a metalloprotease domain, disintegrin- like and cysteine- rich domains, and can be further subdivided into subclasses P-IIIa, P-IIIb, P-IIIc and P-IIId, based on unique post-translational modifications such as whether they are subject to dimerization (P-IIIc) or proteolytic processing, (Fox and Serrano 2008) and (Oyama and Takahashi 2017). All SVMPs contain the metalloprotease domain that displays the zinc-binding motif (HEXXHXXGXXH) at the active site and a highly conserved Met-turn sequence, and as such all classes are likely to function as active proteolytic proteinases (Oyama and Takahashi 2017).

SVMPs present arrays of structurally related biological activities, including the metalloprotease-domain associated peptide cleavage, as well as the proteolytically processed disintegrin-domain specific modulation of platelet aggregation. This domain complexity allows SVMPs to exert maximum damage by targeting a wide range of cellular matrix, ligands, connective

tissues and/or coagulation factors. SVMPs are the chief venom constituent in many *Viperidae* (also referred to as viperid or viper) snake venoms, accounting for 66.5- 75.7% of the total *E. ocellatus* proteome (Wagstaff et al. 2009; Albulescu et al. 2020). Thus, clinical manifestations frequently observed in patients bitten by *Echis spp.* or *Bitis spp.* such as local and systemic haemorrhage and local tissue damage correlate with their venom proteome (Gutierrez et al. 2005b). Although small quantities of SVMPs (<5% total venom protein) were identified in venoms from *N. nigricollis* (Petras et al. 2011) and *D. polylepis* (Laustsen et al. 2015), this toxin family is less clinically relevant in *Elapidae* (also referred to as elapid) species (Tasoulis and Isbister 2017).

1.2.1.2 Snake Venom Serine Proteinase (SVSP)

Snake venom serine proteinases (SVSPs) are abundant in viper venoms, especially *Bitis* spp. but less commonly expressed in elapid venoms (Tasoulis and Isbister 2017). There is no evidence that these enzymes are present in the mamba venoms (Laustsen et al. 2015; Ainsworth et al. 2018) or cobras (Petras et al. 2011; Malih et al. 2014; Lauridsen et al. 2017). They are multifunctional enzymes exhibiting various biological and pharmacological activities (Mackessy, 2010).

SVSPs are composed of six β-strands, a short α-helix within the N-terminus (Figure 1.5 A) and a conserved active site triad: His57, Asp102 and Ser195 (chymotrypsin numbering), (Figure1.5 B), with high specificity for macromolecular substrates (Kang et al. 2011). The serine residue (Ser195) is a key component in the formation of the transient acyl- enzyme, whereas the histidine and aspartic acid provide stability for the complex molecule (Serrano 2013). Despite exhibiting exquisite specificity towards their substrates, several SVSPs share homology such as the presence of 12 cysteine residues, five disulphide bridges and the extended C- terminus (Figure 1.5 B)

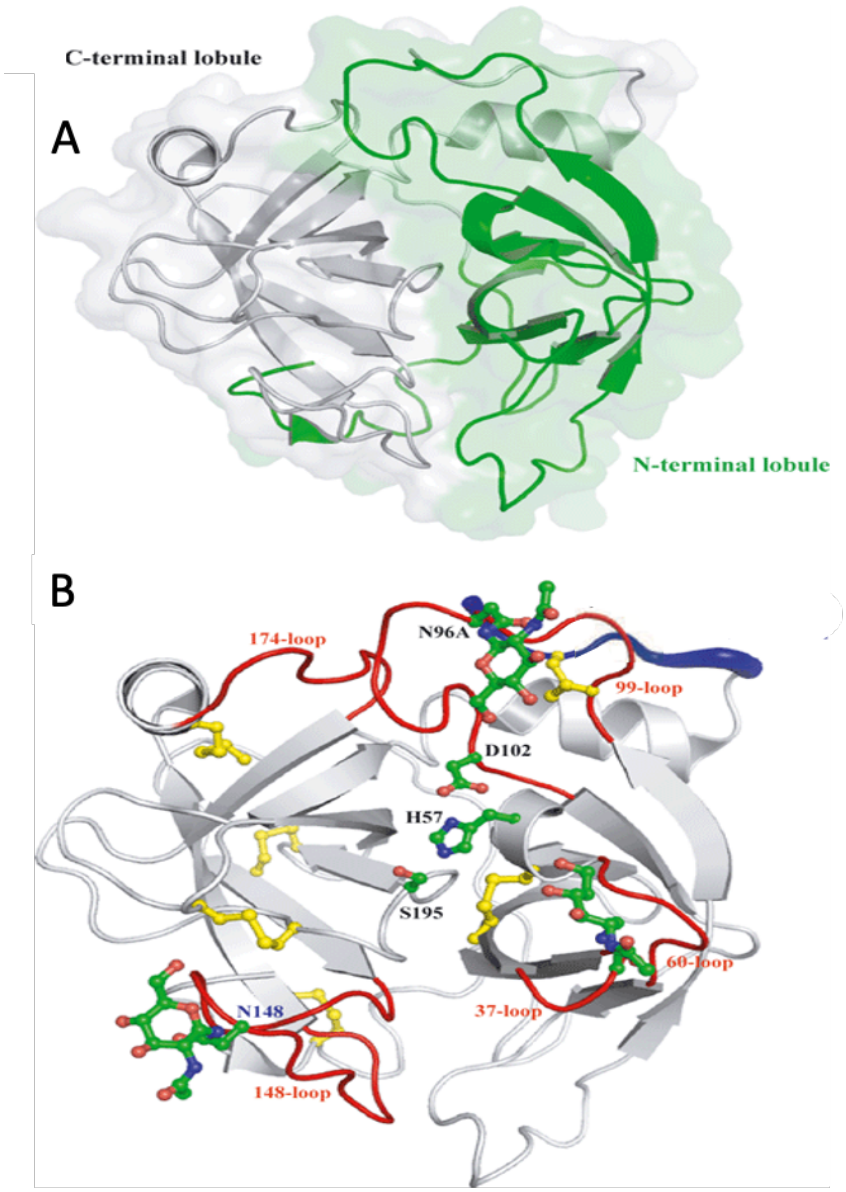

Figure 1.5 Schematic structure of SVSP.

(A) represents the N-terminal subdomain (green) which contains six β – strands and a single short α-helix as the C-terminal subdomain (grey) encompasses a six-stranded β-sheet and two α-helices. (B) represents/ illustrates the extended C-terminal tail which contains additional disulphide bridges (blue), as well as the active serine residue at position 195. The side chains of His57, Asp102 and Ser195 are represented by the atom colour. The putative N-linked glycosylation sited are included and represented by N96A and N148. Cys42/Cys58 represent the intra-chain disulphide bridges whilst Cys22/Cys157 and Cys91/Cys245E are the other two disulphide bridges included in the schematic.

Adapted from (Kang et al. 2011).

SVSPs are known for their ability to alter the haemostasis system and to cause considerable clinical manifestations such oedema and hyperalgesia through still poorly defined mechanisms (Ferraz et al. 2019). Based on their biological roles, SVSPs are classified as procoagulant, anticoagulant, fibrinolytic and platelet aggregation (Serrano and Maroun 2005; Kang et al. 2011).

The procoagulant SVSPs activate several coagulation factors including VIII, X and prothrombin and shorten the coagulation times (Kang et al. 2011). Similarly, the platelet aggregating SVSPs contribute to clot formations by activating platelet receptors which promote the bindings of fibrinogen and clot formations (Ferraz et al. 2019).

On the other hand, the anticoagulant SVSPs are characterised by their ability to activate protein C which in turn inactivate the coagulant factors Va and VIIIa (Kang et al. 2011; Ferraz et al. 2019). Additionally, the fibrinolytic SVSPs are known for playing key role in inducing SBE-associated coagulopathy by eliminating preexisting clots (Kang et al. 2011; Ferraz et al. 2019).

1.2.1.3 Phospholipase A_2 (PLA_2)

Phospholipase A_2 (PLA_2) hydrolyse phospholipid membranes at the *sn*-2 position, producing fatty acids and lysophospholipids (Kang et al. 2011). They are Ca^{2+}-dependent enzymes of approximately 13-15 kDa containing 5-8 disulphide bonds (Schaloske and Dennis 2006). Evidence suggests that $svPLA_2$s were recruited into the snake venom system from non-toxic ancestral proteins, where new multifunctional isomers evolved following rapid evolution and gene duplication (Fry 2005; Ferraz et al. 2019).

The $svPLA_2$ are divided in to two main groups: group-I and group-II which are found in elapids and vipers, respectively (Kang et al. 2011; Xiao et al. 2017). The presence of a third type of $svPLA_2$ (also known as group-II E) in non-front-fanged snakes has been reported, although its role in the venom arsenal is unclear (Ferraz et al. 2019). As demonstrated in the schematic molecular structure (Figure 1.6), all $svPLA_2$ types contain α–helices, β–wings, calcium binding loops and active site residues His48, Asp49, Tyr52 and Asp94 for group-I or Asp99 for group-II; however, these subunits appear to have different binding ligands (Kang et al. 2011). Despite sharing significant structures and 44-99% sequence identity, different $svPLA_2$ types exhibit

variable pharmacological properties (Mackessy 2009). The majority of group-I svPLA$_2$s are Asp49, forming enzymatically active complex toxin, usually associated with post- and pre-synaptic neurotoxicity. On the other hand, group-II svPLA$_2$s are Lys49 and are usually myotoxic, although significant numbers of this isoform are enzymatically inactive (Calvete et al. 2010; Tonello and Rigoni 2017).

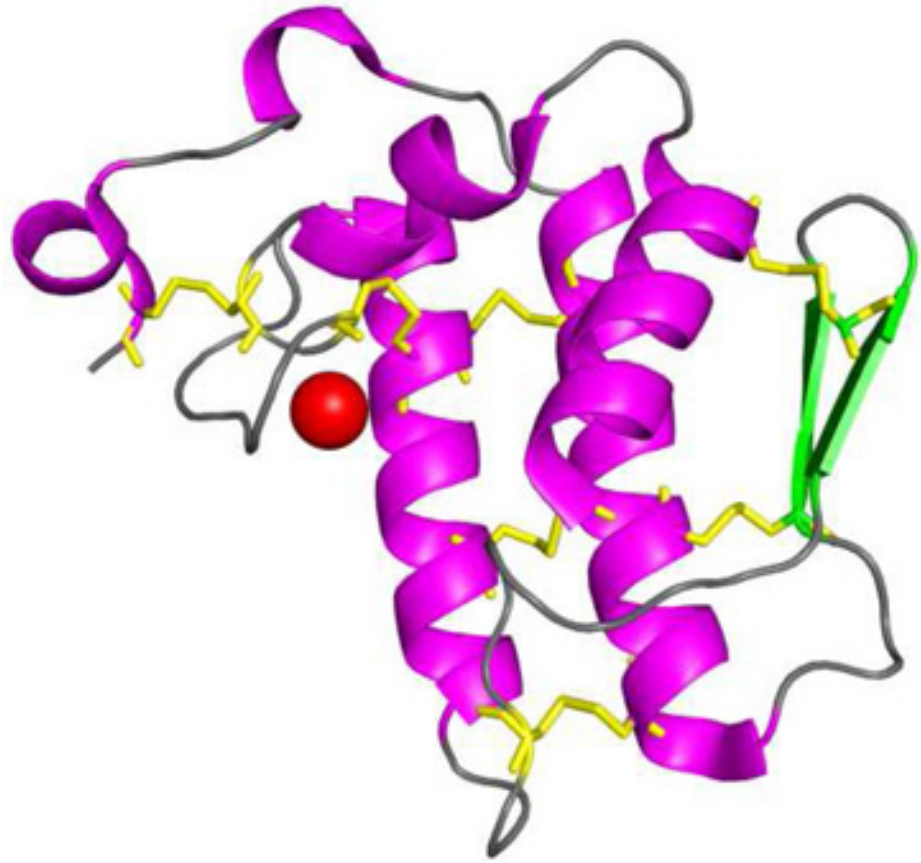

Figure 1.6 Overall structure of svPLA$_2$.

The diagram shows α-helices (magenta), β-strands (green) the six disulphide bonds (yellow) and calcium bound to the loop (red sphere).

Taken from (Dennis et al. 2011) Reprinted with permission.

SvPLA$_2$s are represented by both basic and acidic isoforms, based on overall net charge, toxicity being ascribed to basic svPLA$_2$s. The non-toxic, strongly acidic isoform, is restricted to digestive roles (Tonello and Rigoni 2017). SvPLA$_2$s are amongst the most toxic and abundant venom toxins, but venoms from the *Dendroaspis* spp. contain very few and/or svPLA2s with negligible toxic activity, the lethal neurotoxic effects being attributed to other toxin

families (Laustsen et al. 2015; Petras et al. 2016). Pathologically, this enzyme toxin family is responsible for eliciting a broad spectrum of pathological manifestations including neurotoxicity, myotoxicity, haemorrhage, oedema, inflammation, coagulopathy and hypertension (Ferraz et al. 2019).

1.2.1.4 L–amino acid oxidase (LAAO)

Snake venom L-amino acid oxidases (svLAAOs) are present in many snake venoms in varying proportions, ranging from 0.15% in the Caspian Cobra (*Naja oxiana)* to 30 % in the Malaysian pit viper (*Calloselasma rhodostoma*) (Du and Clemetson 2002). The occurrence of these enzymes in SSA snake venoms is very low, apart from *Echis* and *Bitis* spp., which contain only a slightly higher proportion (Tasoulis and Isbister 2017). Pathophysiologically, svLAAOs have multi-biological functions including inhibition and induction of platelet aggregation, apoptosis, cytotoxicity, haemolysis and haemorrhage (Du and Clemetson 2002; Costa et al. 2014). Hydrogen peroxide (H_2O_2) is produced during these enzymatic reactions, but the mechanism by which these enzymes exert their toxicity is poorly understood and their overall contribution to snake venom toxicity and its mechanism of action on its prey remains unclear.

1.2.1.5 Three- finger toxin (3FTX)

Three-finger toxins (3FTXs or 3FTx) are a group of relatively small non-enzymatic proteins ranging from ~60-74 amino acid residues (Kini and Doley 2010). They are characterised by the presence of 3 highly conserved β–loops extending from a small globular hydrophobic core stabilised by conserved disulphide bonds (Figure 1.7) (Sunagar et al. 2013; Kessler et al. 2017). Snake venom 3FTXs (sv3FTXs) evolved from the scaffold of non-toxic ancestral proteins via gene duplication and accelerated evolution, which resulted in the emergence of structurally and functionally diverse isomers (Sunagar et al. 2013). During evolution, structures that are essential for folding and structural integrity were preserved, resulting in the emergence of multiple isomers with structural similarities but different actions and receptor targets (Kini and Doley 2010).

Most sv3FTXs are monomers with short C and N termini (short chain); however, dimeric 3FTXs also exist as long- chain toxins that contain an

additional 2- 9 amino acids at the C- terminus (Girish et al. 2012). Short chain (or type I) sv3FTXs (e.g., α-neurotoxins, cytotoxins and fasciculins) comprise 57 -62 amino acid residues and 4 disulphide bridges whereas the long chain (or type II) sv3FTXs (e.g., α-neurotoxins and γ-neurotoxins) are typically 66-74 amino acid residues and 5 disulphide bridges (Sunagar et al. 2013; Ferraz et al. 2019). Although different sv3FTXs show minor structural variations, the general structures of sv3FTXs comprise eight highly conserved cysteine residues, crosslinked into four conserved disulphide bonds; these provide structural integrity, stability and aid the folding of the toxins (Kini and Doley 2010). Despite sharing significant homology, individual sv3FTXs exhibit unique mechanisms of actions, targeting pivotal physiological processes. Key pathophysiological properties of sv3FTXs include disruption of the cholinergic system (postsynaptic nicotinic and muscarinic receptors) by various neurotoxin blockade of L-type calcium channels (calciceptine); inhibition of platelet aggregation (dendroaspin); and disruption of the structure and function of phospholipid membranes (cardiotoxins and cytotoxins) (Kini and Doley 2010).

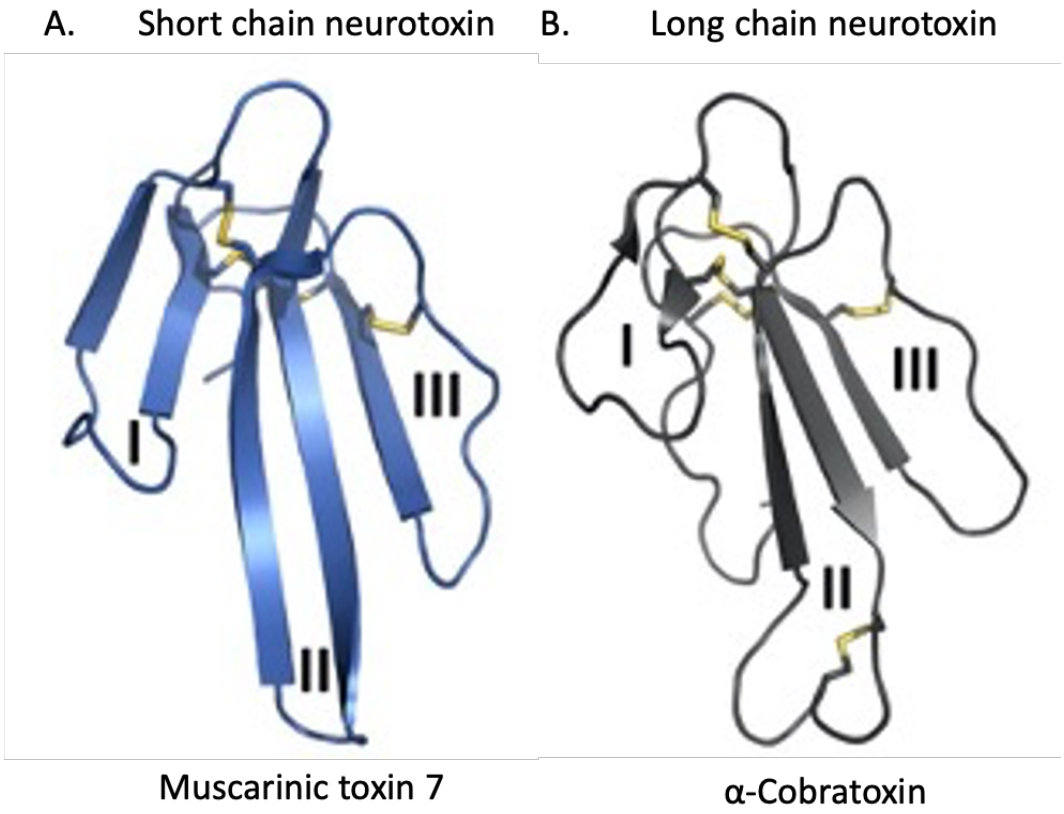

Figure 1.7 Schematic representing 3-dimenstional structure of 3FTXs.

(A) example of short-chain muscarinic toxin 7 (*MT7*) and (B) long chain α-cobratoxin 3FTXs, showing the 3 β–loops (Roman numerals) and the stabilising disulphide bonds (yellow).

Taken from (Kessler et al. 2017). Reprinted with permission.

Proteomic studies reveal that sv3FTXs are found in the venom of almost all elapid snakes. However, 3FTXs are not constituents of viper venoms. They are the chief constituent of elapid venoms, such as those of *Naja* and *Dendroaspis spp.*; and Hydrophiid snake*s* (Mackessy and Saviola 2016; Tasoulis and Isbister 2017). African cobra venom toxins are dominated by neurotoxin and cytotoxin 3FTXs (Petras et al. 2011; Malih et al. 2014; Lauridsen et al. 2017). The majority of sv3FTXs in mamba venoms are short chained neurotoxins of atypical structural and biological functions, for example, muscarinic toxins and fasciculins (Laustsen et al. 2015; Petras et al. 2016; Ainsworth et al. 2018) – also see Figure1.7 A. These toxins are responsible for the paralysis, respiratory failure, arrhythmia, convulsions and death, typically observed following SBE by mambas or cobras (Baldé et al. 2013).

1.2.1.6 Kunitz-type toxin (KTT)

Snake venom Kunitz-type toxins (svKTTs) are small non-enzymatic proteins, around 6.6 kDa, with approximately 60 amino acid residues, stabilised by three disulphide bonds. They are associated with inhibition of serine proteases and K^+ and Ca^{+2} channel blockade (Zupunski et al. 2003; Yuan et al. 2008). On the basis of their function, the KTTs are divided into two main groups: 1) non-neurotoxic; commonly referred to as trypsin and chymotrypsin inhibitor KTTs; 2) homologous neurotoxic groups, which consist of various dendrotoxin (DTX) types (Inagaki 2017). Influenced by gene duplication and rapid diversification, the original action of svKTTs (i.e., the inhibitory mechanism) was replaced by a K^+ channel-blocking action (Zupunski et al. 2003).

The overall structures of dendrotoxin-K (DTX-K) and dendrotoxin-1 (DTX-1), two different K^+ channel blockers, are essentially identical to that of bovine pancreatic trypsin inhibitor (BPTI) (Zupunski et al. 2003; Inagaki 2017). As shown in Figure 1.8., the structure of these proteins consists of two anti-parallel β-sheets, an α- helix and a loop extended from a disulphide bond and

stabilised as a protease- complex molecule by a small segment of amino acids (Inagaki 2017).

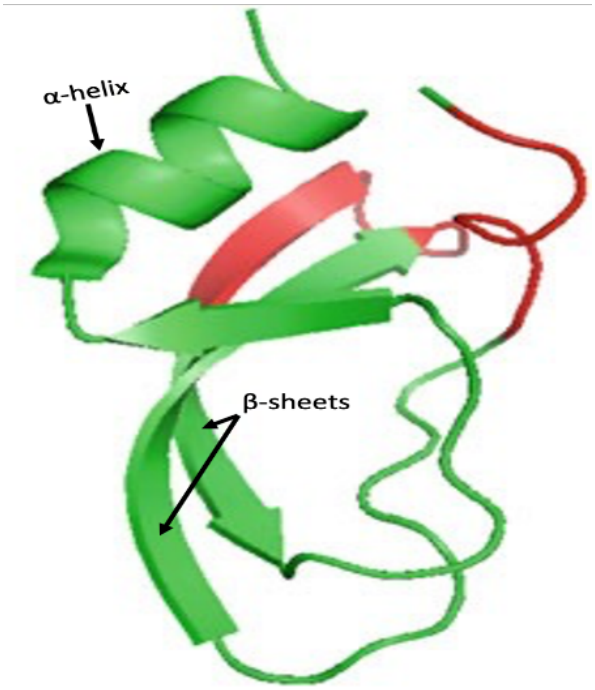

Figure 1.8 Three-dimensional structure of dendrotoxin-K (DTX-K).

The diagram shows the two antiparallel β-sheets, α-helix and the interface with target molecule (highlighted in red).

Adapted from (Inagaki 2017)

SvKTTs are potent neurotoxic compounds present in most viper and elapid venoms. They are the predominant component of *Dendroaspis* venoms, accounting for approximately 61% of *D. polylepis* venom (Laustsen et al. 2015). Various dendrotoxin types, including DTX-1, DTX-K, α-DTX and δ-DTX, were isolated from the venoms of several mamba species (Harvey and Robertson 2004; Laustsen et al. 2015; Ainsworth et al. 2018). In addition to the K^+ channel, as in the cases of dendrotoxins (Harvey and Robertson 2004), potential targets for svKTTs also include coagulation factors Xa, XIIa, and activated protein C (Inagaki 2017). Clinically, K^+ channel blockade of central nervous system (CNS) neurotransmission (Harvey and Robertson 2004), and symptoms such as tachycardia, convulsions and respiratory failure may occur (Lauridsen et al. 2016; Petras et al. 2016). Other clinical signs induced by svKTTs include hypersalivation, local oedema and bleeding (Baldé et al. 2013).

1.2.1.7 C-type lectin (CTL)

Snake venom C-type lectins (svCTLs) are characterised by the presence of a highly conserved carbohydrate-recognising domain of 115- 130 amino acids (Morita 2005). SvCTLs are homodimers or homo-oligomers, consisting of identical subunits, each with a molecular mass of approximately 15 kDa, in addition to the functional Ca^{2+}/ carbohydrate domain responsible for binding sugars (Morita 2005; Arlinghaus and Eble 2012).

This venom toxin family is commonly associated with red blood cell aggregation (Ogawa et al. 2005). The anticoagulant proteins are characterised by their Ca^{2+}-dependent binding to γ-carboxyglutamic acid-containing domains of factor IX and X mediating serious disruption to haemostasis (Arlinghaus and Eble 2012). The platelet aggregation agonists are capable of promoting platelet aggregation by binding to glycoprotein (GPIb) receptors and von Willebrand factor (vWF), facilitating the fibrinogen-integrin αIIbβ3 complex and subsequently platelet adherence to collagen (Ogawa et al. 2005). In contrast, svCTLs that act as platelet aggregation antagonists compete with vWF for binding to platelet GPIb receptors, thereby inhibiting platelet aggregation (Ogawa et al. 2005; Arlinghaus and Eble 2012).

These toxins account for 4.2- 14.3% of total *Bitis* spp venom protein (Calvete et al. 2007) and 7% of *E. ocellatus* venom (Wagstaff et al. 2009). However, there is no evidence to suggest that these toxins are present in the venoms of *Naja spp*. (Petras et al. 2011; Malih et al. 2014) or *Dendroaspis spp.* (Laustsen et al. 2015; Lauridsen et al. 2016; Ainsworth et al. 2018), although traces (<0.3% of total venom proteins) of *selectins* (CTLs) were identified in the venom of *Naja melanoleuca* (Lauridsen et al. 2017). Although the haemorrhage and dysregulated haemostasis observed in SBE by *Echis* and *Bitis spp* are ascribed to SVMPs and SVSPs, respectively, the presence of CTLs in these venoms may amplify toxicity, thus compounding the clinical presentation.

1.2.1.8 Disintegrins (DIS)

Disintegrins are a family of small (40-100 amino acids), cysteine-rich polypeptides (Calvete 2005), commonly present in viper venoms and some hematophagous animals (Chakrabarty and Chanda 2017). Disintegrins/

disintegrin-like domains are released into snake venom as the result of proteolytic cleavage of P-II SVMPs and P-III SVMPs.

Disintegrins evolved numerous integrin-binding motifs such as the arginine-glycine-aspartic acid (RGD), methionine- leucine- aspartic acid (MLD) and valine- glycine- aspartic acid (VGD) sequences (Calvete 2005; Fox and Serrano 2008). The majority of these motifs facilitate interaction of disintegrins / disintegrin- like domains with the distinct binding-ligand profiles formed by the combination of α and β subunits, leading to inhibition of fibrinogen binding to $\alpha IIb\beta_3$ integrins. This, in turn, will inhibit platelet aggregation, dysregulate platelet function and eventually result in significant haemorrhagic onsets (Kamiguti et al. 1998). Furthermore, the motifs act as potent inhibitors of ligand binding to integrins $\alpha_5\beta_1$ and $\alpha_v\beta_3$ expressed on the surface of tumour, fibroblast and endothelial cells (Selistre-de-Araujo et al. 2010; Kuo et al. 2019). Thus, snake venom disintegrins are excellent candidates for therapeutic applications such as antitumor, antithrombotic, and anti-inflammatory agents (Selistre-de-Araujo et al. 2010; Kuo et al. 2019).

Disintegrins / disintegrin-like domains are nonenzymatic venom toxins found in several viper venoms (Calvete 2005; Chakrabarty and Chanda 2017), and are associated with haemorrhage and dysregulated haemostasis in patients envenomated with venoms rich in disintegrins (Calvete et al. 2007). Currently, there is no evidence to suggest the presence of these toxins in elapid venom (Petras et al. 2011; Laustsen et al. 2015; Lauridsen et al. 2016; Tasoulis and Isbister 2017).

1.2.1.9 Cysteine- rich secretory protein (CRiSP)

CRiSPs are nonenzymatic, single chain polypeptides, with a molecular mass of around 20-30 kDa, found in mammals, viper, elapid and colubrid snake venoms (Yamazaki et al. 2003; Yamazaki and Morita 2004). Snake venom CRiSPs (svCRiSPs) are associated with disruption of haemostasis, mainly through interactions with voltage-gated ion channels, cyclic nucleotide-gated (CNG) ion channels and inhibition of smooth muscle contraction (Yamazaki et al. 2003; Yamazaki and Morita 2004; Sunagar et al. 2012). SvCRiSPs were modified into venom components as the result of accelerated evolution, influenced by positive selection and directional mutagenesis, whereas their

mammalian homologs were constrained by negative selection, due to their importance in key biological processes (Sunagar et al. 2012).

Structurally, CRiSPs contain two domains: 1) C- terminus, which forms the highly conserved cysteine-rich domain (CRD) and 2) the N-terminal conserved fold of the pathogenic-related (PR-1) domain. The active site of CRiSPs is still unclear, but the CRD shares structural similarities with other channel blockers and interacts with CNG ion channels and/ or with ryanodine receptors (Wang et al. 2010; Sunagar et al. 2012).

In general, CRiSPs are present in most snake venom, but they are considered minor venom components (Aird 2002). SvCRiSPs represent 10% of total venom proteins of *N. haje* (Malih et al. 2014), and 7.6% *N. melanoleuca* (Lauridsen et al. 2017) but *Echis* and *Bitis* venoms contain svCRiSPs only 0.3-2 % total venom protein (Tasoulis and Isbister 2017), and no trace is found in *Dendroaspis* venoms (Ainsworth et al. 2018).

1.2.1.10 Natriuretic peptide (NP)

Natriuretic peptides (NPs) are a ubiquitous family of small peptides, molecular mass ~24 kDa, found in many animal species, including venomous snakes, and humans (Fry et al. 2006; Vink et al. 2012). NPs play a key role in cardiovascular homeostasis, through regulation of fluid and electrolyte balance, as well as vascular tone (Potter et al. 2009). Structurally, all NPs contain a highly conserved 17 disulphide ring, harbouring the functional 5-amino acid (phenylalanine, aspartic acid, arginine, isoleucine, and isoleucine/ leucine) structure (Munawar et al. 2018). This facilitates the binding of NPs to a transmembrane guanylyl cyclase, which catalyses the synthesis of cyclase guanosine monophosphate (cGMP), thereby initiating vasodilation and hypotension (Potter et al. 2009). Snake venom NPs (svNPs) are significant toxin family in some viper and elapid venoms. NPs are present in considerable quantities in most crotalid venoms, but either constitute a very low percentage or are absent from most Asian, European and African viper venoms (Tasoulis and Isbister 2017). A small percentage of svNPs were identified in all *Dendroaspis* venoms (Ainsworth et al. 2018), they were not found in *Bitis* (Calvete et al. 2007), *Naja* (Petras et al. 2011), or *Echis* (Tasoulis and Isbister 2017) venoms.

1.2.1.11 Bradykinin-potentiating peptide (BPP)

Bradykinin-potentiating peptides (BPPs) are short chain (5- 13 amino acid) oligopeptides characterised by a pyroglutamyl/ proline-rich structure in the N- and C- termini, respectively (Inagaki 2017). The first natural BPP was isolated from *Bothrops jararaca* and then more BPP were subsequently identified from many snake and scorpion venoms (Sciani and Pimenta 2017). Snake venom BPP (svBPPs) primarily act on angiotensin-converting enzyme (ACE) thereby inhibiting the formation of angiotensin II, resulting in the profound hypotension observed in viper SBE patients (Viala et al. 2015). This observation led to the development of Captopril; an ACE-inhibitor drug, widely used in both human and veterinary medicine, derived from *B. jararaca* venom (Munawar et al. 2018).

SvBPPs are found in both viper and elapid venoms (Viala et al. 2015). Indeed, they are present in some *Bitis* (Calvete et al. 2007), and *Echis* venoms and, in conjunction with other hypotensive toxins, contribute to the profound hypotensive shock observed in envenomed patients (Wagstaff and Harrison 2006). Currently they have not been identified in SSA elapid venoms, apart from *N. mossambica* venom (Munawar et al. 2014).

1.2.1.12 Vascular endothelial growth factor (VEGF)

Vascular endothelial growth factor (VEGF) is a diverse but homologous protein family including snake venom VEGFs (svVEGFs) (Yamazaki and Morita 2006; Yamazaki et al. 2009). VEGFs and their receptors play a crucial role in neovascularization, through mediating angiogenesis and vasculogenesis (Yamazaki and Morita 2006). Nevertheless, svVEGFs stimulate cell proliferation, promote hypotension and vascular permeability, and thus could play a role in immobilisation and digestion of prey (Yamazaki and Morita 2006). Unlike the highly conserved snake tissue type VEGFs, venom-derived VEGFs display structural variations, particularly in the functionally-relevant regions including receptor binding loops and C-terminal co-receptor binding regions (Yamazaki and Morita 2006). Despite being scarcely expressed, svVEGFs are found in most viper and some elapid venoms, including those found in SSA (Calvete et al. 2007; Ainsworth et al. 2018).

1.2.1.13 Nerve growth factors (NGF)

Nerve growth factors (NGFs) belong to a closely related protein family, known as neurotrophins, which modulate survival, development and function in both the central and peripheral nervous systems (Skaper 2012). Snake venom NGFs (svNGFs) have been found in a variety of viper and some elapid venoms, including *D. polylepis* (Laustsen et al. 2015), but their role is not fully understood.

The protein families described above are the dominant venom components of the medically important snakes found in SSA. The relative percentage of each of these venom components and their pathophysiological effects, together with common names for these snake species is summarised in Table 1.1.

Other toxins such as phosphomonoesterases, acetyl cholinesterase (AChE), nucleases and nucleotidases have also been identified, but only account for traces of total venom protein.

Table 1.1 key venom components in some of clinically relevant snake species in the SSA region.

Genus	Species	Physiological effects	Percentage of each snake venom constituents												References
			SVMP	SVSP	PLA_2	KTT	3FTX	VEGF	NGF	NP	CRiSP	CTL	DIS	LAAO	Other peptides	
***Bitis* (adders)**	*B. arietans* (Puff adder)	Associated with disrupted haemostasis system leading to severe local and systemic effects such as swelling, haemorrhagic and necrosis onsets.	38.5	19.5	4.3	4.2	ND	ND	ND	ND	ND	13.2	17.8	ND	0.9	(Warrell et al. 1975; Calvete et al. 2007; Currier et al. 2010; Tasoulis and Isbister 2017)
	B. gabonica (Gabon viper)		22.9	26.4	11.4	3	ND	1	ND	ND	2	14.3	3.4	1.3	1.2	
***Dendroaspis* (mambas)**	*D. jamesoni* (Jamesoni mamba)	Associated with neurotoxicity causing fasciculations, ptosis, cardiovascular collapse, respiratory paralysis and death. respiratory paralysis and death.	NA	ND	2.2	16.3	65.5	ND	ND	2	ND	65.5	65.5	65.5	13.4	Warrell et al. 1974; Laustsen et al. 2015; Tasoulis and Isbister 2017; Ainsworth et al. 2018)
	D. polylepis (black mamba)		3.2	ND	<0.1	61.1	31	<0.1	0.3	2.9	ND	ND	ND	ND	1.3	
	D. viridis (western green mamba)		ND	ND	0.2	5.6	76.7	ND	ND	0.5	ND	76.7	76.7	76.7	15.3	
***Echis* (carpet vipers)**	*E. leucogaster* (White-billed carpet viper)	Associated with local and systemic haemorrhage causing spontaneous bleeding, coagulopathy, cardiovascular collapse and intravascular damages.	27.4	3.7	39.7	ND	ND	ND	ND	ND	ND	5.1	14.6	1	ND	(Wagstaff et al. 2009; Calvete et al. 2010; Tasoulis and Isbister 2017; Albulescu et al. 2020)
	E. ocellatus (West African carpet viper)		75.7	2.5	12.6	ND	ND	ND	ND	ND	1.5	7	2.3	2.2	ND	
***Naja* (cobras)**	*N. haje* (Egyptian cobra)	Associated with significant neurotoxicity leading to progressive paralysis leading to respiratory collapse and death	9	ND	4	1.9	60	ND	5	ND	10	ND	ND	ND	9.1	(Warrell et al. 1976a; Malih et al. 2014; Lauridsen et al. 2017; Tasoulis and Isbister 2017)
	N. melanoleuca (forest cobra)		9.7	ND	12.9	3.8	57.1	ND	<0.4	ND	7.6	<0.6	57.1	57.1	<6.6	
	N. nigricollis (black-necked spitting cobra)	Associated with cytotoxicity causing local swelling, oedema, and extensive tissue necrosis.	2.4	ND	21.9	ND	73.3	ND	ND	ND	0.2	73.3	73.3	73.3	0.5	(Warrell et al. 1976b; Petras et al. 2011; Tasoulis and Isbister 2017)

Abbreviations: SVMP; Snake venom Metalloproteinases, SVSP; snake venom serine peptidase, PLA2; Phospholipase A2, KTT; kunitz Type Toxins, 3FTXs; 3 finger toxins, VEGF; Vascular endothelial growth factor, NGF; Nerve growth factor, NP; Natriuretic peptides, CRiSP; Cysteine-rich secretary proteins, CTL; C – type lectins, DIS; disintegrins, LAAO; L-amino acid oxidases, ND; not determined.

1.2.2 Synthesis and storage of snake venom

All of the currently known venomous snakes (~80% of all snake species) belong to the *Colubroidea* superfamily (Vidal 2002; Vidal et al. 2007). Members of the *Colubroidea* superfamily, have evolved highly sophisticated mechanisms for synthesis, storage, and delivery of a highly toxic bioweapon into their prey. However, the molecular and cellular mechanisms underpinning the recruitment and storage of these potent toxins without autodigestion is not fully understood. Recent evolutionary studies have demonstrated that the majority of venom toxins are clustered with their phylogenetically related mammalian proteins, indicating that these proteins originated from common ancestors (Zupunski et al. 2003; Calvete 2005; Fry 2005). Venom toxins were recruited into the snake venom arsenal from normal non-toxic physiological proteins (Figure 1.9), but there is no evidence to show the presence of a specific location for toxin encoding genes (Fry 2005; Fry et al. 2009). Moreover, substantial studies have shown that the diversification and recruitment of venom-related genes into the venom gland was the result of adaptive evolution (Zupunski et al. 2003; Calvete et al. 2005; Fry et al. 2005; Ogawa et al. 2005; Kini and Doley 2010; Sunagar et al. 2012).

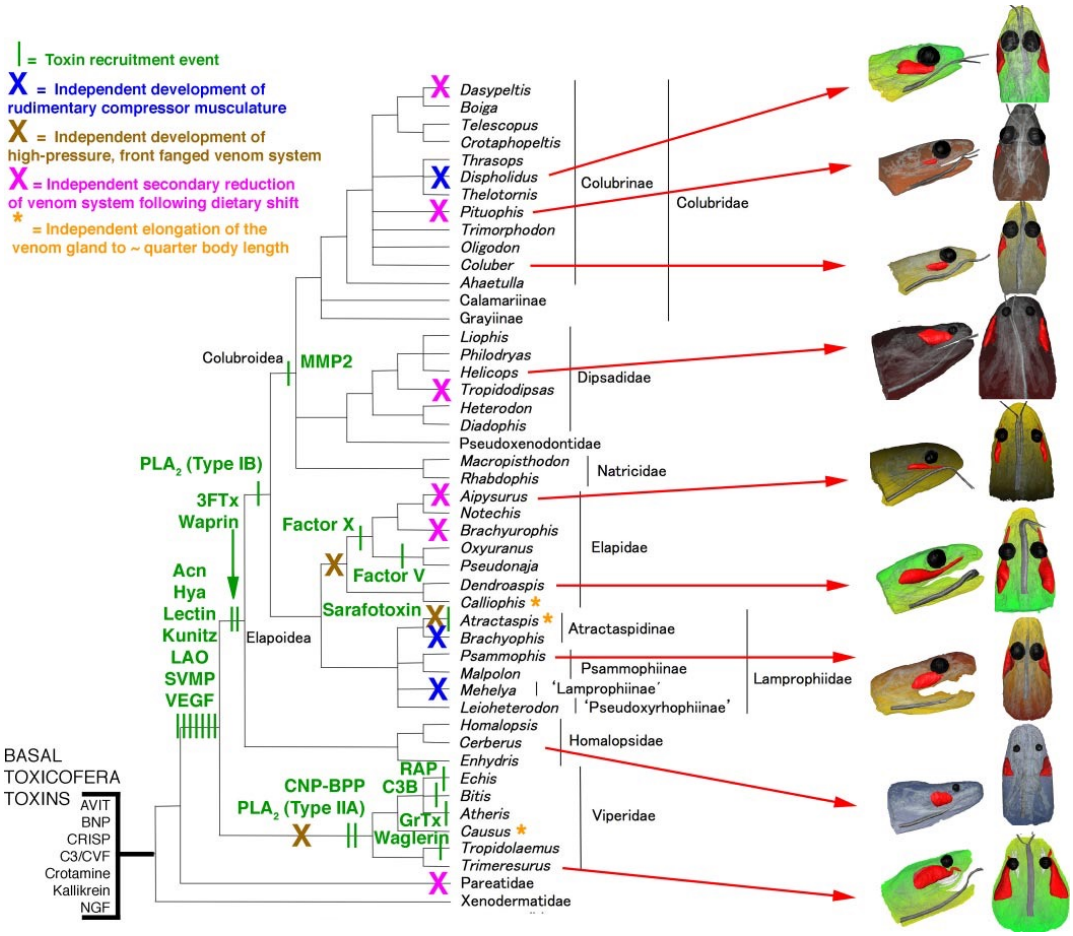

Figure 1.9 Cladogram of evolutionary relationships of advanced snakes.

The diagram shows the relative timing of toxin recruitment events and derivations of the venom system.

Abbreviations: Acn, Acetylcholine esterase; *LAO*, L-amino oxidase; *C3B*, FAMC3B cytokine; *CNP-BPP*, c-type natriuretic peptide-bradykinin-potentiating peptide; *GrTx*, glycine-rich toxin; *Hya*, hyaluronidase; *RAP*, renin-like aspartic protease; *VEGF*, vascular endothelial growth factor.

Taken from (Fry et al. 2008). Licenced under CC-BY.

On the basis of venom storage and synthesis, venomous snakes are classified as front- fanged snakes which contain venom gland, and the rear- fanged snakes that contain the Duvernoy's venom glands (Mackessy and Saviola 2016). Whilst front- fanged snakes occur in *Atractaspidinae*, *Viperidae* and *Elapidae* families (Mackessy and Saviola 2016), rear- fanged snakes are phylogenetically diverse collections of species from families such as C*olubridae, Homalopsidae,* and *Lamprophiidae* (Modahl and Mackessy 2019). Although rear-fanged snakes produce venoms, snakebites that are of medical

concern are predominantly front- fanged snakes from *Viperidae* and *Elapidae* families (Modahl and Mackessy 2019).

Front- fanged snakes contain numerous cells, ducts and glands (Figure 1.10), that work together to provide an efficient system for synthesis, storage and pressurised delivery of venom into prey (Oron and Bdolah 1973; Mackessy and Baxter 2006; Currier et al. 2012). The removal of the venom triggers morphological and biochemical changes in secretory epithelium, where epithelial cells lining the tubules of the venom glands initiate rapid protein synthesis (Mackessy and Baxter 2006; Currier et al. 2012). Synthesised venom proteins are then transferred via secretory vesicles into the gland lumen for storage until required (Mackessy and Baxter 2006; Luna et al. 2013). Following manual extraction, the synthesis process takes approximately 16 days (Mackessy and Baxter 2006). However, complete replacement of depleted venom until the glands return to a quiescent state could take 40-50 days (Portes-Junior et al. 2014).

Snake venom synthesis and storage must be rapid and efficient in order to maintain predatory and defensive capabilities. To minimise venom expenditure, these snakes may meter the venom injected according to the nature of the bite and whether used against prey or defensively (Young and Zahn 2001). The biochemical nature of newly synthesised venom proteins and the mechanism(s) involved in its maturation or activation is not fully elucidated. It was demonstrated that some venom proteins are already present within secretory cells of the venom gland, suggesting that some venom components are synthesised as structurally mature toxins (Luna et al. 2013). Additionally, it has been reported that the peptide composition of these proteins remains unchanged during the toxin's cycle (Mackessy and Baxter 2006). In contrast, other significant proteins, including SVMPs are produced and accumulate in the luminal gland, as proenzymes (Portes-Junior et al. 2014).

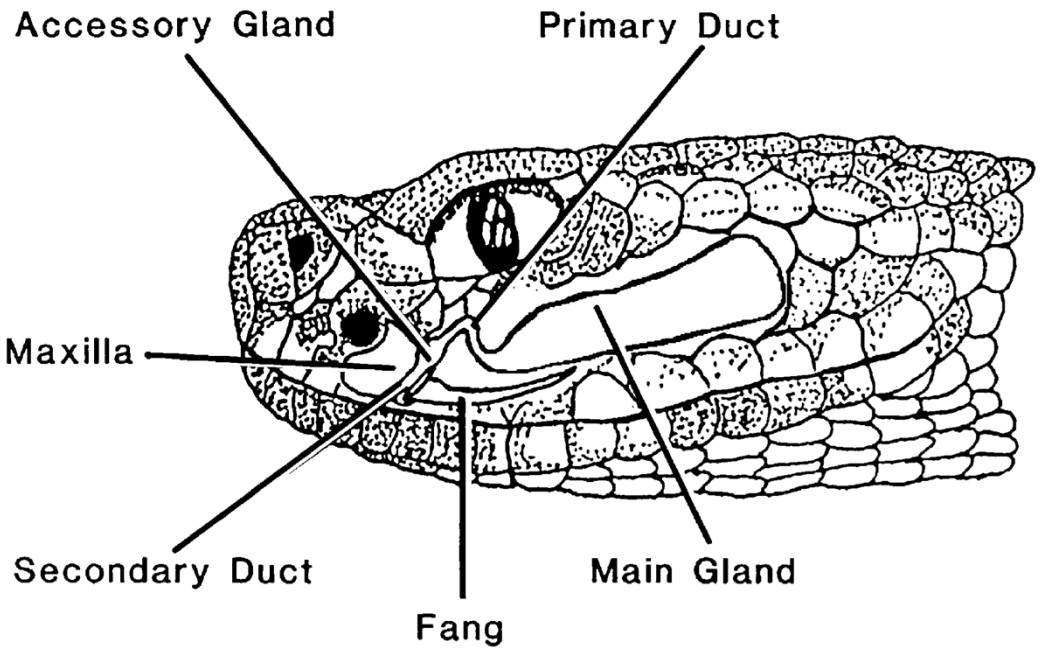

Figure 1.10 Diagram of front-fanged snakes.

The image displays the locations of the main regions: the main glandular lumen, the accessory gland, the primary and the secondary ducts.

Adapted from (Mackessy and Baxter 2006).

Several studies have shown that the morphology of the venom glands consist of: (i) rostral portion; (ii) caudal serous portion; (iii) mitochondria- rich cells and (iv) mucus secreting epithelial cells (Oron and Bdolah 1973; Mackessy and Baxter 2006; Sakai et al. 2012). It is postulated that these structural and cellular compartments play a significant role in maintaining the stability of stored toxins, providing auto-protection against toxic effects, and spontaneously activating the venom during expulsion. In addition to the presence of antibodies and several peptides within stored venom, acidification by the mitochondria-rich cells provides protein stability, inhibits enzymatic activities and ensures that the inactivity of toxins within the central lumen of the gland is maintained (Mackessy and Baxter 2006).

During biting and/or extraction, the venom passes through the rostral portion, a region where mucus-rich epithelial cells are very dense, encounters an alkaline environment and is spontaneously activated by secretion from the caudal serous portion (Mackessy and Baxter 2006). The activation mechanism of venom constituents, which are recruited into the venom arsenal as zymogens, is still unclear. However, it has been reported that peptide cleavage

taking place within the lumen of the venom gland activates enzymes (Portes-Junior et al. 2014). More importantly, for higher efficiency venom delivery, front- fanged snakes have the advantage of highly pressurised glands, allowing rapid expulsion and injection of venom.

1.3 Antivenom

Antivenoms are purified polyclonal antibodies, which specifically bind to and neutralise venom toxins, produced by immunisation of a donor animal. Although various novel therapeutics have been proposed (Alvarenga et al. 2014; Pucca et al. 2019), heterologous antivenoms remain the only commercially available approved treatment for SBE at present (Guidolin et al. 2016). Specific antibody (SpAb) production is induced by repeatedly injecting small quantities of venom into animals, preferably larger farm animals such as horses and sheep, then collecting the resultant hyperimmunized plasma /or serum. Active immunoglobulin G (IgG) is collected by caprylic acid and/or ammonium sulphate precipitations where proteolytic digestions subsequent to produce fragmented antibody [Fab and $F(ab')_2$]. Thus, antivenoms are preparations of heterologous IgG and/or Fab and $F(ab')_2$, usually raised in horses or sheep.

1.3.1 Brief history of the path to the discovery of antivenom

In 1894, Phisalix and Bertrand reported the first attempt to treat envenomed patients using whole blood from a sheep inoculated with detoxified *Viper aspis* (Dias da Silva and V Tambourgi 2011). In 1895 Calmette and colleagues produced the first serum antivenom against cobra snakes that was used to successfully treat a patient envenomed by *Naja kaouthia* (Williams et al. 2018; Pucca et al. 2019). At the time, the anti-cobra serum was presented as a universal antivenom capable of conferring protection against lethality induced by other snake species, even from different species and geographical regions. However, the claim was swiftly contested as the anti-sera failed to offer protection beyond the regional *Naja* spp. (Squaiella-Baptistao et al. 2018), emphasising the antivenom's specificity for the venom(s) used in its production. Thereafter, various countries started producing regionally manufactured crude serum antivenoms effective at treating victims

envenomed by local snakes, although adverse reactions were very common (Dias da Silva and V Tambourgi 2011; Gutierrez et al. 2011).

Despite efficacy at treating envenomed patients, administration of whole serum was associated with dangerous adverse effects attributed to the presence of heterologous proteins (Squaiella-Baptistao et al. 2018). This promoted the need to reduce contaminants, IgG and/or non-Ig serum proteins, where new protocols were proposed to manufacture antivenoms containing purified antibody instead of whole serum. Despite obtaining significant improvements in quality, adverse events were still prevalent leading to the conclusion that whole IgG was a contributory factor (Squaiella-Baptistao et al. 2018). This promoted the introduction of papain and pepsin digestions to cleave-off the fragment crystallisable (Fc) region from whole IgG to produce monomeric and dimeric antigen-binding fragments referred to as Fab and $F(ab')_2$, respectively. In the last two decades, several chromatographic techniques were introduced to capture specific antibodies and remove impurities, including the cleaved Fc fragment (Gutierrez et al. 2011).

1.3.2 Current antivenom formats

There are three different antivenom formats at present, based on their active substance (Figure 1.11): intact IgG, monovalent antigen-binding fragment (Fab), and divalent antigen-binding fragment $F(ab')_2$. Most current antivenoms are horse derived (Laustsen et al. 2018), other larger farm animals such as sheep (Cresswell et al. 2005), and donkeys (Gutiérrez et al. 2007) are also used. Antivenom manufacturers use significantly different methods, but fundamental steps such as precipitation by ammonium (or sodium) sulphate/ caprylic acid and pepsin/papain digestions are universally used.

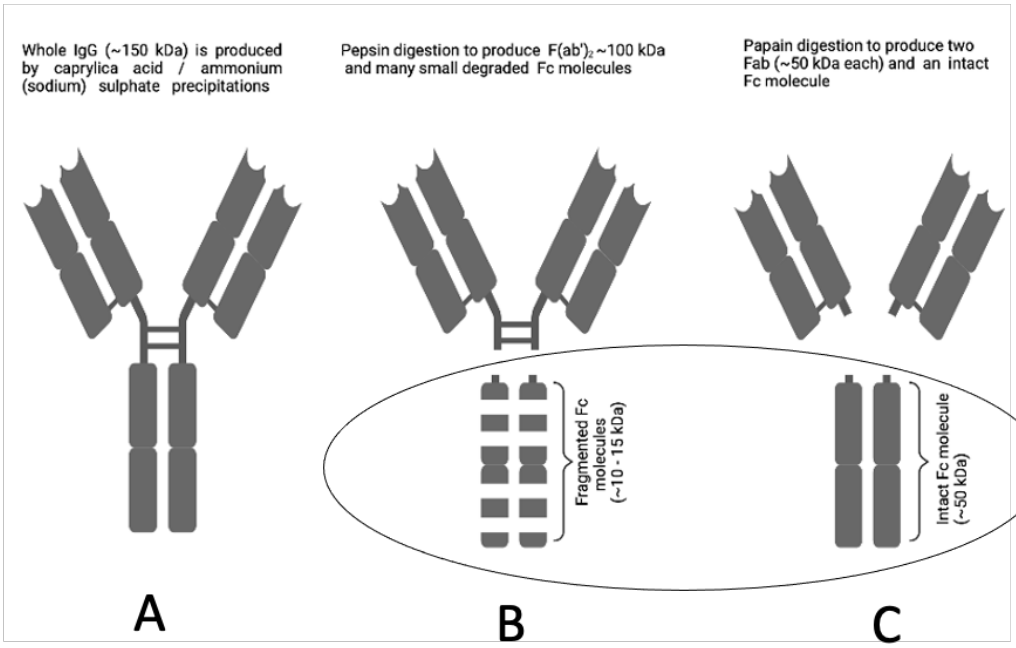

Figure 1.11 Schematic represent the three different antivenom formats.

These are the currently available AVs formats are: whole IgG (A), F(ab')$_2$ (B) and Fab (C). The Fc molecule (encircled) is cleaved by pepsin (B) and papain (C) and is necessarily eliminated from the product in subsequent purification steps (e.g., chromatography). Abbreviations: IgG, immunoglobulin G; kDa, kilodalton; Fab monovalent antigen-binding fragments; F(ab')$_2$, divalent antigen-binding fragments; Fc, Fragment Crystallisable.

Adapted from (Mender et al. 2021).

1.3.2.1 Whole IgG antivenom

Some IgG-based antivenoms have excellent efficacy and safety profiles and are commercially globally available (Otero et al. 2006; Abubakar et al. 2010a; Guidolin et al. 2016; Laustsen et al. 2018). Ammonium sulphate and caprylic acid precipitations are currently the processes of choice used to purify IgG (Otero et al. 1999; Otero-Patiño et al. 2012). The precipitating mechanisms differ significantly but the principles of fractionation to eliminate non-IgG proteins remains similar.

1.3.2.1.1 Ammonium sulphate

The mechanism by which ammonium sulphate ($(NH_4)_2SO_4$) separates proteins depends on altering ionic strength where, at increased salt concentration, the protein solubility is usually decreases leading to precipitation, a process termed as 'salting-out' (Duong-Ly and Gabelli 2014). This will precipitate proteins, such as γ-globulins, that aggregate easily, leaving other

plasma/serum proteins, predominantly albumin, in solution (Duong-Ly and Gabelli 2014). Its main drawback is that contaminants can precipitate with proteins of interest, reflected by the higher occurrence of adverse reactions induced by antivenoms prepared in this way (Otero et al. 1999; Ryan et al. 2016).

1.3.2.1.2 Caprylic acid (octanoic acid)

Caprylic acid precipitates non-IgG proteins including albumin, leaving IgG in solution. This IgG fractionation mechanism shows negligible detection of contaminants and, as such, is reflected by the lower incidence of adverse reactions (Abubakar et al. 2010a; Otero-Patiño et al. 2012; Guidolin et al. 2016). Nonetheless, the precise mechanism involved in this separation remains unclear. However, it was suggested that caprylic acid can directly bind and destabilise the three-dimensional structure of monomeric and multimeric protein molecules, which is a pH and temperature dependent phenomenon (Morais and Massaldi 2012; Nudel et al. 2012). The precipitation equilibrium is thermodynamically controlled, and protein partition relies on the hydrophobicity level. At lower pH the hydrophobicity of the octyl moiety dominates whereby the non-immunoglobulin molecules such as nucleic acids and host cell proteins (HCPs) precipitate whilst IgG, which has sufficient charge to overcome the hydrophobicity, remain in solution (Nudel et al. 2012). In addition to offering higher purity, caprylic acid is considered to be a viral inactivation step, by virtue of its ability to disrupt the integrity of enveloped viruses, despite no evidence of viral transmission associated with antivenom treatment (Burnouf et al. 2004).

1.3.2.2 Monovalent antigen-binding fragment; Fab- based antivenom

A small number of Fab-based antivenom formulations are available, including ViperaTAb®, CroFab™ and DigiFab™ (Cresswell et al. 2005; Casewell et al. 2014a). These commercially available antivenoms are made by papain digestion of sheep IgG, that is primarily purified by $(NH_4)_2SO_4$ fractionation (Smith et al. 1992; Cresswell et al. 2005). Papain cleaves IgG in the region that is on the amino-terminal side of the disulphide bond (Figure 1.12), generating two separate Fab fragments and an intact Fc molecule (Janeway et al. 2001; Cresswell et al. 2005). Papain is a thiol protease that is activated

by the presence of reducing agents such as L-cysteine, dithiothreitol (DTT) or mercaptoethanol (Goding 1996), L-cysteine being used more frequently in biopharmaceuticals (Cresswell et al. 2005; Al-Abdulla et al. 2014). Digestion is terminated by addition of iodoacetamide (Cresswell et al. 2005; Al-Abdulla et al. 2014), which irreversibly alkylates the SH groups on the papain active site (Goding 1996). Efficient cleavage of IgG is controlled by reaction time, temperature and concentration of papain and L-cysteine (Cresswell et al. 2005). The product is purified further by affinity chromatography, where antigen-specific antibodies are collected and formulated (Cresswell et al. 2005; Casewell et al. 2014a).

1.3.2.3 Divalent antigen-binding fragment: F(ab')$_2$-based antivenom

The majority of current commercial antivenoms are F(ab')$_2$ -based formulations (Pepin-Covatta et al. 1997; Bush et al. 2015; Kurtovic et al. 2016; Patra et al. 2018). The pepsin digestion method was first introduced by Pope in the late 1930s (Pope 1939a,b). Pepsin cleaves IgG, at an acidic pH (Gutierrez et al. 2011), at the carboxylic-side of the disulphide bond to generate 2-covalently linked divalent molecules termed as F(ab')$_2$, with preserved antigenic binding activity (Janeway et al. 2001; Boushaba et al. 2003). The digestion process is narrowly controlled by conditions including pepsin concentration, reaction time, pH, and temperature (Morais and Massaldi 2005; Nudel et al. 2012; Kinman and Pompano 2019). The pepsin-cleaved Fc region (Figure 1.12) is degraded into lower molecular weight (LMW) molecules that are removed on subsequent steps by techniques such as chromatography methods or $(NH_4)_2SO_4$ precipitation (Gutierrez et al. 2011). The F(ab')$_2$ containing product is then collected and formulated. It is suggested that the function of pepsin is to cleave selectively at amino acids L234-L235, within the residues responsible for FcγRs recognition (Brezski and Jordan 2010).

1.3.3 Neutralisation by antivenoms

Mammalian IgG (Figure 1.12) consists of two Fab components that are merged together on the Fc moiety by disulphide bonds to form a "Y" shape, molecular weight (MW) approximately 150 kDa (Janeway et al. 2001). The Fab arm has MW 50 kDa and is thought to contain the active antibody site, whereas the role in antivenoms of the Fc moiety, also MW 50 kDa, is unknown.

This might justify the exclusion of Fc fragments from most current commercial antivenom products (Alirol et al. 2015; Potet et al. 2019).

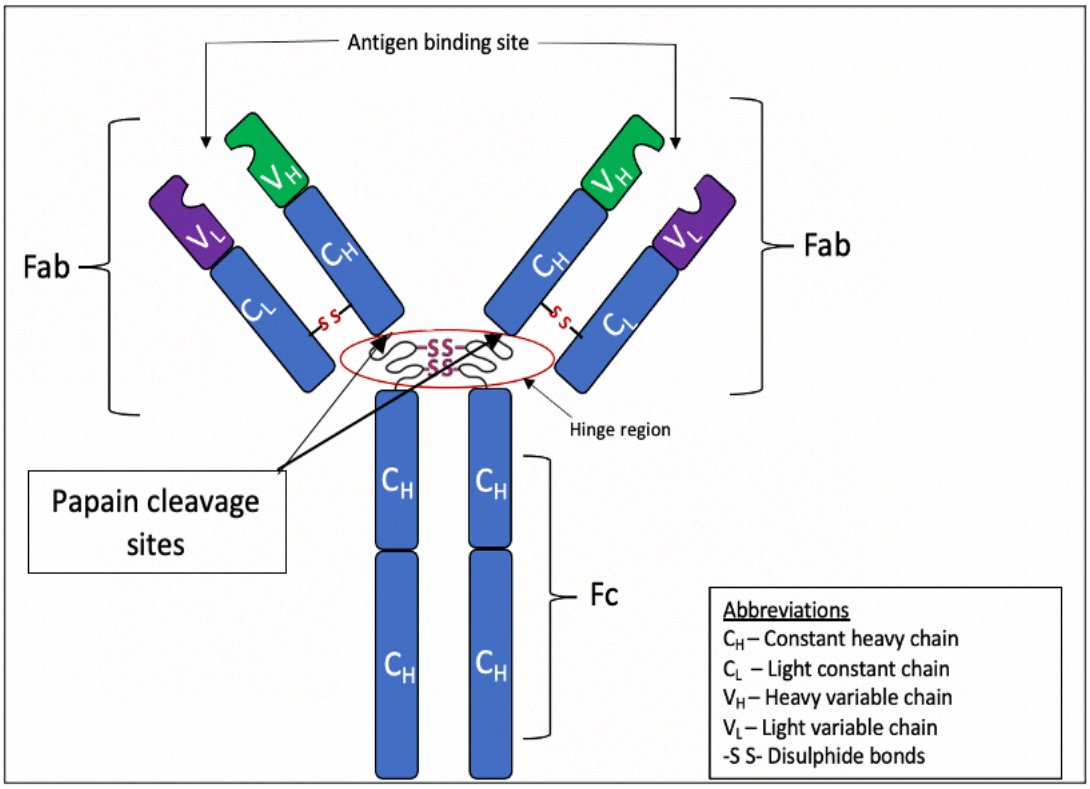

Figure 1.12 Schematic representing basic structure of immunoglobulin G.

Created with BioRender.com.

Most of the current data on the pharmacokinetics of antivenoms were derived from animal studies (Gutiérrez et al. 2003; Rojas et al. 2013), although limited data from clinical studies exist (Gutiérrez et al. 2003). These provide no clear evidence of which antivenom format has the best neutralising efficacy (Laustsen et al. 2018). Indeed, all forms of IgG and its fragments have been found to be effective at neutralising venom toxins, but with highly variable pharmacokinetic and pharmacodynamic properties (Gutiérrez et al. 2003). The success of antivenom is dependent on severity of envenoming, time lapse to administration, efficacy and dose (Silva and Isbister 2020).

1.3.4 Pharmacokinetics (PK) of antivenoms

The Pharmacokinetics (PK) of antivenoms is largely governed by their molecular size, which ranges from whole IgG at 150 kDa to Fab at 50 kDa (Gutiérrez et al. 2003). On the other hand, snake venoms have a larger range

of molecular size (Zupunski et al. 2003; Kang et al. 2011; Sunagar et al. 2013), which together with charge, hydrophobicity and cellular permeability, governs their absorption and distribution to target tissues (Paniagua et al. 2015). Lower molecular weight venom toxins including 3FTXs and KTTs readily distribute to their target sites, despite a lack of evidence for the presence of neurotoxin in the vascular compartment (Baldé et al. 2013). In contrast, venom toxins with a higher molecular weight (HMW), such as SVMPs and SVSPs, are characterised by biphasic pharmacokinetic profiles involved in initial rapid absorption followed by a slower absorption from injection site (Paniagua et al. 2015). Nevertheless, snake venoms are usually delivered subcutaneously and, to a lesser extent, intramuscularly whereas antivenoms are usually administered intravenously (I.V.) conferring an advantage over competition at target sites (Paniagua et al. 2015; Silva and Isbister 2020). Effective neutralisation of irreversible tissue damage is achieved if antivenoms are promptly administered into the circulating compartment at the same time as the venom toxins are absorbed into it. Unfortunately, there is almost always a delay from bite to antivenom administration, and additionally, LMW venom toxins may diffuse faster than antibody fragments to their targets (Silva and Isbister 2020).

Table 1.2 Range of Pharmacokinetic properties for the three antivenom formats within different study models.

Format	Study subject	Vd (ml/kg)	$t_{1/2-\alpha}$ (h)	$t_{1/2-\beta}$ (h)	CL (ml/h/kg)
Whole IgG	Human	58-118	0.22-5.62	34-72	1.1-1.6
	Rabbit	160-164	0.42-0.56*	40.62-44.7	4.86-6.06
F(ab')2	Human	177-387	0.2-2.31	79-132	0.91-2.54
	Rabbit	207-225	0.17-0.27	32.91-34.77	4.86-5.94
Fab	Human	110	2.7	18	No data available
	Rabbit	228-32	0.68-0.72	7.7-8.3	52.5-53.5

*In the rabbit model, both IgG and $F(ab')_2$ antivenoms also have an intermediate phase ($t_{1/2-\alpha}$) of 5.98 ± 0.67 and 2.33 ± 0.45 hours, respectively.

Abbreviations: Vd: volume of distribution; $t_{1/2-\alpha}$: distribution half-time; $t_{1/2-\beta}$: elimination half-life, CL: clearance. Adapted from (Gutiérrez et al. 2003).

As shown in Table 1.2, the volume of distribution (Vd) is largely dependent on MW of antivenoms and, consequently, Fab and $F(ab')_2$ have a larger Vd than whole IgG antivenom (Gutiérrez et al. 2003). Vd is a measure of an agent's tendency to either remain in plasma or to access other compartments. In fact, IgG and $F(ab')_2$ have a similar distribution time and concentration ratio (Boyer et al. 2001; Seifert and Boyer 2001). Given its larger molecular weight, IgG has poor absorption and distribution ratio (Silva and Isbister 2020), which may limit neutralisation of venom toxins already bound to targets on target tissues. It is assumed that $F(ab')_2$ has intermediate PK (Gutiérrez et al. 2003), but intravenous injection of IgG and $F(ab')_2$ showed a biphasic decline in concentration, described as a rapid initial distribution phase (i.e. sum of distribution and elimination process) followed by a slower elimination phase (Gutiérrez et al. 2003; Silva and Isbister 2020). During the early distribution phase, IgG and $F(ab')_2$, antivenoms are rapidly absorbed into target tissues and simultaneously eliminated, perhaps via phagocytosis by the mononuclear phagocyte system, but once distribution equilibrium is reached, elimination becomes the only process causing concentration to decline (Gutiérrez et al. 2003).

Conversely, Fab fragments at 50 kDa, have a higher Vd and concentration ratio making it readily diffusible into extravascular compartments, conferring rapid restoration of damaged tissues (Seifert and Boyer 2001; Gutiérrez et al. 2003). This may enable Fab antivenoms to protect against toxicity caused by smaller neurotoxins. Fab is rapidly eliminated via the renal glomerulus, unlike larger fragments, which remain within the intravascular compartment for longer (Gutiérrez et al. 2003). A clinical study demonstrated that Fab was eliminated 5-7 times faster than $F(ab')_2$ antivenom (Meyer et al. 1997). The pharmacokinetic implications of a short elimination half-life is that recurrence of envenoming is commonplace, and requires repeated antivenom administration (Seifert and Boyer 2001). Furthermore, rapid glomerular elimination of Fab fragments may cause renal impairment, which would, in turn, affect elimination of Fab (Gutiérrez et al. 2003). See Table 1.3.

1.3.5 Pharmacodynamics (PD) of antivenoms

Pharmacodynamics (PD) is the triad interaction between the human/animal body, the toxin and the antivenom. The ability of antivenom to neutralise a given venom effectively is determined by its capacity to provide sufficient specific antibody molecules to neutralise venom toxins absorbed. The polyclonal nature of antivenoms offers the ability to recognise and neutralise multiple venom toxins simultaneously. Theoretically, IgG and $F(ab')_2$ based antivenoms may have higher avidity than Fab fragments, which only contain one antigen-binding fragment. Digestion by proteolytic enzymes, especially pepsin may affect avidity (Morais and Massaldi 2005), but there is no evidence to suggest which antivenom type contains antibodies with the highest neutralising capacity (Laustsen et al. 2018). Several studies have demonstrated that IgG antivenom has a comparable efficacy profile to those containing Fab and $F(ab')_2$ despite the assumption otherwise (Leon et al. 1999; Leon et al. 2001; Otero-Patiño et al. 2012). A clinical study comparing the efficacy of Fab and $F(ab')_2$ antivenoms found that 4 times the dose of Fab was required to induce comparable efficacy to that of $F(ab')_2$ (Meyer et al. 1997; Boyer et al. 2001).

The exact mechanism by which different antivenom formats neutralise various toxins is not fully understood. However, there is a consensus of opinion that they occupy and stereotactically block toxin active sites, or cause conformational changes of enzymatic toxins, making toxin sites inaccessible (Gutiérrez et al. 2003; Laustsen et al. 2018; Nikapitiya and Maduwage 2018). Additionally, antivenoms trap venoms in the central compartment, preventing access to pharmacological sites and preventing toxin dissociation (Laustsen et al. 2018). Being multivalent, IgG and $F(ab')_2$ are capable of forming antibody-venom complexes which may be eliminated by phagocytosis, diminishing the overall presence of toxins (Gutiérrez et al. 2003; Silva and Isbister 2020).

Table 1.3 Advantages and disadvantages of the different types of antivenom

Format	Description	Advantage	Disadvantage
Fab	Monovalent antigen fragment produced by the proteolytic enzyme called papain. Digestion is normally conducted at pH 6 to pH 7.5, and in the presence of L-cysteine.	Has a rapid tissue penetration, larger volume of distribution and decreased risk of immunocomplex formation and complement-mediated anaphylactic reactions.	lower bioavailability, excretion fate is unknown. It is known to inflict renal toxicity. Requires long process involving in affinity purification which adds production cost. Still causes adverse reactions. Lowest yield of final product (i.e., Fab).
$F(ab')_2$	Most commonly manufactured antivenom, consisting of bivalent antigen fragment produced by pepsin digestion of IgG at acidic pH.	It is relatively safer than IgG formulation because over 30% of unwanted proteins have been removed at digestion step. It acts as intermediate product that has elimination half-life ($t_{1/2}$) longer than Fab.	Long process that very often involves a chromatography method for polishing and removal of Fc fragments and pepsin residuals post- digestion step, which will add production cost. Lower yield of final product.
Whole IgG	Intact IgG produced by ammonium (or sodium) sulphate or caprylic acid.	Easy method with great recovery (i.e., highest yield of final product). Cheaper antivenom product	Involves in injecting higher quantity of exogenous proteins compared to Fab and $F(ab')_2$ which may reflect the prevalence of anaphylactic reaction incidence may be more common.

1.3.6 Future direction of antivenoms

Antivenom, in its current format, is the only approved specific treatment for SBE (Silva and Isbister 2020). Adverse effects, especially those related to excess foreign protein, acute anaphylaxis and lack of a universal antivenom led to efforts by the scientific community to derive more advanced therapies. Employing the latest biotechnology, monoclonal antibody (mAb) based antivenoms against several venom toxin types have been developed (Laustsen et al. 2018; Pucca et al. 2019). Preclinical studies demonstrated that these novel antivenoms were effective at neutralising toxins and preventing lethality in mice (Laustsen et al. 2018; Pucca et al. 2019). Phage display techniques were recruited for developing mAb fragments, with specificity for more than one toxin epitope curtailing the need for numerous mAbs or oligoclonal antivenom (Ledsgaard et al. 2018). It was envisaged that the development of a mAb, with multiple cross-reactivity, will pave the way to the production of mAb-based antivenoms that can be used against venoms from multiple species. An equine “experimental antivenom” was developed against biologically active recombinant consensus α-neurotoxin, the whole

IgG-antivenom was preclinically effective at neutralisation of the neurotoxic effects of biogeographically diverse elapid snakes (De la Rosa et al. 2019). Experimental antivenom has been raised in rabbits against recombinant enzymatic venom toxins, including SVMPs, SVSPs and svPLA$_2$s obtained from *Bothrops ammodytoides*. The anti-recombinant venom proteins successfully neutralised the lethal effect of *B. ammodytoides* in mice (Clement et al. 2019). Both approaches support the proof of concept for the use of recombinant enzymatic and/or non-enzymatic toxins to produce antibodies with superior titration, affinity and avidity, and thus herald the next generation antivenoms. However, the complexity and variability of snake toxins imposes a major hurdle for the translation of these strategies into a clinical setting. Therefore, at present, mAb based snake antivenoms have not even reached the clinical study stage, let alone as therapeutics.

1.3.7 Immunisation

In the 1890s, Calmette developed an immunisation protocol for horses using *N. naja* venom which was quickly implemented globally by other institutions (Pucca et al. 2019). With modifications of immunisation protocols, there was a simultaneous improvement of quality and purification methods. The importance of potentiating immune response of host animals to generate larger volumes of potent antisera was promptly recognised. In 1924, the South African Institute of Medical Research (SAIMR) added a tapioca substance to a pool of venom toxins as an “adjuvant” to enhance the immune response of the donor horse (Squaiella-Baptistao et al. 2018). By 1926, aluminium was the first commercially used adjuvant to boost the immune response of diphtheria vaccine (Egli et al. 2014). Currently, Freund’s complete and incomplete adjuvants are commonly used for initial immunisation, and subsequently, with aluminium salts, bentonite or just emulsified in saline (Gutierrez et al. 2011). Different adjuvants enhance the immune response by different mechanisms, but slow release and sequestration of antigens remains an important feature (Awate et al. 2013; Egli et al. 2014). The ideal adjuvant must be safe, cheap and capable of slowly releasing antigens from sites of injection, to stimulate an effective immune response (León et al. 2011).

The diversity of snake venoms makes optimisation of the immunisation protocol key to producing potent antibodies, without compromising the donor animals' welfare. The best protocol is to inject, slowly and repeatedly, small volumes of native, not detoxified, venoms, at several anatomical sites (Gutierrez et al. 2011). The subcutaneous route is most common, but intradermal, intramuscular routes as well as a liposomal delivery are also used to immunise animals for the production of antivenom (León et al. 2011). Venoms used for immunisation should be taken from multiple individuals of snake species relevant to the geographical region in which the antivenom is to be used (World Health Organization 2016). The design of an immunisation protocol requires careful evaluation of snake distribution and toxicity, epidemiological and clinical manifestations. A potent antivenom, designed based on this information, will be effective at neutralising the most clinically important venom toxins. Monospecific antivenoms are appropriate where there is only one species of venomous snake in a region, or if bites from one species are dominant in cases such as *E. ocellatus* bites in West Africa (Visser et al. 2008), particularly Nigeria (Habib et al. 2008). On the other hand, polyspecific antivenoms are preferable in cases where there are multiple clinically relevant species such as in SSA (World Health Organization 2016; Tasoulis and Isbister 2017).

1.3.8 Animals used for production of antivenom

Sheep were the first animals used to produce immunotherapeutic sera against diphtheria (Landon and Smith 2003). The horse became the preferred source for production of antisera and was used for treating diphtheria, tuberculosis (TB) and pneumonia (Walther et al. 2015). Although sheep (Al-Abdulla et al. 2013; Casewell et al. 2014a) and donkey (Gutiérrez et al. 2007) are still used by some manufacturers, horses are most commonly used for manufacturing commercial antivenoms (Gutierrez et al. 2011). Nevertheless, chicken, rabbit, camels and goat are occasionally used (Sells 2003).

Horses are expensive to maintain and, being regarded as companion animals, may not be permitted to be used for this purpose in some countries such as the UK. Avian and Camelid antibodies have been considered as alternatives for the conventional antivenom production due to their economic, ethical and

stability advantages (Gutierrez et al. 2011). Promising efficacy results of IgY-based antivenoms have been reported in a mouse model (Leiva et al. 2019). Experimental Camelid anti *E. ocellatus* whole IgG-based antivenom demonstrated a comparable efficacy to EchiTabG® (Cook et al. 2010), a highly effective sheep-derived antivenom product currently marketed in Nigeria (Abubakar et al. 2010a).

1.3.8.1 Overview of equine immunoglobulins (Igs)

Since the beginning of the immunotherapy era in the 1890s (Squaiella-Baptistao et al. 2018), horse plasma was the mainstay of antivenom preparations, globally. The large plasma volume and versatility of equine IgG made horses the favoured source for antivenom manufacturers (Gutierrez et al. 2011). Equine IgG is composed of five antigenically different subclasses known as IgGa, IgGb, IgGc, and IgG(T), in addition to a fifth subclass known as IgGB (Klinman et al. 1965; Widders et al. 1986). Employing genomic techniques, a recent study has reported seven distinct IgG subclasses designated as IgG_1- IgG_7 (Wagner et al. 2004). Although IgGb represents the highest concentration in the plasma of a healthy adult horse (Sheoran and Holmes 1996), the IgG(T) subclass swiftly becomes dominant in response to infections (McGuire et al. 1972; Widders et al. 1986). IgG(T) is the foremost IgG subclass responsible for neutralisation activities of equine antibodies (Fernandes et al. 1991).

1.3.9 Future direction of immunisations

The current immunisation protocol is based on injecting whole venom proteins with varying degrees of toxicity and immunogenicity (León et al. 2011). The immunogenicity of venom toxins will determine the immune response in the donor animal, and hence the antibody produced. Moreover, some pertinent snake venom toxins are weakly immunogenic because they are either expressed at lower concentration or contain few immunogenic epitopes (León et al. 2011). The α-neurotoxin, an abundant venom component found in cobras (Petras et al. 2011), and mambas (Ainsworth et al. 2018), is notorious for its profoundly lethal activity. Despite being an abundant and highly toxic venom component, these neurotoxins are characterised by significantly weak immunogenicity (León et al. 2011), thus producing antivenoms with low titres.

Sequence analysis has revealed that this tiny molecule (~6-7 kDa), encompasses largely nonimmunogenic residues (de la Rosa et al. 2018). A recombinant consensus short-chain α-neurotoxin (ScNtx) representing the most immunogenic residues within the molecule was identified and reconstructed. The horses produced a potent antibody, following a multi-site immunisation with the biologically active recombinant ScNtx adjuvanted with incomplete Freund's adjuvant and alum initially, followed by no adjuvant (De la Rosa et al. 2019). Likewise, immunising rabbits with reconstructed immunogenic recombinant enzymes (SVMPs, SVSPs and svPLA$_2$) elicited an immune response resulting in the production of potent antisera (Clement et al. 2019). Evidently, this will encourage the search for better immunisation strategies, where potent antibodies are generated without inducing discomfort to host animals. Identifying the most medically important venom toxins for immunisation protocols may pave the road for developing the next generation of antivenom.

1.3.10 Efficacy and effectiveness of antivenoms

Efficacy and effectiveness are two separate entities used to describe the safety of antivenom and its capability to treat the harmful effects of snake venoms successfully. Whilst efficacy is defined as the performance of antivenom under ideal and controlled circumstances, effectiveness refers to its response in the real-world (Isbister 2010). To maintain a high standard of efficacy, effectiveness and safety, numerous preclinical assessments (Gutierrez et al. 2017b), rigorous clinical trials (Chippaux et al. 2007), quality and regulatory control standards should be performed on newly developed antivenoms. Nevertheless, the efficacy and effectiveness of most antivenoms has been poorly studied. In clinical trials, antivenom efficacy is usually determined either by using placebo (if only justified and withholding/delaying treatment pose a negligible risk to participants), or by comparison with gold standard drug product (Williams et al. 2018). Nevertheless, it is unethical to withhold life-saving treatment and choice of the gold standard is always difficult (Chippaux et al. 2007). This dilemma is not exclusive to antivenoms - other well-established medicinal drugs such as insulin and penicillin entered the market without placebo-controlled clinical trials (Williams et al. 2018).

The critical assessments may be circumvented by some manufacturers due to the cost implications of validation achieved from *in vitro* and animal studies (Warrell 2008). Other manufacturers intentionally choose imprecise procedures so that they proceed with minimum requirements; for example, performance of low-quality clinical trials such as non-randomised, one-armed and observational cohort study (Potet et al. 2019). This is true especially for manufacturers targeting the SSA market (Brown 2012).

Despite the recommendation of the African Society of Venomology (ASV) for manufacturers to include meticulous preclinical tests and clinical trials (Chippaux et al. 2010), some of the antivenoms marketed in SSA are inherently ineffective at treating SBE by target snake venoms (Visser et al. 2008; Warrell 2008; Brown 2012). Influenced by corrupt policy makers and poor resources, manufacturers of lower quality and adulterated antivenoms continuously target SSA as a potential market. Nonetheless, despite its small proportion, ~3% of all antivenom stocks (Brown 2012) have demonstrated a proven effectiveness for treating SBEs in SSA (Potet et al. 2019).

To prevent undesired clinical outcomes, replacement of existing antivenom with a new one, must follow critical assessments, such as comparison with the old product. A cheaper antivenom (Asna Antivenom-C; ASNA-C) was introduced as alternative to replace the well-renowned, but expensive Fav-Afrique™ (Alirol et al. 2010). Fav-Afrique™ was a polyspecific antivenom against ten snake species (*B. arietans, B. gabonica, D. jamesoni, D. polylepis, D. viridis, E. leucogaster, E. ocellatus, N. haje, N. melanoleuca* and *N. nigricollis*) native to the SSA region. Despite the manufacturer (Bharat Serum and Vaccine Ltd, India) having claimed it to be effective against *E. ocellatus* envenoming, clinical studies demonstrated that the ASNA-C antivenom offered limited benefits (Visser et al. 2008). In fact, the mortality rate was significantly higher and restoration of blood coagulation required twice the dose in patients who had received ASNA-C, compared to those treated with Fav-Afrique™ (Visser et al. 2008). Today, there are many antivenoms with a target specificity similar to that of Fav-Afrique; for example, Inoserp Pan-Africa and Antivipmyn-Africa, but there is little information on their safety and efficacy (Alirol et al. 2015).

1.3.11 Safety of antivenoms: Side effects associated with antivenoms

Antivenoms are heterologous antibodies produced in animals which have devolved from crude serum, which caused significant adverse events, to highly purified antibodies aided by the latest biotechnology. Despite this, side-effects still occur to all antivenoms, varying from 3% in high quality products to 88% in poorly prepared antivenoms (Leon et al. 2013; Williams et al. 2018). The severity of these events also varies from benign early allergic reactions to rare, life-threatening anaphylactic shock (Williams et al. 2018). Side effects are not exclusive to antivenoms, because no medicinal drug is entirely free from side effects (Alshammari 2016). However, adverse reactions can be minimised with improved manufacturing processes and appropriate quality control measures (Gutiérrez et al. 2003; de Silva et al. 2011).

Despite the current advancement in biomedical research, the precise mechanism triggering adverse events following intravenous administrations of antivenoms is not fully understood. Poorly prepared impure and/or ineffective antivenom, the venom itself and patient's susceptibility to animal serum or plasma are strongly associated with antivenom-induced reactions (Isbister et al. 2008; Stone et al. 2013). It was assumed that the IgG fragments $F(ab')_2$ and Fab were safer and more effective drugs, thus the therapeutic use of intact-IgG has fallen out of favour (Leon et al. 2013). Antivenom-related side effects are broadly classified as early adverse reactions (EARs), anaphylactic reactions, pyrogenic reactions, late adverse reactions (LARs) or serum sickness (Deshmukh et al. 2014).

1.3.11.1 Early Adverse Reaction (EAR)

EARs, usually occur within 2 hours of administrations of antivenom (Chippaux et al. 2015b; de Silva et al. 2016), but may take slightly longer in some patients (Leon et al. 2013). Common symptoms of acute adverse reactions are generally benign such as urticaria, nausea, vomiting, headache and fever, but systemic anaphylaxis may also occur (Malasit et al. 1986; Isbister et al. 2008). Early reactions are very common and often clinicians need to deal with them as much as dealing with envenoming itself (Williams et al. 2018). However, the severity depends on the properties of triggering antigens, most importantly molecular size, but individual predisposition also plays a vital role in the

reaction cascade (Chippaux et al. 2015b). The mechanism of reaction to antivenom is poorly defined, but it is suggested that EARs are most likely to be due to a combination of type I hypersensitivity, a magnified immune response due to allergens, complement activation, aggregates of immunoglobulin (Ig) and its fragmented molecules (Malasit et al. 1986; Lalloo and Theakston 2003; Chippaux et al. 2015b; de Silva et al. 2016; Morais 2018). Depending on the underlying triggering mechanism, EARs are classified as anaphylactic (IgE- and non-IgE mediated) or pyrogenic reactions (Leon et al. 2013).

1.3.11.1.1 IgE-mediated anaphylactic reactions

These occur rarely, but are the most severe and life-threatening reactions, which occur most commonly in known atopic individuals, previously exposed to antivenom products (Morais 2018). However, the fact that it may also occur in individuals that have never been exposed to antivenoms before, requires further study (Lalloo and Theakston 2003; Morais 2018). IgE-mediated anaphylactic reactions are initiated when the allergic-specific IgE is crosslinked with mast cells, which, when activated by a subsequent episode, release potent proinflammatory mediators, which leads to anaphylactic shock (Stone et al. 2013). Anaphylaxis is characterised by oedema, cyanosis, hypotension, and vasodilation (Isbister et al. 2008).

1.3.11.1.2 Non-IgE-mediated anaphylactic reactions

This type of EARs constitutes the vast majority of acute responses to intravenous administration in individuals with no previous exposure to antivenom (Leon et al. 2013). Clinical signs include nausea, vomiting, vasodilation, rash and pain (Morais 2018). The mechanism triggering the non-IgE mediated reactions is not clearly defined.

It was assumed that the Fc fragment in whole IgG antivenoms activated the complement cascade in the classical manner (Leon et al. 2013). Activation is initiated by binding of Fc fragment to complement protein C1q (key subcomponent of complement classical pathway responsible for recognition and binding immune complex), leading to the subsequent generation of anaphylatoxins (Squaiella-Baptistao et al. 2014). Interestingly, this study also showed that antivenoms lacking the Fc domain such as $F(ab')_2$ also activate

the complement system in the same manner as does whole IgG. It was suggested that the hinge portion of the IgG, also preserved in $F(ab')_2$, is responsible for initiating the complement activation (Squaiella-Baptistao et al. 2014). Furthermore, administration of antivenom did not affect the concentration of C3, C4 and C5 (precursors for the potent anaphylatoxins known as C3a, C4a and C5a) in patients who experienced severe anaphylactic reactions (Stone et al. 2013). Despite experiencing significant acute anaphylaxis, absence of anaphylatoxins may suggest that aggregated Ig and macromolecular complexes interact with mast cells eliciting the degranulation process (Stone et al. 2013). Thus, the presence of aggregate proteins in antivenoms initiates the antivenom-induced anaphylactic reactions possibly by activating the complement system (Leon et al. 2013).

There is still a widespread belief that $F(ab')_2$ has a better safety profile compared to IgG antivenoms, mainly due to lack of the Fc portion, which is known to be involved in the complement activation via the classical pathways (Leon et al. 2013). However, preclinical (Squaiella-Baptistao et al. 2014) and substantial clinical studies, (Leon et al. 2013), demonstrated that $F(ab')_2$ also induces comparable early reactions. For instance, a clinical study has reported 23% incidence of acute anaphylactic reaction following administrations of Australian $F(ab')_2$ antivenoms (Ryan et al. 2016). Most importantly, in a randomised-clinical trial comparing the safety and efficacy of whole IgG vs $F(ab')_2$, the incidence of EARs was similar in both group of patients (Otero-Patino et al. 1998). Furthermore, a clinical trial reported 7.6% incidence of anaphylactic reactions with 3% death due to severe reactions in patients treated with ASNA-C antivenom, although administrations of premedication may possibly have skewed the outcome (Visser et al. 2008). Interestingly, patients treated with affinity purified CroFab® (sheep-derived product) that has had its Fc fragment removed chromatographically, induce acute hypersensitivity at a rate of 5.4% (Cannon et al. 2008). The same antivenom (CroFab®) caused serum sickness in 14.3% of treated patients, although the outcome was skewed by a single lot of antivenom (Dart and McNally 2001; Ruha et al. 2002). The implication of Fab and $F(ab')_2$ antivenoms in EARs, although occurring less commonly, may suggest that the non-IgE mediated

anaphylactic reactions are beyond the Fc region, and thus further study is required.

1.3.11.2 Pyrogenic reactions

Pyrogenic substances such as microbial contaminants can be introduced in poorly prepared biologically derived products, mostly during the manufacturing process. Pyrogenic contaminants elicit pyrogenic reactions occurring during the first hour of infusion (de Silva et al. 2016). Pyrogenic reactions are characterised by shivering, sweating, pyrexia, fever, myalgia, tachycardia, hypotension, and vasodilation (Leon et al. 2013; Stone et al. 2013). Bacterial lipopolysaccharides (LPS), also known as endotoxins, are the most common contaminant present in biologically derived pharmaceutical products such as antivenoms (Leon et al. 2013).

Whilst an adequate immune response is required to eradicate pathogenic invasion, if the LPS level exceeds the body's elimination capacity it may lead to aggregated inflammation that, in turn, may result in systemic inflammatory response syndrome (SIRS). SIRS is an over-reaction of the inflammatory response, characterised by hypothermia, tachycardia and tachypnoea, similar to symptoms of EARs (Stone et al. 2013). Preventative control measurements include strict asepsis at all stages of manufacture and handling (including administration), testing final product for endotoxins using either the rabbit pyrogenic test and/or the Limulus Amebocyte Lysate (LAL) test, recommended by WHO as a standard quality release test (World Health Organization 2016).

1.3.11.3 Serum sickness (Delayed adverse reaction; DAR)

Serum sickness is classified as a type III hypersensitivity, where delayed IgG-mediated reactions appear 5-20 days after antivenom treatment (Leon et al. 2013; Ryan et al. 2016). Unlike anaphylaxis, it is not life-threatening but has a higher incidence rate (56%), of clinical signs, than anaphylaxis (Ryan et al. 2015). The incidence, characteristics and treatment of DARs are poorly characterised, mostly because affected patients do not return to medical centres after discharge (Ryan et al. 2016). These reactions are initiated when the immune system recognises the presence of heterologous proteins and responds by generating specific antibodies that react with the antivenom

'foreign proteins', resulting in the formation of a soluble antigen-antibody complex (Morais 2018). This immune complex mediates an immune response by activating the complement cascade, via the classical pathway. It causes ill-defined symptoms such as myalgia, fever, arthralgia, arthritis, urticaria and gastrointestinal disorders (Leon et al. 2013). Delayed reactions are expected to last for approximately 6 days (LoVecchio et al. 2003), although symptoms may persist for up to six weeks in some patients (Ryan et al. 2015). Most of the more serious serum sickness reactions are amenable to a week's course of corticosteroids, but in severe cases an incremental reducing dose for two or more weeks, with oral corticosteroids, is recommended (de Silva et al. 2016; Ryan et al. 2016).

A review of the literature suggested that the incidence of serum sickness varies greatly depending on the type of antivenoms, and perhaps quantity, used (Ryan et al. 2016; Potet et al. 2019). Theoretically, IgG causes more cases of serum-sickness than Fab and $F(ab')_2$ antivenoms because IgG contains highest quantity of non-specific proteins. This hypothesis was supported by experiments on mice (Leon et al. 2001). However, a randomised double-blinded clinical trial was conducted to assess the safety of EchiTAbG and EchiTAb-Plus (Abubakar et al. 2010a). EchiTAbG is a monovalent intact IgG antivenom, targeting bites by *E. ocellatus* and EchiTAb-Plus a polyvalent, also an intact IgG antivenom, is directed against *E. ocellatus*, *N. nigricollis* and *B. arietans* venoms. Both products demonstrated efficacy against envenoming by *E. ocellatus*. The authors reported incidences of serum sickness of 5.2% on patients with EchiTAbG and 10.2% those received EchiTAb-Plus (Abubakar et al. 2010a). In a clinical study, 56% of serum sickness was reported in patients treated with Crotalidae Polyvalent (ACP); an intact IgG antivenom used to treat envenoming by pit vipers (LoVecchio et al. 2003) where there was a greater occurrence of DARs at increased doses, suggesting that the incidence of serum sickness is proportional to the quantity of heterologous proteins (LoVecchio et al. 2003). In contrast, others found that the amount of antivenom is not associated with serum sickness (Ryan et al. 2016). Furthermore, the incidence of serum sickness from Fab and $F(ab)_2$-based antivenoms varies considerably depending on the type of antivenoms

and geographical location. For example, the incidence of serum sickness from Australian antivenoms [all equine $F(ab')_2$], is 29% (Ryan et al. 2016), and 16% due to CroFab® (a sheep derived Fab antivenom), although the results were skewed by the inclusion of a partially purified lot (Ruha et al. 2002). Another clinical study to elucidate efficacy and safety of Antivipmyn® Africa, a polyvalent equine $F(ab')_2$ antivenom, reported 3% of treated patients developed serum sickness (Baldé et al. 2012).

Unfortunately, there is a lack of published data reporting the incidences of DARs related to $F(ab')_2$ antivenoms in SSA, possibly influenced by the fact that follow-up by clinicians of SBE patients from rural regions is difficult because they are unable to return to medical centres after discharge.

In summary, the mechanism controlling early, and delayed adverse reactions is not well understood. Moreover, adverse reactions are generally related to heterologous proteins- even human IgG elicits complement activation (Squaiella-Baptistao et al. 2014). Furthermore, antibodies transferred from horse treatment might be included in final formulations and this might initiate immune reactions (Leon et al. 1999). Thus, whilst removal of the Fc fragment lowers the MW of the administered protein, abiding by 'good manufacturing practice' (GMP) and curtailing impurities play a critical role in improving the safety of antivenoms. Despite the lack of rigorous supporting data, administration of antihistamine, corticosteroids and adrenaline are still widely used to treat and/or reduce adverse reactions (de Silva et al. 2011; Leon et al. 2013).

1.3.12 Current methods for assessing the safety and efficacy of antivenom

Extensive biological studies are essential to characterise each batch of antivenom manufactured, including safety and efficacy, throughout its production process. *In vivo* toxicity tests of a newly developed and/or existing antivenom are the 'gold standard' potency test for antivenom safety before embarking on clinical studies. In cases where no robust and reliable clinical trial data exist, *in vivo* and/or *in vitro* studies can be used to assess the efficacy of antivenoms (Theakston and Reid 1983; Ainsworth et al. 2020).

1.3.12.1 *In vivo* tests for assessing snake venom toxicity and antivenom efficacy

1.3.12.1.1 Median lethal dose (LD_{50}) and Median effective dose (ED_{50})

Murine lethality assays are the 'gold standard' pre-clinical assays of toxicity and treatment efficacy, specifically in relation to neutralisation of venom toxicity with antivenoms (Sells 2003; Parasuraman 2011). Whilst the LD_{50} represents the quantity of venoms required to kills 50% of tested animals, ED_{50} is the quantity of antivenoms that protects 50% of the tested animals (Calvete et al. 2016; World Health Organization 2016). These tests are recommended for every new batch of antivenom prior to their therapeutic use (World Health Organization 2016). Despite physiological and anatomical differences, animal models (most commonly mouse) have been a satisfactory source for quantifying the effect of whole venom on a living system (World Health Organization 2016). The assays themselves are subject to wide variation, in both method and analysis (Gutiérrez et al. 2013), making comparison between laboratories challenging (Ainsworth et al. 2020). ED_{50} may be used to calculate a 'human equivalent dose' as a starting point for clinical trials, in addition to measurement of antivenom efficacy (Saganuwan 2016).

The standard test for LD_{50} of venoms is achieved by injecting intravenously or intramuscularly 5 to 6 mice with different venom concentrations (Theakston and Reid 1979,1983). The number of dead animals is recorded at 24 and 48 hours, respectively (Gutiérrez et al. 2013). Likewise, ED_{50} of antivenom is determined by preparing different volumes of an antivenom pre-mixed with a challenge dose (2 to 5-fold the determined LD_{50}) of relevant venom and intravenously or intraperitoneally injected into mice, and the number of surviving animals are recorded after 24 hours (Sells et al. 2001). The venoms' LD_{50} and/or antivenoms' ED_{50} and 95% confidence interval (95% CI) values are calculated using Probit (Sells et al. 1998), Spearman-Kerber or other non-parametric test analyses (Gutierrez et al. 2017b).

1.3.12.1.2 Minimum Haemorrhagic Dose (MHD)

This *in vivo* study is used to define the local haemorrhagic activities of venom toxins and the potency of antivenom to protect induced lesions, preferably in mice, but rabbits and rats may also be used (Gutierrez et al. 2017b). The

Minimum Haemorrhagic Dose (MHD) test is conducted by intradermally injecting a group of experimental animals with different test sample solutions (venom or venom-antivenom mixtures). The animals are sacrificed and dissected after two hours incubation to assess haemorrhagic lesions. MHD is the quantity of venom which induces a 10 mm haemorrhagic lesion and the antivenom neutralising efficacy is defined as the amount (in mL) required to reduce 50% of the venom activity (Gutiérrez et al. 1985).

1.3.12.1.3 Minimum Necrotising Dose (MND)

Some snakes, for instance *Naja nigricollis*, contain significant cytotoxic venom PLA_2 (Warrell et al. 1976b; Petras et al. 2011), where lethality is of less relevance. With that regard, studying the venom necrosis activity and its neutralisation by a biogeographically relevant antivenom is essential to establish its efficacy. The Minimum Necrotising Dose (MND) test is performed by injecting mice, or rats, subcutaneously, with venom to determine the lowest venom dose causing a necrotic lesion of 5 mm after 3 days (Theakston and Reid 1983; Gutierrez et al. 2005a). Similarly, the ED_{50} is expressed as the amount of antivenom; either as a volume or ratio of antivenom to venom, that results in a 50% reduction of venom toxicity (Gutierrez et al. 2005a).

1.3.12.2 *In vitro* assays for assessing toxicity and potency

It is almost universally accepted that tests using animals should implement the 3Rs (refinement, reduction and replacement of animals in research) whenever possible with *in vitro* methods (Sells 2003). At a WHO Workshop on standardisation and control of antivenoms in 2001, it was agreed that *in vivo* mouse assays inflict significant pain on the test animals, are expensive, and show little or no correlation with SBE therapy in humans (Theakston et al. 2003). The workshop highlighted the importance of devising alternative methods for replacing *in vivo* assays and assessing the antivenom efficacy at neutralising its target venoms.

Since then, several biological assays have been proposed as potential replacements for the murine assays (Nalbantsoy et al. 2012; Ratanabanangkoon et al. 2018; Stransky et al. 2018; Lopes-de-Souza et al. 2019). Furthermore, a panel of *in vivo* and *in vitro* techniques was compared to ascertain the toxic activities of *Bothrops* spp. venoms (de Souza et al. 2015).

The authors reported a correlation between the two sets of results, proposing a possible replacement of animal tests by *in vitro* assays. More recently, proteomics has been introduced into antivenomics with the overall aim of revealing toxicological profile of venoms and the ability of antivenoms to recognise key venom components. The application of antivenomics is now considered a promising alternative to *in vivo* neutralisation tests (Calvete et al. 2014). Despite such coherent efforts, *in vitro* assays have not yet been implemented universally as an accepted alternative to preclinical tests and the use of animal models is still recommended to determine the safety and efficacy of new and/or existing antivenoms (World Health Organization 2016).

To-date, there is no alternative *in vitro* assay that is independently used to assess the potency of antivenoms, and thus correlation to protective and/or therapeutic effect is required. Nevertheless, excellent reviews on the use of *in-vitro* assay are available (Gutierrez et al. 2017b; Harrison et al. 2017). Herein, this review will cover some of the biological assays that are currently under evaluation as potential *in vivo* test replacement.

1.3.12.2.1 Small-scale Affinity Chromatography (SSAC)

Small-scale Affinity Chromatography (SSAC) is an immunoassay that allows venom-antivenom binding, using a gel matrix such as cyanogen bromide (CNBr)-activated sepharose (Smith et al. 1992). In this way, antigen-specific antibodies are captured and subsequently eluted by dropping the pH (Casewell et al. 2010). The method is cheap, rapid, and provides a direct measurement of antibody binding to target venoms. Furthermore, SSAC used by MicroPharm Ltd, UK for release and stability (i.e., quality control tests) of EchiTAbG provides consistent results with good correlation to *in vivo* ED_{50} results (Casewell et al. 2010). However, non-specific binding proves to be a significant limitation for quantitatively measuring specific antibody using this method.

1.3.12.2.2 Enzyme-Linked Immunosorbent Assay (ELISA)

Theakston and colleagues have developed an Enzyme-linked Immunosorbent Assay (ELISA), initially to identify snakes responsible for envenoming patients (Theakston et al. 1977). A few years later, ELISA was introduced as a biological assay for assessing potency of antivenoms (Theakston and Reid

1979). Comparison of *in vivo* ED_{50} with that of *in vitro* ELISA demonstrated an excellent correlation between the two methods. Since then, ELISA has been developed as a standard method to determine the potency of antivenoms and has been used as a substitute for many *in vivo* ED_{50} tests (Maria et al. 2001; Rial et al. 2006; Ratanabanangkoon et al. 2017; Khaing et al. 2018). The method uses samples of known *in vivo* ED_{50} to generate a standard curve, from which sample values are estimated from the linear range within the curve (Theakston and Reid 1979). Despite promising results (Rial et al. 2006; Khaing et al. 2018), WHO still has reservations about the use of ELISA as an independent release test for potency assessment of antivenoms (World Health Organization 2016). However, there are antivenom manufacturers who use ELISA standardised to ED_{50} as a product release assay; for example, Sanofi Pasteur, France has been using ELISA as a release and stability test for ViperFav®. As for most of the current *in vitro* assays, the main limitations of the ELISA assay are that, for use as a release test, it must be validated using *in vivo* studies. Additionally, ELISA is very sensitive to experimental conditions, such as temperature, which may cause greater fluctuations in results compared to the SSAC method. However, such fluctuations would be still lower than that in *in vivo* testing.

1.3.12.2.3 Cytotoxicity assay (CTA) and immunocytotoxicity assay (ICTA)

Snake venom toxicity varies enormously from mild to extreme with different mechanisms of promoting cellular death. Such variations in venom components and their mechanism of action makes it challenging to develop a cell-based model that is universally acceptable to determine a suitable endpoint, such as half-maximal inhibitory concentration (IC_{50}). Various cell lines have been used and IC_{50} values reported for Latin American pit vipers (Oliveira et al. 2002; Lopes-de-Souza et al. 2019), North Africa and Southeast Asia vipers; for example, (Ozverel et al. 2019) and Mediterranean vipers (Nalbantsoy et al. 2012). Recently conducted studies (Stransky et al. 2018; Ozverel et al. 2019; Chong et al. 2020), compared the response of normal (Keratinocytes), immortalised (HEK293 and VERO cells) and cancerous (HeLa, MCF-7) cell lines exposed to venom treatment. These studies found that, although each cell line exhibited a distinct level of cytotoxicity, snake

venoms reduced the growth capacity of all tested cells disproportionally, albeit via various mechanisms.

The search for a cell-based assay as a promising *in vitro* method to screen antivenom potency is ongoing. Lopes-de-Souza et al. (2019) used VERO cells to show a concentration-dependent reduction in cell death, after treatment with 5x IC_{50}. Similarly, Nalbantsoy et al. (2012) used L929 cells to assess antivenom efficacy compared to *in vivo* assays. They reported that antivenom-treatment reduced the venom toxic effects by 65% in cells incubated for up to 48 hours with a mixture of venom-antivenom. Cell-based assays are relatively inexpensive, rapid and, if optimised, a promising *in vitro* candidate for replacement of the *in vivo* test with a venom neutralisation test. However, the inability of antivenoms to prevent death in some cells preincubated with venom toxins (Nalbantsoy et al. 2012), the nature of the assay being susceptible to higher variability, and variation of protocols between different laboratory settings are key limitations of these assays.

Antivenom potency assays remain a conundrum, weighing up the ethics of using *in vivo* studies with the development of *in vitro* assays, which can capture efficacy of antivenoms against all the complex arsenal of venom toxins (Theakston and Reid 1983; Sells 2003; Gutierrez et al. 2005a; Gutiérrez et al. 2013; de Souza et al. 2015).

1.4 Market of antivenoms in the sub-Saharan African region

Despite the call to conduct exhaustive relevant preclinical and clinical studies, there is a dearth of well-designed studies scrutinising the safety and efficacy profiles of antivenoms (Alirol et al. 2015; Ainsworth et al. 2020), and few publications on post-marketing clinical studies on antivenoms currently available on the SSA market. Only three antivenoms (Table 1.4) that are currently available in SSA markets (as of 2019), are supported by robust clinical trial data (Potet et al. 2019). Moreover, half of the clinical studies intended for assessing efficacy and safety of commercial antivenoms in SSA between 2014 – 2018 were single-armed studies (Potet et al. 2019). It is unethical to withhold a life-saving medicine and thus a deterrent for conducting placebo controlled antivenom clinical trials (Hamza et al. 2016). A randomised clinical trial (RCT) (Abubakar et al. 2010a) and non-randomised comparative

clinical study (CCS) (Visser et al. 2008) were used to successfully ascertain the efficacy and safety of SSA antivenoms. Nevertheless, factors such as poor resources and the difficulty of following up snakebite victims post-discharge are inherent challenges for initiating robustly designed clinical studies in the region.

Worryingly, four (~27%) of the antivenoms described in Table 1.4 had no published data supporting *in vivo* neutralisation efficacy (Ainsworth et al. 2020). Interestingly, at least one of the antivenoms not supported by available data from appropriate clinical and/or preclinical studies did not prevent fatalities (Visser et al. 2008). Although it is not recommended to be used alone, the murine lethality neutralisation study is essential to assess an antivenom's efficacy, particularly in the absence of well-designed clinical studies (Ainsworth et al. 2020).

In 2018, there were 15 different antivenoms marketed in SSA (Table 1.4), predominantly equine derived $F(ab')_2$ polyvalent products with only two intact IgG products (Potet et al. 2019). As mentioned earlier, most of these drugs entered the market with limited, if any, clinical studies. Although promoted as effective by the manufacturer of these antivenoms, when assessed independently, were found to be deficient in relevant venom antibodies, and were catastrophically ineffective (Visser et al. 2008). Therefore, healthcare, and associated personnel must be vigilant about the geobiological content, efficacy, and safety of antivenom. In response to the increased mortality rate from SBE in the region, during their meeting in 2015, the African Society of Venimology (ASV) aimed to reduce death by 90% by 2020. The organisation envisaged a plan of educating health professionals, setting-up a snakebite database and promotion of financial support for victims (Chippaux and Habib 2015). However, there is no evidence of whether this target was achieved.

In the SSA region, more than 500,000 doses of antivenom are required to treat snakebite incidence accounting for ~300,000 envenomations annually (Chippaux and Habib 2015). The current antivenom output in the region is not known, but in 2010/2011 antivenom manufactures combined to produce 377, 500 vials per year that provided only ~83,000 effective treatments (Brown 2012). Since then, discontinuation of Fav-Afrique™ in 2014 (Potet et al. 2019)

has worsened the situation(Chippaux and Habib 2015). Although, many antivenom products have entered the market as potential replacements, so far none of these antivenoms have demonstrated comparable quality, efficacy, and safety (Visser et al. 2008; Alirol et al. 2015; Potet et al. 2019).

Table 1.4 Commercial antivenoms available in sub-Saharan African countries, as of 2018

Polyvalent Antivenoms		
Product Name / Country of origin	**venoms used for immunisation**	**Format**
ASNA-C , India	*B. arietans, B. gabonica, B. nasicornis, D. angusticeps, D. jamesoni, D. polylepis, E. carinatus, N. haje, N. melanoleuca, N. nigricollis, N. nivea*	Equine - $F(ab')_2$
ASNA-D, India	*B. arietans, B. gabonica, B. nasicornis, D. angusticeps, D. jamesoni, D. polylepis, E.ocellatus, N. haje, N. melanoleuca, N. nigricollis, N. nivea*	Equine - $F(ab')_2$
EchiTab-Plus, Costa - Rica	*B.arietans, E. ocellatus, N. nigricollis*	Equine - IgG
Inoserp Pan-Africa, Mexico/Spain	*B. arietans, B. gabonica, B. rhinoceros, D. angusticeps, D. jamesoni, D. polylepis, D. viridis, Echis leucogaster, E. ocellatus, E. pyramidum, N. haje, N. katiensis, N. melanoleuca, N. nigricollis, N. nivea, N. pallida*	Equine - $F(ab')_2$
Antivipmyn-Africa, Mexico	*B. arietans, B. gabonica, B. rhinoceros, D. angusticeps, D. jamesoni, D. polylepis, D. viridis, E. leucogaster, E. ocellatus, E. pyramidum, N.haje, N. katiensis, N. melanoleuca, N. nigricollis, N. nivea*	Equine - $F(ab')_2$
Snake Venom Antiserum (Pan Africa), Inida	*B. arietans, B. gabonica, B. nasicornis, B. rhinoceros, Dendroaspis angusticeps, D. jamesoni, D. polylepis, D. viridis, E. carinatus, E. leucogaster, E. ocellatus, Naja nigricollis, N. haje, N. melanoleuca*	Equine - $F(ab')_2$
Snake Venom Antiserum (Central Africa), India	*B.rhinoceros, E. carinatus, Daboia russelli, D.polylepis*	Equine - $F(ab')_2$
SAIMR Polyvalent, South Africa	*B.arietans, B. gabonica, D. angusticeps, D. jamesoni, D. polylepis, Hemachatus haemachatus, N. annulifera, N. melanoleuca, N. mossambica, N. nivea*	Equine - $F(ab')_2$
VACSERA-Poly, Egypt	*B. arietans, B. gabonica, Cerastes cerastes, C. vipera, Echis carinatus, E. coloratus, M. lebetina, M. palestinae, N.haje, N. melanoleuca, N. mossambica, N. nigricollis, N. oxiana, P. persicus, V.ammodytes, V.xanthina, W. aegyptia*	Equine - $F(ab')_2$
VINS-A, India	*B. arietans, B. gabonica, D. jamesoni, D. polylepis, D. viridis, E.leucogaster, E. ocellatus, N. haje, N. melanoleuca, N. nigricollis*	Equine - $F(ab')_2$
VINS-CA, India	*B. gabonica, Echis carinatus, Daboia russelli, Dendroaspis polylepis*	Equine - $F(ab')_2$
Monovalent Antivenoms		
Product Name / Country of origin	**venoms used for immunisations**	**Format**
SAIMR Echis ocellatus / Echis pyramidum, South Africa	*E. carinatus, E. ocellatus, E. coloratus, Cerastes spp.*	Equine - $F(ab')_2$
EchiTab-G, UK	*E. ocellatus*	Ovine - IgG
SAIMR-Boomslang, South Africa	*Dispholidus typus*	Equine - $F(ab')_2$
VINS-Echis, India	*E. ocellatus*	Equine - $F(ab')_2$

(Adapted from Potet et al. 2015).

On the other hand, antivenom manufacturers face enormous pressure to increase production making antivenoms reasonably affordable whilst fulfilling quality regulation standards. Antivenoms marketed in SSA cost in the region of $100 – $300 (Chippaux and Habib 2015), but significantly cheaper antivenoms are available (Harrison et al. 2017) which, in many cases, are the choice of those who are looking for the cheapest product, but without consideration for its safety and efficacy. In a meta-analysis study, the price for average treatment is estimated to be $124 (55 – 640$) where full treatment (including caring, service, transportation and food for a 7-day hospital-stay), could cost up to $153 (Hamza et al. 2016). This exceeds the monthly income of most snakebite victims in the SSA (Mitra and Mawson 2017), thus, financial intervention by government institutions and organisations is especially needed (Chippaux and Habib 2015). The cost of the major antivenoms currently marketed in SSA are summarised by (Habib et al. 2015b; Hamza et al. 2016).

1.5 Key Target Product Profile (TPP) for antivenom currently marketed in SSA

The majority of the antivenoms marketed in the SSA region are horse-derived $F(ab')_2$-based polyspecific antivenoms (See table 1. 3). Antivenoms are generally packed in containers such as vials, ampoules, or intravenous infusion bags. Antivenoms are generally stored at 2℃ - 8℃ with a demonstratable shelf-life of at least 3 years for liquid formulation (World Health Organization 2016), although it is highly recommended to demonstrate extended stability at 30℃ ±2℃ and relative humidity of 75% ±5%. Freeze-dried antivenom has a 5-year shelf-life (World Health Organization 2016), but there is an additional cost associated with its manufacture (Hamza et al. 2016). Antivenoms are generally administered by controlled intravenous infusion, all patients, regardless of their age and sex or body weight, receiving the same dose that is sufficient to neutralise 100% of the average venom administered per bite by an adult snake (World Health Organization 2010).

1.6 Aim and objectives of the study

Despite the increased incidence of snakebite across SSA, there is unprecedented shortage of supply of effective and affordable antivenoms. In response to this issue, the African authorities started to import poor quality antivenoms, which often led to disastrous consequences. Amongst other factors, the decision to rely on cheaper markets is hugely influenced by the high cost of antivenom, which exceeds several months income of many families living in SSA (Mitra and Mawson 2017; Habib et al. 2020). In response to this, the Wellcome Trust and WHO have jointly devised a roadmap to halve snakebite related death and disability by 2030. As a top priority, the organisations are committed to facilitating a sustainable supply, and accessibility to safe, effective and affordable antivenom in the region (Williams et al. 2019a). Towards this goal, antivenom manufacturers are being encouraged to upgrade their facilities to conform with modern pharmaceutical technology.

Although many antivenom producers have attempted to emulate Fav-Afrique™, the current 'gold standard' antivenom for SSA, but there is no evidence to suggest that the current antivenoms meet its specifications. Thus, the search for developing affordable, safe, and effective antivenom continues. The initial aim of this study is to develop a manufacturing process for a Polyspecific antivenom for use in SSA. Making use of access to the manufacturing process for Fav-Afrique™, this study has the potential to fulfil the requirement to reinstate an antivenom with comparable qualities. Affordability was the main reason for cessation of Fav-Afrique™ manufacture (Warrell et al. 1976b), the project aims to create a cost effective manufacturing process without compromising the quality of the product. Towards that goal, the study will benefit from the existing modern pharmaceutical technology at MicroPharm Ltd to develop manufacturing processes to generate two of the most common formats of antivenom:

- Whole IgG-based antivenom: A relatively cheap method based on caprylic acid fractionation of IgG from hyperimmunised horse plasma.

- F(ab')$_2$-based antivenom: a purer antivenom produced by cleavage of IgG at its hinges using the proteolytic enzyme pepsin.

This will be covered in chapter three. However, it is important to note that the study has no control on the immunisation protocol, it will be using hyperimmune horse plasma (HHP) against ten medically relevant snake species belonging to the *Bitis*, *Dendroaspis*, *Echis* and *Naja* genera.

It is known that the neutralisation ability of equine-derived antivenom is largely attributable to the IgG(T) subclass (Fernandes et al. 1991). On the basis of these findings, a few commercially available IgG(T)-derived antivenoms were manufactured (Grandgeorge et al. 1996; Pepin-Covatta et al. 1997). Given the significantly increased cost implication with their preparations, these antivenoms are not available in SSA at present. Indeed, the quality of these antivenoms reported warrants further investigation of the possibility of their manufacture for SSA. The second aim of this study is therefore to assess the binding activity and the relative quantity of each of the equine IgG subclasses, and it is covered in chapter four. To achieve this, different techniques and assays are employed to isolate and purify equine IgG(T), IgGa and IgGb IgG subclasses.

Currently, preclinical assessment of antivenoms largely relies on the *in vivo* murine tests of venom toxicity and antivenom efficacy. Despite being considered the 'gold standard' potency test, their use is associated with ethical, technical, logistical and financial restrictions. In response to the current global trend to implement the 3Rs, it is almost universally accepted that tests using animals should, wherever possible, be replaced by alternative *in vitro* methods (Sells 2003; Clark 2018). The final aim of this study is to develop a *Galleria mellonella* larval model and Vero cell-based assay to assess the lethality and potency of snake venom and antivenom, respectively. This will be covered in chapter five of this study. In addition to being rapid, inexpensive and being 3Rs compliant, it is the ultimate objective of this study that the assays, particularly the larvae assay, should compare with murine studies in their sensitivity and reproducibility. Finally, the assays will be used to examine and assess the toxicity profiles of both viper and elapid snake venoms. The

polyvalent antivenom will then be used to validate the capacity of the invertebrate model and the *in vitro* cell assay to measure antivenom potency.

Chapter 2: Materials and Method

2.1 Materials

Prominence HPLC Shimadzu and UV-VIS Shimadzu 180 Spectrophotometer were purchased from Shimadzu Corporation (Kyoto, Japan). AdvanceBio SEC 300Å 4.6 x 150 mm (or 7.8 x 300 mm) columns were purchased from Agilent Technologies (Cheshire, UK). PolarStar Omega plate reader, BMG LABTECH Ltd (Aylesbury, UK). AKTAPure 150 system, x50 column and QXL Sepharose were purchased from GE Healthcare (Buckinghamshire, UK). Avanti-26S Centrifuge was purchased from Beckman Coulter (Higher Wycombe, UK) where bench (Eppendorf) centrifuge was obtained from ThermoFisher Scientific (Paisley, UK). Reagents such as 10x running buffer (Tris/Glycine/SDS) and 10xTris Buffered Saline (TBS) as well as consumables and equipment used for SDS-PAGE and Western blot assays were obtained from Bio-Rad (Watford, UK). Unless otherwise stated, all HRP-conjugated antibodies (Abs) including goat anti-horse IgG(T), goat anti-pepsin, goat anti horse IgG (Fc), goat anti horse IgG $F(ab')_2$, and sheep anti-horse albumin were purchased from Cambridge Bioscience (Cambridge, UK). Similarly, standard proteins including horse albumin, horse IgG (Fc) and IgG $F(ab')_2$ were purchased from Cambridge Bioscience (Cambridge, UK).

Mouse anti-horse IgGa, mouse anti-horse IgGb (Bio-Rad, Watford, UK) and the goat anti-mouse IgG (H+L) HRP-conjugated was purchased from Bio-Rad (Watford, UK). Goat anti-horse IgG (H+L) HRP was obtained from Sigma-Aldrich (Gillingham, UK). Caprylic acid and other general chemicals and consumables were obtained from Merck (Watford, UK) and Sigma-Aldrich (Gillingham, UK). Water For Irrigation (WFI) and 0.9% NaCl were obtained from Baxter Healthcare Ltd (Newbury, UK). Activated carbon filters (Millistak+® Pod Depth Filter, CR40) were obtained from Merck (Watford, UK). All other filters, unless stated otherwise, were obtained from Sartorius Stedim, (Surrey, UK). Lyophilised pepsin (from porcine gastrin mucosa) was purchased from Sigma-Aldrich (Gillingham, UK).

Lyophilised venoms were obtained from Latoxan (Portes-les-Valence, France). These venoms were extracted from: *Bitis arietans, Bitis gabonica, Dendroaspis polylepis, Dendroaspis viridis, Dendroaspis jamesoni, Echis*

ocellatus, Echis leucogaster, Naja haje, Naja nigricollis and *Naja melanoleuca.* Hyperimmune Horse Plasma (HHP) against venoms of each genus (*Bitis, Dendroaspis, Echis and Naja*) were obtained from Sanofi Pasteur (Lyon, France). Non-hyperimmune horse plasma (NHP) was purchased from Tebu-bio (Peterborough, UK).

Galleria mellonella larvae were purchased from Reptile Cymru (Cardiff, UK). Insulin syringes (0.5mL) were obtained from VWR International (Lutterworth, UK). XE series Inverted Microscope was purchased from Pyser SGI (Edinburgh, UK). Class II biological safety cabinet was purchased from ESCO Lifescience (Barnsley, UK). Binder incubator was purchased from Binder International (Germany). Microplate shaker was purchased from VWR international (Lutterworth, UK). Vero cells were purchased from European Collection of Authenticated Cell Cultures (ECACC) (Porton Down, UK) and kindly provided by MicroPharm Ltd. Fav-Afrique antivenom (lot G9921, EXP 10/2013) was kindly provided by Prof. Nicholas Casewell. EchiTab-Plus ICP (lot6190319PALQ, EXP 03/2022) was kindly provided by MicroPharm Ltd (see table 2.1). Cell culture reagents such as Dulbecco's modified Eagle's medium (DMEM), sterile Dulbecco's Phosphate Buffered Saline (DPBS), heat inactivated foetal Bovine Serum (FBS), 200mM L-glutamine, penicillin-streptomycin, Trypsin/ EDTA (ethylenediaminetetraacetic acid), Dimethyl sulfoxide (DMSO) and Trypan blue were purchased from Sigma-Aldrich (Gillingham, UK). CellTiter-Blue dye was purchased from Promega (Chilworth Southampton UK). Sterilised consumables such as serological pipettes, BD falcon culture tissue plates and dilution plates were purchased from VWR International (Lutterworth, UK). GraphPad Prism v9.0 was purchased from GraphPad Software, San Diego, California, USA. IBM SPSS Statistics version 27.0 (Armonk, New York; IBM Corp) was accessed through Cardiff university.

Table 2.1 details of antivenoms used in this study

Name of Antivenom	Format	Manufacturer	Protein content	Lot number	Production year	Expiry year
Fav-Afrique™	$F(ab')_2$	Sanofi	76 g/L	G9921	Not recorded*	Oct-13
EchiTab Plus-ICP	IgG	ICP	60 g/L	6190319PALQ	Mar-19	Mar-22
Polyvalent $F(ab')_2$	$F(ab')_2$	in-house	50 g/L	150421	Apr-21	N/A
Polyvalent IgG	IgG	in-house	50 g/L	240820	Aug-20	N/A

Descriptions: *production year was not recorded at experiment time, N/A; not applicable.

2.2 Methods

Detailed recipes and concentrations of buffers and solutions used through the study are inserted in Appendix I.

2.2.1 Hyperimmune Horse Plasma (HHP) against snake venom mixtures

The Hyperimmune Horse Plasma (HHP) used for this study was prepared by immunising four groups of horses against venom mixtures from four snake genera. One group of horses received a mixture of venoms from *B. arietans* and *B. gabonica*, the second group with venoms from *D. jamesoni, D. polylepis* and *D. viridis*, the third group with venoms from *E. leucogaster* and *E. ocellatus*, and the final group with venoms from *N. haje, N. melanoleuca* and *N. nigricollis*. HHP was obtained from Sanofi Pasteur (Lyon, France). Access to further information is restricted. The precise composition of additives to the plasma is confidential, but it contained M-cresol and sodium citrate as preservative and anticoagulant agents, respectively.

Water For Irrigation (WFI) is a sterile, distilled, nonpyrogenic intended only for sterile irrigation, washing, rinsing and dilution purposes. It has a specification of clear and colourless appearance, a conductivity of <5.0 µS/cm, endotoxin level of <0.25 EU/mL and a pH 5.5 (5.0 to 7.0). At MicroPharm Ltd, WFI is the standard solution that is used in laboratory experiments such as dilutions, formulations, and development studies.

2.2.2 Purification and preparation of caprylic acid precipitated IgG product

Horse IgG was prepared by caprylic acid fractionation following the method first reported by Rojas and colleagues (Rojas et al. 1994), with some modifications. M-cresol was removed by passing the HHP sample through Millistak+® Pod Depth Filter CR40 (Merck; Watford, UK) at ~80 mL/min using Watson Marlow pump 323S (Falmouth, England). HHP was then thermally treated at 56°C±1°C for 1 hour (h) and allowed to cool to 22°C (±1°C) before being diluted by 0.5x starting plasma volume with WFI. The pH of the plasma was adjusted to 4.88±0.05 using 1.74 M acetic acid (Merck; Watford, UK) before being treated with 3% (v/v) caprylic acid (Merck; Watford, UK) and mixed vigorously, using a magnetic stirrer for 1 h at 22°C±1°C. The slurry was

centrifuged (4500 RCF, 45 minutes 22°C) and the supernatant, which contained the IgG, was collected, and filtered through a serially connected glass fibre (GF) (0.65 µm) and 0.2 µm filters (Sartorius Stedim; Surrey, UK). M-cresol and caprylic acid residuals were removed by passing the product through Millistak+® Pod Depth Filter, CR40 filter at ~80mL/min using Watson Marlow pump 323S. The product was filtered through a serially connected GF (0.65µm) and 0.2 µm filters and split into two for manufacturing intact IgG and F(ab')$_2$ antivenom products. Also, for a detailed process map, see Appendix II (a).

The product was concentrated and diafiltrated against 7x the sample volume with 0.9% NaCl (Baxter Healthcare Ltd; Newbury, UK), using 100 kDa nominal molecular weight cut-off (nMWCO) Polyethersulfone (PES) membrane at pH 7.4 ±0.2. The whole IgG-based antivenom product was formulated in 0.9% NaCl and 0.05% (v/v) polysorbate 80 (PS80), also known as Tween-80, at pH 7.4 ±0.2. Finally, the formulated product was sterilised by passing through 0.2 µm filters and filled in grade A vials (10 mL) in a laminar flow cabinet.

2.2.3 Manufacturing F(ab')2-based antivenom

F(ab')$_2$ cleavage was achieved by pepsin digestion of purified equine IgG following the method described by Kurtovic and colleagues (Kurtović et al. 2019), with some modifications. Following pH adjustment to 3.05±0.05 using 0.5 M HCl, caprylic acid purified IgG (section 2.2.2) was treated with 2% (w/w) pepsin for 1 h at 30°C. As described in Figure 2.1, the digest was terminated by adjusting the pH to 5.0 (4.8 – 5.2) using 1 M NaOH, and the product was concentrated and diafiltrated against 7x the sample volume with 20 mM piperazine buffer (comprising 20 mM piperazine, 65 mM NaCl, pH 5.0±0.1) using 50 kDa nMWCO PES membrane. The product was filtered through serially connected GF (0.65 µm) and 0.2 µm filters. To enhance the purity, the F(ab')$_2$ containing sample was passed through a x50 column packed with QXL sepharose matrix (196 mL column volume) at 20 mL/ minute using AKTA Pure 150. In the presence of 20 mM piperazine buffer (pH 5.0±0.1 and conductivity 8.5±2.0 mS/cm), the column was conditioned so that it permits the passage of ultrapure F(ab')$_2$ whilst simultaneously trapping impurities including pepsin and Fc residues. The F(ab')$_2$ product was concentrated using a 30 kDa

nMWCO PES membrane and formulated in 0.9% NaCl and 0.05% (v/v) PS80 at pH 7.4±0.2 (Figure 2.1). The final product was sterilised by passing it through 0.2 µm filters and the drug product was stored in grade A vials (10 mL) in a laminar flow cabinet.

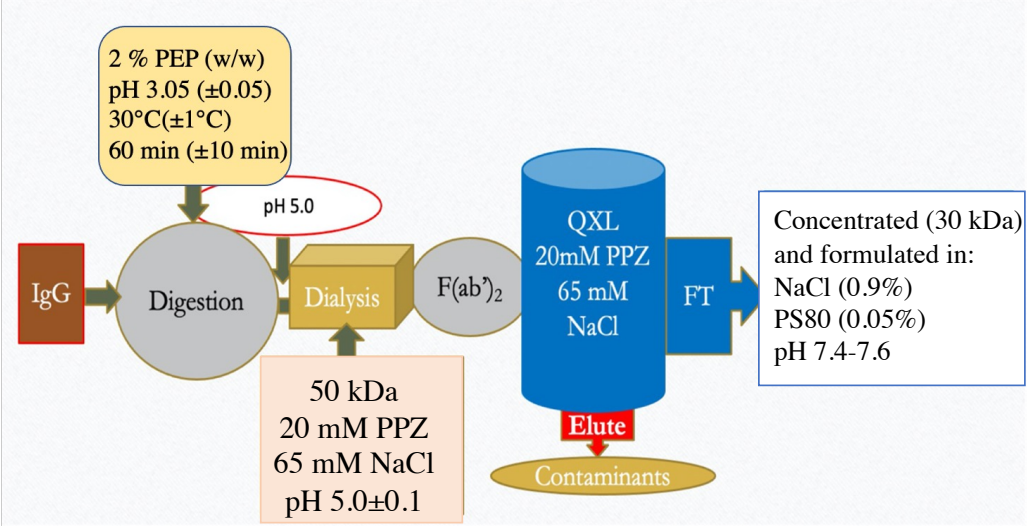

Figure 2.1. Process map for manufacturing F(ab')2- antivenom.

Caprylic acid purified equine IgG was digested with 2% (w/w) pepsin enzyme for 60 min (±10 min) at 30℃±1℃ and pH 3.0 – 3.10. impurities such as fragmented Fc were reduced during the diafiltration stage (50 kDa PES). The $F(ab')_2$ product further purified by passing through the QXL Sepharose packed column. The product was concentrated and formulated in 0.9% NaCl and 0.05% PS80, pH7.4±0.2. Further details are available in Appendix II (B).

Abbreviations: IgG, immunoglobulin; $F(ab')_2$, antigen binding fragment (divalent); PEP, pepsin; kDa, kilodalton; PS80, polysorbate 80 (also known as tween 80); NaCl, sodium chloride; PPZ, piperazine buffer; w/w, weight-for-weight; mM, millimolar; min, minute.

2.2.4 Protein concentration

Protein concentrations were measured at 280 nm, using an extinction coefficient of 1.36 for horse IgG (Pla et al. 2017). Concentrations were calculated from the mean of triplicate readings. However, there is no universal method for measuring snake venom protein concentration (Bocian et al. 2020). To avoid underrepresented results, protein concentration for snake venoms was determined by their dry-weight where 200 mg±2 mg of lyophilised venoms was dissolved in 20 mL 0.9% NaCl to achieve 10 mg/mL stock concentration.

The venom solutions were filtered through GF (0.65µm) and 0.2 µm filters and stored at -80℃ until required.

2.2.5 Reconstituting lyophilised pepsin

Lyophilised pepsin enzyme was dissolved in citrate buffered saline (18.36 mM tri-sodium citrate dihydrate, 1.66 mM citric acid monohydrate and 150 NaCl; pH 6.0±0.2) at 100 g/L. To ensure the removal of contaminants such as lipopolysaccharides (LPS) endotoxins, the solution was diafiltered against the reconstituting buffer using 100 kDa nMWCO PES membrane and filtered through a 0.2 µm filter. The protein measurement was determined spectrophotometrically (180 UV-VIS spectrophotometer Shimadzu) using the following equation:

$$\{(\mathrm{A1\ x\ 1.55}) - (\mathrm{A2\ x\ 0.76})\}\ x\ DF$$

A_1 = absorbance at 280 nm,

A_2 = absorbance at 260 nm

And DF is dilution factor.

2.2.6 Quality Control Assays for antivenoms

The quality control of the final drug products was conducted in accordance with WHO recommendations (World Health Organization 2016). Some of these standard quality tests (for e.g., extractable volume, neutralising efficacy, osmolality, pyrogen, sterility test and abnormality toxicity assays) were not part of this study, only process-related assays being performed.

2.2.7 Stability

The stability studies were conducted following the International Conference on Harmonisation (ICH) guidelines for stability of new drug substance and products (European Medicines Agency 2003). The Apollo II Liquid (Haywards Heath, UK) Viewing Station method was used for visual inspection of possible discolouration, particle formation and/or protein degradation in the liquid-filled vials.

Apollo II viewer provides a simple method for the detection of visible particles in ampoules, vials, and bottles. Although its use may vary among different laboratories, the system operates by gently swirling each individual container in front the black and white panels (see Figure 2.2). According to MicroPharm

protocols, containers are observed for approximately 5 seconds and particles (others than air bubbles) are reported accordingly. White particles (e.g., glass) will be viewed under the black panel whereas black coloured particles will be viewed under the white panel.

Figure 2.2. Apollo II Liquid Viewer Station

2.2.8 Yield

The yield was the direct measurement of the total amount of equine IgG/ $F(ab')_2$ obtained from a litre of HHP. As described in Section 2.2.4, protein concentrations of the antivenom products were measured at 280 nm, using an extinction coefficient of 1.36 for horse IgG.

2.2.9 Purity assessment using Sodium dodecyl Sulphate-Polyacrylamide Gel Electrophoresis (SDS-PAGE) and Western Blot

2.2.9.1 SDS-PAGE

Plasma proteins, IgG and whole venoms were analysed using Sodium dodecyl Sulphate-Polyacrylamide Gel Electrophoresis (SDS-PAGE) under reducing and non-reducing conditions. Electrophoresis of proteins was performed following the method first described by (Laemmli 1970), with minor adjustments. Samples were diluted in 150 mM NaCl then further diluted 1:1 with 2x Laemmli buffer, mixed gently and heated for 5 minutes at 95°C. For reduced conditions, the 2x Laemmli buffer was supplemented with 1:20 volume of 2-mercaptoethanol (Sigma-Aldrich; Gillingham, UK). Denatured

samples were mixed, centrifuged at 14000x *g* for 1 minute at 20ºC, then allowed to cool to room temperature (15-25ºC) before loading on 4-15% acrylamide gradient Mini-PROTEAN TGX gel (Bio-Rad; Watford, UK). All laboratory temperatures were set to 15-25ºC, hereinafter referred to as room temperature. Unless stated otherwise, all proteins were loaded at 5 µg/well. Electrophoresis was run at 50 volt (V) for 5 minutes followed by 150 V for 60 minutes, or until the blue dye reached the bottom of the gel. Proteins were stained with Coomassie Brilliant Blue R-250 (Thermo Fisher Scientific; Paisley, UK) diluted to 0.25 g/L in 10% acetic acid. Excess Coomassie was removed by destaining the gel with 10% acetic acid.

2.2.9.2 Western blotting

Electrophoresed proteins were transferred onto a 0.45 µm nitrocellulose membrane (Bio-Rad; Watford, UK), using a Trans-Blot Turbo Transfer system (Bio-Rad; Watford, UK) and run for 3 minutes at 1.3 V. Membranes were blocked at 4°C for overnight (19 – 24 h) with blocking buffer (TBST-milk). The TBST-milk constitute a ready-made 10x TBS, 5% (w/v) non-fat milk (CK's Food store, Newcastle Emlyn, UK) and 0.1% (v/v) tween-20, pH 7.4. Blots were washed at least 3x with washing buffer [TBS containing 0.1% (v/v) tween-20, pH 7.4]. The molecular weight marker (Precision Plus Protein Western C Standard: WC) (Bio-Rad, Watford, UK) lanes were carefully cut and placed in a 1:5000 solution of Strep-Tactin-HRP (Bio-Rad, Watford, UK) in blocking buffer.

To detect Fc, pepsin and albumin impurities, blots were washed as above and incubated in their respective HRP-conjugated antibodies (diluted at 1:5000 in blocking buffer) for at least 1 h at room temperature mixing continuously on a gyratory mixer (full blot) and roller mixer (strips). Blots were washed 3x with washing buffer before immersing in in enhancer chemiluminescent substrate (ECL) (Bio-Rad, Watford, UK) for five minutes. Images were collected using the ChemiDoc XRS chemiluminescent detection system and analysed using ImageLab software.

Analysis of venom-antivenom interactions was performed as above with a few modifications. Following the blocking step, all antivenoms [HHP, purified venom-specific IgG, Fav-Afrique^{TM}, intact IgG and F(ab')$_2$ antivenom products]

were diluted to 1 g/L in 150 mM NaCl firstly and then further diluted to 1:500 in blocking buffer. Venom blots were incubated in their respective sample for at least 1 h at room temperature, mixing continuously on a gyratory mixer (full blot) and roller mixer (strips). Blots were washed as above and incubated for at least 1 h at room temperature in goat anti horse $F(ab')_2$-HRP conjugated [for Fav-Afrique™ and $F(ab')_2$ antivenom] or in HRP-conjugated goat anti-horse IgG (for intact IgG antivenom). The WC lanes were processed as above. All HRP-conjugated antibodies were diluted to 1:5000 in blocking buffer. Blots were washed 3x with washing buffer before immersing in ECL for five minutes. Images were collected using the ChemiDoc XRS chemiluminescent detection system and analysed using ImageLab software.

To detect equine IgGa and IgGb, blots were firstly incubated with mouse anti horse IgGa or IgGb, diluted at 1: 5000 in blocking buffer, for at least 1 h at room temperature, mixing continuously on a gyratory mixer. Then, the blots were washed (as above) and probed with goat anti-mouse IgG (H+L) HRP conjugated antibody, diluted at 1:5,000 in blocking buffer, unless stated otherwise. Following the blocking and washing steps (as above), the IgG(T) blot was probed against HRP-conjugated goat anti-horse IgG(T) diluted at 1:5,000 (non-reduced) and 1:10,000 (reduced) conditions. All blots were incubated for at least 1 h at room temperature. Blots were washed 3x with washing buffer then immersed ECL for five minutes. Images were collected using the ChemiDoc XRS chemiluminescent detection system and analysed using ImageLab software (Bio-Rad, Watford, UK).

2.2.10 Enzyme-Linked Immunosorbent Assay (ELISA)

The enzyme-Linked Immunosorbent Assay (ELISA) was performed according to the method previously reported by (Theakston and Reid 1979) and (Harrison et al. 2017) with some modifications. Ninety-six wells ELISA Immulon 4BX plates (Thermo Fisher Scientific; Paisley, UK) were coated with 100 µL/well of 2.5 µg/mL venom in PBS (100mM phosphate buffer containing 150 mM NaCl, pH 7.4) at 2-8℃ overnight (16-24 h). Plates were washed 3x with 350 µL/well PBST containing 0.1% (v/v) Tween-20 using a plate washer (BioTek, Swindon, UK) and blocked with 150 µL PBS containing 2.5% (w/v) Foetal Bovine Serum (FBS), for 2 h at 37℃. Plates were washed as above and

antivenoms or control (non-hyperimmune horse plasma; NHP) were added as a 3-folds serial dilution starting at 1:100 dilution and plates were incubated at 37°C for 1 hour. The plates were washed as above then 100 µL/well of a 1:30,000- dilution (in PBST) of goat anti-horse IgG (H+L) HRP (for whole IgG-based samples) or goat anti horse $F(ab')_2$-HRP conjugated diluted in PBST at 1:100,000 [for $F(ab')_2$ -based samples] was added and plates were incubated for 1 h at 37°C. The plates were washed as above before adding 100 µL/well of 3, 3′, 5, 5′-Tetramethylbenzidine (TMB), then incubated for approximately 12 minutes at room temperature. The reaction was stopped by adding 50 µL per well of 1 M HCl. The plates were read using a PolarStar Omega plate reader, BMG LABTECH Ltd (Aylesbury, UK) at 450 and 690 nm wavelengths. Data was obtained and processed using MARS Data Analysis Software. Further data analysis was performed using GraphPad Prism 9 software (see section 2.2.23).

2.2.11 Size-exclusion chromatography-high pressure liquid chromatography

The presence of aggregates within the product was assessed using size-exclusion chromatography-high pressure liquid chromatography (SEC-HPLC) on a Prominence HPLC system with an Agilent AdvanceBio SEC 300Å, 2.7 µm, 4.6 x 150 mm (or 7.8 x 300 mm) column equilibrated and eluted with 20 mM sodium phosphate, 130 mM sodium chloride, 0.02% sodium azide, pH 6.0±0.2, at a flow rate of 0.5 mL/min. The Gel Filtration Standards (Bio-Rad; Watford, UK) used for molecular weight (MW) determination were thyroglobulin (Mr 670,000), γ-globulin (M_r 158,000), ovalbumin (M_r 44,000), Myoglobin (M_r 17, 000) and Vitamin B12 (M_r 1,350). Data analysis was performed using LabSolutions software, Shimadzu corporation (Kyoto, Japan).

2.2.12 Preparations of IgG(T)-enriched and IgG(T)-depleted antivenom products

An anion exchanger Q-sepharose XL (QXL) Fast Flow matrix connected to AKTAPure 150 system (GE Healthcare; Buckinghamshire, UK) was used to isolate IgGa, IgGb & IgG(T) subclasses. Following the manufacturer's

instructions, a 15.6 mL column volume was packed with QXL. For the anion exchange chromatography (AEX) step, whole IgG [which is referred to through this study as Total IgG (TIgG)] was used as a stock solution. TIgG was derived from the whole IgG product (described in section 2.2.2) prior to formulating in 0.9% NaCl and 0.05% PS80.

The TIgG sample was diluted to 5 g/L in washing buffer (10 mM phosphate buffered saline: ~6 mM disodium hydrogen phosphate anhydrous, ~ 4 mM sodium phosphate monobasic dihydrate and 10 mM NaCl, pH7.1±0.1). The column was equilibrated against washing buffer until the effluent pH was 7.1±0.1 and conductivity 2.6 mS/cm. Total IgG samples were loaded at ~25 mg/mL of QXL matrix and run at a flow rate of 5 mL/min. Flow-through (FT) and unbound wash were collected in a clean container by washing the column using washing buffer until no protein was detected in the effluent (absorbance at 280 nm ≤0.05). Bound proteins were eluted using 10 mM phosphate buffer containing 1 M NaCl, pH 7.1±0.1. Both bound and unbound protein samples were concentrated and diafiltered as above (sections 2.2.2 &2.2.3) and formulated in 0.9% NaCl (Baxter Healthcare Ltd; Newbury, UK). The final products were filtered through GF (0.65 µm) + 0.2 µm filters and stored temporarily at 2–8℃ or -20℃ for prolonged storage.

2.2.13 Conjugating venoms to CNBr-activated Sepharose matrix

CNBr-activated Sepharose matrix (GE Healthcare; Buckinghamshire, UK), was used for coupling either *Echis spp.* (*E. leucogaster* and *E. ocellatus*) venoms or *Naja spp. (N. haje, N. nigricollis* and *N. melanoleuca)* venoms. Coupling solutions were freshly prepared by dilution of lyophilised venoms to 10 g/L with coupling buffer (100 mM sodium carbonate/bicarbonate and 0.5 M NaCl, pH 8.3±0.1) and filtered through GF (0.65 µm) + 0.2 µm filters, serially connected. Conjugations were performed at a ratio of 5 mg (lyophilised venoms): 1g (dry CNBr matrix).

Following the manufacturer's instructions, the freeze-dried CNBr-activated sepharose was suspended in a chilled 1 mM HCl and mixed in a roller mixer for 1 hour at room temperature. The swollen matrix was transferred into a glass sintered filter (Gallenkamp; Cambridge, England) and washed 5x with 30 mL 1 mM HCl before it was activated with 3x 30 mL coupling buffer.

Coupling solution containing 15 mg of venom proteins (equal amounts of each species, e.g., *E. leucogaster* and *E. ocellatus*) was added to the swollen CNBr-activated matrix at 5:1 ratio (venom: dry CNBr-activated sepharose) and coupled at room temperature overnight on a roller mixer. The coupled medium was washed with 3x 30 mL coupling buffer and filtrates retained for assessment of coupling efficiency. Uncoupled sites were blocked by the addition of 1 M ethanolamine, pH 8.0, for 2 h at room temperature on a roller mixer. Coupled medium was transferred to a glass sintered filter for washing alternately 5x with equal volumes of coupling buffer and 100 mM sodium acetate buffer containing 500 mM NaCl; pH 3.8. Venom coupling efficiency was determined by collecting filtrates and measuring absorbance at 280 nm. After determination of coupling efficiency, coupled matrix was packed into different size columns. The packed columns and unused venom-coupled matrix were stored in PBS (100 mM Phosphate buffer, 150 mM NaCl: pH 7.4±0.2) containing 0.01% thiomersal (storage buffer) and kept at 2–8 °C.

2.2.14 Small-scale Affinity Purification (SSAP)

Venom conjugated CNBr-matrices (section 2.2.13) were packed into gravity columns. The columns were equilibrated by washing with 10x column volumes of a variant phosphate buffered saline containing 0.5 M NaCl (PBW: 85 mM di-sodium hydrogen phosphate, 15 mM sodium dihydrogen phosphate and 500 mM sodium chloride; pH 7.4±0.2). Samples were diluted in PBW, filtered through GF (0.65µm) and 0.2 µm filters then loaded into the column at ~25 mg per mL venom-coupled matrix. To ensure maximum binding, columns were mixed for 2-4 h at room temperature. Non-specific, non-binding antibodies were allowed to pass through the column by gravity, and columns washed with PBW until absorbance at 280 nm was ≤0.05. Venom specific antibodies were eluted by adding 100 mM glycine-HCl, pH 1.5. Samples were collected and their protein concentrations were determined at 280 nm as described in section 2.2.4. Three columns were run concurrently, and data were collected as a mean ± SD of three independent replicates.

2.2.15 Preparations of Affinity Purified Antivenoms

Venom conjugated CNBr-matrices (section 2.2.13) were packed into 10 mL columns (MerckMillipore; Watford, UK) and the columns were connected to the AKTA Pure 150 system. Each column was equilibrated, and samples were prepared as described in section 2.2.14. According to the manufacturer instruction, the CNBr-activated Sepharose matrix has a capacity of 25 mg protein per mL matrix, and samples were loaded slowly at 1 mL/min. To maximise the capture of the specific antibody, the samples were allowed to cycle on the column 3x whilst maintaining the slow flowrate at 1 mL/min. Unbound proteins were washed with PBW until the UV signal fell to <0.10 milli-absorbance unit (mAU) and/or absorbance at 280 nm was ≤0.05. Venom-specific antibodies were dissociated using 100 mM glycine-HCl, pH 2.5±0.2. To preserve the biological activities for downstream assays, samples were neutralised immediately using 1 M Tris-HCl, pH 8.0. Samples were diafiltered and formulated as described in sections 2.2.2 and 2.2.3 and all procedures were conducted at room temperature. Protein concentrations were determined as described in section 2.2.4.

2.2.16 Separation of equine IgG subclasses using Protein G

Separation of equine IgG subclasses was performed on a Protein G column, as described previously (Sheoran and Holmes 1996; Sugiura et al. 2000), with some modification. A 5 mL HiTrap Protein G column (GE Healthcare; Buckinghamshire, UK) was connected to the AKTA Pure 150 system and equilibrated with 5x column volumes PBS, pH 7.5±0.1 at a flow rate of 1 mL/minute. Experiments were performed at room temperature. Highly purified equine IgG samples (i.e., Flow-through fraction) obtained from the AEX step (section 2.2.12) were loaded at ≤25 mg/mL of matrix and flow rate of 1 mL/minute, following the manufacturer instruction. The unbound proteins were extensively washed using PBS; pH 7.5±0.1 until no protein could be detected in the effluent (UV signal fell to <0.10 mAU and/or absorbance at 280 nm was ≤0.05). Bound fractions were eluted in two steps: using 100 mM glycine-HCl, pH 2.9 and pH 2.5. Under these conditions, it is expected that equine IgGa and IgGb subclasses are eluted at pH 2.9 and pH 2.5, respectively (Sugiura et al. 2000). To preserve the biological activities for downstream assays,

eluted samples were immediately neutralised to ~ pH 7.4 with 1 M Tris-HCl pH 8.0.

2.2.17 *Galleria mellonella* larval injection assays

The F(ab')$_2$-based polyvalent antivenom (described in section 2.2.3) was prepared by pepsin digestion of caprylic acid fractionated IgG (as described in section 2.2.2). Snake venom toxins used through this study were reconstituted and stored as described in section 2.2.4. Insects were placed in experimental groups of similar weights where only larvae at 200 – 300 mg (average 250 mg) were selected. In the presence of food, the larvae were stored at room temperature for overnight to induce torpidity.

To avoid needle stick injury (Dalton et al. 2017), larval movement was eliminated by chilling in ice for 30-60 minutes and larvae were then immobilised by placing in a clamp (Figure 2.3). This experiment was performed as described by (Ramarao et al. 2012; Dalton et al. 2017; Gorr et al. 2019) with some modifications. For each concentration of venom (or antivenom, or controls), ten larvae (n = 10) of approximately 250 mg (body weight) were slowly injected with approximately 50 µL sample per larva into the haemocoel via the last (fourth) left proleg. Preliminary studies were conducted to determine the sample size, and based on results obtained from these experiments, a sample size of n=10 was sufficient to generate reliable data and also increased the statistical power of the study (result is not shown). An assay control constituting only DPBS was included for every experiment, to demonstrate that needle injury was not responsible for changes observed. In addition, the highest doses of venom and antivenom used were included as negative and positive controls, respectively.

Figure 2.3. Holding *G. mellonella* during injections

Larvae were chilled by incubating in ice for 30-60 minutes then the chilled larvae were immobilised by placing in a clamp. Approximately 50 µL of a prediluted sample was injected into the haemocoel via the last (fourth) left proleg. The larvae were maintained at room temperature for up to 48 h after injection with regular monitoring.

Following injection, larvae were transferred into clean plastic container (special container contain small openings) and incubated at room temperature. The responses of the injected larvae to toxins were carefully monitored at 6, 24 and 48 h when an endpoint of mortality was recorded. During the experiments, onsets such as change on appearance, fluid discharges, mobility and death time of injected larvae were monitored. Furthermore, health status of injected larvae was assessed by tapping the tail

and head of the insects and their responses were observed for ~1 minute. Thus, lack of movement was taken to indicate death. At the end of the experiment, larvae were stored at -80 for at least 24 hours before autoclaved and discarded in clinical waste. Mortality (or survival) was recorded and transferred into Probits and presented as LD_{50} and ED_{50} for venom toxicity and antivenom potency, respectively.

2.2.18 Median lethal Dose (LD_{50})

To assess the LD_{50} of snake venoms on *G. mellonella,* different venom concentrations were prepared by diluting in DPBS. Reconstitution and quantification of snake venoms were performed as described in section 2.2.4. Firstly, a "range-finding experiment" was performed for each snake species [(see Appendix IV(A). This was involved in defining the minimum venom concentration that kills 100 % of the tested larvae and the maximum tolerated dose which is defined as the lowest venom concentration at which there was no death observed.

Subsequently, a range of venom concentrations (eight for *B. arietans*; *seven* for *B. gabonica*, *E. leucogaster, E. ocellatus, N. haje* and *N. melanoleuca*; and six for *N. nigricollis*) were prepared (Table 2.2). The assay control was DPBS (vehicle). The highest venom dose used resulted in 100% mortality for the assay to be valid.

Table 2.2 Preparation of snake venom doses for *G. mellonella* injections

Snake species	Snake Venom Toxins Dose (µg/Larvae)								DPBS only (µL/larvae)
B. arietans	40	30	25	20	15	10	5	2.5	50
B. gabonica	125	100	75	50	25	10	5		50
E. leucogaster	50	25	20	15	10	5	2.5		50
E. ocellatus	50	25	20	15	10	5	2.5		50
N. haje	50	30	25	20	15	10	5		50
N. melanoleuca	25	10	7.5	5	2.5	1	0.1		50
N. nigricollis	5	4	3	2	1	0.5			50

2.2.19 Median effective Dose (ED_{50})

Assessment of antivenom ED_{50} was conducted in a manner based on the murine model (Casasola et al. 2009; Gutierrez et al. 2014). Accordingly, six different antivenom concentrations (see table 2.3) were prepared by mixing a prediluted amount of the antivenom with a fixed 'challenge dose' (ranging from 2.5-5x LD_{50}) of the corresponding venom. The venom-antivenom mixtures

were incubated at 37℃ for 30 minutes, gently vortexed and immediately administered as described above (section 2.2.17). In addition to the assay control (DPBS), positive (antivenom) and negative (venom challenge dose) controls were also included in each experiment.

Table 2.3 Preparation of antivenom doses for G. mellonella injections

	Dose (µg/Larvae)					
Antivenom	1000	250	62.5	15.6	3.9	1.0

Following injection, larvae were incubated and monitored as described above in section 2.2.17. Similarly, mortality (or survival) was recorded and transferred into Probits and presented as LD_{50} and ED_{50} for venom toxicity and antivenom potency, respectively. The calculated LD_{50} and ED_{50} values, together with the challenge dose, were used to estimate the Potency of the antivenom using the following equation as previously reported (Ainsworth et al. 2020).

$$\text{Potency (P)} = \frac{(\text{n} - 1)x\text{LD}_{50}}{\text{ED}_{50}(\frac{\text{mg}}{\text{mL}})}$$

Where P is the amount of venom that is completely neutralised per 1 mL antivenom, and "n" is the number of LD_{50}s used in the assay to determine the ED_{50}.

2.2.20 Cell culture

Vero cells used in the assays were between passages 20 and 29 and were maintained using Dulbecco's modified Eagle's medium (DMEM) supplemented with 10% heat inactivated foetal Bovine Serum (FBS), 1% (v/v) penicillin-streptomycin and 2 mM L-glutamine. The cells were routinely maintained in a humidified atmosphere at 37°C and 5% carbon dioxide (CO_2). Cells were passaged in accordance with ECACC protocol and cryopreserved in DMEM medium containing 10% dimethyl sulfoxide (DMSO) and transferred into vapour phase liquid nitrogen. Cells were maintained in 75 cm^2 flasks seeded at a density of 6.7 x 10^3 cells/mL DMEM. Cells were harvested by adding approximately 3 mL trypsin-EDTA (Ethylenediaminetetraacetic acid) (0.05% trypsin and 0.02% EDTA). Following incubation for 15 minutes at 37°C, 5% CO_2, trypsinised cells were neutralised by adding approximately 7 mL DMEM and cells were thoroughly mixed to achieve a good cell suspension.

Cell count was performed by diluting the trypsinised cells 10x in Trypan blue (0.4%) and cells were counted on a haemocytometer using a Pyser SGI inverted XE series Microscope. All samples were diluted in DMEM. All experimental procedures, apart from reading results, were conducted in a Class II Biological Safety cabinet using a sterile technique.

2.2.21 Cell viability assay

The method was performed in accordance with previously reported studies (Lopes-de-Souza et al. 2019; Chong et al. 2020), but with some adjustments. Ninety-six well microplates were seeded with Vero cells at 1.0 x 10^5 cells /mL, in a volume of 100 µL, and grown for 16 to 24 h in a humidified incubator at 37^{o}C and 5% CO_2. To assess the cytotoxicity (IC_{50}) of snake venoms on Vero cells, different concentrations were prepared by diluting venom toxins in DMEM medium, mixing thoroughly and serially diluting across a separate "dilution" plate. Venom concentrations and serial dilutions are included in Appendix V(A). The plate was then placed on a microplate shaker and the samples mixed at 500 rpm for 1-minute pre and post incubation for 1 h at 37^{o}C and 5% CO_2. Following incubation, 100 µL sample was transferred from each dilution plate to corresponding wells of the cell culture plate. Assays were performed either in triplicate (*Bitis* and *Echis* species) or duplicate (*Naja* species). Blank wells containing DMEM medium without cells, positive control (untreated cells) wells containing only cells in DMEM and negative control wells containing cells treated with the maximum venom concentration were included.

After 48 h incubation, cell viability was quantified using a CellTiter-Blue based assay. The cell variability for cytotoxicity (IC_{50}) was calculated in relation to positive control (DMEM-only treated cells) where viability considered 100%. Briefly, CellTiter-Blue was added at 10%, according to the manufacturer's instructions, and the plate was incubated for 4-5 h at 37^{o}C and 5% CO_2. The ratio of viable cells was measured using fluorescence at 544 nm excitation and 590 nm emission filter sets.

Percentage cell viability was determined using an equation derived from (Chong et al. 2020):

$$\frac{(\text{Fluorescence of experimental sample}) - (\text{Fluorescence of negative})}{(\text{Fluorescence of positive sample}) - (\text{Fluorescence of negative})} \text{x}100$$

Where the positive control is the untreated cells (DMEM-only treated cells) for cytotoxicity assay (or antivenom only treated cells for immunocytotoxicity assay), negative control is cells treated with maximum venom concentration with Relative Fluorescence Unit (RFU) equivalent to the blank.

2.2.22 Half-maximal effective concentration (EC_{50})

To assess the EC_{50} of antivenoms against their target venoms, cells seeded and incubated overnight as described above (section 2.2.21) were treated with different antivenom concentrations mixed with a challenge dose of venom [see Appendix V(B)]. To achieve this, antivenom was added to the wells, mixed thoroughly and serially diluted across the plate. A prediluted venom was then added across the plate that contained the serially diluted antivenom and mixed thoroughly by pipetting up and down at least three times. As mentioned above (section 2.2.21), untreated cells (i.e., DMEM-only treated cells), negative (venom dose inducing maximum cell death) and positive (antivenom only treated cells) controls were included. The dilution plate containing the venom-antivenom mixture was placed on a microplate shaker for 1 minute before and after being incubated for 1 h at 37°C and 5% CO_2. Following incubation, 100 µL of the venom-antivenom mixture was transferred to the seeded cell culture plate, which was incubated for 48h at 37°C and 5% CO_2.

After 48 h incubation, cell viability was quantified using a CellTiter-Blue based assay as described above (section 2.2.21). The cell variability for the neutralisation assay (EC_{50}) was calculated in relation to positive control (antivenoms only treated cells) where viability considered 100%, using the equation shown in section 2.2.21.

2.2.23 Data analysis

Unless stated otherwise, data analysis was performed using GraphPad Prism 9 software (San Diego, California, USA). Nonlinear curve, 4- parameters (Top, bottom, logIC50 and Hillslope) were performed to calculate the Half-maximal inhibitory concentration (IC_{50}) values / Half-maximal effective concentration (EC_{50}). Results were expressed as mean ± SD of three independent biological repeats comprising three technical replicates, unless stated otherwise. Statistical significance was determined using either unpaired *t-test* with Welch's correction or One-Way Analysis of Variance (ANOVA) with Tukey post hoc test method, unless stated otherwise. Data were considered significant at $p<0.05$.

The median lethal dose (LD_{50}) and median effective dose (ED_{50}) of snake venom and antivenoms, respectively, on *G. mellonella* were determined using Probit analysis (World Health Organization 2016) with SPSS software (Version 27.0). Probit is derived from probability + unit, and it is a type of regression that used to analyse binomial variables. Basically, it works by transferring sigmoidal dose-response curve into straight line which is analysed by regressions using techniques such as least square and maximum likelihood.

For the Probit analysis, mortality / survival was the 'response frequency'; dose was the 'covariate', and the total number of tested larvae was set as the 'total observed'. LD_{50} values were expressed as mean ± SD of three independent biological repeats for each concentration of venoms/ antivenom. Similarly, ED_{50} values were expressed as mean ± SD of at least two independent biological repeats for antivenom used against each venom.

Chapter 3: Developing a manufacturing process for polyvalent antivenoms

3.1 Introduction

Snakebite envenoming (SBE) constitutes a major health and economical challenge, particularly to subsistence farmers in the tropical regions of Africa, Asia, and Latin America (Kasturiratne et al. 2008; Chippaux 2011; Benjamin et al. 2018). In sub-Saharan Africa (SSA), an increase in the incidence of SBE is accompanied by lack of adequate infrastructure and effective medical interventions resulting in the use of traditional remedies being favoured. Despite the global burden of this health problem (Kasturiratne et al. 2008; Gutierrez et al. 2017a), parenteral administration of heterologous antivenom remains the only approved therapeutic agent currently available to treat the mortality and morbidity associated with SBE (Gutierrez et al. 2014). Factors such as antivenom efficacy, timing of administration and venom toxicity are amongst the key factors which affect the outcome of the intervention. Thus, if managed appropriately, antivenom can potentially reverse the major effects of systemic envenoming, e.g., haemorrhage and coagulopathy (Habib 2015). Sadly, there is no evidence to suggest that conditions such as psychological, post-traumatic stress disorders (PTDs) and amputations can be improved by antivenom interventions (Wijesinghe et al. 2015).

Antivenoms were first introduced to Africa in the 1950s, and since then has saved many lives, whereby SBE related deaths have reduced by 70% (Stock et al. 2007). Despite such a tremendous achievement, the sale of antivenom has progressively declined since the 1970s reportedly by 60-80% (Chippaux 1998). Initially, the Bheringwerke (Germany), Aventis Pasteur (institute Pasteur, France) and the South African Institute for Medical Research (SAIMR) were the only three antivenom suppliers across the African continent (Laing et al. 2003). Currently, there are 15 antivenoms (11 polyvalent and 4 monovalent) available in the SSA market (Potet et al. 2019) supplying approximately 400,000 vials annually (Chippaux 2011; Brown 2012). However, this provides only around 2.5% effective treatment of the current need to treat SBE occurring in SSA (Brown 2012) estimated to be between 435,000 and 580,000 cases per annum (Gutierrez et al. 2017a). The result is 1.03 million disability-adjusted life years (DALYs) being incurred annually

(Halilu et al. 2019). DALY is a universal metric used to estimate the disease burden based on robust economic and ethical principles which can guide policies which deliver cost-effective healthcare (Kasturiratne et al. 2017). Therefore, it will require 1.5 – 2 million doses per annum, to successfully treat the morbidity and mortality currently associated with SBE in SSA region (Stock et al. 2007).

Antivenom is a relative expensive therapy, with a highly variable price between $40 and $24,000 (Brown 2012). The cost of antivenom in SSA is between $18 to $200 per vial (Brown 2012) with an estimated average recommended retail price of $124 per dose (Hamza et al. 2016). With the exception of the relatively expensive ($315) South African antivenoms; SAVP-SAIMR (*Echis* monovalent) and SAVP-SAIMR polyvalent (Harrison et al. 2017), the cost of life-saving treatment in SSA ranges from $1,997 to $6,205 whereas each reduction in DALY requires between $73 and $247 (Hamza et al. 2016). This variation is likely to be due to variable antivenom efficacy, for example, when a double dose is required as well as the complexity of the healthcare set up. Antivenom itself accounts for approximately 64% of the total treatment cost, the remaining expenses being for healthcare services (Habib et al. 2020). Nevertheless, the majority of communities most affected by SBE live below the poverty line, and in addition face the risk of contracting other tropical diseases, both communicable and non-communicable. All in all, it is obvious that antivenom in SSA is neither sufficiently available nor affordable for all, particularly for those who most need it.

In response to the current antivenom crisis in Africa (Brown 2012), a few new antivenoms were introduced in the 2000s (Laing et al. 2003; Ramos-Cerrillo et al. 2008). Although it was hoped that this would resolve the paucity of antivenom across the continent, the cessation of Fav-Afrique™ (section 1.3.10) in 2014 has raised concerns and left unmet challenges (Potet et al. 2019). The result was that low quality antivenoms were imported from India and other Asian producers, some of which were biogeographically irrelevant, and their administration led to tragic treatment failures (Visser et al. 2008; Guidolin et al. 2016). The acute shortage of antivenom together with global recognition of SBE in 2017 (Chippaux 2017), were key factors in promoting the WHO to establish a Roadmap with the overall aim to halve SBE mortality

and morbidity by 2030 (Habib et al. 2020). Towards this goal, the WHO project has four main objectives: (1) To ensure that safe and effective antivenom are affordable and accessible to all, (2) To empower and engage communities, (3) To improve healthcare systems, and (4) To establish partnerships, coordination and resources (Williams et al. 2019a).

All of the commercially available antivenom formats [Fab, $F(ab')_2$ and intact IgG] are effective at neutralising snake venoms, albeit presenting different pharmacokinetics (Gutiérrez et al. 2003). This suggests that the efficacy of an antivenom is dependent on factors such as immunisation strategy, manufacturing process, venom toxicity and time to administration (León et al. 2011). Immunisation strategy and time to administration are outside the remit of this Thesis, thus focusing on the manufacturing process.

Despite being over 100 years since development of antivenom, few changes have been introduced to the original method, first developed by Calmette and colleagues (Squaiella-Baptistao et al. 2018). Modifications include the introduction of steps such as pepsin digestion, chromatography and caprylic acid precipitation. Although whole IgG antivenom is still in use, primarily in SSA (Potet et al. 2019) and Latin America (Otero et al. 1999; Otero-Patiño et al. 2012), the $F(ab')_2$ -based polyvalent antivenom is the most common commercial product worldwide (Laustsen et al. 2018). This is because the Fc fragment is thought to be responsible for initiating the anaphylaxis and serum sickness, frequently observed during antivenom administrations (Leon et al. 2013). However, antivenom adverse reaction appears to be outside the Fc domain, because even the highly pure affinity purified Fab antivenom products (e.g., CroFab®) may induce allergic reactions (Dart and McNally 2001; Ruha et al. 2002; Cannon et al. 2008). Whilst the removal of the Fc domain will reduce protein load, there is growing evidence to suggest that process-related impurities are significant triggers of adverse reactions in patients treated with antivenom (Malasit et al. 1986; Lalloo and Theakston 2003; Chippaux et al. 2015b; de Silva et al. 2016; Morais 2018).

It is important that antivenom manufacturers implement ‘Good Manufacturing Practice’ (GMP) to improve the safety of antivenoms. Globally, some excellent methods exist and are producing consistently safe and effective antivenoms, mainly for the USA (Dart and McNally 2001), Europe (Smith et al. 1992; Pepin-

Covatta et al. 1997) and Australia (Herrera et al. 2014). Because most of the technology behind these methods are complex and expensive, they have not been considered for global production. However, in most cases, the major expense is setting-up the manufacturing facility. Once the initial set-up has been successfully implemented, a harmonised and sustainable supply of antivenom can be maintained. More importantly, it is down to the quality system and regulatory bodies of the country of origin to ensure that strict measurements are in place for producing consistently high-quality antivenom.

3.2 Aims and objectives

With this in mind, Chapter 3 aims to develop a robust and inexpensive manufacturing method for developing affordable and effective polyvalent antivenom for use in SSA. The starting material used for this study was the hyperimmune horse plasma (HHP) used for the manufacture of Fav-Afrique™ prior to its termination in 2014 (Potet et al. 2019). Therefore, the antivenom produced in this study must meet the key quality specifications defined for Fav-Afrique™ including purity, efficacy and excellent formulation stability.

The process used to manufacture Fav-Afrique™ was exhaustively complex and significantly expensive, which was the main reason for its cessation (Chippaux and Habib 2015). To avoid this happening again, the present study has envisaged a simple and relatively inexpensive but realistic and scalable manufacturing process to generate intact IgG and $F(ab')_2$ antivenoms. It is important to emphasise that if successful, it would enable the commercial sponsor of this project (MicroPharm) to consider implementation of this method into their manufacturing pipeline.

3.3 Results

3.3.1 Preparations of IgG-based antivenom

3.3.1.1 Identifying the optimum operating parameters for the caprylic acid precipitation of equine IgG

In contrast to an earlier study which suggested the use of 5% (v/v) caprylic acid (Rojas et al. 1994), 3% was the optimum concentration selected for this study. Initially, the optimum operating range of different factors were investigated for the caprylic acid precipitation of equine IgG. These factors were: caprylic acid concentration [1 to 10% (v/v)], temperature (22℃, 25℃ and 37℃), pH (4.5, 5.0 and 5.5) and solubilisers (WFI and 0.9% NaCl). This was performed during the early stage of research and development. Following the determination of these parameters, 4.0 L of HHP constituting 1.0 L from each group of immunised horses (see section 2.2.1) were mixed. The study has revealed that increasing the caprylic acid concentration favours the purity (Figure 3.1 A-D) but not the yield (Table 3.1). Although all the samples presented on Table 3.1 (except 10%) were analysed on SEC-HPLC, only samples 1%, 2%, 4% & 5% are shown on Figure 3.1A-D. Although the caprylic acid concentrations at 2% and 3% (v/v) have shown negligible difference on purity and yield, the 3% (v/v) was selected for this study because it is supported by historical protocols at MicroPharm Ltd. This is because 3% caprylic acid is supported by validated data; for example, for viral clearance as per MicroPharm protocols. Consistent with (Kurtović et al. 2019), caprylic acid concentrations at ≥5% were associated with higher turbidity and slow filtration (data is not shown here).

Table 3.1 Yield of IgG at different caprylic acid concentration.

Caprylic acid %(v/v)	1%	2%	3%	4%	5%	6%	7%	8%	9%	10%
Yield (g/L)	24.2	18.9	18.7	16.6	13.5	15.1	15.8	16.3	15.2	ND

The sample treated with 10% caprylic acid- denoted by “ND; for not determined” was difficult to filter.

Together with the 3% (v/v) caprylic acid, a temperature of 22°C ±1°C and pH 4. 88 ±0.05 were identified as the optimum parameter for a maximised yield (Figure 3.2) and enhanced purity of IgG (Figure 3.3 D). pH data is not shown. Solubilising the heated plasma with WFI (at 0.5x its volume) also enhanced

the yield whilst heat-inactivation improved the purity of IgG, but adversely affected its yield.

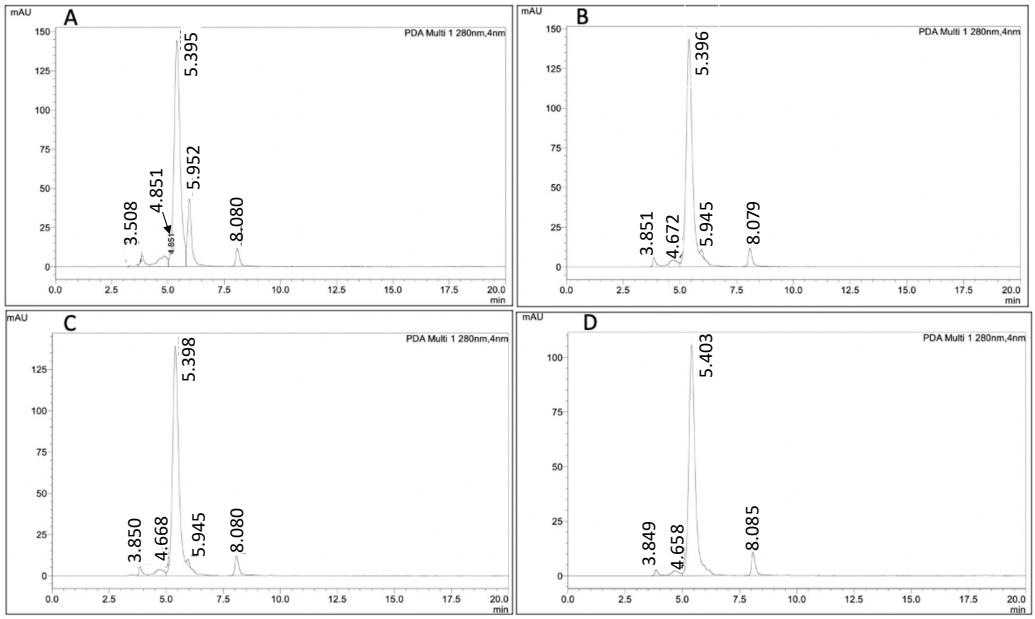

Figure 3.1 SEC-HPLC profiles for IgG samples purified with different caprylic acidic concentrations (v/v).

A (1%), B (2%), C (3%) and D (5%) caprylic acidic concentrations (v/v). SEC-HPLC was performed using Agilent AdvanceBio SEC 300 Å, 2.7 µm, 4.6 x 150 mm column connected to Shimadzu Prominence HPLC. Analysis was performed at a flow rate of 0.5 mL/min using 20 mM phosphate, 130 mM sodium chloride, 0.02% sodium azide, pH 6.0±0.2 at room temperature and the absorbance was monitored at 280 nm. Based on the molecular weight of components present within equine plasma, molecules at peaks ~Rt 3.5 min could be aggregates, peak at ~Rt 3.8 min is likely to be IgM (~ ≥ Mr 700 kDa), peak at ~Rt 4.7 and 4.8 min appears to be IgA and/or IgG dimer, peak at ~Rt 5.4 corresponds to IgG, peak at Rt 6.0 could be albumin. The peak at ~Rt 8.1 min appears to be caprylic acid and/or LMW impurities. Data analysis was performed using LabSolutions software, Shimadzu corporation.

Abbreviations: SEC-HPLC, Size-Exclusion Chromatography-High-performance Liquid Chromatography, Rt; retention time; kDa, kilodalton; IgA, immunoglobulin A; IgM, immunoglobulin M; LMW, low molecular weight.

3.3.1.2 Improving purity of IgG-based antivenoms

The effects of factors such as heat-inactivation, solubilisation agents and mixing temperature on the purification of HHP were determined and results are shown on Figure 3.2. All samples presented in Figure 3.2 were thermally treated at 56°C ±1°C for 1 h and allowed to cool to 22°C (±1°C) before being

diluted by 0.5x starting plasma volume with either WFI or 0.9% NaCl. The pH of all samples was adjusted to 4.88±0.05 using 1.74 M acetic acid before being treated with 3% (v/v) caprylic acid. All samples were then mixed vigorously, using a magnetic stirrer for 1 h at either 22°C or 25°C or 37°C. Although a maximum of 66.5% yield of IgG was achieved at a mixing temperature of 22°C, when all factors considered, the experiment has a starting yield of 58.7%.

The heat-inactivation step (1 h at 56°C) facilitated the removal of high molecular weight (HMW) species and Ig aggregates. However, as shown in Figure 3.2, this step is associated with product loss where approximately 53% of IgG was recovered from caprylic acid treatment of heated plasma compared to approximately 60 to 70% with caprylic acid alone.

These results correlate with previous studies that showed heat inactivation only slightly affected yield of IgG (Kurtović et al. 2019). However, it improved the purity and removal of HMW impurities, which may persist throughout the process if not removed at this stage.

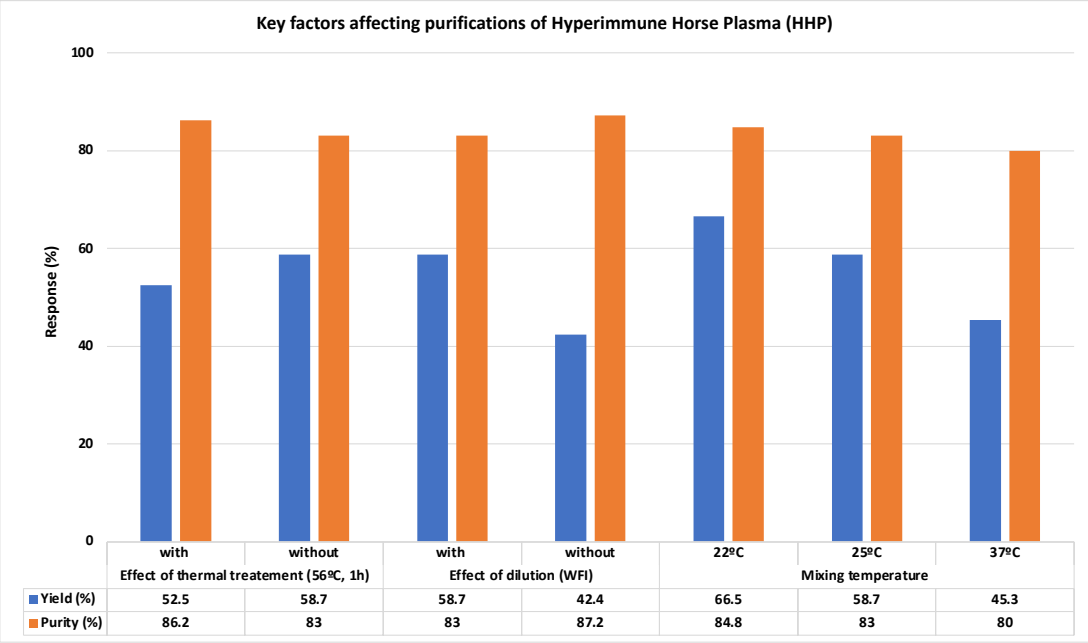

Figure 3.2 Key factors affecting the yield and purity of caprylic acid fractionated equine IgG.

All samples were treated with 3% (v/v) caprylic acid. Protein concentration was measured as described in section 2.2.4. Data were collected from at least three independent replicates and were analysed on Microsoft Excel.

Abbreviation: WFI, Water for Irrigation.

Under the optimum conditions identified in this study (section 3.3.1.1), the majority of non-immunoglobulin molecules, particularly albumin (Figure 3.3 A), were significantly reduced by the caprylic acid precipitation (Figure 3.3 B).

The removal of low molecular weight (LMW) species such as m-cresol (108.14 g/mol) and caprylic acid (144.21 g/mol) required a diafiltration (100 kDa nMWCO) step (Figure 3.3 C) followed by passage through an activated carbon filter (Figure 3.3 D). The formulated final drug product (Figure 3.3 D) was greatly purified IgG with a SEC-HPLC purity profile of approximately 96%. Also see Appendix II (A) for a detailed whole IgG manufacturing process map.

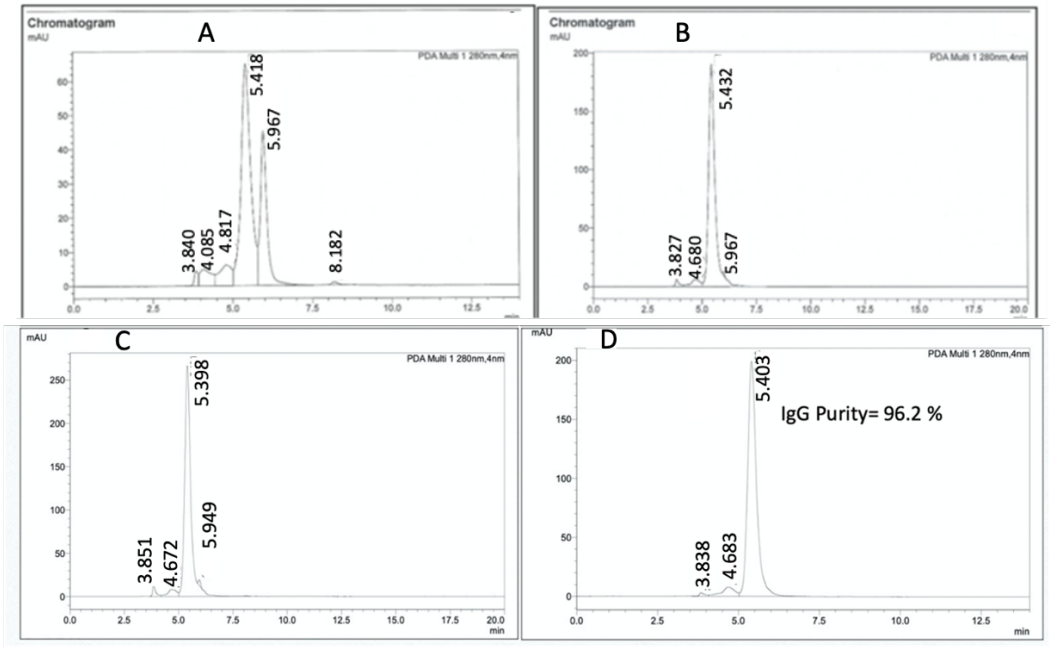

Figure 3.3 SEC profiles demonstrating the purity of equine IgG at different purification stages.

Description: Hyper immune horse plasma (A), activated carbon filtered caprylic acid precipitated IgG (B), diafiltered IgG product (C), and formulated IgG based antivenom product (D). SEC was performed using Agilent AdvanceBio SEC 150 Å, 2.7 µm 4.6 x 150 mm column connected to Shimadzu Prominence HPLC. Analysis was performed at a flow rate of 0.5 mL/min using 20 mM phosphate, 130 mM sodium chloride, 0.02% sodium azide, pH 6.0±0.2 at room temperature and the absorbance was monitored at 280 nm. Based on the molecular weight of components present within equine plasma, molecules at peaks ~R_t 3.8 min could be aggregates (or fibrinogen), peak at ~R_t 4.1 min is likely to be IgM (~ ≥ M_r 700 kDa), peaks at ~R_t 4.7 & 4.8 min appears to be IgA and/or IgG dimer, peak at R_t 5.4 min corresponds to IgG, peak at ~R_t 6.0 min could be albumin. Peaks at *Rt* 8.2 min to be caprylic acid and/or LMW impurities.

Descriptions of data analysis and abbreviations are consistent with Fig. 3.1.

Consistent with WHO recommendations (World Health Organization 2016), the purity of the IgG-based antivenom was further analysed using SDS-PAGE under non-reducing (Figure 3.4 A) and reducing conditions (Figure 3.4 B). Using a Coomassie stain, an intense double-band was visualised at approximately 150 kDa (non-reducing; Figure 3.4 A) and at approximately 60 kDa (reducing condition; Figure 3.4 B). This may suggest that this band represents an equine IgG isotype which comprises more than one IgG subclass with slightly different MWs (Sugiura et al. 2000; Lewis et al. 2008); also see section 4.3.2, Figure 4.2 and Figure 4.3 in chapter 4 of this Thesis. Additional faint bands were detected at ~250 kDa and ~125 kDa (Figure 3.4 A), which is likely to indicate the presence of minor aggregates and/or equine Ig components. Overall, the final product has a purity profile ≥95% (see Figure 3.3 D), which meets the current WHO recommendation for purity of antivenom products of >90% (World Health Organization 2016).

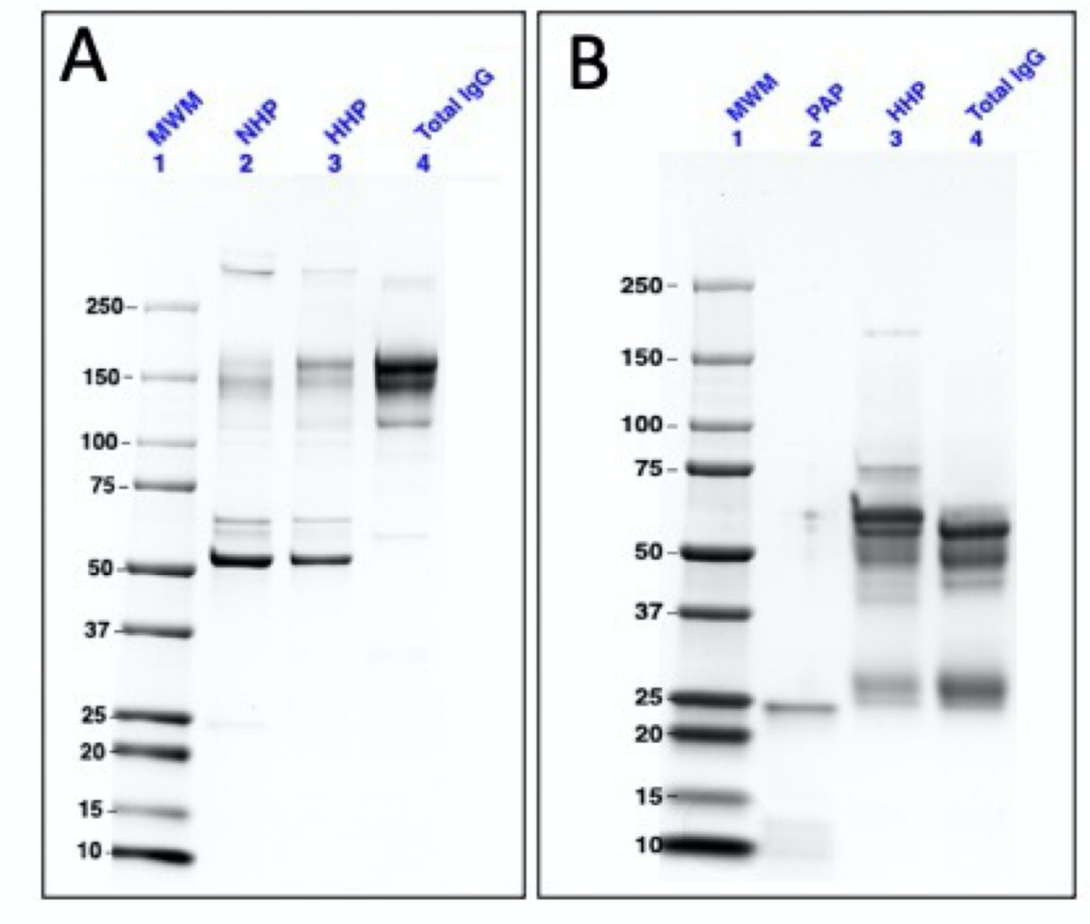

Figure 3.4 Assessing purity profile of IgG AV under SDS-PAGE.

The image represents Coomassie stain of electrophoresed proteins under non-reducing (A) and reducing (B) conditions. All proteins were loaded at 5 µg/well. NHP and PAP are

negative controls. All proteins were loaded at 5 µg/well. NHP and PAP are negative controls. HR-conjugated goat anti-horse IgG (H+L) was diluted at 1: 5000 dilutions in blocking buffer. Full details are given in section 2.2.9.1. HHP is the starting material prior to purifications and the total IgG is the final formulated IgG-based AV. Full details of SDS-PAGE method is given in section 2.2.9.1. Abbreviations: MWM, molecular weight marker (Dual Colour standard protein, Bio-Rad); NHP, Non-Hyperimmune Horse Plasma; PAP, papain; HHP, Hyperimmune Horse Plasma; AV, antivenom.
Note that, the two experiments were run independently and with a different experimental time.

3.3.1.3 Optimising pepsin digestion for generating F(ab')$_2$ -based antivenom

The IgG product that was used for the F(ab')$_2$ preparation was generated using caprylic acid precipitation, as described on section 2.2.2. Whilst providing complete IgG digestion, the process was carefully optimised to prevent denaturing the antibodies. To achieve this, the optimum operating parameters for pepsin digestion was determined as follows: pepsin concentration of 2% (w/w) pepsin to IgG, reaction time of 60 min (±10 min), temperature 30℃±1℃ and pH 3.05 ± 0.05. These process-related parameters were developed following historical data from MicroPharm Ltd. Most of the LMW species and/or degraded impurities including Fc and pepsin residues were removed using diafiltration against a 50 kDa nMWCO PES membrane. Also, see Appendix II (B) for a detailed F(ab')$_2$ manufacturing process map.
As determined by SEC-HPLC (Figure 3.5), a F(ab')$_2$ antivenom with purity of 97% was generated by passing the diafiltered product through QXL column (20 mM piperazine, 65 mM NaCl; pH 5.0±01). Under these chromatographic conditions, impurities such as residual Fc and pepsin were eliminated from the product by selectively binding these impurities to the matrix, whilst permitting the purer F(ab')$_2$ product to flow through the chromatography column.

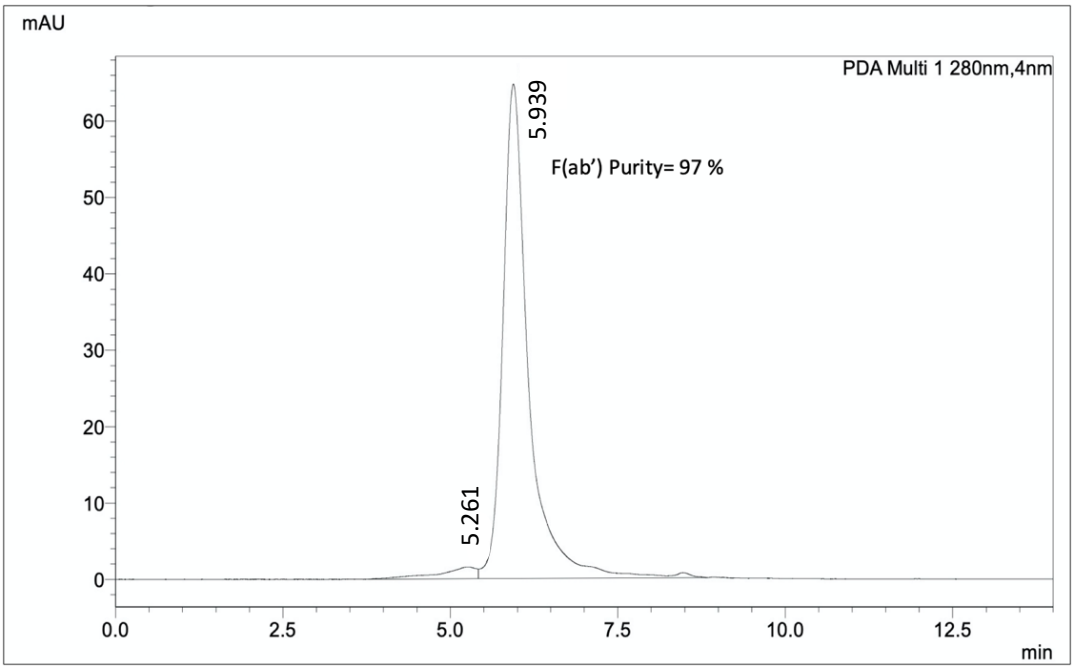

Figure 3.5 SEC profile demonstrating the molecular distribution of F(ab')$_2$.

F(ab')$_2$ represents 97% of the total protein content. SEC-HPLC was performed using Agilent AdvanceBio SEC 300 Å, 2.7 µm 4.6 x 150 mm column connected to Shimadzu Prominence HPLC. Analysis was performed at a flow rate of 0.5 mL/min using 20 mM phosphate, 130 mM sodium chloride, 0.02% sodium azide, pH 6.0±0.2 at RT and the absorbance was monitored at 280 nm. Based on the molecular weight of components present within equine plasma, molecules at peaks ~R_t 5.3 min could be soluble dimer and peak at ~R_t 5.9 corresponds to F(ab')$_2$. Data analysis was performed using LabSolutions software, Shimadzu corporation.

Abbreviations are consistent with Fig. 3.1.

3.3.1.4 Purity assessments

Consistent with WHO recommendations (World Health Organization 2016), the purity of the F(ab')$_2$ product was further analysed by SDS-PAGE under reduced (Figure 3.6 A) and non-reduced (Figure 3.6 B) conditions showing clearance of HMW species /aggregates. Furthermore, results obtained by Western blot analysis have demonstrated that the chromatography step effectively removed impurities, including pepsin (Figure 3.6 C) and Fc (Figure 3.6 D) residuals.

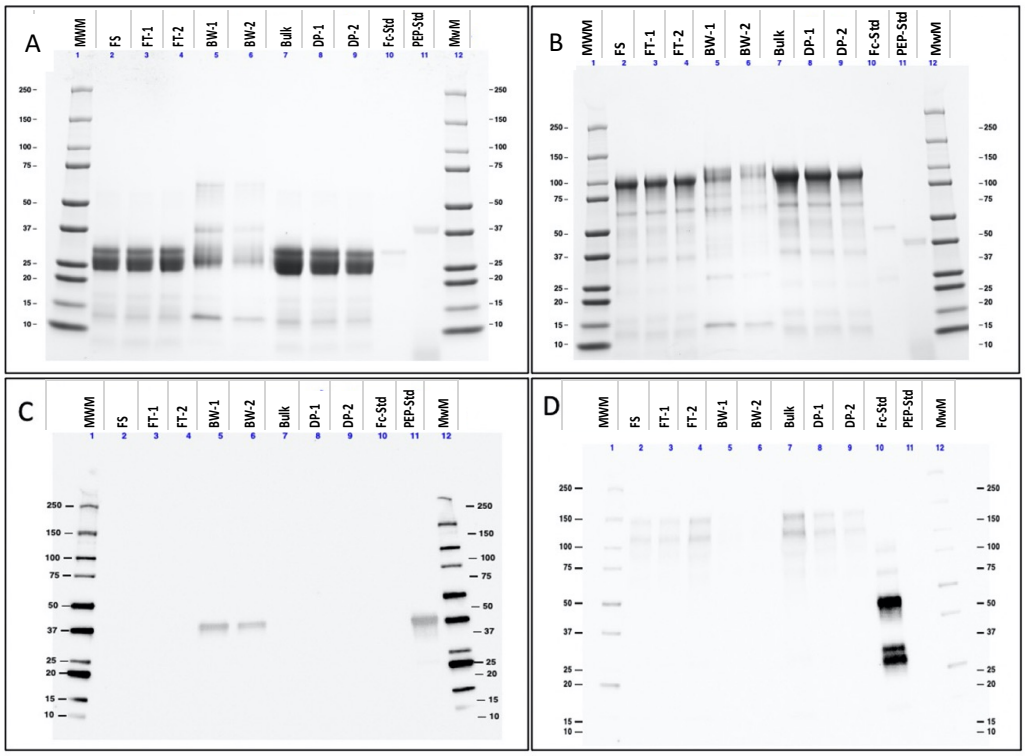

Figure 3.6 Gel electrophoresis to assess the purity of F(ab')$_2$ AV product:
Electrophoresed proteins represent A) reduced Coomassie stain, B) non-reduced Coomassie stain, C) Western blot (under non-reduced conditions) against pepsin, D) Western Blot (under non-reduced condition) against Fc. All proteins were loaded at 5 µg/well and the HRP-conjugated goat anti-pepsin (C) and goat anti-horse IgG Fc (D) antibodies were diluted in blocking buffer at 1:5,000. Full details of SDS-PAGE and Western blot methods are given in sections 2.2.9.1 and 2.2.9.2, respectively.
Descriptions and abbreviations: FS, feed stock for AEX; FT-1 & FT-2, flow through fractions (from run 1 & run 2, respectively); BW-1 & BW-2, bound wash (from run 1 & run 2, respectively); Bulk, Active Pharmaceutical ingredient (API) prior to formulation; DP-1 & DP-2 final drug product (from run 1 and run 2, respectively) formulated in 0.9% NaCl + 0.05% PS80; MWM, molecular weight marker

Furthermore, SDS-PAGE using Coomassie stain and Western blot analysis were used to assess the presence of residual albumin within the antivenoms. As shown in lane 2, Figure 3.7 A, under non-reducing conditions, horse albumin band is detected at approximately 65 kDa (Ramos-Cerrillo et al. 2008). The absence of this band in lanes 3&5 for Coomassie stained SDS-PAGE (Figure 3.7 A) may indicate that both the F(ab')$_2$ and IgG antivenom products are free from albumin contaminants. Complete absence was, however, confirmed by the more sensitive Western blotting method (Figure 3.7

B). Surprisingly, both the SDS-PAGE and Western blot results have shown some residual albumin in the EchiTab Plus ICP (Figure 3.7 A&B, lanes 6).

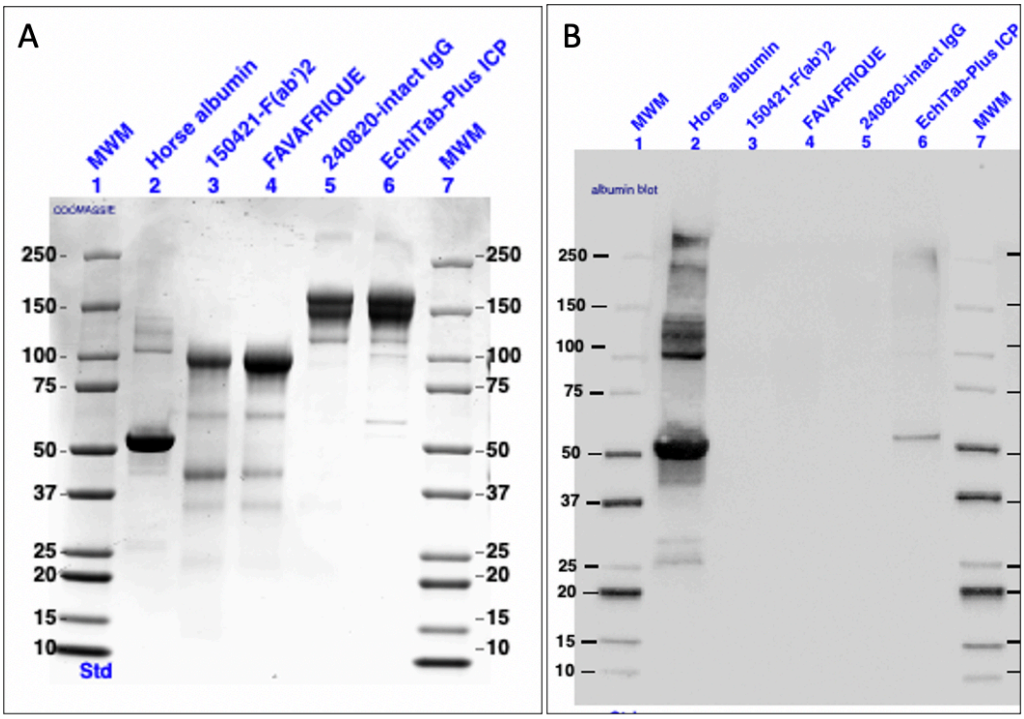

Figure 3.7 Gel electrophoresis to detect residual albumin in IgG and F(ab')$_2$ AVs.

The diagram represents electrophoresed proteins under non-reduced conditions for: a) Coomassie stained SDS-PAGE and B) western blot analysis against albumin. All proteins were loaded at 5 µg/well and HRP-conjugated goat anti-horse albumin (B) was prediluted in blocking buffer at 1:5,000. Full details of SDS-PAGE and Western blot methods are given in sections 2.2.9.1 and 2.2.9.2, respectively.

Descriptions: EchiTab G Plus is whole IgG AV; 150421-F(ab')2 is the polyvalent F(ab')$_2$ AV; 240821 is the polyvalent intact IgG AV (the numbers in both cases indicate for batch number); FAVAFRIQUE is the Fav-AfriqueTM product reported in this study.

Abbreviations: MWM, molecular weight marker; HRP, Horseradish peroxidase

3.3.1.5 Stability profile of the antivenoms

Both the IgG and F(ab')$_2$ antivenom products have demonstrated excellent stability in both accelerated temperature (37℃, relative humidity of 75% ±5%) and real-time temperature (2℃ - 8℃) studies for eight months. Although there is not a fixed rule to predict a long-term stability at real time from accelerated temperatures, particularly for biologics, there is a general consensus suggesting that 6 months at 37℃ is equivalent to 2 years at 2-8℃ (Matt Aldridge and Hayley Jekeman, personal communications). However, each

formulation should be studied independently to accurately determine the extrapolation of accelerated temperature to real-time. This is because the stability mechanism in biologics is primarily affected by factors such as excipients, pH and protein concentration (Segura et al. 2009; Manning et al. 2010; Al-Abdulla et al. 2013).

The antivenoms presented a colourless and slightly opalescent appearance, with no particles or fibres, following visual assessment using the Apollo II system (Figure 3.8 A&B), See Appendix II (C). Thus, the antivenom produced in this study has demonstrated excellent and essential shelf-life stability features, suggesting that the antivenom product may stay stable and efficacious for the indicated period of time.

Antivenoms passed visual assessment until the end of the study, after which access to the samples was no longer possible. This protocol is consistent with the WHO recommendations (World Health Organization 2016).

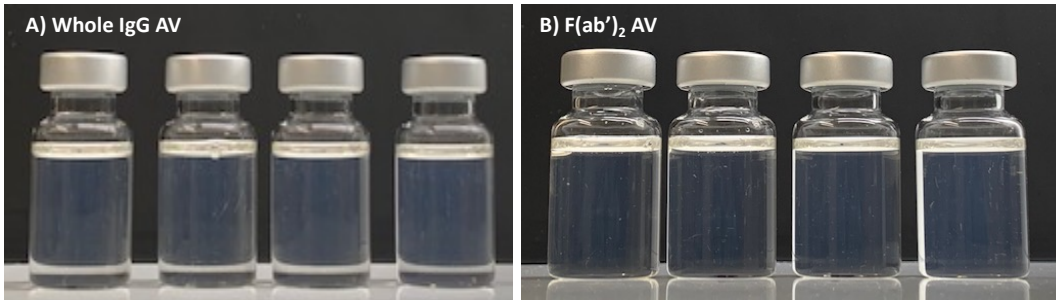

Figure 3.8 Visual assessment for (A) IgG and (B) F(ab')$_2$ antivenoms at 37℃.

Descriptions: Whole IgG and F(ab')$_2$ are polyvalent AVs (against the ten snake species endemic to the SSA region). Visual assessment was performed using the Apollo II system as per MicroPharm Ltd QC protocol. All samples presented here were from 37℃ stability condition. Abbreviations: AV, antivenom; IgG, immunoglobulin

3.3.1.6 Recognition of snake venoms by different antivenoms

The capacity of the antivenoms to interact with the different venom toxins was analysed using Western blot analysis (Figure 3.9 A-D) and their ability to recognise the relevant venom constituents was compared to that of FAV-Afrique™. The FAV-Afrique™ antivenom product has used the same HHP material that was used to prepare the antivenoms in this study (see sections 1.3.10 and 2.2.1). The manufacturing process for FAV-Afrique™ involved

harvesting IgG by ammonium sulphate precipitation followed by pepsin digestion and DEAE purification.

The Coomassie stained SDS-PAGE revealed venom proteins in the range of 10 kDa to 150 kDa with venoms from the viper species dominated by HMW toxins (Figure 3. 9 A; Lanes 2, 3, 7& 8) and elapid by LMW toxins (Figure 3.9 A; Lanes 4, 5, 6, 9, 10&11). This is consistent with published proteomic studies (Calvete et al. 2007; Wagstaff et al. 2009; Petras et al. 2011; Malih et al. 2014; Laustsen et al. 2015; Lauridsen et al. 2016; Petras et al. 2016; Lauridsen et al. 2017).

Western blot analysis revealed that both the IgG (Figure 3.9 B) and $F(ab')_2$ (Figure 3.9 C) antivenom products were effective at recognising the major venom constituents of *Echis* and *Bitis* species seen in Coomassie stained SDS-PAGE gels (Figure 3.9 A; Lanes 2, 3, 7& 8). The IgG antivenom (Figure 3.9 B) has shown poor binding with some of the key LMW venom toxins visualised in the Coomassie stained gels (Figure 3.9 A), particularly those from *Dendroaspis* and *Naja* species (Figure 3.9 A; Lanes 4, 5, 6, 9, 10& 11). On the other hand, the $F(ab')_2$ antivenom (Figure 3.9 C) was as effective as the FAV-Afrique product (Figure 3.9 D) at recognising all the major toxin bands revealed in the Coomassie stained gels (Figure 3.9 A). It is interesting that, despite having been derived from the same HHP material, the IgG failed to recognise the LMW toxins which may indicate that a higher protein concentration of the antivenom was required to generate equivalent band intensity.

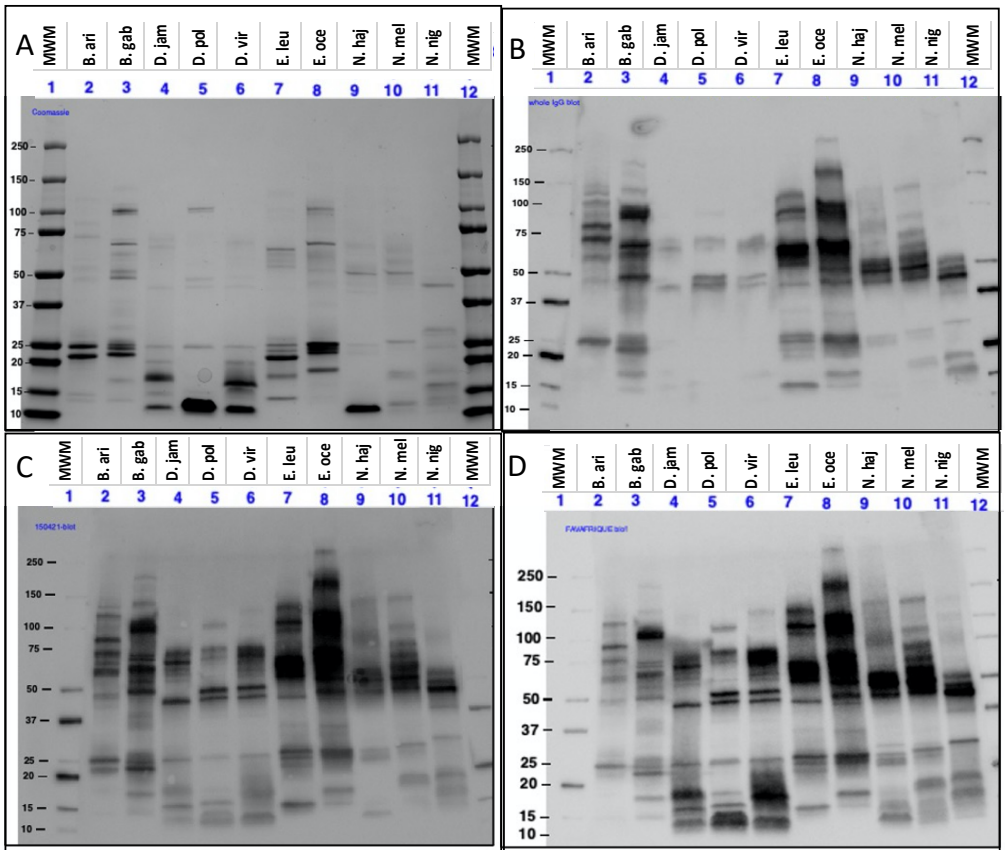

Figure 3.9 SDS-PAGE and Western blot analysis of venom: antivenom interactions:

The diagram represents electrophoresed snake venoms under non-reduced conditions for: a) Coomassie stain of Electrophoresed snake venom proteins B) Western blot against whole IgG antivenoms, C) Western blot against F(ab')$_2$, and D) Western blot against FAV-Afrique^{TM} products. To achieve high separation resolution, all venom proteins were loaded at 2.5 µg/well. Antivenoms were diluted in blocking buffer at 2 µg/mL and HRP-conjugated goat anti-horse IgG (B) and goat anti horse F(ab')$_2$ (C&D) antibodies were diluted 1:5000 in blocking buffer. Full details of SDS-PAGE and Western blot methods are given in sections 2.2.9.1 and 2.2.9.2, respectively.

Abbreviations: MWM, molecular weight marker; B. ari, *Bitis arietans*; B. gab, *B. gabonica*; D. jam; *Dendroaspis jamesoni*; D. pol, *D. polylepis*; D. vir, *D. viridis*; E. leu, *Echis leucogaster*; E. oce, *E. ocellatus*; N. haj, *Naja haje*; N. mel, *N. melanoleuca* and N. nig, *N. nigricollis*.

3.3.1.7 Yield of antivenom

This study reports an excellent yield, where approximately 15 g of a highly purified IgG product (~96%, by SEC-HPLC) was recovered from each litre of HHP. Similarly, about 7 g of F(ab')$_2$ was collected from each litre of HHP with

an enhanced purity of 97% (SEC-HPLC). As summarised in Table 3.2, the final formulation of IgG-based drug product is composed of 0.9% NaCl, 0.05% (v/v) polysorbate 80 (also known as Tween-80) and formulated at pH 7.5±0.1.

Table 3.3.2 Physiochemical properties of the IgG and F(ab')$_2$ antivenoms

Characteristics	Whole IgG AV	F(ab')$_2$ AV
Protein (g/L)	50±1	50±1
NaCl (g/L)	9	9
pH	7.4±0.2	7.4±0.2
Tween-80 (v/v)	0.05	0.05
Monomer content (%)	≥96	≥97
Fc content	N/A	Not detected
Albumin content	Not detected	Not detected
Aggregate content (%)	< 5	< 3

Abbreviations: g/L, gram per litre; v/v, volume-to-volume; N/A, not applicable.

3.3.1.8 Antivenom titres

To validate comparisons, all antivenoms were firstly diluted to 0.5 mg/mL then samples were serially diluted 3-fold in duplicate, starting at 1: 100 dilutions. Further details are given in section 2.2.10. As shown in Figure 3.10 A-D, the F(ab')$_2$ antivenom product has similar titration values compared to the control, i.e., Fav-Afrique™, against the *Bitis* and *Echis* species. This is indicated by the two curves [F(ab')$_2$ vs Fav-Afrique™; Figure 3.10 A-D], which have almost identical trends. In contrast, the IgG antivenom showed a considerably lower binding capacity against these *Viperidae* species, which shows the curve shifted slightly to the left (Figure 3.10 A-D). Such differences could arise due to the biochemical disparity between the IgG and F(ab')$_2$ molecules.

In this case, the titre of the antivenoms can be defined as the highest dilution (i.e., least concentration) that increased the signal response by 50% (or half-way on the linear section of the curve) compared to the OD of the negative control (i.e., NHP). This is equivalent to dilution 8100 (Figure 3.10, A-D and Figure 3.11, A-D).

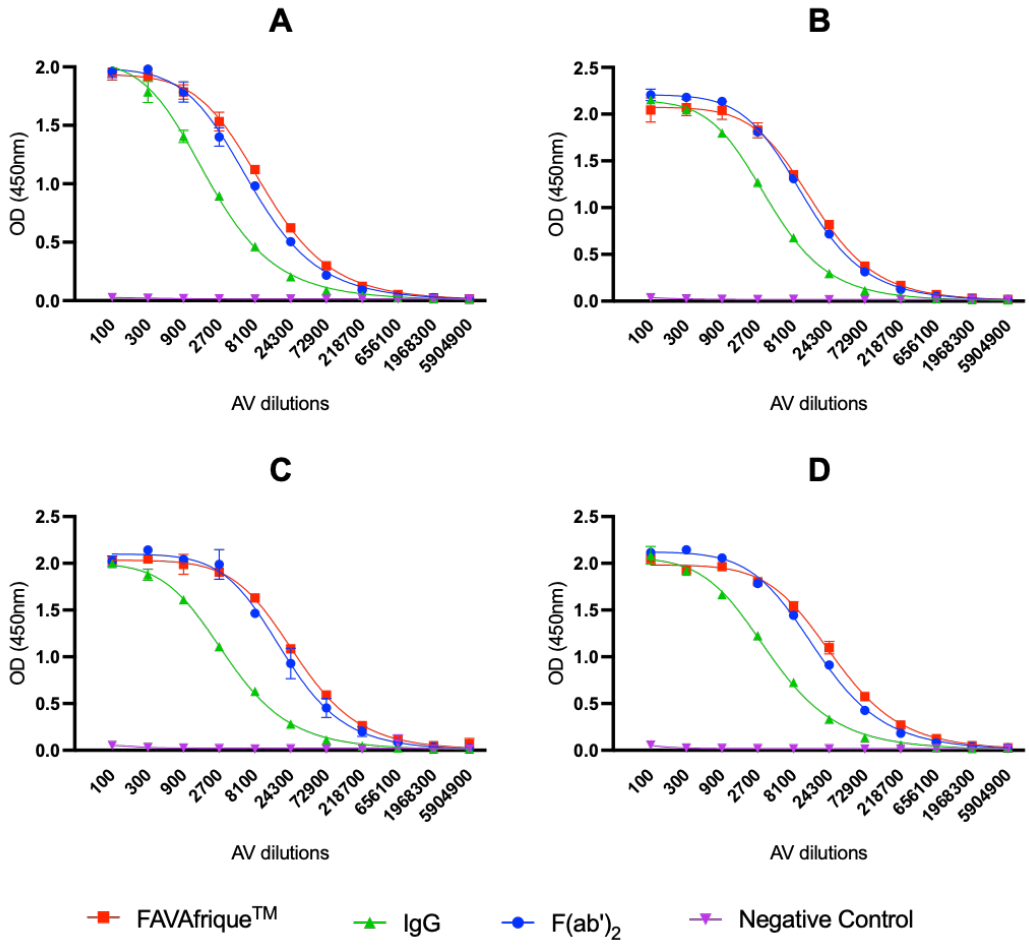

Figure 3.10 Titre for different AVs against a panel of *Viperidae* snake species.

Description: (A) *Bitis arietans*, (B) *B. gabonica*, (C) *Echis leucogaster* and (D) *E. ocellatus.* In compliance with QC protocols, results were obtained from a single data set. Data were analysed using Prism GraphPad 9. Non-linear curve representing log (agonist) vs response 4- parameters (top, bottom, hillslope and log EC_{50}) analysis was used to compare the titre of each antivenom against each snake venom. Error bars indicate mean ± SD from duplicates.

Abbreviations: AV, antivenom; OD, optical density; QC, quality control; IgG, immunoglobulin; F(ab')$_2$, divalent antigen-binding fragment

Compared to Fav-Afrique™, the F(ab')$_2$ antivenom shows a slightly lower titre against the *Naja and Dendroaspis* (both *Elapidae* genus); however, the Whole IgG product produced the weakest titre against the elapid venoms. This is indicated by the curves pattern shown on Figure 3.11 A-F. Thus, Fav-Afrique™ has the highest titre values against elapid venoms compared to the F(ab')$_2$ and IgG antivenom products. The Negative control was from non-

hyperimmunised horse plasma, and as expected, it produced a negligible signal against all of the tested snake venoms.

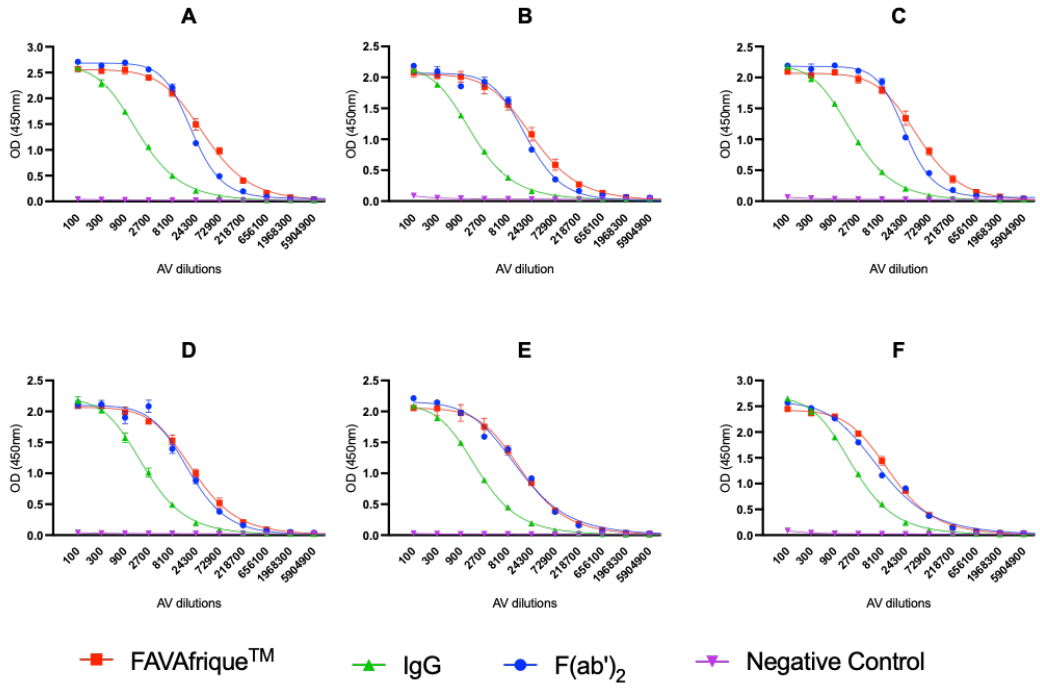

Figure 3.11 Titre for three different AVs against a panel of *Elapidae* snakes.

Description: *Dendroaspis jamesoni* (A)*, D. polylepis* (B)*, D. viridis* (C), *Naja haje* (D)*, N. melanoleuca* (E) and *N. nigricollis* (F). In compliance with QC protocols, results were obtained from a single data set. Data were analysed using Prism GraphPad 9. Non-linear curve representing log (agonist) vs response 4- parameters (top, bottom, hillslope and log EC_{50}) analysis was used to compare the titre level of each antivenom against individual venom. Error bars indicate mean ± SD from duplicates.

Abbreviations are consistent with Fig. 3.10.

3.3.1.9 Process development, optimisation and scalability

During the early research and development phases, small batches of 20 - 50 mL of HHP were used to cover several factors concurrently (see section 3.3.1.1). Once a suitable process was identified, a study of 2 x 1 L batches was performed to ensure the method is robust and reproducible. Data generated from the laboratory batches were used to assess purity, yield and the suitability of the process, generally. Once satisfactory results were obtained, a 4 L batch was used for manufacturing the antivenom products reported here. Key steps are outlined in the diagram shown in Figure 3.12.

The method was easy to perform, robust and reproducible, which may indicate this process would be fit to perform in production facilities, if considered for large-scale antivenom production.

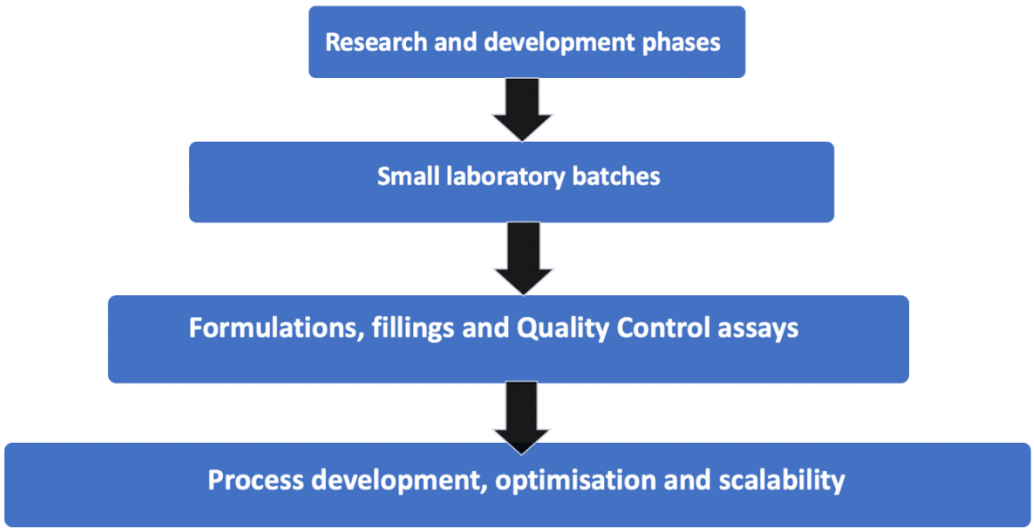

Figure 3.12 Hierarchy diagram showing main steps during antivenom development

3.4 Discussion

The manufacture of antivenom requires significant effort and resources, which increases cost, making it one of the most expensive medicinal drugs to produce (Stock et al. 2007). On the other hand, antivenom manufacturers need to make a profit in order to continue business. Where this balance was not achieved, multinational biopharmaceuticals, such as Sanofi Pasteur have ceased their supply of antivenom to Africa and switched to more profitable product pipelines (Potet et al. 2019).

The majority of the current commercially available antivenoms in the SSA are liquid formulations although a few lyophilised products exist (Habib et al. 2015b; Habib et al. 2020). As well as adding a significant cost (Hamza et al. 2016), lyophilisation of antivenom has several technical issues, including delayed treatment whilst reconstituting the product before use, making Ready-To-Administer (RTA) antivenoms the favoured drug products by clinicians. However, liquid formulations, particularly those which are protein-based, are prone to degradation and formation of particles, which may impact on the potency and, more importantly, the safety of antivenoms. The WHO recommends the comprehensive assessment of several physiochemical and biochemical parameters to ensure the safety and efficacy of antivenoms (World Health Organization 2016).

This study reports the development of optimised manufacturing processes for generating IgG and $F(ab')_2$ based liquid formulation antivenoms using caprylic acid precipitation followed by several downstream process steps. The pepsin cleavage of IgG method for generating the $F(ab')_2$ product was carefully optimised and adapted to prevent antibody denaturation. Thus, the operating parameters adapted for this study fall within the safe window for pepsin digestion of equine IgG (Morais and Massaldi 2005).

Although ammonium/sodium sulphates are still in use (Cresswell et al. 2005; World Health Organization 2016; García-Arredondo et al. 2019), caprylic acid precipitation is increasingly becoming the process of choice for many antivenom manufacturers (Otero et al. 1999; Gutierrez et al. 2005a; Abubakar et al. 2010b; Guidolin et al. 2016; Kurtović et al. 2019). This is because,

antivenom prepared by caprylic acid precipitation demonstrated excellent safety profiles at clinical trials, in addition to offering a higher yield and purity (Abubakar et al. 2010a; Abubakar et al. 2010b; Otero-Patiño et al. 2012). Furthermore, caprylic acid precipitation offers technical simplicity by enabling the proteins of interest (i.e., IgG) to be harvested from the supernatant which prevents the precipitate labile antibody from possible damage and degradation (Al-Abdulla et al. 2014). More importantly, caprylic acid is considered to be a viral removal/inactivation step, apparently by virtue of its ability to disrupt the integrity of enveloped viruses (Burnouf et al. 2004; Mpandi et al. 2007). Although there is no evidence suggesting that transfer of virus to humans from animal derived IgG, viral clearance constitutes an essential assessment for antivenom production (Caricati et al. 2013).

In compliance with WHO guidance for viral reduction measurements (World Health Organization 2016), the antivenoms produced in this study used an optimised caprylic acid precipitation at 3% (v/v) and pH 4.87, a critical parameter for the viral removal step. This is despite the report by (Kurtović et al. 2019), which showed that increasing the percentage of caprylic acid beyond 2% (v/v) does not necessarily lead to improved yield and purity and instead, it may adversely affect the process by causing filter blockages and slowing progress. However, existing data support that caprylic acid at 3% to 6% (v/v) is capable of offering viral removal/inactivation as recommended by the WHO (Mpandi et al. 2007) and (Al-Abdulla, personal communication).

In addition to offering process-related technical advantages (Guidolin et al. 2016; Kurtović et al. 2019), heat inactivation is an effective step for removal/inactivation of enveloped and non-enveloped viruses in human/animal derived immunoglobulin (Mpandi et al. 2007; Caricati et al. 2013). Heat treatment particularly can efficiently neutralise viruses that survived the caprylic acid precipitation step. Although heat treatment at 56˚C for ≥1 hour could be associated with a slightly poorer yield (Table 3.1), it can certainly improve the purity (Figure 3.3 D and Figure 3.7 A&B, lane 5), stability (Kurtović et al. 2019) and safety of the drug products (Mpandi et al. 2007; Caricati et al. 2013).

Additionally, for the $F(ab')_2$-based antivenom, pepsin digestion is also considered as a viral removal step, although to a lesser extent than heat

inactivation and caprylic acid precipitation (Caricati et al. 2013). In this respect, the F(ab')$_2$-based antivenom was produced by implementing process parameters (pH 3.05 ±0.05, and 30℃ for 1 h), which have shown enhanced removal/inactivation of different types of viruses associated with antivenoms, in previous studies (Caricati et al. 2013; World Health Organization 2016). It is worth emphasising that nanofiltration (≤50 nm pore-size), phenol (≤2.5 g/L) and m-cresol (≤3.5 g/L) are all effective methods for eliminating and/or preventing microbial contamination of antivenom drug products (World Health Organization 2016). However, phenolic derivatives are associated with the formation of considerable amounts of aggregates (data not shown) and nanofiltration adds significant production costs that may exceed the budget of the target marketing region.

According to the WHO guidance on quality requirement, the total protein concentration of antivenom product should not exceed 100 g/L (World Health Organization 2016). In compliance with this guidance, the antivenom products produced in this study have a protein concentration of 50 g/L where monomeric IgG and F(ab')$_2$ constitute ≥96% (by SEC-HPLC) of the total protein content. As confirmed by the highly sensitive Western blot assays (see Figure 3.6 and Figure 3.7), Fc, pepsin and albumin contaminants were below the lowest detectable limit of the assay. This is a mandatory QC assessment currently recommended by the WHO as part of the safety profile for antivenom products (World Health Organization 2016). In addition to residual albumin and pepsin, the presence of Fc fragments in F(ab')$_2$-based product is associated with increased adverse reactions (Ramos-Cerrillo et al. 2008).

The absence of contaminants (i.e., residual albumin, Fc and pepsin), as demonstrated by the purity profiles, make the antivenom produced in this study superior to most antivenoms in the SSA region (Pepin-Covatta et al. 1997; Ramos-Cerrillo et al. 2008). However, it is worth mentioning that, as with most other antivenoms (Ramos-Cerrillo et al. 2008; Kurtović et al. 2019), both the IgG and F(ab')$_2$ antivenoms usually contain significant quantities of non-specific antibodies. In fact, the specific antibodies (SpAb) account for approximately 16% of the total protein content of antivenoms prepared by ammonium sulphate or caprylic acid precipitation (Al-Abdulla et al. 2014). In

contrast, affinity purified antivenoms such as CroFab™ and ViperaTAb®, contain higher quantities of SpAb (Dart et al. 1997; Casewell et al. 2014a). However, this purification method is highly expensive and, therefore, its application has not been introduced into antivenom manufacture for the African market.

The venom-binding capacity of the antivenoms produced in this study was assessed using an ELISA assay. The results obtained from this study demonstrated that both antivenoms had high titres, which can be attributed to their high purity profile. Whilst it is not guaranteed that antivenoms with strong venom-binding activities will also neutralise venom toxicity *in vivo*, binding can be used as a preclinical predictor of antivenom efficacy (World Health Organization 2016). It must be emphasised that venom binding and toxicity are two distinct and possibly unrelated phenomena (Theakston and Reid 1979). This may explain why an antivenom, with excellent binding activity with a matrix-adsorbed venom, may fail to induce equivalent neutralisation activity *in vivo* (Calvete et al. 2016). Indeed, all immunogenic venom proteins are not necessarily toxic, and vice versa. For instance, highly toxic short peptides such as 3FTXs and disintegrins are amongst the least immunogenic venom components (Gutierrez et al. 2014). Nevertheless, plotting the optical density (OD) of a new batch of antivenom against a reference that has been prepared identically and with a known ED_{50} value may improve the sensitivity of ELISA assay. The ELISA assay used to assess antivenom potency was first developed by (Theakston and Reid 1979), and since then, several studies have reported an excellent correlation between ELISA titre and *in* vivo ED_{50} assays (Rial et al. 2006; Khaing et al. 2018). In fact, the ELISA assay is used as a QC batch release assay in some pharmaceutical companies (Al-Abdulla, personal communications).

To validate the assay for this project, the ELISA titre of antivenom was compared to that of the Fav-Afrique™ drug product. Although the Fav-Afrique™ batch used (lot G69921) had expired in 2013, it was clear and without any particles, and it had an excellent purity profile as demonstrated by SDS-PAGE assay (see Figure 3.7). Interestingly, a recent study (Sánchez et al. 2019) has shown that antivenom maintains its pharmacological activities for up to 20 years, which correlates with earlier observations that an

antivenom's colour changes before its potency deteriorates (Theakston and Reid 1979). The hyperimmune plasma used had also expired about the same time, although hyperimmune plasma/serum can be used for up to 20 years if stored appropriately (John Landon and Ibrahim Al-Abdulla, personal communication). It must be noted that the Fav-Afrique™ and the F(ab')$_2$ antivenom were prepared using different methods and in different laboratories. As the work described in this thesis was a proof-of-concept study, the use of Fav-Afrique™ as a reference product was acceptable. The results showed that the F(ab')$_2$ antivenom has a similar ELISA titre to that of Fav-Afrique™ for viper venoms, but a slightly lower titre for the elapid venoms. In addition, Western blots showed similar binding by the F(ab')$_2$ and Fav-Afrique™ products, irrespective of snake species.

Therefore, it appears that the mixing ratio of HHP (i.e., 1:1:1:1; see section 3.3.1.1), is not sufficient to provide the polyvalent antivenoms with a balanced efficacy against the elapid venoms. These results are consistent with published data, which demonstrated that polyvalent antivenoms had a lower efficacy against *Elapidae* species (Guidolin et al. 2016). This suggests that larger volumes of HHP against *Naja* and *Dendroaspis* species, compared to the anti-*Echis* and anti-*Bitis* HHP must be used. Alternatively, purifying each group separately and pooling them together afterwards on the basis of their potency could improve overall antivenom potency against elapid venoms. However, this requires animal studies and, therefore, would impose significant expense. It appears from preclinical (Ramos-Cerrillo et al. 2008; Casasola et al. 2009) and clinical studies (Baldé et al. 2013; Potet et al. 2019) that most of the major polyvalent antivenoms targeting a mixture of viper and elapid venoms fail to provide a balanced efficacy against them all. To counter these problems, Guidolin and colleagues proposed making anti-*Viperidae* and anti-*Elapidae* antivenoms separately (Guidolin et al. 2016).

Despite reporting promising results, to my knowledge, these antivenom products have not been manufactured commercially. This could be due to: 1) delayed treatment because most SBE patients do not correctly identify the snake species responsible, and/or (2) it has significant financial implications because clinical centres would be required to double their antivenom stock. The IgG had a lower binding titre despite all three antivenoms [i.e., the IgG,

F(ab')$_2$, and Fav-Afrique^{TM}) being derived from common HHP. Interestingly, the IgG antivenom failed to recognise some of the key elapid venom LMW toxins particularly those of *Dendroaspis* venoms. *Naja* venoms are dominated by LMW components including 3FTXs and PLA$_2$s, which are typically ~6 kDa and ~14 kDa respectively, as identified by proteomic studies (Petras et al. 2011; Malih et al. 2014; Lauridsen et al. 2017). Similarly, LMW toxins such as 3FTXs and KTT (around 6 kDa) dominate the venom composition of the *Dendroaspis* species included in this study (Laustsen et al. 2015; Ainsworth et al. 2018). Being poorly immunogenic venom components (Gutiérrez et al. 2009; Calvete et al. 2010), the antivenom may already contain fewer antibodies against toxins such as 3FTXs and KTT.

Furthermore, the antigen binding fragment accounts for 66.7% of the whole IgG molecule. Therefore, increasing the IgG concentration could improve antivenom efficacy and provide enhanced detection by immunoassays such as Western blot and ELISA. This is corroborated by a venomics study (Petras et al. 2011) that demonstrated an enhanced recognition of venom toxins was achieved by increasing the IgG concentration in the antivenom: venom mixture. Additionally, the same study (Petras et al. 2011) reported enhanced recognition of 3FTXs and PLA$_2$ from *N. nigricollis* by EchiTab G Plus, an intact IgG antivenom, produced using caprylic acid precipitation (Gutierrez et al. 2005a). Furthermore, *in vivo* studies demonstrated that whole IgG antivenom has a neutralising efficacy comparable to Fab (León et al. 2000) and F(ab')$_2$ (Leon et al. 1999; Leon et al. 2001), albeit at slightly increased quantity of IgG. This would suggest that observance of poor binding in Western blot analysis does not necessarily equate to ineffectiveness.

Whilst providing equal potency against the four genera would have been desirable, this was not an issue because: firstly, the potency assay was not within the scope of this study and, second, the main objective of this study was to develop a process method that can be adapted to large-scale production with a particular focus on formulation stability.

Subsequently, this study reports stability assessment for the antivenom. The SSA region is considered to be in the ICH climatic zone III (hot and dry), Iva (hot and humid) or IVb (hot and very humid), which necessitates the

development of liquid formulations with tolerance range of 30℃ ± 2℃ (European Medicines Agency 2003). Additionally, the supply of electricity is continuously disrupted throughout the day in most of the SSA countries (Ramos-Cerrillo et al. 2008), thus producing an antivenom stable at these temperatures is highly desirable (World Health Organization 2016). Keeping this in mind, both the IgG and $F(ab')_2$ antivenoms demonstrated excellent stability at both refrigerated (2-8℃) and accelerated (37℃) temperatures for over 8 months, with no visible particles or evidence of protein degradation. Although the actual accelerated temperature is usually 40℃ ± 2℃ (European Medicines Agency 2003), most of the QC assays were conducted in accordance with MicroPharm‘s existing standard procedures; for e.g., stability is monitored for up 6 months at 37.5 ℃.

Stability of antivenoms at a neutral pH (pH 7.0±0.5), without the use of potentially toxic excipients, is desirable (World Health Organization 2016). All of the reagents and excipients used for the formulation developed in this chapter have been reported in many recent USA Food and Drug Administration (FDA)-approved injectable medicines (Schwartzberg and Navari 2018; Kriegel et al. 2019; Ionova and Wilson 2020).

In compliance with MicroPharm’s privacy policy, providing a breakdown of manufacturing cost is inappropriate. However, the production method reported in this study is generally cheaper (Gutierrez et al. 2005a) compared to affinity-purified antivenoms (LoVecchio et al. 2003), IgG(T)-precipitation (Pepin-Covatta et al. 1997) and lyophilisation methods. In Latin America, the antivenom production cost, using traditional manufacturing methods (i.e., by caprylic acid and/or ammonium sulphate precipitation), is $2.40 to $25 per 10 mL vial, depending on production volume, immunisation strategy and manufacturing technology (Morais and Massaldi 2006). According to (Morais and Massaldi 2006), the production costs for antivenom can be divided into three stages:

1) stage 1 collection of snake venoms, immunisation of donor animals, and collection of hyperimmune plasma.
2) stage 2 research and development (R&D) and the manufacturing process, including manpower and consumables.

3) stage 3 Quality Assurance (QA), quality control (QC) assays, murine test, filling and shipments.

Although all stages contribute to the production cost, stage 3 and, particularly the murine test, is responsible for increased manufacturing cost. One way to reduce the production expenditure is by introducing *in vitro* assays (for e.g., ELISA) to be used as a surrogate assay where a reference from murine test is retained to be used across the subsequent batches. Furthermore, usually antivenom manufacturers produce smaller batches due to low demand and thus the production expense remains almost the same with the exception of stage 1 (i.e., production and collection of hyperimmune plasma). Therefore, increasing the batch size would significantly reduce the cost of the antivenom product. Finally, the collaboration between antivenom manufacturers to jointly manufacture one sufficiently bigger batch is another way for curtailing the production cost (Morais and Massaldi 2006).

3.5 Limitation of the study

The study has a number of limitations including disproportionate titres of $F(ab')_2$ directed against venoms from the *Viperidae* and *Elapidae* species. This could be improved/corrected by, either running each group separately and blending the final drug substances on the basis of their potency, or by carefully developing a blending ratio that provides balanced antibody titres against all four genera, or at least the same as that for the Fav-Afrique™.

The ELISA potency assay should have provided more data for statistical analysis, but time constraints due to the pandemic adversely affected the progress of the project. This is despite the fact that, for QC assays, only a single ELISA plate is sufficient.

Full treatment in many SBE cases could require a staggering antivenom dosage of up to 40 mL, equivalent to ≥4000 mg protein (Potet et al. 2019). Therefore, it would have been advantageous if the study had included stability studies on bags (e.g., 50 mL-100 mL) which would offer a flexible packaging option.

Finally, this Thesis would have benefited from studying antivenomics to precisely determine the venom components recognised by the antivenom.

However, neither expertise nor the technology existed to support this study platform at the university or MicroPharm Ltd.

3.6 Conclusion and future direction

The study provides a simple, robust and cheap manufacturing process, which constitutes a potentially valuable solution to the antivenom crisis in SSA. Preliminary data suggest that the method was reproducible and readily adaptable for scaling-up and transfer to production with minimal risk. The formulation reported in this study demonstrated an excellent shelf-life at both refrigerated and accelerated temperature. Stability of liquid formulations at temperatures exceeding 30℃ can provide unparalleled advantages for antivenoms targeting the SSA.

Additionally, the antivenoms produced in this study demonstrated excellent purity (≥96%). Quality control assays confirmed that the contaminants such as albumin, pepsin and Fc residuals, were below their detection limit which is a critical step for antivenom safety. As confirmed by Western blot assay, the $F(ab')_2$ antivenom product has an excellent capacity to recognise key venom toxins for both viper and elapid venoms. A realistic yield of approximately 15 g and 7 g of whole IgG and $F(ab')_2$, respectively, was extracted from each litre of HHP.

Next, we aim to assess the efficacy of the antivenom produced in this study using a novel invertebrate "*Galleria mellonella*" model.

Chapter 4: Characterisations of equine immunoglobulin G subclasses and assessing their role in neutralisation of snake venom toxins

4.1 Introduction

Since the beginning of the immunotherapy era in the 1890s (Squaiella-Baptistao et al. 2018), horse plasma still continues to be an indispensable source, specifically for global preparations of antivenoms. The large plasma volume and the versatility of equine immunoglobulin G (IgG) make horses favourite sources for most antivenom manufacturers (Gutierrez et al. 2011). Horse plasma is rich in α, β and γ globulins, dominated by prealbumin, and albumin (Tothova et al. 2016).

All blood proteins are made and secreted by hepatocyte cells, with the exception of immunoglobulins (Igs), which are produced exclusively by activated B lymphocytes and plasma cells (Janeway et al. 2001; Bowen and Casadevall 2018). Igs are glycoproteins primarily responsible for mediating immune responses, including complement activation and phagocytosis via interaction with Fcγ receptors. All Igs share a similar basic structure, comprising two identical heavy (H) chains (each ~50 kDa) coupled together by a disulphide bond, and two identical light (L) chains (~25 kDa each) linked to the heavy chains by disulphide bonds (Walther et al. 2015). Each heavy and light chain is composed of one variable domain (V_H or V_L), and, for the heavy chains, three or four constant domains (C_H1, C_H2, C_H3 and C_H4), but the light chains only have a single constant domain (C_L). The variable (V) region, formed from both heavy and light chains (V_H and V_L), confers specific binding of a unique antigen. A schematic representing basic structure of IgG is available in Figure 1.12. On the other hand, the constant domains impact on the variable domains, thereby priming the immune response to a specific antigen (Bowen and Casadevall 2018). As is the case in the entire mammalian Ig repertoire, the equine light chain is composed of two isotypes; lambda (λ) and kappa (κ) of which lambda light chains are predominant (Wagner et al. 2004; Walther et al. 2015). The nucleotide sequence for the Ig heavy chain (IGH) is located on chromosome 14q32 (human) and chromosome 24 (horse). It is composed of variable heavy (IGHV), diversity heavy (IGHD), joining heavy (IGHJ) and constant heavy (IGHC) gene segments (Wagner 2006).

Previous studies identified antigenically distinct groups of horse immunoglobulins including IgM, IgD, IgA, IgE, and IgG (McGuire et al. 1972). Equine IgM is the first endogenous immunoglobulin isotype to be produced by the immune system of a newly born foal, followed by the synthesis of other Ig isotypes including IgG, IgA and IgD. IgM is a pentamer and is responsible for the primary immune response and, together with IgA and IgG, is the predominant Ig in horse plasma (Wagner et al. 2004). In equine plasma, IgD is represented at a low concentration (Keggan et al. 2013), and its role in the equine immune system is not fully established (Walther et al. 2015).

In mammals, IgG is the most versatile Ig isotype and is responsible for the majority of immune responses (Bowen and Casadevall 2018). Mammalian IgG is characterised by diversity within subclasses and expression of distinct biological functions (Butler 1997; Butler et al. 2009). In mammals, the number of IgG subclasses varies from a single sub-isotype such as in rabbits (Butler 1997; Weber et al. 2017), four in humans (Hjelholt et al. 2013; Irani et al. 2015) and mice (Han et al. 2020), two in cattle (Butler 1969; Ulfman et al. 2018), six in pigs (Butler et al. 2009) and seven in horses (Wagner et al. 2004).

On the basis of antigenic differences, serological and electrophoretic features, horse IgGs were previously assigned to four well-defined subclasses: IgGa, IgGb, IgGc (Klinman et al. 1965), and IgG(T) (Widders et al. 1986), in addition to a fifth subclass known as IgGB, reviewed by (Sheoran and Holmes 1996). However, genomic studies have revealed that equine IgG can be expanded to include seven subclasses: IgG_1 – IgG_7 (Wagner et al. 2004; Wagner 2006; Lewis et al. 2008; Walther et al. 2015). Currently, eleven IGHC genes have been characterised and are aligned in the IGH locus – 5' *IGHM, IGHD, IGHG1, IGHG2, IGHG3, IGHG7, IGHG4, IGHG6, IGHG5, IGHE* and *IGHA 3'* (Wagner et al. 2004). It is postulated that all IGHC genes have diverged from a single ancestral IGH gene as the result of duplication events early in mammalian evolution (Wagner et al. 2002). Accordingly, the previous nomenclatures were replaced by: IgG_1 and IgG_2 (IgGa); IgG_4 and IgG_7 (IgGb); IgG_6 (IgGc); IgG_3 and IgG_5 [IgG(T)], where IgGB is initially reported as aggregated Ig (Wagner et al. 2004; Wagner 2006). Nevertheless, only anti-horse IgG subclass antibodies (anti-IgGa; anti-IgGb; anti-IgG(T) and anti IgGc) are currently

available (Cunha et al. 2006; Lewis et al. 2008) so the subtypes cannot be distinguished in practice. In spite of the newly identified subclasses, therefore, the old nomenclature system is still in use in more recent publications relating to equine IgG subclasses (McKenzie et al. 2014; Mateljak Lukačević et al. 2020). Thus, this nomenclature will be used throughout the thesis because the major and relevant antibodies are still marketed under these names.

Despite increased efforts, the structures and individual functions of equine IgG subclasses are not fully elucidated. However, substantial studies have attempted to characterise equine IgG quantitatively (McGuire et al. 1972; Sheoran et al. 2000) and qualitatively (Lewis et al. 2008; Rocha et al. 2019). In common with other mammals, all horse IgG subclasses have molecular weights (MW) of ~150 kDa and comprise a crystallisable fragment (Fc) domain and two antigen binding fragments (Fab), each MW ~50 kDa assembled with disulphide bonds to make a "Y" shaped intact molecule (see Figure 1.12). Equine IgGs are *N-glycosylated* molecules and the IgG_3 sub-isotype contains an additional *O-glycan* attached to the heavy chain (Lewis et al. 2008). Studies on rabbit IgG and mouse IgG2b have shown that the *O-glycans* are attached to threonine and serine residues within the hinge of IgG (Lewis et al. 2008). A recent study on mouse IgG demonstrated that glycosylation is key to determining effector function of IgG subclasses (Kao et al. 2017).

Quantitatively, IgGb was found to be the most abundant IgG subclass, followed by IgG(T) and IgGa, whereas the presence of IgGc was almost negligible in serum from healthy adult horses (Sheoran et al. 2000). There is a general consensus of opinion that the level of IgG(T) (comprising IgG_3 and IgG_5) is markedly increased in hyperimmune horses (McGuire et al. 1972; Widders et al. 1986). Others demonstrated a significantly increased level of IgGa and IgGb in infected horses (Lopez et al. 2002; Cunha et al. 2006). Although antigen type and cellular response may affect the IgG profile in horses, the exact mechanisms that regulate the synthesis and class switching phenomena are poorly understood. However, class switching of B cells to producing antigen specific IgG subclasses is commonly dependent on T-lymphocyte cell-mediated proinflammatory and anti-inflammatory agents. In mice, the presence of T-helper 1 (Th1)-mediated proinflammatory agents such

as interferon gamma (IFN-γ) stimulate B cells to produce IgG2a/c and IgG3, whereas in the presence of Th2-dependent interleukin-4 (IL-4) and transforming growth factor-β (TGF-β), B cells favour the production of IgG1 and IgG2b (Weber et al. 2014).

More importantly, it has been shown that in horses infected with bacteria, there is a significant increase of antigen-specific IgGa and IgGb subclasses, which was correlated with the upregulation of cluster of differentiation-4 (CD4)-mediated IFN-γ (Lopez et al. 2002). Additionally, it has been reported that the administration of aluminium-hydroxide adjuvanted influenza vaccine elicits the production of IgG(T) (Hooper-McGrevy et al. 2003). Although there is a lack of substantial evidence about antigenic associations with equine IgG subclass production, in mice, the production of IgG1 is preferentially elicited by protein antigens, IgG2a/c by viral antigens and IgG_3 by bacterial polysaccharide antigens (Weber et al. 2014). Furthermore, Hooper-McGrevy and colleagues (2003) demonstrated that the production of IgG(T) and IgGb in horses is associated with the Th2-response whilst IgGa is linked with the Th1-driven immune response.

There is conflicting evidence regarding the function of equine IgG subclasses (Rocha et al. 2019). Early studies proposed that IgGa and IgGb are involved in opsonisation and complement activation (McGuire et al. 1972; Cunha et al. 2006). These studies also advocated that IgG(T) inhibits complement fixation by blocking interactions between IgGa and IgGb with complement components. In contrast, a recent study by Lewis et al., 2008, demonstrated that IgG_3, a component of IgG(T), is the most potent equine IgG subclass to elicit complement activation. There is a lack of evidence about the factors regulating the function of horse IgG which, to some extent, may explain the inconsistency of data between studies. A corresponding study in mice demonstrated that glycosylation is key to regulation of the effector function of IgG subclasses (Kao et al. 2017). For example, O-glycans, such as those that are present in IgG_3, were shown to have a role in IgG protection from degradation by proteolytic enzymes, such as pepsin and trypsin (Lewis et al. 2008).

In venom-hyperimmune plasma, IgG(T) represents the majority of circulating antibodies, followed by IgGa and IgGb whereas IgGc is scarcely detectable (Fernandes et al. 1997; Krifi et al. 1999). Additionally, earlier studies have reported that the neutralising activities of antivenom reside within the IgG(T) subclass (Fernandes et al. 1991; Fernandes et al. 1997; Fernandes et al. 2000b). These findings led to the manufacture of the currently commercially available IgG(T)-based antivenoms (Grandgeorge et al. 1996; Pepin-Covatta et al. 1997). Subsequent studies have shown that IgGa antivenom is also capable of neutralising major venom toxins, albeit, at a lower efficacy than IgG(T) antivenom (Fernandes et al. 2000a; Toro et al. 2006).

Furthermore, the study reported by Fernandes and colleagues (2000a) compared the neutralisation capacity for IgG(T) and IgGa subclasses on two differently prepared antivenoms. These were a bothropic antivenom (against *Bothrops jararaca*, *B. jararacussu, B. moojeni, B. neuwiedi and B. alternatus*) manufactured by Instituto Butantan, Brazil, and a polyvalent antivenom (against *Bothrops asper*, *Crolatus durrisus durissus* and *Lachesis muta stenophrys*) manufactured by Instituto Clodomiro Picado (ICP), Costa Rica (Fernandes et al. 2000a). In the Butantan antivenom, IgG(T) was ~3 times more effective than the IgGa in neutralising lethality, whereas the neutralising activities for the ICP antivenom was almost exclusive to the IgG(T) subclass (Fernandes et al. 2000a). It is not known if such discrepancies can be attributed to antigen variations (different snake species), immunisation protocols or purification methods used for manufacturing the antivenoms or possibly, a combination of all these factors. Furthermore, IgGa could have suffered higher losses during the ICP purification processes, which involved in caprylic acid precipitation method (Rojas et al. 1994). However, a previously conducted study suggested that a caprylic acid precipitation method does not affect the distribution of IgG subclasses (Halassy et al. 2019).

In conclusion, it is clear that there are significant discrepancies between reported results of quantity (w/w) and quality (affinity of IgG subclasses), of HHP. There is a dearth of information on the neutralising profiles of IgG subclasses of Sub-Saharan antivenoms. Despite compelling evidence that suggests that IgGa provides substantial protection against venom toxins, there

are currently no reports of the efficacy of antivenoms containing a combination of IgG(T) and IgGa. Although partially reported by (Halassy et al. 2019), the precise quantification of equine IgG subclasses in HHP has yet to be fully elucidated.

4.2 Aims and objectives:

The primary aim of this study was to assess the binding capacity and specific antibody content of IgGa, IgGb and IgG(T) harvested from horses that have been immunised with venoms from snakes native to sub-Saharan Africa. This study also aimed to investigate the relative quantities (w/w) of IgGa, IgGb and IgG(T) in this HHP. The ultimate aim of this study was to define and develop a suitable method to manufacture antivenom enriched with the most efficacious neutralising antibodies.

4.3 Results

4.3.1 Analysis the purity of IgG using SEC-HPLC method

Total IgG (TIgG) was generated from HHP using several purification stages that includes heat inactivation, caprylic acid precipitation and diafiltration (see section 2.2.2). Analysis of the various IgG purification stages by SEC-HPLC showed that caprylic acid effectively precipitated most of the non-IgG protein components of horse plasma (Figure 4.1 A), generating TIgG with purity of ~96% (Figure 4.1 B). The TIgG products (section 2.2.12) were fractionated by slowly passing them through a Q-Sepharose XL (QXL) gel. The QXL matrix is a strong anion exchanger containing extra charged quaternary ammonium ligands that partition proteins on the basis of their net surface charge, permitting positively charged molecules to flow-through whilst firmly adsorbing the negatively charged proteins. Under the conditions described in section 2.2.12, two fractions were collected:

1) FT (or unbound fraction) containing proteins that do not bind to QXL, which represents the IgG(T)-depleted sample (Figure 4.1 C)

2) Strongly bound fraction eluted with 10 mM phosphate buffer (pH 7.1±0.1) containing 1 M NaCl (Figure 4.1 D), which represents the IgG(T)-enriched sample.

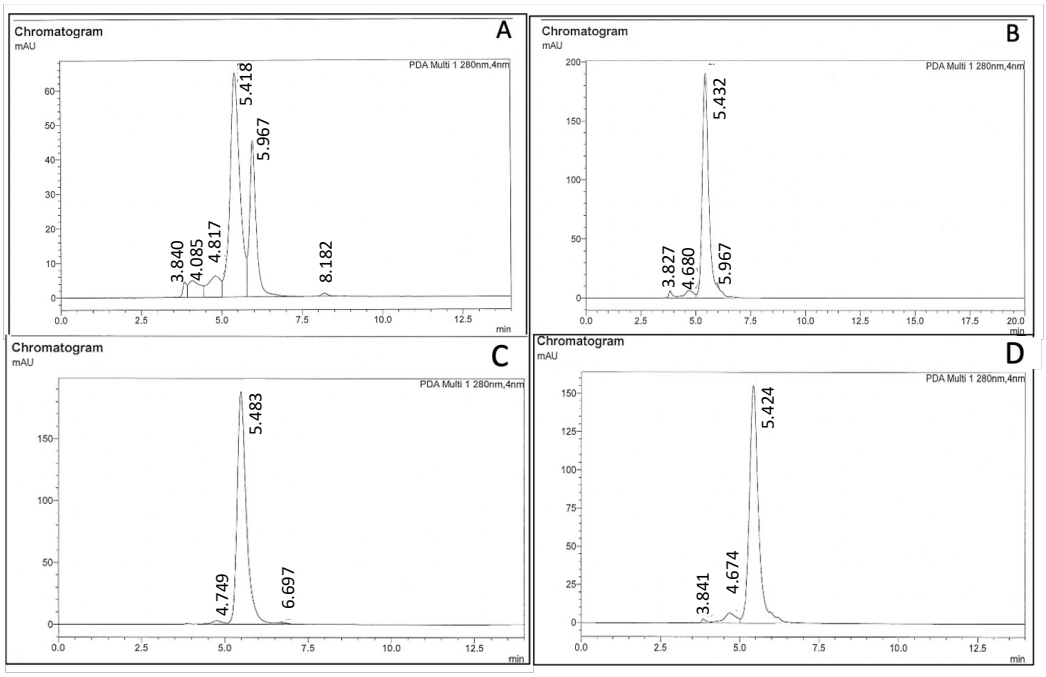

Figure 4.1 Size-exclusion Chromatography (SEC) profiles.

A) hyperimmune horse plasma (HHP) raised against *E. leucogaster* and *E. ocellatus,* B) Total IgG (TIgG) AV after caprylic acid purification, C) IgG(T)-depleted AV, and D) IgG(T)-enriched AV. Anti *Naja* samples have identical profiles (not shown). SEC was performed using Agilent AdvanceBio SEC 300 Å, 2.7 µm, 4.6 x 150 mm column connected to Shimadzu Prominence HPLC. Analysis was performed at a flow rate of 0.5 mL/min using 20 mM sodium phosphate, 130 mM sodium chloride, 0.02% sodium azide, pH 6.0±0.2 at RT and the absorbance was monitored at 280 nm. Based on the molecular weight of components of equine plasma, molecules at the peak ~R_t 3.8 min are thought to be aggregates; the peak at ~R_t 4.1 min is IgM (~ ≥ M_r 700 kDa); peak at ~R_t 4.7 & 4.8 min is IgA and/or IgG dimer; the peak at ~R_t 5.4 is IgG; and the peak at ~R_t 6.0 min is albumin and peak at ~R_t 6.7 min is LMW related substance.

All abbreviations are consistent with Fig. 3.2.

4.3.2 Verification of horse IgG subclasses

All samples collected from AEX were analysed using Western blot to verify the presence or absence of IgG(T) using non-reducing (Figure 4.2) and reducing conditions (Figure 4.3). To minimise experimental variation, all samples were prepared identically, by diluting with 0.9% NaCl to the same protein concentration and pH 7.5 ± 0.1. Electrophoresed protein gels, under non-reducing (Figure 4.2) and reducing (Figure 4.3) conditions, were stained with Coomassie Blue (panel A).

Under both conditions, a clear difference is seen between the IgG(T)-enriched (Figures 4.2 A and 4.3 A: lanes 5 and 10) and IgG(T)-depleted samples (Figures 4.2 A and 4.3 A: lanes 6, and 11).

The non-reduced gel (Figure 4.2 A) allows comparison of IgG bands. It is evident that lanes 4 and 9 (Figure 4.2 A) which contain Total IgG, suggests the presence of two IgG subclasses with different MWs. One appears to be ~145 kDa and the other ~170 kDa. Under reduced conditions, the corresponding heavy chain bands were detected at ~60 kDa and ~50 kDa (Figure 4.3 A, lanes 4&9).

Lanes 5 and 10 (Figures 4.2 &4.3) contain IgG(T)-enriched samples and are dominated by a single IgG subclass around 160 kDa (non-reduced; Figure 4.2 A) and ~60 kDa (reduced; Figure 4.2 A). Lanes 6 and 11 (Figures 4.2 & 4.3) contain samples from the flow through of the AEX step [IgG(T)-depleted sample] and are dominated by single IgG molecules of approximately 150 kDa (non-reduced; Figure 4.2 A) and ~50 kDa (reduced). These findings are consistent with published data which reported that equine IgGa and IgGb subclasses have lower molecular weight than the IgG(T) components under reduced SDS-PAGE (Lewis et al. 2008).

The bands visualised in HHP (lanes 2, 3 & 8) at ~55 kDa (Figure 4.2 A) may represent equine albumin which is ~65 kDa (Ramos-Cerrillo et al. 2008). Additionally, the bands at ~25 kDa under reducing conditions (Figure 4.3 A), are light chain bands. These bands were also detected by Western blot analysis (Figure 4.3 B-D), but at low intensity.

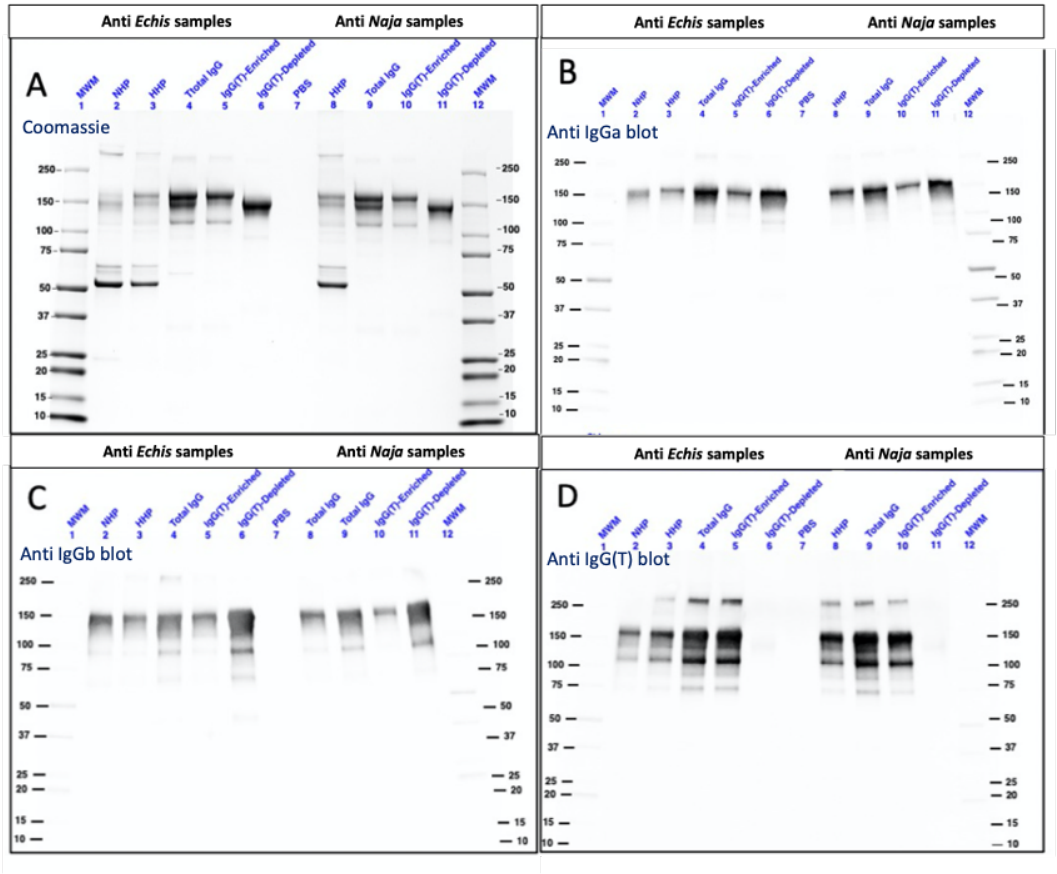

Figure 4.2 Coomassie stain and Western analysis for different equine IgG subclasses (non-reducing condition).

Non-reducing SDS PAGE of proteins stained with Coomassie blue (A); Western blotting against mouse anti-horse IgGa (B); mouse anti-horse IgGb (C); and goat anti-horse IgG(T) (D). To obtain higher resolution of protein separation, all proteins were loaded at 2.5 µg/well. Both mouse anti IgGa and anti IgGb were diluted at 1:5000 in blocking buffer. All HRP-conjugated antibodies were also diluted similarly. Full details of SDS-PAGE and Western blot methods are given in sections 2.2.9.1 and 2.2.9.2, respectively.
Results were visualised using ECL reagents and the ChemiDoc system.
Abbreviation: MWM; molecular weight marker, NHP; (non) or pre-immune horse plasma, HHP; hyperimmune horse plasma; PBS: phosphate buffered saline (negative control).

By Western blot analysis, IgG(T) band was detected on the AEX bound fraction [expected to be IgG(T)-enriched; lanes 5&10, Figure 4.2 D & Figure 4.3 D] but the IgG(T) band was completely absent in the AEX FT samples [expected to be IgG(T)-depleted; lanes 6&11, Figure 4.2 D and Figure 4.3 D]. The anti-IgGa and IgGb blots have revealed a relatively concentrated level of IgGa in lanes 6&11 (Figure 4.2 B & Figure 4.3 B) and IgGb in lanes 6&11 (Figure 4.2 C & Figure 4.3 C). Also, the presence of lower levels of IgGa and

IgGb were detected in the AEX bound fraction (lanes 5 & 10, Figure 4.2 B&C, and Figure 4.3 B&C). However, it should be noted that the specificity of these monoclonal mouse antibodies for horse IgGa and IgGb in Western blot analysis is not validated. As stated by the manufacturer, there could be some cross-reactivity with other horse Ig isotypes (for example, IgA & IgM). Furthermore, analysis by SEC-HPLC indicated that the IgG(T)-depleted fraction (Figure 4.1 C) is purer and appears to consist of IgG subclasses only. In contrast, the IgG(T)-enriched fraction (Figure 4.1 D) appears to contain other Ig classes, such as IgM, IgA, and/or aggregates which are not examined in this study.

Thus, the complete absence of IgG(T) from the unbound (FT) fraction (Figure 4.2 D and Figure 4.3 D, lanes 6&11), may suggest that this method is successful in separating IgG(T) from the rest of the equine IgG subclasses. Others, (Sheoran and Holmes 1996; Sugiura et al. 2000), have reported separations of horse IgG subclasses using a weaker anion exchanger, namely diethylaminoethyl (DEAE). It is interesting that we were unable to achieve the desired results using the same matrix (results not shown). It may be that DEAE is suitable for separating pre-immune horse plasma whereas QXL works better for HHP.

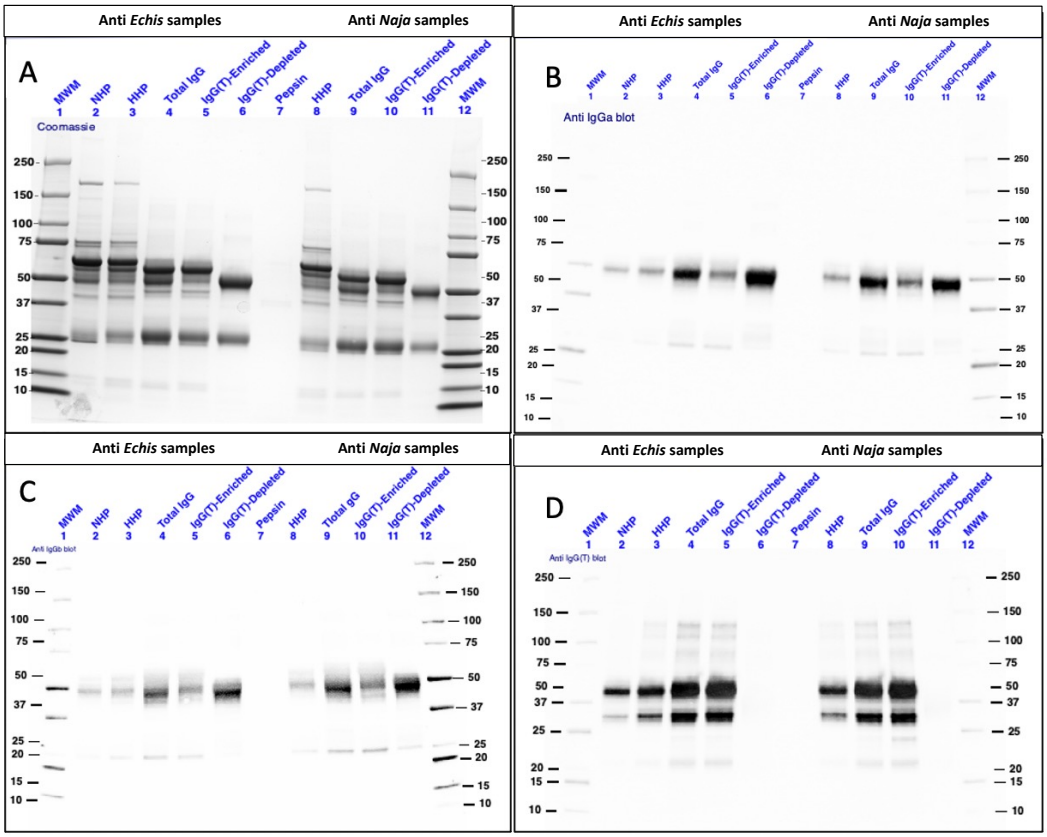

Figure 4.3 Coomassie stain and Western analysis for different equine IgG subclasses (under reducing condition).

Reducing SDS-PAGE of proteins stained with Coomassie blue (A); Western blotting with mouse anti-horse IgGa (B); mouse anti-horse IgGb (C); and goat anti-horse IgG(T) (D). All proteins were loaded at 2.5 µg/well. Mouse anti-horse IgGa, mouse anti-horse IgGb and the HRP-conjugated anti-mouse IgG (H+L) were all diluted at 1: 5,000 in blocking buffer. HRP-conjugated goat anti-horse IgG(T) was diluted at 1:10,000. Full details of SDS-PAGE and Western blot methods are given in sections 2.2.9.1 and 2.2.9.2, respectively. Blots were visualised using ECL reagents and the ChemiDoc system.
All abbreviations are consistent with Fig. 4.2.

4.3.3 Relative quantity of IgG(T)-enriched and IgG(T)-depleted samples in HHP

The relative quantity (w/w) of each subclass was determined chromatographically. Figure 4.4 shows that IgG(T) makes up the majority (~67%) of equine IgG in HHP. These results agree with earlier studies (Widders et al. 1986; Fernandes et al. 1991; Pepin-Covatta et al. 1997). However, the IgG(T)-depleted sample represents ~24 % of the equine TIgG.

Both the IgG(T)-enriched, and IgG(T)-depleted samples were generated from the AEX purification step using the TIgG sample as a feedstock (section 2.2.12).

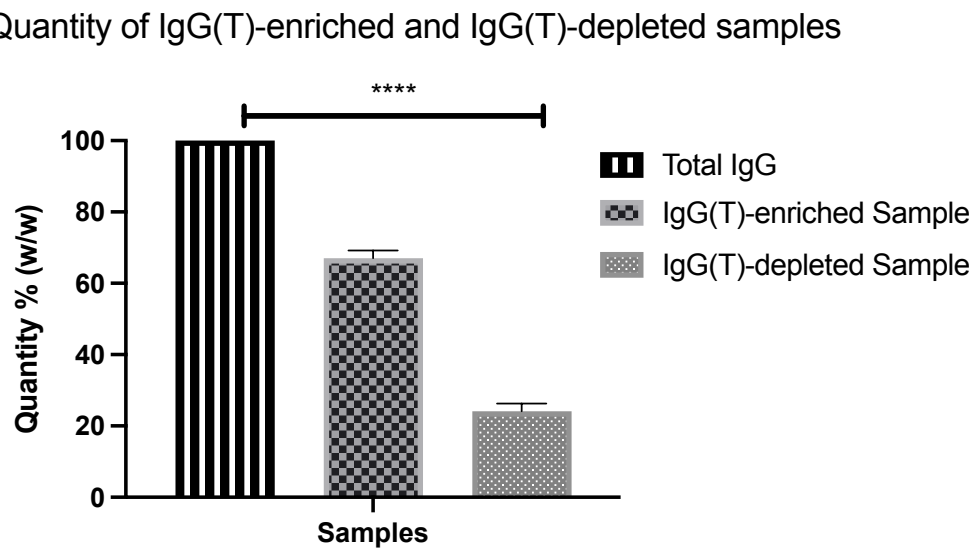

Figure 4.4 Relative quantification of different IgG subclasses in HHP.

Protein quantity of each fraction was measured using a 180 Spectrophotometer at 280 nm as described in section 2.2.4. Data was analysed using GraphPad Prism 9. One-way ANOVA with Dunnett's method *post-hoc* test was used to determine statistical significance, where **** indicates for $P < 0.0001$. Values are mean ± SD of replicates from three biologically independent experiments.

Descriptions: Total IgG is the feed stock used for the AEX QXL step; IgG(T)-enriched is the protein quantity collected from elute (i.e., bound fraction); IgG(T)-depleted is the protein quantity collected from flow-through (i.e., unbound fraction).

4.3.4 Quantification of Specific antibody (SpAb) content of IgG(T)-enriched and IgG(T)-depleted samples.

IgG(T) may represent the majority of the total IgG, but it is of interest to know whether this fraction contains a greater proportion of antivenom activity than the IgG(T)-depleted sample. The proportion of antivenom specific antibody (SpAb) within HHP, TIgG, IgG(T)-enriched, and IgG(T)-depleted samples was measured by small scale affinity chromatography (SSAC) against venoms from *E. leucogaster* and *E. ocellatus* prepared at equal proportion (for more details, see sections 2.2.13 & 2.2.14). Unprocessed HHP was used as a control to which all groups were compared. As described in section 2.2.14, samples were passed through a column bearing bound venoms and captured

antibodies were subsequently eluted and measured spectrophotometrically to calculate the % of the fraction that had bound. Raw plasma (i.e., HHP) appears to contain the highest proportion of specific antibodies (~16% of total IgG present in the unrefined plasma) when compared to the purified samples (Figure 4.5). The relatively lower proportions in TIgG (15.5%) and IgG(T)-enriched (14%) samples (Figure 4.5) may reflect the loss of the specific antibodies during the purification process. Nevertheless, there was no statistically significant difference between these groups when compared to HHP. On the other hand, the IgG(T)-depleted sample, which has the highest purity profile (Figure 4.1 C), has the lowest proportion of specific antibodies (10.1%). Also, there was a statistically significant difference ($P < 0.003$) between the IgG(T)-depleted sample and control (HHP), as determined by one-way ANOVA (Figure 4.5). Ideally, the percentage of SpAb in a sample should increase as purity improves. Contrary results could mirror non-specific proteins bound to the column, which are then included in the eluted sample denoting the quantity of SpAb.

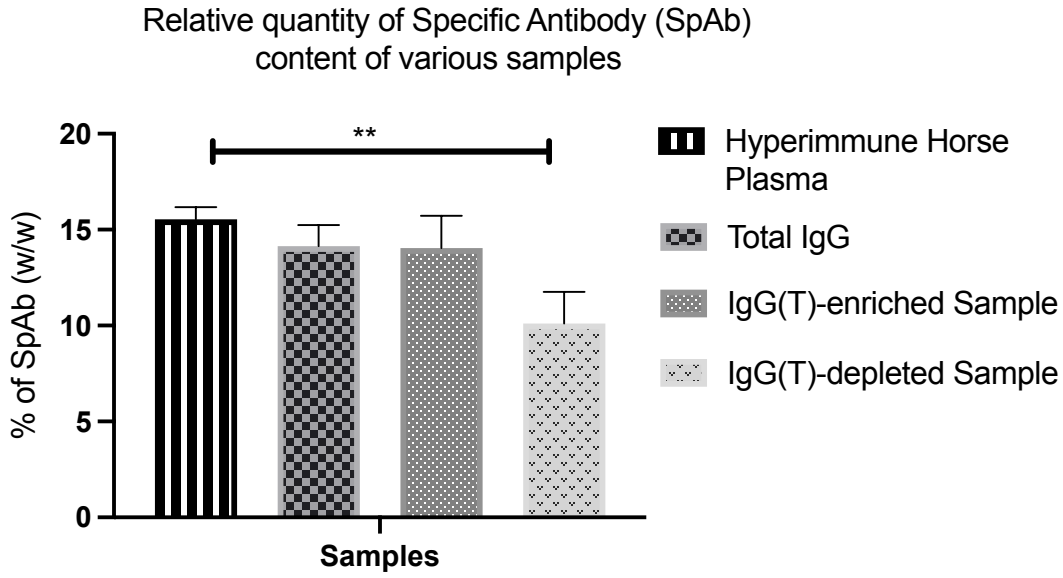

Figure 4.5 quantification of SpAb in anti- *Echis* samples.

Comparisons of specific antibody present within HHP, TIgG, IgG(T)-enriched and IgG(T)-depleted samples against *E. leucogaster* and *E. ocellatus.* SSAC quantification performed as described in section 2.2.14 and protein concentration was measured as described in section 2.2.4. Data was analysed with Prism GraphPad 9 using one-way ANOVA with Dunnett's method *post-hoc* test to determine statistical significance, where ** indicates

for $P < 0.0034$. Values are the mean ± SD of replicates from three biologically independent experiments.

Whilst the SSAC method is easy, cheap and rapid for preliminary assessments of specific antibodies, non-specific binding proves to be a significant shortcoming for quantitatively measuring SpAb using this method (Bolton 2017). This might be reflected by the presence of relatively increased quantity of non-IgG molecules (e.g., IgM, IgA or albumin as in the case of HHP) in all samples except the IgG(T)-depleted sample. Thus, this drawback has inspired the development of a more robust and sensitive quantitative assay, namely indirect ELISA.

4.3.5 Indirect ELISA: an alternative method to assess the binding activity of antivenoms

An ELISA method was optimised as an alternative platform for measuring the binding activity of the prepared antivenom samples at different purification stages. To minimise assay variations, a single dilution was performed (instead of serial dilutions) for all samples, with all the remaining steps were the same as detailed in section 2.2.10.

Compared to the SSAC, the ELISA method was superior in reproducibility, robustness and sensitivity. In fact, the non-hyperimmune horse plasma (NHP), a negative control sample, showed a negligible optical density (OD) reading, which is within the range of the blank used throughout this assay. The ELISA standard curve was constructed with affinity purified IgG (AffiPureIgG) that has generated by affinity purifications against target venoms (section 2.2.15). Additionally, the AffiPureIgG sample was used as a reference. This is an affinity purified antigen-specific antibody sample which possesses the highest binding activities against the target venom. The activity of the samples was then determined by interpolating their values from the curve using Prism GraphPad 9 software. The relative percentage binding of each sample was calculated from the following equation:

$$\%\ binding = \frac{interpolated\ value\ for\ a\ sample}{interpolated\ value\ for\ Ref\ (AffiPureIgG)} x100$$

This approach was consistent with other published results (Khaing et al. 2018), which used OD value of a reference with a known potency from an animal test- unfortunately this option was not available for the present study.

This experiment was conducted with samples from horses immunised with a mixture of venoms from different snake species, therefore, it was essential to establish the binding capacity of each sample to the individual venoms used in the immunisation protocol for the antivenom in test (see section 2.2.1). Herein, the binding activities of IgG(T)-enriched, and IgG(T)-depleted samples were determined using indirect ELISA. Eight standards were prepared as shown in Appendix III (A) and used to generate a standard curve [see Appendix III (B)] that is used to interpolate the binding values of the tested samples [see Appendix III (C)]. To minimise experimental errors, all samples were pre-diluted in PBST (containing 0.1% Tween-20) to 0.5 µg/mL, which was within the linear range of the standard curve, except for the negative control (NHP).

As shown in Figure 4.6 A, the IgG(T)-depleted sample has statistically significantly higher binding than IgG(T)-enriched antivenom for both *Echis* species. Similarly, the fractions for the plasma raised against a mix of *Naja* venoms showed that IgG(T)-depleted sample has statistically significantly higher binding capacity than IgG(T)-enriched fraction (Figure 4.6 B), additional data is available in Appendix III(C). This shows that, despite IgG(T) being the major IgG component, the proportion of the non-IgG(T) antibodies reacting with target venom epitopes is higher than the proportion in IgG(T).

Furthermore, the HHP produced against mixed *E. leucogaster* and *E. ocellatus* venoms, showed similar binding trends of IgG(T)-enriched and IgG(T)-depleted samples to *E. leucogaster* and *E. ocellatus* venoms respectively (Figure 4.6 A). As the two species are closely related (Pook et al. 2009), these findings suggest that venom compositions from these two *Echis spp.* may contain a similar quantity of immunogenic toxins. This has also been suggested previously by (Calvete et al. 2010). Similarly, there was no statistically significant difference between binding of the IgG(T)-enriched sample to the three *Naja species* (Figure 4.6 B). There was also no statistically significant difference in binding of the IgG(T)-depleted sample between *N. haje*

and *N. melanoleuca* venoms. In contrast, there was statistically significant difference between binding activity of IgG(T)-depleted samples between *N. haje* and *N. nigricollis* venoms, and between the *N. melanoleuca* and *N. nigricollis* venoms. A summary of statistical significance is given in Figure 4.6.

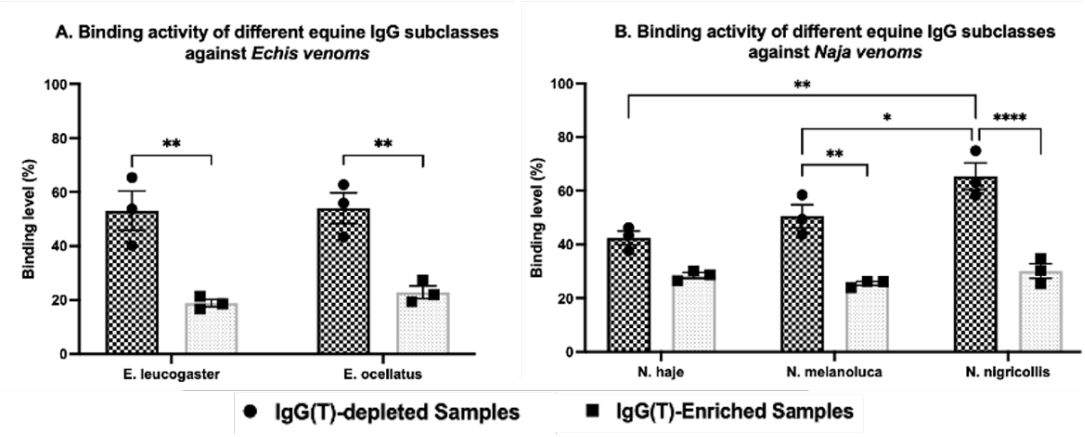

Figure 4.6 Binding capacity for IgG(T)-enriched and IgG(T)-depleted samples against individual venoms from (A) *Echis* and (B) *Naja* species.

ELISA results comparing the binding capacity of IgG(T)-enriched and IgG(T)-depleted antivenoms against *Echis* spp. (A) and *N.* spp. (B). As described in section 4.3.5, all results were calculated in relative to the reference (AffiPureIgG). Further methodological details are available in section 2.2.10.

Data were analysed using Prism GraphPad 9. Two-way ANOVA with Tukey's method *post-hoc* test was used to determine statistical significance. Values are mean ± SD of triplicates from three biologically independent experiments, comprising three technical replicates.

In Fig.4.6A, ** indicates for p= 0.0044 and p=0.0078 for *E. leucogaster* and *E. ocellatus* respectively. Whilst in Fig. 4.6B, * indicates for P=0.0048, ** (*N. melanoleuca)* indicates for p= 0.0023, ** (*N. haje: N. nigricollis*) indicates for p< 0.001 and **** indicates for P < 0.0001.

These results suggest that binding of IgG(T) is not significantly affected by species of venom. In contrast, the IgG(T)-depleted sample indicated considerable disparity of binding between different *Naja* species, which may reflect intraspecies and interspecies venom variation (Mackessy 2009; Petras et al. 2011). Previous studies (Fernandes et al. 2000a; Toro et al. 2006) demonstrated that IgG(T) has the greatest binding capacity, which may reflect the content of IgG(T) which makes up the highest proportion of the equine IgG

isotype (Fernandes et al. 1991). In contrast, the data obtained from this study have shown that other IgG subclasses have a considerably greater binding capacity than IgG(T). Although these subclasses represent only about 24% of the total equine IgG isotype (Figure 4.4), their binding superiority could be due to the fact that they are highly potent or may contain higher venom-specific activities compared to the IgG(T) subclass. Because of physicochemical relationships between IgG(T), IgGc and IgA, the IgG(T)-enriched samples may contain small residual amounts of these other horse Ig class/ IgG subclasses. However, the separation method is reported to be exquisitely effective so that the presence of IgA is negligible, and IgGc is reported to be almost undetectable in HHP (Fernandes et al. 1997; Krifi et al. 1999).

As summarised in Table 4.2, the IgG(T)-depleted sample showed the highest binding capacity against all tested venoms. In the anti-*Echis* antivenom, the IgG(T)-depleted antivenom showed a binding capacity greater than 2.8 and 2.4 times that of IgG(T)-enriched samples against *E. leucogaster* and *E. ocellatus,* respectively. Similarly, within the antivenom raised against the *Naja* species, the IgG(T)-depleted antivenom demonstrated a binding capacity greater than 2.2, 2.0 and 1.5 times that of IgG(T)-enriched against *N. nigricollis, N. melanoleuca* and *N. haje,* respectively. The IgG(T)-depleted antivenom also showed a binding capacity greater than 2.2 and 1.9 times that of TIgG sample against *E. leucogaster* and *E. ocellatus* venoms*,* respectively (for group *Echis*)*.* For the anti-*Naja* sample, the binding capacity of the IgG(T)-depleted antivenom was greater than 1.6, 1.5 and 1.3 times of total IgG sample against *N. nigricollis, N. melanoleuca* and *N. haje*, respectively.

Table 4.1 ELISA results comparing the relative percentage of binding capacity for the different AVs against individual venoms

	Snake species	IgG(T)-depleted AV	IgG(T)-enriched AV	TIgG AV
***Echis* group**	*E. leucogaster*	53.1	18.9	24.7
	E. ocellatus	54.0	22.9	27.9
***Naja* group**	*N. haje*	42.4	28.4	32.6
	N. melanoleuca	50.5	25.5	33.0
	N. nigricollis	65.4	30.1	40.9

Abbreviations: AV, antivenom, TIgG, Total IgG

4.3.6 ELISA: binding efficacy of different antivenoms against venom mixtures

Further to the individual venoms, the study evaluated the binding capacity of TIgG, IgG(T)-enriched and IgG(T)-depleted antivenoms against a mixture of venoms that used in the immunisation protocol for the antivenom in test. To achieve this, ELISA plates were coated using a venom mixture (2.5 µg/mL) comprising equal quantity from *Echis* species (for group *Echis*) or equal quantity from the *Naja* species (for group *Naja*). All antivenom samples had a starting protein concentration of 125 µg/mL and were then serially diluted 4-fold, in duplicate. All other steps were performed as described in section 2.2.10.

Plotting the OD results against their concentrations has generated a sigmoidal curve (Figure 4.7 A&B). This provided visual comparisons of binding trends for the different antivenoms against a mixture of venoms used to immunise each group. As shown in Figure 4.7 A, the IgG(T)-depleted antivenom (indicated by green colour) has the highest titre followed by TIgG (indicated by blue colour) and IgG(T)-enriched (indicated by red colour) with least titration values against the *Echis* group. Similar titre trends were also observed against the *Naja* group (Figure 4.7 B). As expected, the negative control (indicated by purple colour) has negligible titre values against all tested venoms. Additional data are available in Appendix III (D).

As shown in Figure 4.7, nonlinear curve representing log (agonist) vs response with four- parameters (Top, Bottom, Hillslope and the EC_{50}), was used to determine the half-maximal effective concentration (EC_{50}) values for each subclass.

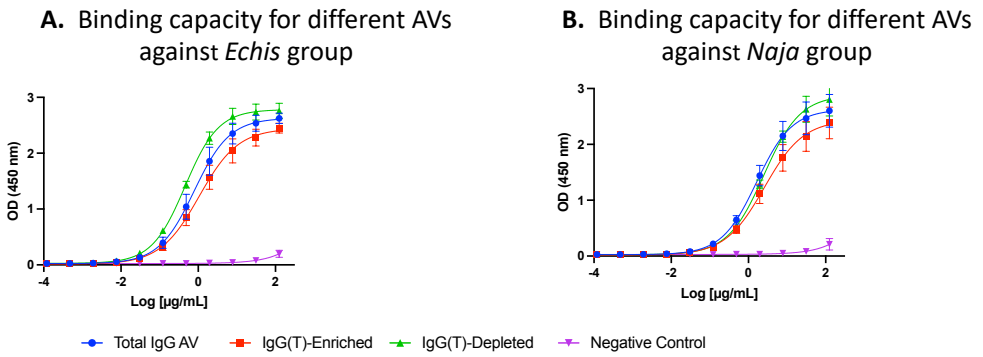

Figure 4.7 ELISA titre curves illustrating the binding efficacy of the different AVs against snake venom mixtures.

Nonlinear sigmoidal curves illustrating the binding capacity of TIgG, IgG(T)-enriched, IgG(T)-depleted and negative control samples against *Echis* spp. (A) and *N. spp.* (B). ELISA plates were coated with venom mixture containing equal quantity of venoms that used in the immunising protocol.

Data were analysed using Prism GraphPad 9. Bars represent mean ± SD of triplicates from at least three biologically independent experiments, comprising three technical replicates. Abbreviations: µg microgram; mL, millilitre; AVs, antivenoms.

The half-maximal effective concentration (EC_{50}) can also be used to signify the quantity of an antivenom that is required to inhibit venom activities by, for example, occupying and effectively blocking the venoms' active sites (Gutiérrez et al. 2003). In respect to our ELISA result, this is equivalent to the lowest concentration (highest dilution) of the antivenom that increased the OD by 50% from the NHP sample (negative control), which showed a signal close to baseline (Figure 4.7 A&B). Therefore, the lower the EC_{50} value (Table 4.2), the more potent is the antivenom, and hence lower quantities are likely to be required to promote effective neutralisation against a given snakebite envenoming.

In all antivenoms tested, IgG(T)-depleted samples had lower EC_{50} values than IgG(T)-enriched samples, or that of TIgG antivenom (Table 4.2). Compared to IgG(T)-depleted antivenom, the IgG(T)-enriched antivenom showed a higher EC_{50} values of approximately 2.4 and 2-fold higher in the *Echis* and *Naja* groups, respectively. Similarly, the TIgG had EC_{50} values of approximately 1.7 and 1.2-fold higher than that of IgG(T)-depleted EC_{50} value for *Echis* spp. and *Naja* spp., respectively.

Table 4.2 EC_{50} for antivenoms against A) Echis and (B) Naja venoms.

Unit	Antigen	Total IgG (TIgG) AV	IgG(T)-Enriched AV	IgG(T)-Depleted AV	Negative Control (NHP)
EC_{50} (µg/mL)	A- *Echis*	0.91	1.26	0.52	157700
	B- *Naja*	1.71	2.8	1.43	65820

IC_{50}s were obtained from at least three biologically independent experiments, comprising three technical replicates [see Appendix III(D)]. Data were analysed using GraphPad 9.0. Simple regression curve and sigmoidal 4- parameters (top, bottom, hillslope and log EC_{50}) analysis was used to determine the EC_{50}s for each antivenom. The negative control was a Non-Hyperimmune Horse Plasma denoted NHP.

Abbreviations: AV, antivenom; IC_{50}, half-maximal effective concentration.

4.3.7 Correlating venom toxin families with IgG subclasses

The ability of total IgG, IgG(T)-enriched and IgG(T)-depleted antivenoms to recognise venom toxins was determined using Western blotting (Figure 4.8 C&D). These results demonstrate that both IgG(T)-enriched and IgG(T)-depleted antivenoms are effective at recognising the same proteins but at variable intensity (Figure 4.8, C&D). Almost all of the *Echis* venom proteins visualised under Coomassie stained gel (Figure 4.8 A) were recognised by the two antivenoms but at a slightly different intensity: there were more prominent bands in the IgG(T)-depleted samples for *Echis* venoms in lanes 8&9 of Figure 4.8 C than for IgG(T)-enriched (lanes 5&6). For the *Naja* species, the Coomassie-stained venom gels (Figure 4.8 B) showed intense bands corresponding to proteins ≤ 20 kDa, whereas in the corresponding Western blot (Figure 4.8 D), proteins with molecular weight ≥ 40 kDa appeared with greater intensity.

Moreover, Coomassie stain revealed a highly intense protein band at ~15 kDa for *E. leucogaster* venom (indicated by arrow in Figure 4.8 A) where the same band has shown less intensity for *E. ocellatus* venom (Figure 4.8 A). This may suggest that the specific venom protein present at different concentrations within the two *Echis* species. Similarly, a band of the same size (~15 kDa) was seen in electrophoresed *Naja* venoms (indicated by arrow in Figure 4.8 B). Despite being of small MW, this band was still seen, particularly in

electrophoresed *E. leucogaster* and *N. nigricollis* venoms, in the corresponding Western blots, shown in lane 8 (Figure 4.8 C) and lane 12 (Figure 4.8 D), respectively. This may suggest that the venom protein corresponding to this band is immunogenic. Interestingly, the IgG(T)-depleted antivenom showed more intense bands, suggesting higher binding with these proteins. In snake venoms, this band is likely to represent PLA_2s with a MW of 13–15 kDa (Schaloske and Dennis 2006). A similar band, which was visualised using SDS-PAGE and Western blotting techniques was subsequently identified as PLA_2s from *N. nigricollis* venom using venomics (Petras et al. 2011). PLA_2s make up 12.6 % of total venom proteins in *E.* ocellatus (Wagstaff et al. 2009) but the more intense band seen in the Coomassie stained gel (Figure 4.8 A) suggests the predominance of this toxin in *E. leucogaster* venom which represent 39.7% of its total venom composition (Albulescu et al. 2020). Snake venom PLA_2s were characterised from spitting cobra (Petras et al. 2011) and *Echis* spp. (Calvete et al. 2010) but at different ratios (Tasoulis and Isbister 2017). Nevertheless, excellent characterisations of *Echis* and *Naja* venoms have been extensively described elsewhere: (Casewell et al. 2009; Wagstaff et al. 2009; Calvete et al. 2010; Petras et al. 2011; Malih et al. 2014; Lauridsen et al. 2017).

These results and our data (Figure 4.8) suggest that this toxin family is a key venom component of many snake venoms, particularly *E. leucogaster, E. ocellatus* and *N. nigricollis.*

Furthermore, under the Coomassie staining (Figure 4.8 B), two of almost equal size bands (~10kDa) were visualised for *N. haje* venom (lanes 2, 6 &10, Figure 4.8 B)- also indicated by arrow in lane 6, Figure 4.8 B. Given to the bands' intensity and migration distances, these could be 3FTXs (~6.6 – 8.2 kDa) which make about 60% of the total venom composition in *N. haje* (Malih et al. 2014). Although it was faint bands, these venom components were recognised by Total IgG and IgG(T)-enriched antivenoms (lanes, 2 & 6 Figure 4.8 B). Interestingly, the IgG(T)-depleted antivenom recognised only one band (lane 10, Figure 4.8 D), but at a lower intensity compared to the other IgG subclasses.

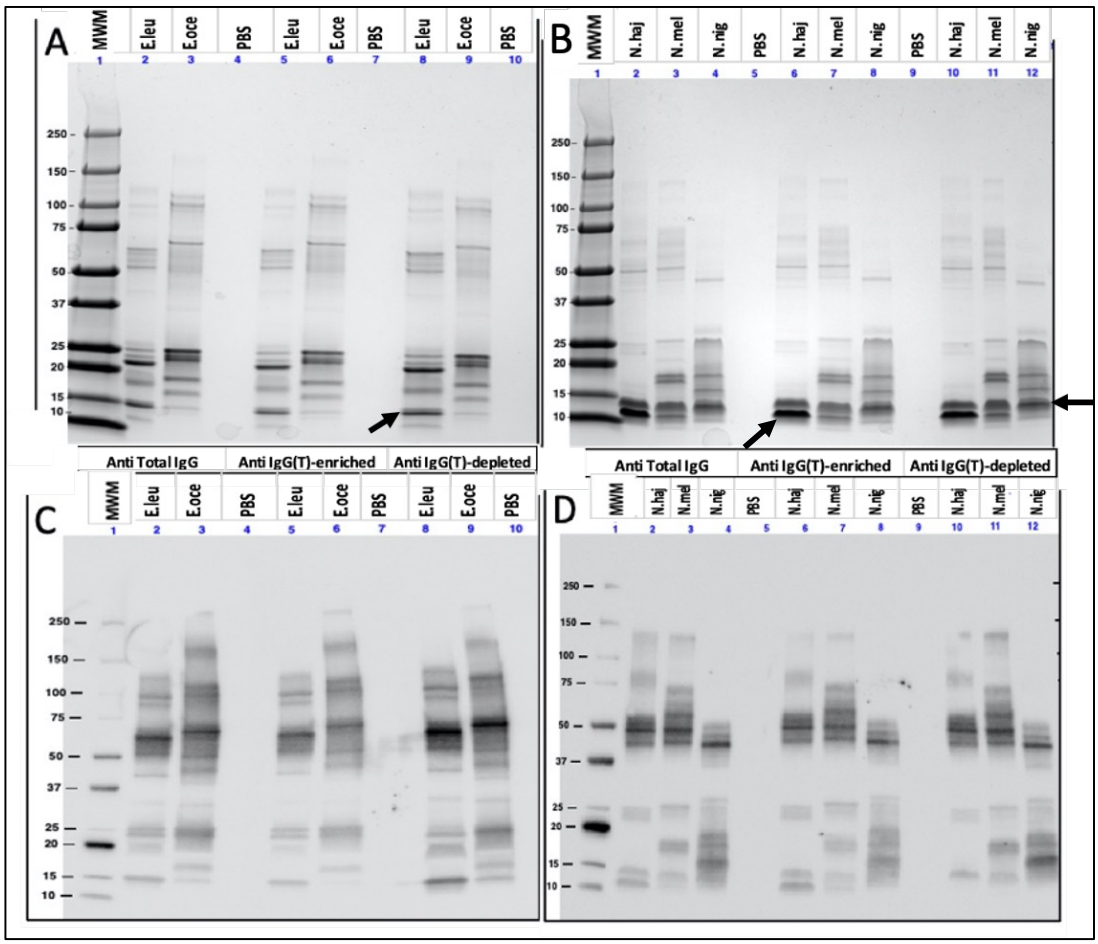

Figure 4.8 electrophoresis of snake venom proteins and their detection by Western blot analysis.

Non-reducing Coomassie stain (A&B) and Western blot analysis (C&D) for venom toxins from *Echis leucogaster* and *E. ocellatus* (A & C) and from *Naja haje*, *N. melanoleuca* and *N. nigricollis* (B & D). All proteins were loaded at 2.5 µg/well. Further details are available in section 2.2.9.1 & 2.2.9.2. Electrophoresed proteins were stained with Coomassie Brilliant blue dye and blots were probed against HRP-conjugated goat anti-horse IgG, diluted at 1: 5,000 in blocking buffer. Blots were visualised using ECL reagents, and images were captured using a ChemiDoc imaging system.

Abbreviations: MWM, molecular weight marker; E. leu, *Echis leucogaster;* E. oce, *Echis ocellatus*; PBS, phosphate buffered saline; N. haj, *Naja haje;* N. mel, *Naja melanoleuca;* and N. nig*, Naja nigricollis.*

4.3.8 Separation of IgGa and IgGb isotypes using Protein G purification

The separation of horse Ig isotypes and IgG subclasses is described by (Sheoran and Holmes 1996; Sugiura et al. 2000). Using this method, a relatively pure separation of IgGa and IgGb subclasses was achieved. The FT or IgG(T)-depleted sample collected from the AEX step, was passed through a Protein G column. After washing the column extensively, a larger quantity of proteins was eluted at a pH of 2.9 (Figure 4.9, A-C, lane 7) and a relatively small amount collected at pH 2.5 (Figure 4.9, A-C, lane 8).

Following Western blot analysis (Figure 4.9, B-C), the likely identification of the two fractions eluted at pH of 2.9 and 2.5 (lanes 7 & 8 respectively) were, as expected, IgGa and IgGb although separation appears to be incomplete. This is consistent with previous published data (Sheoran and Holmes 1996; Sugiura et al. 2000). The purity of the samples was assessed by performing SDS-PAGE under reducing conditions with Coomassie blue staining (Figure 4.9 A). The presence of clear bands at ~55 kDa, particularly in lanes 7 and 8, may suggest that a single IgG subclass (or biochemically related subclass) has been obtained under these conditions. Additionally, the bands detected at ~25 kDa (Figure 4.9 A), are light chain bands.

A previous study, conducted by Lewis et al., 2008, showed that polyclonal anti horse IgG(T) at a 1:10,000 dilution cross-reacted with the IgG_2, component of IgGa, under reduced conditions. The presence of a faint band at ~50 kDa in lane 7 (Figure 4.9 D), but not in lane 8 (Figure 4.9 D), indicates successful separation of IgGa and IgGb from IgG(T). Bands of different intensity were visualised using Western blotting with mouse anti-horse IgGa (Figure 4.9 B) and mouse anti-horse IgGb (Figure 4.9 C). However, the band at ~50 kDa in lane 8 (Figure 4.9 C) and its lower intensity in lane 8 (Figure 4.9 B), suggests that IgGb was eluted at pH 2.5. There is a dearth of published data on the use of these antibodies in Western blotting. Thus, the presence of bands at other molecular weights may be due to the inherent cross-reactivity of the monoclonal mouse anti-horse IgGa and anti-horse IgGb antibodies or maybe separation of the two subtypes was not complete.

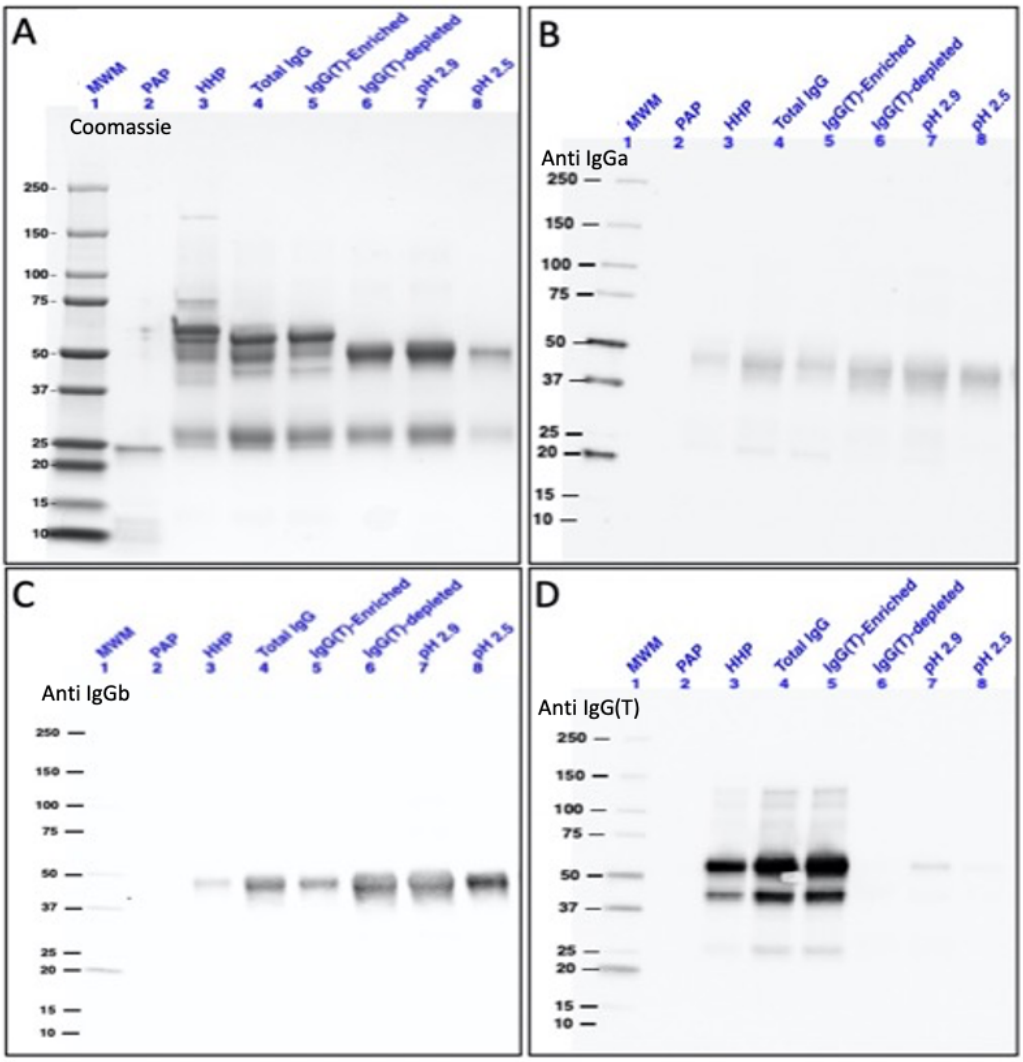

Figure 4.9 SDS-PAGE and Western blotting analysis for IgGa and IgGb subclasses separated by Protein G method.

Electrophoresed proteins were stained with Coomassie blue (A), Western blotting with mouse anti-horse IgGa (B), mouse anti-horse IgGb (C), and goat anti-horse IgG(T) (D). All proteins were loaded at 2.5 µg/well. HRP-conjugated goat anti-mouse IgG (H+L) and goat anti-horse IgG(T) were diluted 1:5000 and 1:10,000, respectively, in blocking buffer. Blots were visualised using ECL reagents and images were captured using the ChemiDoc imaging system. Full details of SDS-PAGE and Western blot methods are given in sections 2.2.9.1 and 2.2.9.2, respectively.

Abbreviation: MWM; molecular weight marker, HHP; hyperimmune horse plasma, PAP; papain (negative control).

4.3.9 Quantification of different IgG-subclasses

Following the separation of IgG(T), IgGa and IgGb using AEX and Protein G columns, their relative quantity (w/w) in HHP was determined (assuming full separation). Based on the protein concentration (described in section 2.2.4), it is estimated that IgGa makes up ~81 %, IgGb ~15% of the IgG(T)-depleted sample (Figure 4.10). As described in section 4.3.3, the IgG(T)-depleted sample represents approximately 24% of the TIgG (total IgG). Therefore, within the TIgG sample, IgGa and IgGb will be equivalent to ~20% and ~4%, respectively. These findings are consistent with published data which reported that IgG(T) and IgGa constitute the majority of equine IgG in HHP (Toro et al. 2006).

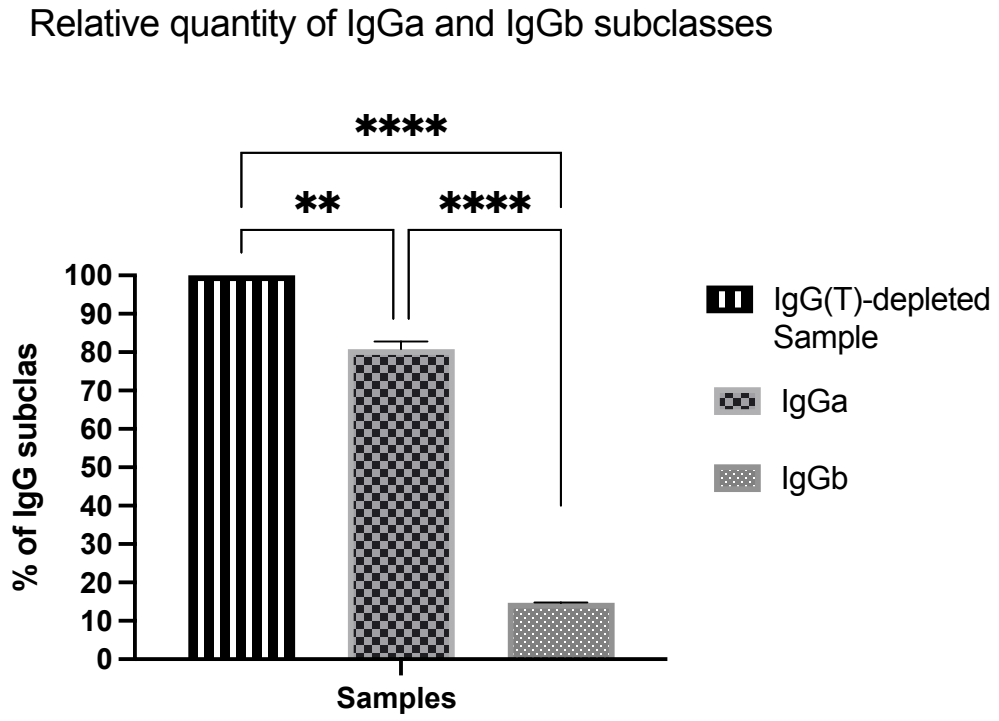

Figure 4.10 Quantity of IgGa and IgGb subclasses in the total IgG sample.

IgGa and IgGb were separated from the IgG(T)-depleted sample using Protein G chromatography. Protein concentrations were measured as described in section 2.2.4. Data were analysed using Prism GraphPad 9. One-way ANOVA was performed with *post-hoc* Tukey's multiple comparison test to determine statistical significance, ** indicates P <0.0063 and **** < 0.0001. Values are mean ± SD of three biologically independent experiments.

4.4 Discussion

Gene duplication in mammals has led to the expression of multiple IgG subclasses that are variable in number and function (Butler 1997). Equine IgG consists of seven IgG subclasses (IgG_1 – IgG_7), that are characterised by physicochemical similarities (Lewis et al. 2008). Such similarity creates inherent difficulties in the separation of these IgG subclasses. Although several studies (Fernandes et al. 1991; Sheoran and Holmes 1996; Fernandes et al. 1997; Fernandes et al. 2000a; Toro et al. 2006) reported successful separation, obtaining a single and pure equine IgG subclass remains a challenging task. Here, we report the optimisation of methods to fractionate equine IgGa, IgGb and IgG(T) subclasses.

The use of the AEX matrix; Q sepharose XL (QXL), allows the partition of IgGa/IgGb (IgGab) and IgG(T) according to their surface charge at the selected pH. The IgG(T)-depleted antivenom comprised pure IgGa and IgGb (IgGab), the absence of IgG(T) being confirmed using Western blotting. These results were consistent with earlier publications reporting the use of anion exchangers, such as DEAE, to selectively purify IgGab from equine IgG (Sheoran and Holmes 1996; Sugiura et al. 2000). Given the physicochemical similarities between IgA, IgG(T) and IgGc (Sugiura et al. 2000), the IgG(T)-enriched sample may contain very small residual amounts of IgA and IgGc. The proportion of IgGc in HHP is negligible (Toro et al. 2006), so the purification method was optimised to minimise contamination, including that of other Ig isotypes, in the downstream process.

Quantitatively, the results presented show that together IgGa and IgGb represent 20-30% (w/w) of the total IgG isotype content in HHP. However, IgG(T), the predominant IgG subclass in HHP (Toro et al. 2006), represents 60-70% of IgG. Subsequently, IgGa and IgGb were separated using a Protein G column to produce relatively pure IgGa (~20%) and IgGb (~4%) of TIgG (Figure 4.10). This is corroborated by published data (Fernandes et al. 1991; Fernandes et al. 1997; Fernandes et al. 2000a; Fernandes et al. 2000b), and others demonstrate that IgG(T) and IgGa together make up around 80% of IgG (Toro et al. 2006). Despite the lack of understanding of the mechanisms which regulate IgG subclass production in the horse, antigen type (Lopez et

al. 2002) and immunisation method (Hooper-McGrevy et al. 2003) play critical roles in priming B cells to produce distinctive populations of IgG subclasses. To some extent, this could be the reason for the discrepancies in subclass composition reported in the literature.

Previous studies (Fernandes et al. 2000a; Toro et al. 2006) demonstrated that IgGa confers significant protection against venom toxins in mouse neutralisation studies. Toro et al., 2006 demonstrated that both IgGa and IgG(T) possess considerable ELISA antibody titres against venoms from scorpions. Consistent with these findings, the data presented provide evidence that the neutralising efficacy of horse plasma-derived antivenoms may not be ascribed to IgG(T) alone. Indeed, the IgG(T)-depleted antivenom shows significantly higher binding capacity than that of the IgG(T)-enriched antivenom.

Considering the binding capacity values, the IgG(T)-depleted samples were superior when compared to TIgG and IgG(T)-enriched antivenoms against all tested venoms. As shown in Table 4.1, the IgG(T)-depleted sample (group *Echis*) demonstrate binding capacity greater than 2.4 and 1.9 times that of IgG(T)-enriched and TIgG samples, respectively. Within the *Naja* group, the IgG(T)-depleted antivenom demonstrate binding capacity greater than 1.5 and 1.3 times that of IgG(T)-enriched and TIgG samples, respectively. A higher binding capacity, therefore, signifies antibodies with higher avidity (binding strength between venom and antivenom), which may predict the performance of the antivenom *in vivo* potency measures.

Similarly, the IgG(T)-depleted antivenom still demonstrated the highest titre (Figure 4.7) when assayed against a mixture of venoms used in the immunisation strategy for each group of snake species. EC_{50} is the concentration of antivenoms required to inhibit the activities of a given venom by 50% and we propose that our EC_{50} values may represent a surrogate for the effectiveness of the products. A lower EC_{50} (see Table 4.2) signifies antibodies with higher avidity (binding strength between venom and antivenom), which may be equivalent to *in vivo* potency measures.

Although it is plausible to predict that antivenom with higher avidity to target venoms is more likely to elicit a greater potency, careful assessment should

be made when correlating to *in vivo* data. This is because venom is made up of highly complex biologically active proteins and thus, predicting the harm-causing molecule could be challenging. Moreover, some highly toxic venom components are less immunogenic, thereby producing fewer antibodies and/or antibodies of lower affinity (Calvete et al. 2010; León et al. 2011). Such antivenoms will fail to neutralise lethality effectively. Nonetheless, substantial studies have demonstrated that binding activities from ELISA studies correlated to *in vivo* potency (Theakston and Reid 1979; Rial et al. 2006; Khaing et al. 2018). In contrast, others have shown poor correlations between results obtained from ELISA assays and *in vivo* studies (Barbosa et al. 1995; Alape-Girón et al. 1997). This could be due to the fact that snake venoms constitute many different proteins making estimations of lethality-causing toxin very challenging. Additionally, toxicologically irrelevant venom component could be highly immunogenic and thus, unlike the potency assay which assess the overall venom lethality, the ELISA result will reflect the immune response (Gutiérrez et al. 2021). For example, ELISA results against venoms from the *D. polylepis* snake have shown a higher titre against the larger non-toxic SVMPs than the highly lethal smaller venom components such as 3FTXs and dendrotoxins (Laustsen et al. 2015). Therefore, that the use of ELISA assays for assessing antivenom efficacy should be assessed for each snake venom individually.

These results (also see section 4.3.5) demonstrate that binding of antivenoms raised against a combination of *E. leucogaster* and *E. ocellatus* venoms is similar for each of the two *Echis* venoms. This suggest that *E. leucogaster* and *E. ocellatus* venoms contain similar components. Although *Echis* venoms are typically dominated by HMW toxins, such as SVMPs, LMW toxins such as PLA_2 and C-type lectins (CTL), are also considered significant venom components (Wagstaff et al. 2009; Tasoulis and Isbister 2017). The HMW venom enzymatic toxins are more immunogenic than the smaller ones, such as PLA_2 which have been shown to have variable immunogenicity (Calvete et al. 2010; Ainsworth et al. 2020). PLA_2 make up about 40% within the proteomic of *E. leucogaster* (Albulescu et al. 2020) compared to 8.5 – 12.6% of the total

venom proteins in *E. ocellatus* (Wagstaff and Harrison 2006; Casewell et al. 2009; Tasoulis and Isbister 2017)

Furthermore, PLA_2 from *E. ocellatus* venom was reported to be more immunogenic (45–67%) compared to that from *E. leucogaster* venom (25-40%) (Calvete et al. 2010). Coomassie stain (Figure 4.8 A), showed a higher staining density of bands with a MW that are consistent with PLA_2s in *E. leucogaster* venom compared to *E. ocellatus.* Although *E. ocellatus* may contain PLA_2 of high immunogenicity, the slightly higher binding capacity (Table 4.1) of the IgG(T)-depleted antivenom towards the *E. leucogaster*, may reflect that *E. leucogaster* contain higher content of PLA_2 than *E. ocellatus*. This $svPLA_2$s molecule is comprehensively described in the literature (Schaloske and Dennis 2006; Kang et al. 2011; Harris and Scott-Davey 2013; Ferraz et al. 2019).

Binding activity of IgG(T)-enriched antivenom raised against a mix of 3 *Naja* venoms was also similar for the three individual *Naja* venoms. However, the IgG(T)-depleted antivenom showed an inconsistent response, the highest binding being with *N. nigricollis* venom and the least with *N. haje* venom (see Table 4.1). These cobra venom toxins are dominated by 3FTXs and $svPLA_2$s, albeit, with different quantities and qualities (Tasoulis and Isbister 2017). The 3FTXs are LMW neurotoxins which are poorly immunogenic and are therefore likely to induce production of qualitatively and/or quantitatively defected antibodies (Calvete et al. 2010). This may explain the absence of distinct LMW bands on Western blot (Figure 4.8 C), despite being prominent on SDS-PAGE gels (Figure 4.8 B). Antivenomic studies of EchiTab Plus-ICP demonstrated that some types of PLA_2 were effectively immunodepleted whilst others were only partially immunodepleted (Calvete et al. 2010).

Proteomic studies revealed that *N. nigricollis* venom contains 21.9% PLA_2, *N. melanoleuca* 12% and *N. haje 4%* of total venom protein (Tasoulis and Isbister 2017). Interestingly, the IgG(T)-depleted Western blot (Figure 4.8 B) is consistent with the high PLA_2 content within the *Naja* species venoms. *Naja nigricollis* venom is rich in PLA_2s which are implicated in severe local pathological lesions (Warrell et al. 1976b). Its venom is less neurotoxic compared to the non-spitting, *Naja* spp., but may result in extensive necrosis

attributed to the cytotoxic PLA_2s associated with spitting cobra venom (Petras et al. 2011). In agreement with these findings (Petras et al., 2011), there was an intense band on the *N. nigricollis* venom SDS-PAGE gel (Figure 4.8 D), of a MW corresponding to PLA_2s (~15 kDa). It was also demonstrated (Petras et al., 2011) that PLA_2 was recognised by EchiTabG-Plus-ICP, a polyspecific equine IgG- antivenom raised against *B. arietans, E. ocellatus and N. nigricollis* venoms (Petras et al. 2011). In spite, EchiTab-Plus-ICP has much higher ED_{50} value (lower neutralisation efficacy) for *N. nigricollis* venom (Petras et al. 2011), than that for *Echis ocellatus,* (Ainsworth et al. 2020). This disparity may be explained by the presence of higher molecular weight SVMPs in *Echis* spp. accounting for nearly 70% of total venom protein (Wagstaff et al. 2009), which are responsible for consumptive coagulopathy, systemic haemorrhage and spontaneous bleeding (Warrell et al. 1974).

Besides being more immunogenic (Ainsworth et al. 2020), these results (Figure 4.8 C and 4.8 D) show that IgG(T)-enriched antivenom has high binding with SVMPs, which are 20 – 100 kDa (Fox and Serrano 2008). This is consistent with antivenomic studies (Petras et al. 2011; Sánchez et al. 2015b), that have shown polyvalent antivenoms were effective in recognising HMW venom toxins, particularly the PIII-SVMPs which are 60 -100kDa (Fox and Serrano 2008). Clinical symptoms of envenoming by *N. nigricollis* include local swelling, extensive tissue necrosis, spontaneous haemorrhage and depleted platelets (Warrell et al. 1976b), these manifestations being consistent with cytotoxic PLA_2s (Ferraz et al. 2019). Therefore, the lower potency observed for EchiTab-Plus-ICP antivenom against *N. nigricollis* could be, at least partially, due to the presence of IgGa at lower quantity generally within whole IgG-based antivenoms.

A neutralisation efficacy of a Latin American polyvalent antivenom (manufactured by ICP, Costa Rica) was reported to be exclusively due to the IgG(T) subclass (Fernandes et al. 2000a). The authors have reported that the IgGa subclass from this antivenom has failed to neutralise $svPLA_2$ and as a consequence, this antivenom has a significantly lower neutralising efficacy against $svPLA_2$ compared to a parallel antivenom with IgGa of higher neutralising activity. Despite being a completely different antivenom targeting

venoms from a different geographical region, both antivenoms were produced by the same manufacturer and thus, antigen and immunisation strategy may influence production of IgG subclasses (Hooper-McGrevy et al. 2003).

Taken together, the current study demonstrates that the IgGab are proportionally less represented than IgG(T) (Figure 4.10), but due to their superior potency, IgGab exhibit higher binding titres than IgG(T)-enriched antivenoms (see Figure 4.7 A&B and Table 4.1). Additionally, alongside the HMW venom toxins, this study shows that IgGab antivenom has a higher affinity than IgG(T) for svPLA$_2$. This may suggest that IgGab may confer potent neutralising activities, particularly against svPLA$_2$-induced toxicity profiles. In contrast, IgG(T)-enriched antivenom, which shows effective binding to the HMW venom toxins, shows less binding to svPLA$_2$s. The higher the binding efficacy of an antivenom may equate to: a) removal of venom toxins already bound to target tissues, b) effective blockade of target sites and c) induce conformational changes of toxins, making toxin binding sites inaccessible (Gutiérrez et al. 2003; Laustsen et al. 2018; Nikapitiya and Maduwage 2018). It is unclear if the superior binding ability of IgGab extends to other LMW venom toxins. The western blot results (Figure 4.8 D) have shown that the 3FTXs in *Naja* venoms were poorly recognised by all IgG subclasses.

Although, the IgG(T)-depleted sample is reported here as IgGab- antivenom, IgGb is thought to have the lowest binding efficacy to venom toxins (Fernandes et al. 2000a). Quantitively, these results (Figure 4.10) suggest that IgGb accounts for ≤15% of the IgG(T)-depleted sample, which is dominated by IgGa (≥81%). Furthermore, IgG$_1$, component of IgGa, is reported to provide more protection against the activity of bacterial infection in horses than IgG$_4$/$_7$ (IgGb) and IgG$_3$/$_5$, [IgG(T)] (Rocha et al. 2019). This provides a parallel suggesting that most of the binding observed by the IgG(T)-depleted antivenom may be empirically due to IgGa. Nevertheless, the extrapolation of these results to cell and/or *in vivo* assays remains to be completed. The results would suggest that combining IgG(T) and IgGa, would improve the efficacy and safety of antivenoms by reducing the dose required and, therefore, administration of irrelevant exogenous protein. Separation of IgGa and IgGb using a Protein G column requires a pH of ≤2.5 which leads to irreversible aggregation.

Despite the formation of acid-induced aggregations, human IgG has been shown to preserve its antigen binding activities (Lopez et al. 2019). Nonetheless, in current therapeutics, acidic elution aggregates are removed from final monoclonal antibody product. Precipitate formation due to aggregates commonly results in the rejection of liquid formulation products during stability testing (Al-Abdulla, personal communication). Removal of aggregates was beyond the scope of this study. Formation of precipitates after prolonged storage of samples was observed, making the individual downstream analysis of IgGa and IgGb futile.

4.5 Limitation of the study

This study lacks the sensitivity to identify the specific venom toxins recognised by each IgG subclass. This would require more rigorous separation of venom proteins and the application of techniques such as venomics (Pla et al. 2017) to determine which toxins are recognised by which IgG subclass. Additionally, the study would have benefited from using techniques such as Biacore to assess the real-time affinity measurements of the equine IgG subclasses in respect to the venom toxins.

4.6 Conclusion and Future direction

Here we demonstrate that the binding of venom toxins of snakes residing in SSA region, by horse-derived antivenoms is not limited to IgG(T). In fact, IgGab showed significantly higher binding activity to all tested venoms than that of IgG(T). The results have shown that the IgGab antivenom demonstrated a higher binding capacity to PLA_2 than IgG(T)-antivenom. This may explain the lower neutralising efficacy for treatment of *N. nigricollis* envenoming by some antivenoms marketed in Sub-Saharan Africa (Ainsworth et al. 2020). However, none of the tested IgG subclasses bound effectively to LMW toxins, which include the 3FTXs found in abundance in the venoms of neurotoxic *Naja* species.

Currently, the manufacture of IgGab-based antivenom is not a logistically feasible option; however, optimisation of immunisation techniques to enrich the production of these subclasses might improve the efficacy of antivenoms. Moreover, their omission from antivenom preparations could potentially lead

to antivenoms with inferior efficacy. Next, we aim to investigate whether these binding activities are extrapolated to neutralisation of cell cytotoxicity assays and in an invertebrate model. If successful, preparation, using a combination of IgG subclasses and proven neutralising properties, will provide a highly efficacious and safe antivenom for the treatment of envenoming in sub-Saharan Africa.

Chapter 5: Developing an invertebrate model and Vero cell assay for assessing snake venom toxicity and antivenom potency

5.1 Introduction

Assessment of venom toxicity and antivenom efficacy are two integral contemporaneous requirements in the discovery, design and development of medicinal drugs such as antivenoms (Parasuraman 2011). This requires validation of relevant biological assays, including animal studies, which are fundamental in establishing key properties, including safety and efficacy, of an antivenom throughout its life cycle. Sadly, antivenom marketed with insufficient preclinical testing has resulted in tragedy when administered to envenomed patients (Visser et al. 2008; Alirol et al. 2015). This has led to the ever-increased demands to establish robust methods for preclinical characterisation of antivenoms.

Snake venoms have an enormously variable toxicity profile consequent to their venom composition, occurring at all biological and taxological levels (Chippaux and Goyffon 1998). Toxicity is expressed in a median lethal dose (LD_{50}) which is the quantity of venom (µg) that kills 50% of the tested animals (Erhirhie et al. 2018). Currently, snake venom toxicity is measured using *in vivo* assays, the mouse being the most commonly used animal (Chippaux and Goyffon 1998). Similarly, the efficacy of antivenom (or neutralisation capacity) on annulling the lethal activities of venom is expressed as a median effective dose (ED_{50}), (World Health Organization 2016). ED_{50} is the amount of antivenom (µL) required to neutralise lethality of a challenge dose of venom (µg) in 50% of tested animals (Ainsworth et al. 2020). Challenge dose is the quantity of venom toxins capable of inducing submaximal responses in assay system or a supralethal response in animals (Gutierrez et al. 2014), usually 2.5 – 5x LD_{50} (Ainsworth et al. 2020), although others suggest 3 to 6x LD_{50} (World Health Organization 2016; Gutierrez et al. 2017b) of the corresponding snake venom. Although other routes of injection may be used (Chippaux and Goyffon 1998; Gutierrez et al. 2017b), intravenous injection of 5 – 6 mice/dose group is the most commonly used method of administration in these assays (Casasola et al. 2009; Casewell et al. 2010; Segura et al. 2010). The LD_{50} and ED_{50} can be calculated using Probit analysis (Sells et al. 1998), Spearman-Kerber or other

non-parametric test analysis (World Health Organization 2016; Gutierrez et al. 2017b).

Despite being the gold standard assay of antivenom safety and efficacy, *in vivo* murine lethality testing has a number of limitations, including cost, reproducibility and the suffering induced on the test animals (Ainsworth et al. 2020). Moreover, there is not a universally agreed method for these LD_{50} assays, such discrepancies making comparison of results generated by different laboratories difficult. Such variations may arise from use of a different strain of animal, dose, route of administration, exposure time, data analysis and/ or interpretation (Gutierrez 2017). Additionally, the inherent complexity of snake venoms which may constitute over 100 different toxin proteins (Mackessy 2010; Petras et al. 2016), together with inter-and intra-species variations (Casewell 2012), make the conventional LD_{50} and ED_{50} studies a challenging task. More importantly, there is evidence that *in vivo* neutralising efficacy of antivenoms fail to translate to clinical settings (Baldé et al. 2013). This may require an in-depth understanding the toxicity profile of each venom independently, to determine the suitability of LD_{50}/ ED_{50} studies. This is because the exact venom toxin responsible for lethality may not be known thus, neutralising ability of whole venom may not be sufficient to assess the overall efficacy of antivenom (Gutiérrez et al. 2013).

Depending on the venom under investigation, the performance of more specific *in vivo* tests, such as Minimum Haemorrhagic Dose (Gutiérrez et al. 1985) and Minimum Necrotising Dose (Theakston and Reid 1983; Gutierrez et al. 2005a) may also be required. This would consume an extortionate number of experimental animals for a single study, which is unacceptable ethically, financially and logistically. Following the current social and scientific principles to apply the 3Rs (Reduction, Replacement and Refinement of animals in research), there is a demand to replace the current *in vivo* with *in vitro* assays (Gutierrez et al. 2017b).

To this end, several biomedical assays, including insensate fertile hen eggs (Sells et al. 1997; Sells et al. 1998), ELISA (Theakston et al. 1977; Theakston and Reid 1979; Maria et al. 2001; Rial et al. 2006; Ratanabanangkoon et al. 2017; Khaing et al. 2018) and cytotoxicity studies (Oliveira et al. 2002; Lopes-de-Souza et al. 2019) have been explored as a possible replacements for

murine studies (Theakston and Reid 1979,1983). Furthermore, proteomics of venom and venom/ antivenom binding has been introduced as 'antivenomics' with the overall aim of revealing the toxicological profile of venoms and subsequent ability of antivenoms to recognise key venom components (Calvete et al. 2014). Despite such coherent efforts, the *in vivo* murine test remains the 'gold standard' for preclinical assessment of newly developed and/or existing antivenom (World Health Organization 2016).

The currently available toxicological data for snake venoms and their components are determined predominately from animal studies (Lyons et al. 2020). In recent years, various cell lines have been used to estimate the cytotoxicity of different snake venoms from Latin American (Oliveira et al. 2002; Lopes-de-Souza et al. 2019), North Africa and Southeast Asia (Ozverel et al. 2019) and the Mediterranean (Nalbantsoy et al. 2012) snakes. Recent studies (Stransky et al. 2018; Ozverel et al. 2019; Chong et al. 2020) have reported an excellent response by normal (HEK293 and Keratinocytes), immortalised (Vero) and cancerous (HeLa and MCF-7) cells exposed to snake venom toxins. All these studies demonstrated variable degrees of cytotoxicity, albeit by different mechanisms, depending on venom and cell line. Furthermore, (Lopes-de-Souza et al. 2019) used Vero cells to measure venom toxicity and antivenom efficacy, where they reported an excellent correlation with data obtained from *in vivo* studies. Use of cell lines, such as Vero cells, in optimised cytotoxicity assays are a promising platform for Replacement or Reduction of *in vivo* testing for screening of antivenom efficacy.

Vero cells are derived from the kidney epithelial cells of the African Green Monkey (Lopes-de-Souza et al. 2019). They are a highly sensitive and well-established cell line, frequently used to assess cytotoxicity of numerous substances, including bacterial (Freire et al. 2005; Postnikova et al. 2018; To and Bhunia 2019; Burtscher et al. 2021) and chemical (Freire et al. 2005) toxins.

The use of insects such as *Diatraea saccharalis* (sugarcane borer), *Apis mellifera* (honeybee) and *Gryllus assimilis* (Jamaican field cricket) to assess the toxicity of scorpion and spider venoms (Manzoli-Palma et al. 2003) have been reported. In a different study, the use of invertebrate models to study the biological effects of Australian *Chironex fleckeri* (box jellyfish) and

Chiropsalmus species (Carrette and Seymour 2006) has also been reported. Other invertebrate models, such as *Drosophila* (fruitflies) and *Caenorhabditis elegans* (a free living nematode), have been used to study the mechanisms of a number of neurodegenerative diseases, including Alzheimer's (Link 2005; Ségalat 2007). Despite being phylogenetically distant from humans, the presence of key genetic and molecular tools in *Drosophila* and *C. elegans* make them valid models to study these diseases and also as screening tools in drug discovery and design (Link 2005).

The use of *Galleria mellonella* (Greater wax moth, honeycomb moth or waxworm) is becoming increasingly popular as a model for studying a number of human pathogens, including bacterial and fungal infections in recent years (Junquiera 2012, Tsai et al. 2016). With over 1000 publications (Tsai et al. 2016), it is evident that the use of *G. mellonella* offers an encouraging platform to characterise snake venom toxicity.

Galleria mellonella belongs to the subfamily *Glariinae* of the *Pyralidae* family within the order Lepidoptera (Kwadha et al. 2017). Morphologically, the wax moth larva is 1-3 mm long in its first instar, whereas larvae at their later instar are 20-30 mm in length and 5-7 mm in diameter (Kwadha et al. 2017). Prior to pupation, larvae weight approximately 250 mg and have a creamy white appearance that serves as an indicator of health during experimental procedures (Ramarao et al. 2012). *G. mellonella* has six legs located on the frontal (thorax) and a number of prolegs (false legs) situated along the abdominal segments (Kwadha et al. 2017).

Recently, *G. mellonella* has become a well-established invertebrate model for studying the pathogenicity of a range of microbes (Fedhila et al. 2010; Ramarao et al. 2012; Malmquist et al. 2019), and for investigating antimicrobial resistance (Gorr et al. 2019; Kay et al. 2019). *G. mellonella* offers several technical and biological advantages over other invertebrate models that make it suitable for biomedical research. As well as being inexpensive and easily maintained, *G. mellonella* offers multiple administrative routes, including parenterally (Ramarao et al. 2012; Kay et al. 2019), and orally (Fedhila et al. 2010; Lange et al. 2018). Compared to other-established insect models (Escoubas et al. 1995; Manzoli-Palma et al. 2003), *G. mellonella* larvae are larger in size, facilitating injection with a practical sample volume. The

preferred route of administration is by injection into the haemocoel, which allows more accurate dosing (Ramarao et al. 2012). Currently, the use of *G. mellonella* does not require ethical approval and, in addition, its ability to survive at 37˚C makes it the most suitable invertebrate model to mimic vertebrate model conditions (Kay et al. 2019), particularly for experiments that require a higher temperature (Malmquist et al. 2019).

G. mellonella possesses a complex innate immune system, comprising humoral and cellular responses, which effectively fight pathogen invasion (Pereira et al. 2018). However, prior to mounting an immune response, structural defences include the gut peritrophic matrix, and the tracheal lining, which prevent pathogens entering into the haemocoel (De Gregorio et al. 2002). Interestingly, this innate immunity of *G. mellonella* exhibits a remarkable similarity to that of mammals potentially generating valuable information relevant to the mechanisms of mammalian immunity; e.g., pathogen recognition receptors, production of antimicrobial peptides (AMPs) and phagocytosis (Ramarao et al. 2012; Kay et al. 2019). Haemocytes, opsonin, AMPs and melanisation are the key innate immune components of *G. mellonella* (Kay et al. 2019). In particular, the haemocytes, comprising plasmacytes and granular cells, play a critical role in phagocytosis of pathogens (Kay et al. 2019), also a key mechanism for eradicating invading pathogens in mammals (Lee et al. 2020). AMPs are synthesised in the fat body, equivalent to the liver in mammals, and are secreted into the haemolymph where they are actively involved in the eradication of pathogens (De Gregorio et al. 2002). Additionally, opsonin facilitates the binding to pathogens, thereby inducing cellular phagocytosis, an analogue to pattern recognition peptide in mammals (Kay et al. 2019). In insects such as *Drosophila, G. mellonella* and *D. saccharalis*, melanisation “or blackening” is the most dramatic and immediate manifestation of the immune response, which is triggered by injury and/or microbial infections (De Gregorio et al. 2002). Melanisation occurs in response to synthesis and deposition of melanin at the site of injury, thereby encapsulating the invading pathogen or toxin and is equivalent to abscess formations in mammals (De Gregorio et al. 2002; Tsai et al. 2016).

Another key similarity with mammals is that *G. mellonella* encompasses coagulocytes which are involved in the haemolymph coagulation process (Ménard et al. 2021). Additionally, Lepidoptera express clottable proteins such as lipophorin and vitellogenin-like proteins which function similar to vWF in mammals (Vilmos and Kurucz 1998; Maguire 2017), and these proteins, particularly lipophorin, represent a major haemolymph component in *G. mellonella* (Maguire 2017). Moreover, voltage-gated sodium channel (Na_v) was recently identified by (Cordero et al. 2016) from ganglia nerve cord of *G. mellonella*. It has been suggested that receptors such as L-type voltage gated ion channels (K_v, Ca_v &Na_v) and coagulation proteins such as fibrin, platelets, vWF and prothrombin represent key targets for snake venom toxins (Frangieh et al. 2021). Thus, together with the similarity in the innate immunity, the presence of Na_v and coagulation system validate *G. mellonella* as a suitability model for characterising snake venom toxicity and antivenom potency.

For standardised injections, *G. mellonella* are used at their last instar larval stage before pupation to allow administration of a reliable injectable volume (Ramarao et al. 2012). The most commonly adapted route is the intra-haemocoelic injection where relatively smaller volume is injected into the haemocoel region, ideally, via the fourth proleg (Ramarao et al. 2012; Gorr et al. 2019; Kay et al. 2019). Experiments using *G. mellonella* are generally reported as survival or as an LD_{50} using an endpoint of 48 h (Gorr et al. 2019) or 72 h (Kay et al. 2019). In murine assays, mortality is typically recorded at 24 h for intravenous injections and 48 h for intraperitoneal administrations (Gutiérrez et al. 2013; World Health Organization 2016).

Clearly, it is worthwhile considering that the use of an experimental model such as a mammal, which reflects the natural predatory habits of the snake, is essential for understanding the interaction between its venom and its target (Richards et al. 2012). However, in addition to the venom complexity and interspecific variability, the murine assays are associated with biological, logistic and ethical limitations. Thus, establishing a rapid and inexpensive assay that reflect the murine features is necessarily required for implementing the 3Rs' principles. Surprisingly, despite the extensive use of *G. mellonella* in

various research applications (Junqueira 2012; Tsai et al. 2016), its use for screening snake venom toxicity has not been reported previously.

5.2 Aims and objectives of the study

Despite potentially promising results, cell-based assays have not been extensively explored for assessment of venom toxicity and antivenom efficacy, particularly those relevant to SSA. To date, excluding those studies which reported diet-venom toxicity relationship (Barlow et al. 2009; Richards et al. 2012), to our knowledge, invertebrate models have not been used to assess snake venom toxicity and antivenom efficacy, respectively. Therefore, this study has the following objectives: To develop, and assess the suitability of, firstly, an assay using *G. mellonella* and, secondly, an *in vitro* cytotoxicity assay using Vero cells to determine venom lethality and antivenom efficacy.

5.3 Results

A representative selection of neurotoxic, haemorrhagic and cytotoxic snake venoms were used to assess the ability of invertebrate and cell-based models to determine venom lethality and efficacy of a polyvalent $F(ab')_2$-based antivenom. To ensure the validity of the model, the assay tolerance was set at ≤10% for larvae injected with DPBS (assay controls) or antivenom (positive control) and ≥90% mortality for those injected with the highest venom dose (negative controls). The LD_{50} of snake venoms and ED_{50} of antivenom on *G. mellonella* (larvae) was determined from the average of three biologically independent replicates by Probit analysis (Finney et al, 1972) using SPSS software. Full experiment description is given in sections 2.2.18 & 2.2.19. The larvae mortality records at each venom concentrations are available in Appendix IV (B) whereas the larvae survivals data at each antivenom dose is available in Appendix IV (C).

Initially, injected larvae exhibited staggering and firm attachment to a surface. This lasts for up to 12 hours (h), after which, larvae injected with DPBS or antivenom had completely recovered. Larvae injected with snake venoms demonstrated a remarkable variety of clinical manifestations, such as melanisation, instability, and death, which occurred within 2 – 36 h after

injections. These phenomena were venom species and 'dose' dependent. Incubations for more than 48 h did not necessarily affect the mortality and therefore the experimental endpoint was taken as 48 h.

5.3.1 Toxic activities of *Viperidae* snakes on *G. mellonella* used in this study

Injections with venoms from *Bitis* (*B. areitans* and *B. gabonica*) and *Echis* (*E. leucogaster* and *E. ocellatus*), resulted in immediate discolouration (melanisation) and writhing of larvae, followed by leakage of dark-coloured fluids, appeared to be, from the entire surface of the body, and yellow spots. Colour change, which started approximately 1 h after injection, was noticeably dependent on dose and species of venom used (see Figure 5.1, A-F). After injection, larval movement gradually reduced, and they became covered with a sticky fluid. Although similar symptoms were observed with all test venoms, the severity differed between venoms injected. For example, melanisation predominated in larvae injected with *B. arietans,* whereas fluid exudation predominated in those injected with *Echis* leucogaster. This is reflected by the toxicity profiles (Table 5.1) demonstrating that *E. leucogaster* was the most toxic viper venom to the larvae (8.4 µg/larvae) and *B. gabonica* was the least toxic venom which required doses in excess of 100 µg to induce 100% mortality.

Interestingly, despite causing significant toxicity effects including discolouration and fluid exudation, the larvae have shown a remarkable resistance to venoms, particularly against *B. gabonica.* Lethality caused by these snakes was assessed as µg per larvae, and the study has reported an LD_{50} range from 8.4 µg (95% Confidence interval limit: 5.9 – 11.3) for *E. leucogaster* to 45.9 µg (95% Confidence interval limit: 32.2 – 62.8) for *B. gabonica*: full description is given in Table 5.1. Approximately, 40 µg of venom toxins (*B. arietans*), 125 µg (*B. gabonica*), 50 µg (*E. leucogaster* and *E. ocellatus*) was required to cause 100% mortality of *G. mellonella* (see Table 2.2). Venom from the *Viperidae* spp. less than 5 µg/ larvae have negligible toxicity effects [(see Appendix IV(B)]. Murine tests (Casewell et al. 2010; Segura et al. 2010) revealed a slightly different toxicity rank with *E. ocellatus*

being the most toxic to mouse followed by *B. arietans, E. leucogaster* and *B.* gabonica as the least toxic.

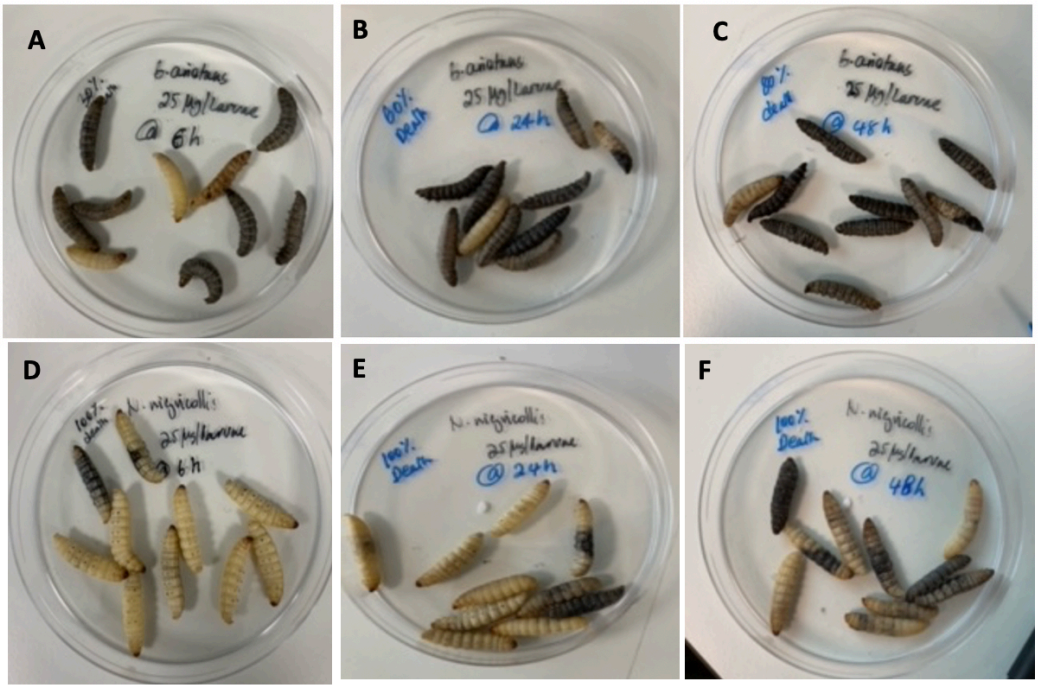

Figure 5.1. response of *G. mellonella* larvae to snake venom injections.

Larvae displaying different degrees of melanisation at different time-points (h) following injection with venoms from *Bitis arietans* (panel A-C) and with *N. nigricollis* (panel D-F). Immediate responses (in less than 1 h) were observed in the *Bitis* group whereas the *Naja* group has shown a delayed response (over 24 h).

Abbreviations: µg, microgram; h, hour.

5.3.2 Toxic activities of *Elapidae* snakes on *G. mellonella*

Venoms from *Naja* (*Elapidae*) species (*N. haje, N. melanoleuca,* and *N. nigricollis*) displayed a completely different toxicity profile to that observed with the viper venoms. Administration of these venoms caused flaccidity and loss of righting reflex, an immediate reduction in movement was observed, progressing to complete paralysis and death. A gradual recovery from neurotoxicity took approximately 24 to 36 h post-injection in the larvae injected with lower doses of venom. However, these were venom-specific and dose-dependent effects. *G. mellonella* were highly sensitive to *N. nigricollis* venom which was more active than *N. melanoleuca* and *N. haje* venoms, respectively. Thus, 5 µg/ larvae of *N. nigricollis* venom killed 100% of the tested larvae

whereas 25 µg/ larva of *N. melanoleuca* venom and 50 µg/ larva of *N. haje* venom were required for 100% mortality (see Appendix IV(B)). Lethality (LD_{50}) values for all the tested snake species is given in Table 5.1. In contrast to these results, *N. melanoleuca* was the most lethal followed by *N. haje* and *N. nigricollis* in murine toxicity tests (Casasola et al. 2009). As observed with venoms from the *Viperidae* species, injected larvae showed mild melanisation, particularly *N. nigricollis* venom (Figure 5.1). Additionally, injections with *Naja* venoms caused minimal fluid exudation.

Table 5.1 Toxicity profiles of medically relevant SSA snake venoms as determined by *G. mellonella* and Vero cells.

Snake venoms	LD_{50} (µg/Larvae; 95% CI) against *G. mellonella*	IC_{50} (µg/mL; 95% CI) against Vero cells
B. arietans	15.0 (11.3 - 19.1)	10.1 (8.4 - 12.3)
B. gabonica	45.9 (32.2 - 62.8)	9.3 (6.6 - 12.7)
E. leucogaster	8.4 (5.8 - 11.3)	5.3 (3.6 - 8.1)
E. ocellatus	12.7 (8.9 - 18.0)	5.2 (3.1 - 9.1)
N. haje	11.2 (8.0 - 14.3)	10.6 (8.3- 13.8)
N. melanoleuca	3.2 (0.02 - 28.9)	8.3 (6.7 - 10.9)
N. nigricollis	1.6 (1.1 - 2.1)	9.4 (7.7 - 11.62)

Data were collected from 3 biologically independent experiments and analysed by Probits using SPSS software (LD_{50}) or GraphPad (IC_{50}). Further data are available in Appendices IV(B) and V(A) for the LD_{50} and IC_{50} cells, respectively. As it is described in section 2.2.17 & 2.2.18, for each concentration of venom, ten larvae (n = 10) were injected with 50 µL sample.

Abbreviations: LD_{50}, median lethal dose; IC_{50}, Half-maximal inhibitory concentration; CI, confidence interval; µg, microgram.

Statistical analysis of the LD_{50} for the different venoms is summarised in Figure 5.2. Although there were some differences in toxicity induced by venoms from the *Bitis* species (Figure 5.2 A) and the *Echis* species (Figure 5.2 B), such differences were not statistically significant. However, the difference in toxicity induced by the *Naja* species was statistically significant (Figure 5.2 C). Similarly, comparisons of toxicity across all tested venoms showed that *B. gabonica* has been the least toxic venom to *G. mellonella* compared to the other snake species, and the difference was statistically significant (Figure 5.2 D). Additional statistical analysis was also performed by comparing toxicities

for all snake species (other than *G. gabonica*) against each other (data not shown); however, no statistically significant differences were observed.

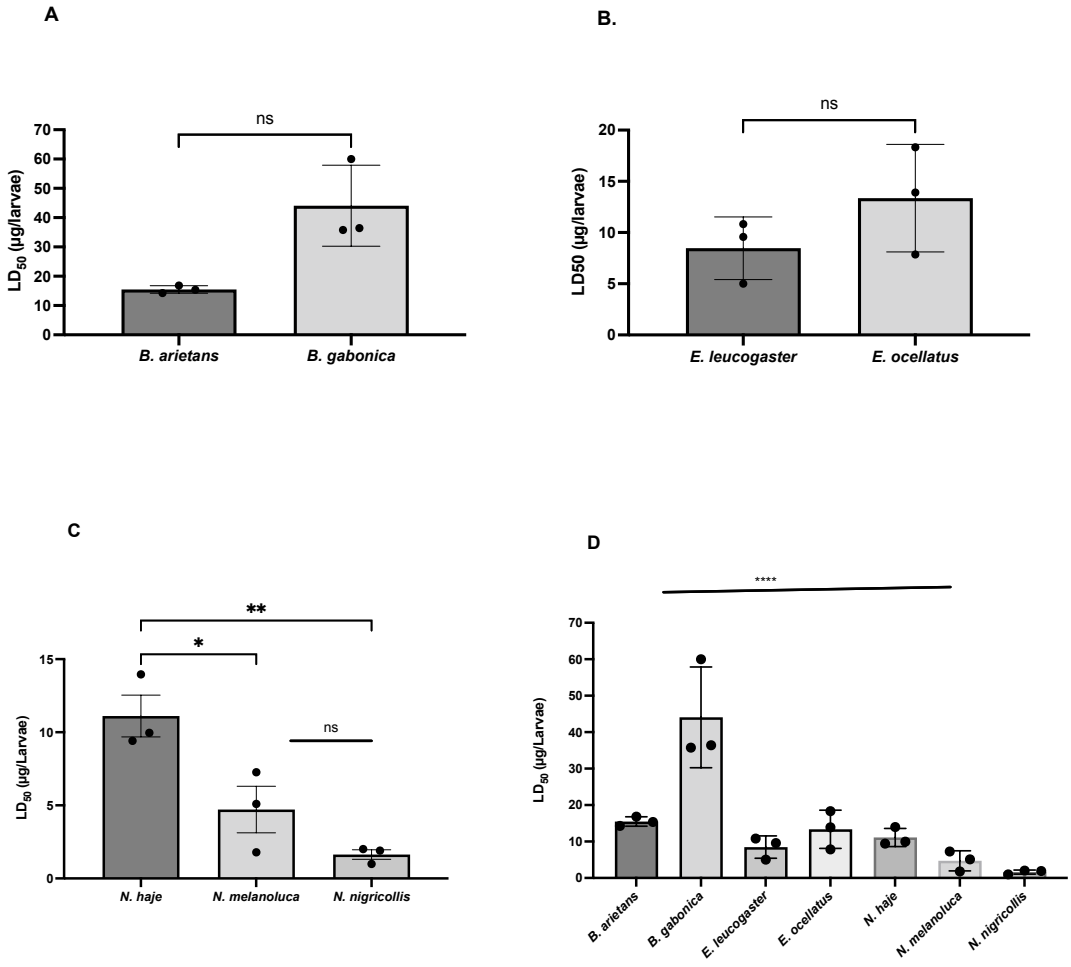

Figure 5.2 Assessment of LD50 for snake venoms in G. mellonella larvae.

Data were analysed using Prism GraphPad 9. Unpaired *t-test* with Welch's correction was used to determine statistical significance for the *Bitis* (Fig. 5.5 A) and *Echis* (Fig. 5.5 B) species. Statistical significance for the *Naja* species (Fig. 5.5 C) and for all groups (Fig. 5.2 D) was determined using one-way ANOVA, with Tukey's method *post-hoc* test. Statistical analysis in panel D (Fig. 5.2) represent comparison of toxicity for all tested snake species against *B. gabonica* in *G. mellonella*. Error bars indicate mean ± SD of triplicates from three biologically independent experiments. Pairwise statistical comparisons are shown by asterisks (*indicates *P* =0.0259, ** in indicates *P = 0.0042,* and **** indicates *p<0.0001*).

Abbreviations: ns, not significant; LD_{50}, median lethal dose; µg, microgram.

5.3.3 Cytotoxic Effects of snake venoms in Vero cells

A Vero cell line was selected to perform all cytotoxicity assays, taking into consideration its suitability for both toxicological studies and microscopic analysis, although the latter was not the primary aim of the current study. Venom cytotoxicity was evaluated after 4 h incubation with CellTiter-Blue, a dye used to monitor cell viability, including metabolic function and cellular health index. Only viable cells can convert the non-fluorescent blue resazurin to the readily fluorescence-absorbed resorufin. The Half-maximal inhibitory concentration (IC_{50}) can be defined as the quantity of venom which reduces cell viability by 50% compared to positive control (DMEM only treated) cells. The cytotoxicity (IC_{50}) values for the different snake venoms are summarised in Table 5.1.

Vero cells were highly sensitive to snake venoms where morphological changes could be observed immediately, example image are shown in Figure 5.3 (A-F). After incubation with the cells for an hour, a reduced number of intact lysosomes and/or lysosomal damage was observed, possibly indicating changes in membrane permeability. Loss of integrity and adherence was also observed immediately after adding the venom toxins (Figure 5.3 B-F). These changes were time and dose-dependent phenomena, with significant cytotoxicity occurring after 48 h incubation with venom toxins. Punctured mitochondria and cell organelles, in which integrity was severely damaged, were observed after exposure to neurotoxin-rich venoms from *Naja* species.

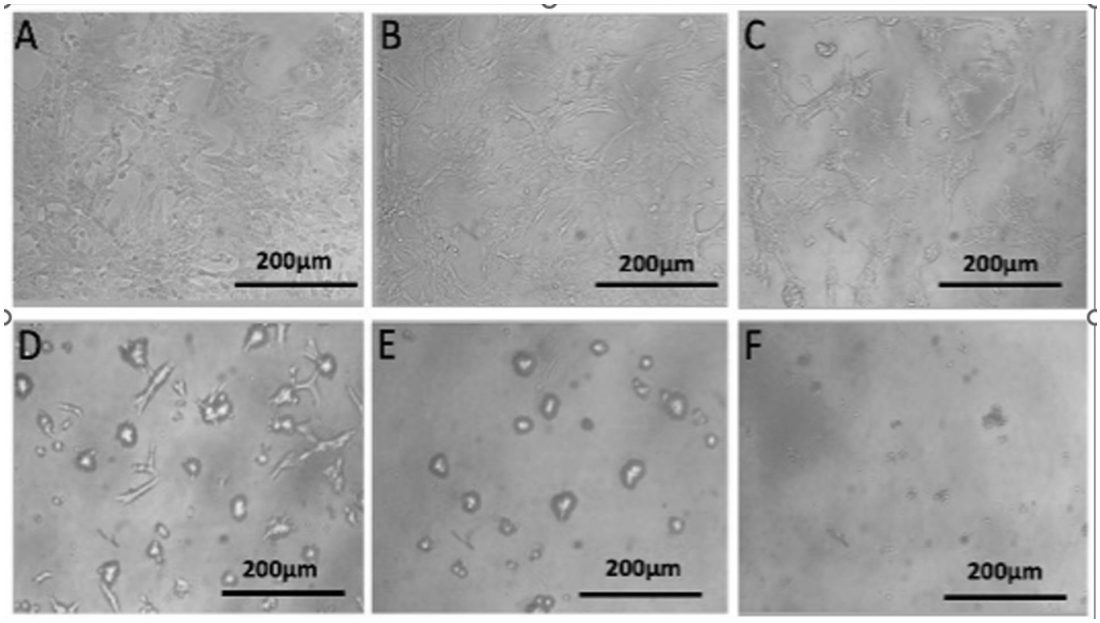

Figure 5.3. morphological changes for Vero cells treated with venoms from *E. leucogaster*.

A) control-untreated cells, B) 0.13 µg/mL, C) 2.05 µg/mL, D) 12.80 µg/mL, E) 80 µg/mL and F) 500 µg/mL venoms from *E. leucogaster*. Images were viewed at 48 h post treatment with venom toxins using Pyser SGI inverted XE series Microscope (magnification: 400x). Abbreviations: µm, micrometre.

Interestingly, in cells treated with some of the lowest venom concentrations, cell viability was slightly higher than that of untreated cells. This phenomenon could be explained by a sublethal effect of venom on cell metabolism and was observed in cells treated with all venoms tested.

Incubations with all tested snake venoms resulted in a dose-dependent inhibition of cell viability (Figure 5.4 A-D). However, the cytotoxicity level varied between the different species, with IC_{50} ranging from 5.2 µg/mL (95% Confidence interval: 3.1 – 9.1) for *E. ocellatus* to 10.1 µg/mL (95% Confidence interval limit: 8.4 – 12.3) for *B. arietans* (Table 5.1). Although there were minor differences in cytotoxicity induced by the difference venoms, such differences were not statistically significant (Figure 5.5 A-D).

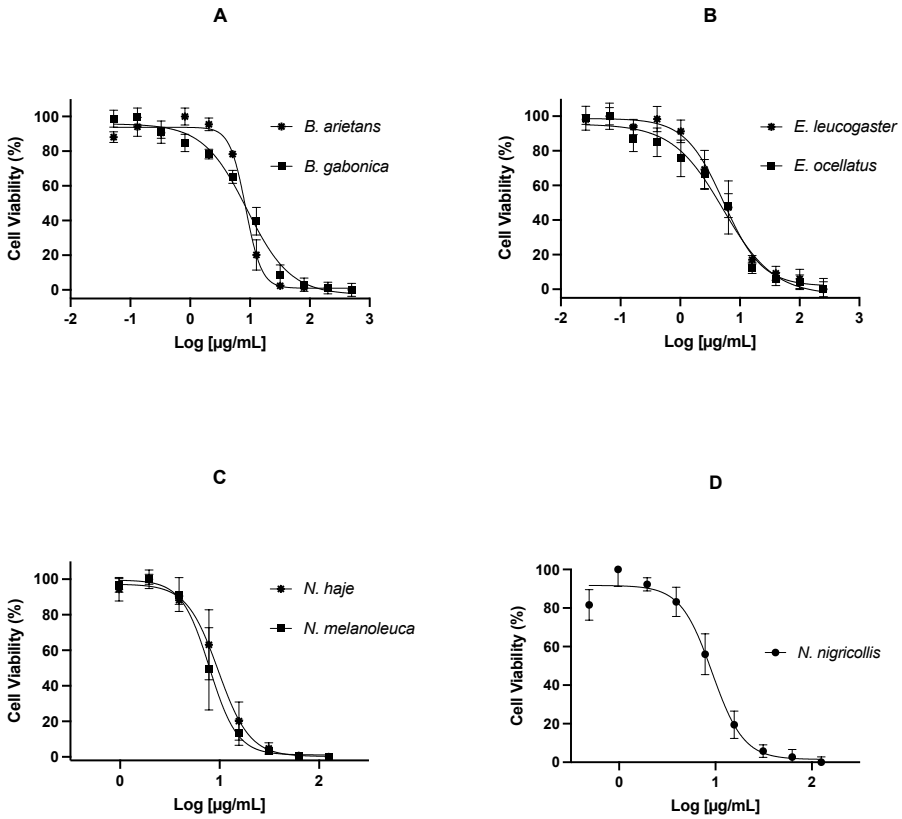

Figure 5.4. normalised sigmoidal curves showing Dose-dependent inhibition of Vero cells treated with snake venoms.

Data were analysed using Prism GraphPad 9. Nonlinear sigmoidal curves were generated by using 4- parameters (top, bottom, hillslope and log IC_{50}) and used to determine IC_{50} for each snake venom. Error bars indicate mean ± SD of triplicates from three biologically independent experiments, comprising three technical replicates. Cell viability was determined by CellTiter-Blue assay and data were normalised to represent actual percentage (0 – 100%). Venom concentrations, dilutions and unnormalised cytotoxicity data are available in Appendix V(A).

Abbreviations: µg, microgram; mL, millilitre.

The CellTiter-Blue assay results were subject to substantial variability, indicated by the wide standard deviation (Figure 5.5 A-D). However, this is an inherent challenge frequently encountered in cell-based assays, which is influenced by 'technical noise' and intrinsic biological variations. Nevertheless, consistent data with minor variations was generated from experimental replicates (Figure 5.4 A-D).

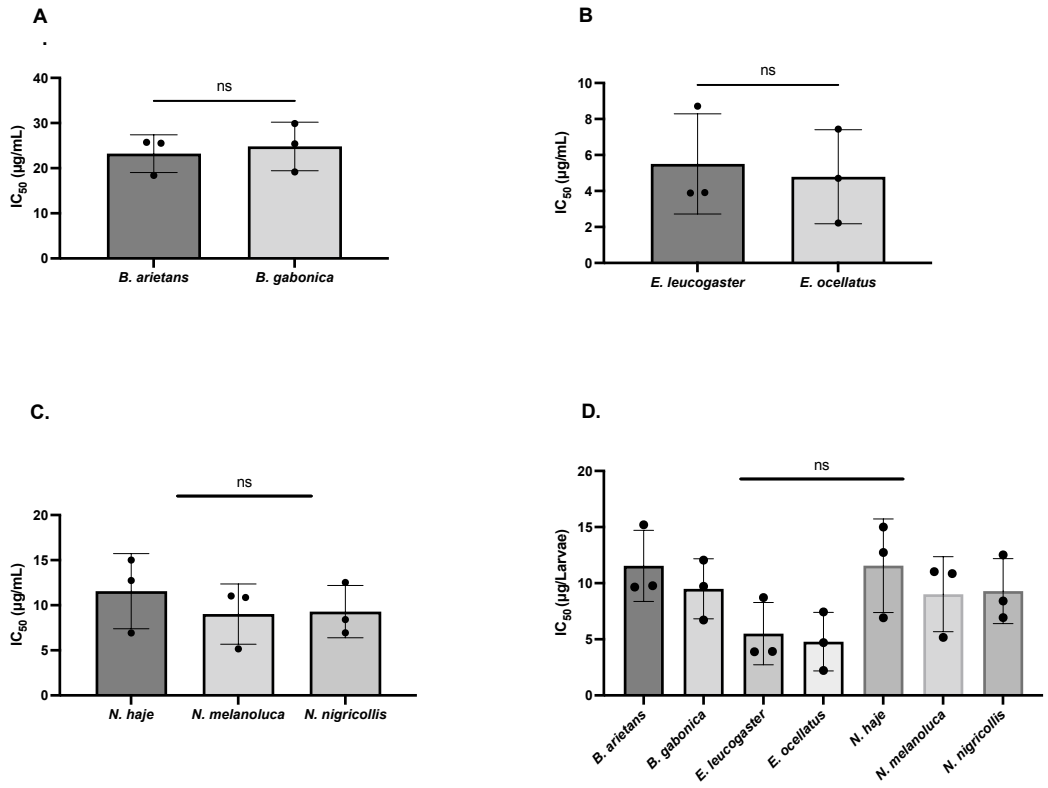

Figure 5.5. Assessing IC_{50} of snake venoms using VERO cell line.

Data were analysed using Prism GraphPad 9. Unpaired *t-test* with Welch's correction was used to determine statistical significance for the *Bitis* (Fig. 5.5 A) and *Echis* (Fig. 5.5 B) species. Statistical significance for the *Naja* species (Fig. 5.5 C) and all groups (Fig. 5.5 D) was determined using the one-way ANOVA with Tukey's method *post-hoc* test. Statistical analysis in panel D (Fig. 5.5) was performed by comparing cytotoxicity for all tested snake species against each other in Vero cell line. Values are mean ± SD of triplicates from three biologically independent experiments, comprising three technical replicates.

Abbreviations: IC_{50}, Half-maximal inhibitory concentrations; ns, not significant; µg, microgram; mL, millilitre.

5.3.4 Antivenom potency

5.3.4.1 Galleria mellonella

This study next addressed whether *G. mellonella* is a suitable model to assess antivenom efficacy. A polyvalent $F(ab')_2$-based antivenom (section 2.2.3) was employed to assess its ability to protect larvae from the toxic, including lethal, effects of snake venoms. The ability of antivenom to neutralise the snake venoms is expressed as either a median effective dose (ED_{50}) or Potency

(Table 5.2). ED_{50} is the quantity of antivenom required to protect 50% of the test animals injected with lethal dose (typically 2.5 – 5x LD_{50}) and it can be expressed as either a) µL of antivenom required to neutralise the "challenge dose" (i.e., µL/ mouse) or b) µL of antivenom required to neutralise a mg of venom (µL/mg) or mg venom neutralised by 1 mL antivenom (mg/mL) (Ainsworth et al. 2020). A quantity of venom that induces 100% lethality to the tested larvae population was chosen as a "challenge dose" for each venom [see Appendix IV(C)]. As shown on Table 5.2, the challenge dose (µg) varied between snake venoms based on the species-specific LD_{50} values.

Table 5.2. ED_{50} and Potency values for the polyvalent $F(ab')_2$ antivenom against the different snake venoms.

Snake species	LD_{50} (µg/ larvae)	LD_{50}s used (n)	Challenge dose (µg)	ED_{50} (µL/ larvae; 95% CI)	ED_{50} (mg/mL)	Potency (mg/mL)
B. arietans	15.0	2.0	30.1	10.4 (2.13 - 2613.4)	2.9	0.2
E. leucogaster	8.4	4.0	33.7	1.2 (0.6 - 2.8)	27.9	1.1
E. ocellatus	12.7	3.0	38.1	0.7 (0.3 - 2.1)	53.3	2.1
N. nigricollis	1.6	3.0	4.8	5.4 (2.5 - 16.4)	0.9	0.3

ED_{50}s were obtained from three biologically independent experiments. As it is described in section 2.2.17 & 2.2.19, for each concentration of antivenom, ten larvae (n = 10) were injected with 50 µL sample. Further data (including calculations) are available in Appendix IV(D). Abbreviations: LD_{50}, median lethal dose; ED_{50}, median effective dose; µL, microliter; mL, millilitre; µg, microgram; mg, milligram.

Potency is the amount of venom that is completely neutralised per 1 mL antivenom (Table 5.2), and would protect 100% of the tested animals, in contrast to the ED_{50} which protect 50% of them. The expression (n-1) xLD_{50} (equation section 2.2.19) is used instead of the total amount of the venom (nxLD_{50}) because at the endpoint of the neutralisation assay, one LD_{50} remains unneutralised and causes the death of 50% of the test animals (Morais et al. 2010). Although neutralisation efficacy of antivenom is frequently reported as ED_{50} which estimates protection of 50% of the test animals (Casasola et al. 2009; Sanchez et al. 2017), potency (Table 5.2) is more relevant because it estimates 100% lethality neutralisation.

As summarised on Figure 5.6, antivenom offered difference in neutralising potency against the different species of snake venom, most of which were statistically significant (see Figure 5.6).

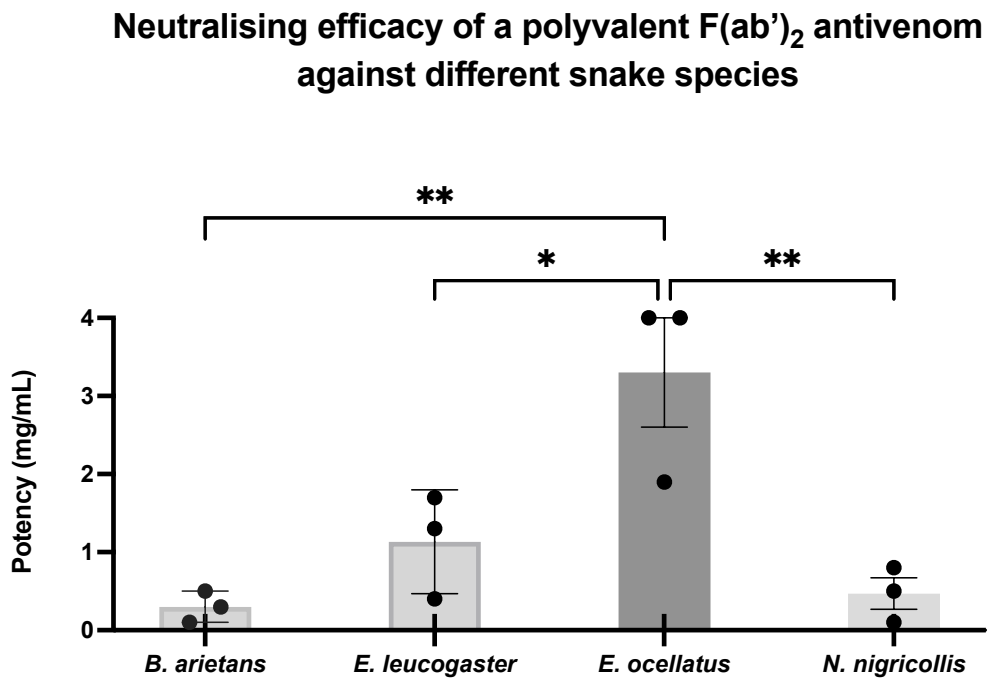

Figure 5.6. Potency of Polyvalent F(ab')$_2$ antivenom in a *G. mellonella* model.
Potency is expressed as mg venom completely neutralised per 1 mL antivenom. Error bars represent mean ±SD of three biologically independent experiments. Statistical significance was determined using one-way ANOVA with Tukey's method post-hoc test. Pairwise statistical comparisons are shown by asterisks (* indicates P =0.0026, ** for E. ocellatus v B. arietans indicates P= 0.004, and **for E. ocellatus v N. nigricollis indicates P= 0.0058).

Injections of positive controls (DPBS or antivenom) did not demonstrate any signs of toxicity (Figure 5.7 E&F), and the experiment was considered invalid if mortality exceeded 10 %. However, there is ±20 tolerability range in murine test (personal communication, Matt Aldridge). Larvae injected with venom preincubated with antivenom generally showed full survival, but the time and severity of clinical signs of toxicity varied tremendously within the surviving larvae.

It must be emphasised that, due to time constraints, we were unable to collect enough data to perform statistical analysis on the antivenom potency against the *B. gabonica* and *N. melanoleuca.* Thus, the neutralisation efficacy data against these two snake species is only preliminary. However, despite being a single technical replicate, the antivenom demonstrated a higher neutralising efficacy against *B. gabonica* but weak potency against *N. melanoleuca*, also see Appendix IV(E). This is reflected by the toxicity-associated effects (Figure

5.7 C&D), where the antivenom protected the larvae from *B. gabonica* toxicity at a challenge dose of 3xLD$_{50}$ (~138 µg venom).

Nevertheless, the antivenom demonstrated excellent protective efficacy against all associated toxic effects of *B. gabonica* and *E. ocellatus* venoms in the larvae, where larvae were fully protected (Figure 5.7 C&D and also Figure 5.8 A&B).

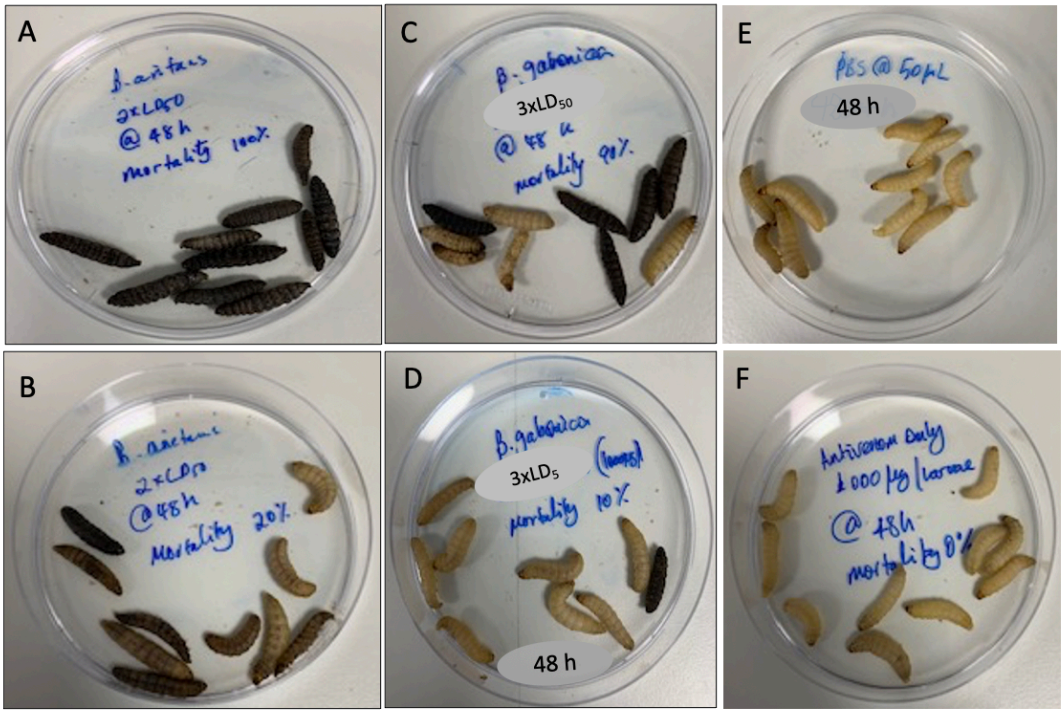

Figure 5.7. Protection of *G. mellonella* larvae from *Bitis* toxicity in response to antivenom treatment.

The diagram shows larvae displaying different signs of toxicity after injection with 30 µg of *B. arietans venom* (A); a mixture of 30 µg *B. arietans* venom and 1000 µg F(ab')$_2$ antivenom (B); 137.7 µg of *B. gabonica* venom (C); a mixture of 137.7 µg *B. gabonica* venom and 1000 µg F(ab')$_2$ antivenom (D); controls of DPBS (E); and F(ab')$_2$ antivenom only (F). All outcomes were recorded at 48-hour post injection.

Abbreviations: LD$_{50}$, median lethal dose; h, hour; µg, microgram; µL microliter; PBS, Dulbecco's Phosphate Buffered Saline.

The polyvalent F(ab')$_2$-based antivenom was particularly effective against *E. ocellatus* venom. Even when a challenge dose of 5xLD$_{50}$ was used, 100% of tested larvae were protected (Figure 5.8 A&B). Secondly, despite offering 90% protection, the antivenom failed to neutralise toxic effects such as melanisation and fluid exudation induced by *E. leucogaster* venom (image is not included).

Similarly, the antivenom was less protective against the lethal effects of *N. nigricollis* venom, only offering 90% protection (see Figure 5.8 D). However, when administered at a higher dose (1000 µg/larvae), the antivenom was very effective at reversing all associated signs of toxicity induced by *N. nigricollis* venom (Figure 5.8 C&D). It took slightly longer (approximately 20 h) for the larvae treated with antivenom to recover fully from the *N. melanoleuca* venom induced toxicity (image not included). Finally, the polyvalent antivenom was ineffective at reversing clinical signs such as melanisation and fluid exudation associated with *N. melanoleuca* with only 80% of larvae surviving, even at the highest antivenom dose of 1000 µg/larvae.

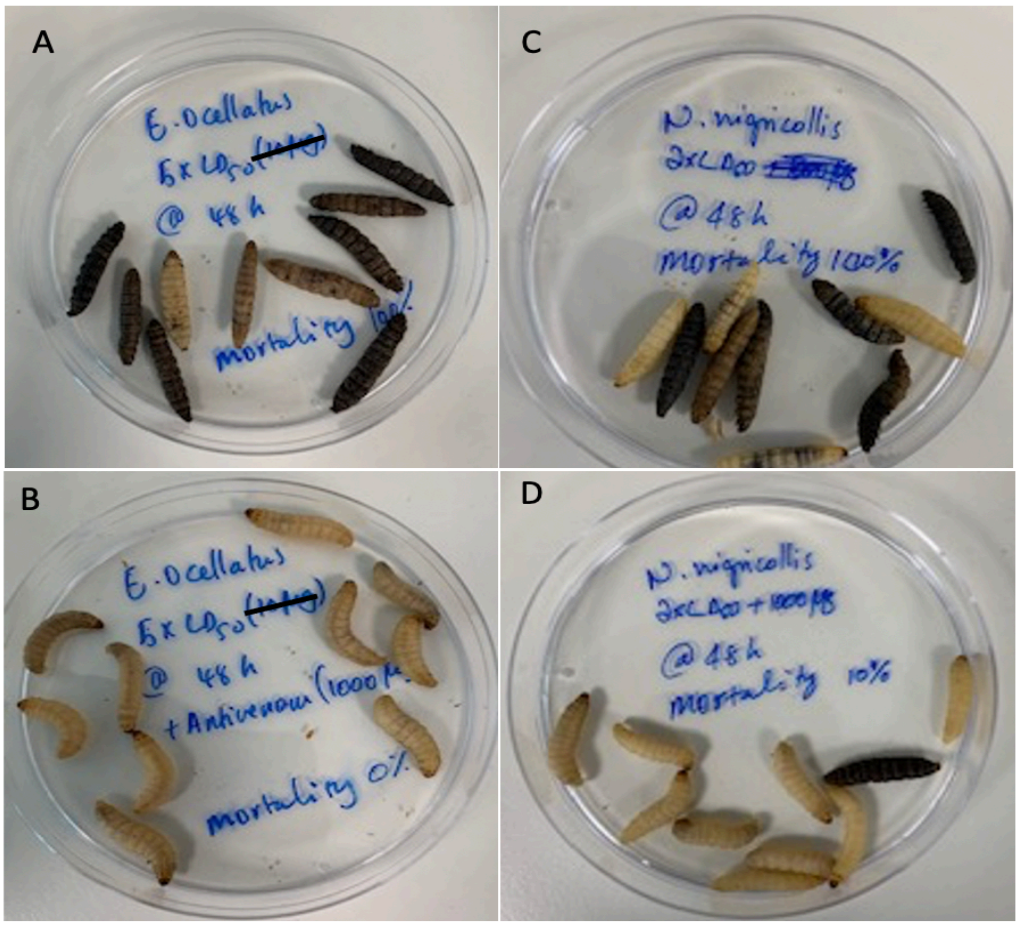

Figure 5.8. Protection of *G. mellonella* larvae from *E. ocellatus* and *N. nigricollis* toxicity in response to antivenom treatment.

The image illustrates *G. mellonella* larvae displaying different signs of toxicity after injection with 63.5 µg of *E. ocellatus* venom (A), a mixture of 63.5 µg *E. ocellatus* venom and 1000 µg antivenom (B), 3.2 µg of *N. nigricollis* venom (C), a mixture of 3.2 µg *N. nigricollis* venom and 1000 µg antivenom (D). controls are shown in Fig. 5.7.

Abbreviations are consistent with Fig. 5.7.

As summarised in Table 5.2, the polyvalent F(ab')$_2$ antivenom has its maximum neutralisation potency (mg venom/ mL antivenom) against *E. ocellatus* followed by *E. leucogaster* > *N. nigricollis* and *B. arietans*.

In contrast, published *in vivo* data showed that Fav-Afrique™ antivenom has its highest potency against *B. arietans* (3.9 mg/mL) followed by *E. ocellatus* (1.8 mg/mL), *E. leucogaster* (0.5 mg/mL) but no *in vivo* data are available against *N. nigricollis* to draw direct comparisons (Ainsworth et al. 2020). However, such variations are common even within murine assay, mainly due to difference in venom geographical origin, mouse strain, experimental settings.

Further to the *G. mellonella,* the neutralisation of cytotoxicity was assess using Vero cell line; however, this study lacks the support of biologically independent replicates (see Appendix VI).

5.4 Discussions

It is now universally recognised that research involving the use of animals must implement the 3Rs (Refinement, Reduction and Replacement of animals in research) and, ideally, replacement with *in vitro* methods (Sells 2003). Embracing this mindset, the current study established an invertebrate larval model using *Galleria mellonella* to assess lethality (LD_{50}) of snake venoms and neutralisation efficacy (ED_{50}) of antivenoms. The suitability of the *G. mellonella* platform was assessed using a panel of six contrasting snake venoms from the haemorrhagic- *Echis* species, cytotoxic *Bitis spp.* (Warrell et al. 1977; Habib et al. 2008; Paixão-Cavalcante et al. 2015) and *Naja spp.* representing both neurotoxic species (Warrell et al. 1976a; Baldé et al. 2013) and cytotoxic spitting cobra species (Warrell et al. 1976b).

The study demonstrated a highly variable toxicity between venoms, where statistically significant differences in LD_{50} were observed. Accordingly, *N. nigricollis* was found to be the most lethal snake species to *G. mellonella*, followed by *N. melanoleuca*, *E. leucogaster*, *N. haje*, *E. ocellatus, B. arietans* and *B. gabonica* (Table 5.3). These findings agree with lethality studies reported in the literature using the natural invertebrate prey of these snakes. *Echis pyramidum leakeyi,* representative of a group of phylogenetically related species (Okuda et al. 2001; Pook et al. 2009), including *E. leucogaster*, was the most toxic to scorpion followed by *E. ocellatus* and *B. arietans* (Barlow et al. 2009; Richards et al. 2012). In contrast, against mammalian targets, *Naja melanoleuca* was the most potent venom to mice, followed by *N. haje, E. ocellatus, B. arietans, N. nigricollis* and *B. gabonica* (Casasola et al. 2009; Casewell et al. 2010; Segura et al. 2010).

Comparing the LD_{50} values (Table 5.3) with those from published murine studies (Casasola et al. 2009; Casewell et al. 2010; Segura et al. 2010), the *G. mellonella* model provided a different relative toxicity ranking for the venoms tested. *Bitis arietans* and *B. gabonica* were comparable to the toxicity rankings reported in mice (Table 5.3), but those of *Echis and Naja* species were not. Interestingly, comparison of dose on a body weight basis (mg venom/ kg animal body weight), snake venoms were found to have a considerably lower lethality to invertebrates than to mice (Table 5.3),

corroborated by findings of previously published data (Barlow et al. 2009; Richards et al. 2012).

Table 5.3. comparison of snake venom lethality on *G. mellonella*, murine and Vero cells

	lethality of snake venoms in mouse vs larvae					Cytotoxicity on Vero cells
	Larvae experiment (LD_{50})		LD_{50} - Literatures			
Snake venoms	µg/Larvae	µg/g (Larvae*)	µg/ mouse	µg/g (mouse**)	Sources	IC_{50} (µg/mL)
B. arietans	15.0	60.2	13.3	0.7	Segura et al. 2010	10.1
B. gabonica	45.9	183.8	29.9	1.5		9.3
E. leucogaster	8.4	33.7	24.9	1.2		5.3
E. ocellatus	12.7	50.7	12.4	0.6	Casewell et al. 2010	5.2
N. haje	11.2	44.8	12	0.6	Casasola et al. 2009	10.6
N. melanoleuca	3.2	12.8	6.5	0.3		8.3
N. nigricollis	1.6	6.3	18.7	0.9		9.4

* larvae weight was considered at 0.25 g, ** mouse weight was considered at 20g

Snake venom is characterised by significant variations in toxin composition and lethality influenced by factors such as age, sex, diet specificity, geographical location and phylogenic relationship (Chippaux et al. 1991; da Silva Jr and Aird 2001). Poor cross reactivity against heterologous *Echis spp.* (Casewell et al. 2010) resulted in failure of treatment of envenoming due to use of antivenoms directed against inappropriate *Echis* venoms (Visser et al. 2008). SDS-PAGE separation of venom proteins (see Figure 3.10 A) highlighted significant venom variations between venom from different snake species, even those from the same genus.

The exact mechanism governing snake venom specificity for prey remains unclear. However, several studies have correlated venom composition to diet, suggesting that venoms are more toxic to their natural prey than, for example, an experimental model such as the mouse (Daltry et al. 1996; da Silva Jr and Aird 2001; Barlow et al. 2009; Richards et al. 2012). This suggests that the sensitivity of an experimental model will, at least in part, depend on the diet-specificity for that species. Rodents such as mice and rats are the staple diet of the majority of venomous snakes including the *Bitis, Echis* and *Naja* genus (Kang et al. 2011). Previously, it has been demonstrated that the arthropod-consuming *Echis pyramidum leakeyi*, the phylogenetically closest snake species to *E. leucogaster* (amongst the snake species reported in this thesis) (Okuda et al. 2001), was found to be more toxic in invertebrate models than the vertebrate-consuming *E. ocellatus* (Barlow et al. 2009; Richards et al.

2012). However, accumulated evidence from *in vivo* studies have shown that *E. ocellatus* has the most potent venom of sub-Saharan vipers (Ainsworth et al. 2020). The increased toxicity of *E. leucogaster* to *G. mellonella* larvae reported in this study may reflect diet-specific toxicity. Despite primarily feeding on lizards, birds and small mammals (Luiselli et al. 2002), the overwhelmingly greater toxicity of *Naja nigricollis* venom to *G. mellonella* larvae may suggest that this species may consume phylogenetically related invertebrates to *G. mellonella*. Nevertheless, the toxicity ranking of *N. melanoleuca* and *N. haje* venoms in the larval model correlates with that of the murine model (Table 5.3).

On the other hand, it has been postulated that the toxicity of venoms results from their toxin composition (Richards et al. 2012). This hypothesis is supported by transcriptome analysis of venom glands, which did not provide evidence linking specific venom proteins to diet-specificity but suggested that isoform diversification is responsible for intrageneric venom variation between medically important species of the *Echis* genus (Casewell et al. 2009). This may suggest that there is increased lethality, irrespective of diet for snake venoms to vertebrate versus invertebrate models. Taken together, the venom-prey interaction and mechanism governing venom toxicity towards specific prey is complex. Indeed, working with an animal model using the snake's natural prey is advantageous at demonstrating the pathological consequences of the venom toxins present (Richards et al. 2012). However, any *ex vivo* model capable of demonstrating venom-sensitivity must be considered to avoid the logistical and ethical barriers associated with mammalian *in vivo* studies. This study has demonstrated that the *G. mellonella* larval model is a sensitive and robust method of assessing snake venom toxicity and antivenom efficacy potentially providing Replacement or, at least, Reduction of the use of the murine lethality assays, in accordance with the spirit of the 3Rs.

In addition to lethality, the *G. mellonella* model provided valuable information on the predominant pathological effects induced by different venoms which may correlate specifically to the toxin profile of each species. For example, *Bitis spp.* resulted in melanisation of larvae, whereas neurotoxic venoms resulted in paralysis of larvae resulting in their loss of attachment. Studies elucidating the proteome of venoms (Calvete et al. 2007; Casewell et al. 2009;

Wagstaff et al. 2009; Casewell et al. 2014b), have identified venom metalloproteinases (SVMPs), snake venom serine proteinases (SVSPs) and snake venom phospholipase A_2 (svPLA_2) as the major venom constituents of *Bitis* and *Echis* species. These toxins target key tissue components such as ligands, cellular matrix, connective tissue and coagulation factors, resulting in profound local and systemic tissue damage in envenomed patients (Gutierrez et al. 2005b). *G. mellonella* larvae injected with venom from *Bitis* or *Echis* spp. exhibit a species and dose-dependent writhing, melanisation and exudation of fluids. In invertebrates, melanisation is evidence of local and/or systemic inflammation, and it corresponds to oedema and abscess formation in mammals (De Gregorio et al. 2002; Tsai et al. 2016). The exudation of fluids observed in *G. mellonella* larvae treated with viper venoms indicate disruption of the haemolymph system, which is analogous to blood in mammals (De Gregorio et al. 2002; Pereira et al. 2018). Bites by *Bitis* and *Echis* species, particularly, *B. arietans* and *E. ocellatus,* are strongly associated with swelling, disruption of haemostasis and significant local/systemic haemorrhage, coagulopathy and, if untreated, death occurred mainly due to cerebral haemorrhage (Warrell et al. 1974; Warrell et al. 1975).

On the other hand, 3FTXs are the major toxins in *Naja* venoms, constituting 60% (*N. haje*), 57.1% (*N. melanoleuca*) and 73.3% (*N. nigricollis*) of the total venom proteome (Tasoulis and Isbister 2017). PLA_2s are the next most abundant toxin in these venoms, particularly in *N. nigricollis* (Petras et al. 2011) and *N. melanoleuca* (Lauridsen et al. 2017). However, PLA_2 represents only 4% of the total venom proteins in *N. haje* which also contains SVMPs (10%) and CRiSPs (9%), amongst others, as major venom toxin constituents (Malih et al. 2014). The 3FTXs exhibit unique mechanisms to target and interfere with pivotal physiological processes thereby causing disruption of the cholinergic system, blockages of L-type calcium channel, inhibition of platelet aggregation and interference with the structure and function of phospholipid membranes (Kini and Doley 2010). The 3FTXs comprise short and long postsynaptic α-neurotoxins which compete and specifically bind to the nicotinic acetyl cholinesterase receptors (nAChR) on the motor end plate, leading to neuromuscular blockage and irreversible paralysis (Silva et al. 2018). Venoms from the spitting cobras induce flaccidity and disruption of

conduction through the neuromuscular junction. Clinically, envenomings by *Naja* spp., particularly *N. haje* and *N. melanoleuca* present with drowsiness, ptosis, blurred vision, loss of consciousness, paralysis, convulsion, respiratory failure, arrhythmias and death (Warrell et al. 1976a; Warrell et al. 1976b; Baldé et al. 2013). Despite the dominance of 3FTX in its venom proteome, *N. nigricollis* is not associated with the neurotoxicity signs induced by elapid envenoming, but, in contrast, it induces extensive necrosis, which may be attributed to cytotoxic PLA_2s (Warrell et al. 1976b). PLA_2s are generally implicated in severe local pathological lesions, myotoxicity, haemorrhage, oedema, inflammation, coagulopathy and hypertension (Warrell et al. 1976b; Ferraz et al. 2019). Therefore, its ability to verify the toxicity difference expressed by different snake species may validate that the *G. mellonella* is a useful model for assessing snake venom lethality.

Furthermore, this study has demonstrated that a cytotoxicity assay using Vero cells offers a rapid screening for cytotoxicity of snake venoms. Vero cells have a high sensitivity to snake venoms (Stransky et al. 2018). Although correlations between *in vivo* toxicity with some *in vitro* activities were reported (Lopes-de-Souza et al. 2019), clarification of these observations may require further studies. Snake venoms are rich in proteolytic enzymes, particularly metalloproteinases (Munawar et al. 2018; Ferraz et al. 2019), which may interfere with cellular adherence as cells are easily dislodged by washing. To overcome these issues, this study employed the simple and rapid CellTiter-Blue assay, which measures the metabolic function of viable cells without the need for washing or solubilising solvents such as those used in other methods such as the Neutral Red Uptake (Repetto et al. 2008), and 3-(4,5-dimethylthiazol-2-yl)-2,5-diphenyl-tetrazolium bromide (MTT) assays (Chong et al. 2020). Viable cells continuously convert resazurin (blue nonfluorescent) to resorufin (pink fluorescent) mainly via intracellular organelles such as mitochondria and nucleus, although the exact mechanism is unknown (O'brien et al. 2000). The cytotoxicity data obtained from these experiments strongly correlated with those of published murine data, particularly for the *Echis* venoms, (see Table 5.3). This may suggest that in this Vero cell line, cytotoxicity is more consistently induced by viper venoms generally considered as haemorrhagic and coagulopathic than by neurotoxic elapid

venoms (Gutierrez et al. 2005b). Overall, the assay provided highly consistent and reproducible data, supporting their use in the portfolio of quality control assays necessary for the preclinical assessment of snake venom toxicity and antivenom efficacy.

Occasionally, cells treated with the lowest venom concentrations showed a higher cell viability compared to untreated cells (i.e., control cells treated with DMEM only), regardless of snake species or incubation time. Such observations were present on CellTiter-Blue assays when Vero cells were treated with toxins from *Clostridium difficile* bacteria and also on L929 cell linage treated with TNF α (Rossen Donev, personal communications). Although it is not clear how this happened, CellTiter-Blue relies on enzymatic activities, and venom toxins at concentrations below the lethal threshold may stress the cells thereby increasing the enzymatic activities of the organelles involved in the reduction of resazurin to resorufin without actually affecting the cell viability. The other possibility could be that the toxins below the lethal concentration threshold could be used as supplementary items by the cells and that increases the metabolic functions.

Further to the snake venom toxicity studies, the larval model showed a species-specific variable antivenom neutralisation efficacy. However, the *G. mellonella* model still requires optimisation and standardisation. These results corroborate the current problems associated with polyvalent antivenoms, which lack universal efficacy against all their target venom toxins, particularly against *Elapidae* species (Baldé et al. 2013). The lethality and toxicity-associated effects were amenable to antivenom treatment, when induced by *E. ocellatus* but to a lesser extent for the toxicity profiles induced by *B. gabonica* and *E. leucogaster*. These results concur with findings from *in vivo* studies, which demonstrate that a polyvalent antivenom almost always demonstrates a significantly higher neutralising potency against viper venoms compared to those from elapid species (Harrison et al. 2017; Ainsworth et al. 2020). Although inconsistent results were reported using murine preclinical assays (Abubakar et al. 2010b; Sánchez et al. 2015b; Ainsworth et al. 2020), almost all geographically relevant antivenoms were effective at neutralising *E. ocellatus* venom (Ainsworth et al. 2020). Furthermore, findings from *in vivo* studies suggested that polyvalent antivenoms are equally effective at

neutralising toxicity induced by *B. arietans* and *E. ocellatus* (Segura et al. 2010; Harrison et al. 2017; Ainsworth et al. 2020). It is concerning that there are no comparative clinical data form human subjects to support the findings from murine studies of antivenom efficacy against envenoming by *B. arietans*. In fact, available clinical data have suggested that almost all polyvalent antivenoms are effective against *E. ocellatus* beside offering limited protection against other *Echis* species, including *E. leucogaster* (Potet et al. 2019). This may suggest that *E. ocellatus* is dominated by highly immunogenic toxins (Calvete et al. 2010; Ainsworth et al. 2020) that may skew the immune response of, e.g., horses, during immunisation stages: thereby antibodies with higher affinity towards these components may prevail (León et al. 2011). The other explanation is that venom toxins from *E. ocellatus* which is dominated by HMW proteins, i.e.,≥ 20 kDa, (Casewell et al. 2009), which could be easily accessible by antivenoms. This is because HMW venom toxins such as SVMPs and SVSPs are not readily diffusible to the extravascular compartments and are, therefore, available for neutralisation by the intravenously administered antivenom (Seifert and Boyer 2001; Gutiérrez et al. 2003; Paniagua et al. 2015). Nevertheless, pharmacokinetics of venom/ antivenom have not yet been studied in *G. mellonella* larvae.

Furthermore, these results demonstrated that antivenom offered limited protection against toxicity profiles associated with the *Naja* venoms where it was ineffective at preventing melanisation induced by *N. nigricollis* venom. Interestingly, the potency ranking for *Naja* venoms reflects the data obtained from preclinical studies where antivenoms demonstrated the lowest neutralising efficacy for *N. nigricollis* followed by *N. melanoleuca* and *N. haje* the highest (Ramos-Cerrillo et al. 2008; Casasola et al. 2009). From a clinical perspective, it would appear that all of the current antivenoms appear to offer very limited efficacy at treating envenoming by *Naja* species (Baldé et al. 2013; Potet et al. 2019), but, at present, there are insufficient data to confirm this view. This is attributed to the poorly immunogenic (Petras et al. 2011), yet the readily diffusible low molecular weight 3FTXs (Baldé et al. 2013) which are predominant in the proteome of *Naja* venoms (Tasoulis and Isbister 2017). Although it is difficult to achieve, it is desirable for an antivenom (i.e., polyspecific/pan-specific) to offer a relatively high potency against all target

snake venoms. This relies on factors such as immunisation strategies, venom properties, timing of administration and the ability of antivenoms to penetrate less vascular tissues with removal of tissue-bound toxins (Gutiérrez et al. 2003; León et al. 2011; Silva and Isbister 2020).

Similarly, the results obtained here from *in vitro* immunocytotoxicity (Vero cells) reflects the clinical and murine study findings where the polyvalent $F(ab')_2$-based antivenom demonstrated a better neutralising efficacy against the cytotoxicity induced by *Echis ocellatus* venom than that for *E. leucogaster* venom. However, these preliminary data were not obtained from a validated assay to comprehensively study the efficacy of antivenom to neutralise venom-induced cytotoxicity of Vero cells.

5.5 Limitation of the larval model

Despite being a useful tool for assessing snake venom toxicity and antivenom's potency, the *G. mellonella* model study has some limitations: Firstly, as larvae were obtained from high street shop, there was no control of age, sex and genetic background which might cause variations in some of the results collected from the different experimental repeats. Secondly, in addition to mortality data, inclusion of the recently established health index scoring system involving assessing activity, cocoon formation and melanisation (Loh et al. 2013) might have increased the sensitivity of the assay. Finally, the significantly reduced LD_{50} g/kg body weight (venom: testing animal) compared to the murine tests, highlights the limitation of the *G. mellonella* of being an absolute lethality determinant model. However, such variations exist between murine data generated from different studies (Ainsworth et al. 2020). Finally, it is worth mentioning that the method reported here, i.e., injections of venom: antivenom mixtures do not represent the natural snakebites. Thus, it would have been very interesting to test an assay that would involve injecting venoms first and rescuing the larvae with antivenom afterwards; a situation mimicking the actual circumstance of snakebite.

5.6 Conclusion and future direction

In summary, the *G. mellonella* model has the potential to become an invaluable tool for assessing the toxicity profile of snake venoms and

neutralising potency of antivenoms. Although inconsistencies were observed, overall, the assay corroborates findings from murine and clinical studies. Indeed, this invertebrate model has verified the existing variations in toxicity amongst the venoms of different snake species and their neutralisation by antivenoms. Yet, it has provided reliable data for both the LD_{50} and ED_{50} measurements, where death is the endpoint. In addition to lethality, the *G. mellonella* model could potentially incorporate the health index scoring system currently used to assess bacterial virulence (Loh et al. 2013; Malmquist et al. 2019). Results obtained from the cytotoxicity assay demonstrated that Vero cells are sensitive to different cytotoxicity levels induced by snake venoms, particularly those from Viperidae species. This study demonstrates that this cytotoxicity assay, using Vero cells, could be validated as a potency assay for assessment of antivenom efficacy, especially those directed against *Viperidae* venoms.

The current study highlights the necessity of developing several assay options to measure venom toxicity and antivenom efficacy, that currently relies on a vertebrate animal model. Given the ethical, financial, and logistic constraints associated with the gold standard murine lethality assay, this study has demonstrated that an invertebrate model is well-suited to provide a preliminary characterisation of venom toxicity and antivenom efficacy. Although it will still require the support from the murine study, introduction of the *G. mellonella* model and Vero cell cytotoxicity assays to the current *in vitro* potency assays may ultimately reduce the number of animals required and, hence, implement the 3Rs principles.

Chapter 6: General Discussion

Venomous snakes have evolved an important bioweapon system for deterring and/or subduing animals. Venom is a highly complex mixture of biologically and pharmacologically active enzymatic and non-enzymatic proteins with a primary function to deter, incapacitate and subdue prey. Bites by venomous snakes cause a spectrum of potentially fatal medical consequences, including systemic haemorrhage, neurotoxicity and cytotoxicity. There are about 500,000 snakebites annually in SSA alone, which result in approximately 30,000 deaths every year (Chippaux 2011). Antivenom has been effective at treating and preventing the morbidity and mortality associated with snakebite envenoming (SBE). However, the availability and accessibility of good quality antivenoms is extremely rare particularly in SSA. Prior to the discontinuation of the prestigious antivenom, Fav-Afrique™ in 2014, efficacious antivenom available in the region was estimated to cover only around 2.5% of the projected need for the region (Potet et al. 2019). More recently, the establishment of safe and effective treatment has been introduced by WHO as part of a comprehensive roadmap aiming to halve SBE-related mortality and morbidity by 2030 (Williams et al. 2019a).

The overarching aim of the work described here was to establish a simple manufacturing process to produce affordable, safe, and effective polyvalent antivenom for use in SSA. The study provides a detailed investigation into the recent technology used for manufacturing antivenom with particular emphasis on affordability and efficacy. To enhance the quality specifications of the newly developed antivenom, the study has taken advantage of using the same HHP that was used to manufacture the now-ceased Fav-Afrique™. The intact IgG was, however, produced alongside the $F(ab')_2$ product mainly to assess the robustness of the manufacturing process as well as the formulation during optimisation and stability stages. This was followed by characterising equine IgG subclasses and defining their role and capacity in venom neutralisation. Several immunological and physicochemical assays were used to evaluate the quality of the newly developed antivenom. As an alternative to the current *in vivo* murine lethality tests, herein the study reports, for the first time, the development of a *Galleria mellonella* larval model to assess snake venom toxicity and antivenom efficacy. To this end, snake venoms from different species were used to assess the suitability and capacity of this invertebrate

model. A concurrently developed Vero cell cytotoxicity assay was used in parallel to measure different snake venom cytotoxicity and corresponding antivenom efficacy. In this respect, the CellTitre-Blue assay was used to overcome some of the inherent major setbacks (e.g., impact of washing step on cellular adherence) when using cell lines.

6.1 Development of an inexpensive manufacturing process for polyvalent Antivenoms

In an effort to resolve the recent antivenom crisis in SSA, global manufacturers have used the opportunity to supply the region with new wave of cheaper but poor-quality antivenoms (Harrison et al. 2017). Very few of these antivenom products have demonstrated adequate efficacy (Brown 2012), for example, Inoserp® Pan Africa antivenom (Chippaux et al. 2015a), nor were these products affordable (Harrison et al. 2017). However, the current study predicted that a good quality antivenom can be produced at a considerably reduced cost. This was achieved by establishing a simple and inexpensive manufacturing process involving caprylic acid precipitation followed by pepsin digestion and chromatographic steps. Both $F(ab')_2$ and whole IgG antivenom products were developed in parallel and their quality compared to Fav-Afrique™. The manufacturing process appeared to be robust, and it can be used to manufacture either intact IgG antivenom or $F(ab')_2$ antivenom with minor but appropriate parameter switching. Generally, production of whole IgG is considered simpler and costs less but may require a higher dose to achieve the protection afforded by $F(ab')_2$.

6.1.1 Liquid formulations with Improved stability

Lyophilisation of antivenom is an unaffordable process for SSA (Harrison et al. 2017; Mitra and Mawson 2017), thus this study has developed a robust method to produce a liquid formulation which demonstrates excellent stability at real (2-8℃) and accelerated (37.5℃) temperatures. Both the intact IgG and $F(ab')_2$-based antivenoms were comparable in terms of stability and physicochemical properties.

6.1.2 Comparisons between the newly manufactured $F(ab')_2$ antivenom and Fav-Afrique™

Whilst it is the 'gold standard' to perform murine potency tests for every new antivenom batch, it has been proposed that antivenom potency can be accurately predicted using a carefully optimised ELISA assay (Theakston and Reid 1979; Rial et al. 2006). Furthermore, there is a call to incorporate ELISA assays into the quality control system for antivenom manufacturers, some producers having already used the method for batch release. In addition to reducing production cost, the ELISA assay provides more consistent data between batches. However, this method still relies on murine neutralisation tests to generate a "reference sample" to provide equivalent data between the *in vivo* and ELISA assays. This still significantly reduces the number of animals used per study.

Inspired by these findings, the study described in this thesis used an ELISA assay to assess the potency titre of the newly formulated antivenom compared to the original Fav-Afrique™ product. The ELISA results have demonstrated that the F(ab')$_2$ antivenom produced a potency titre equivalent to that of Fav-Afrique™, particularly against the viper venoms. However, Fav-Afrique™ has a slightly better potency titre against the *Dendroaspis* and *Naja* venoms, which could be due to the result of HHP mixing ratios. Additionally, the two F(ab')$_2$-based antivenom products have offered a similar recognition pattern of snake venom components which showed effective venom- antivenom interactions against major toxin families within all the target snake species.

In contrast, the whole IgG-based antivenom was ineffective at recognising all the major snake venom toxins and also showed the lowest potency titre compared to the F(ab')$_2$ and Fav-Afrique™ antivenoms, within the ELISA assay. In spite of this, both EchiTab and EchiTabG Plus, which are intact IgG monovalent ovine (*Echis ocellatus*) and trivalent equine (*Echis ocellatus*, *Bitis arietans* and *Naja nigricollis*) antivenoms, respectively, demonstrated excellent efficacy and safety profiles in clinical trials (Abubakar et al. 2010a). This may suggest that intact IgG directed against many snake species constitute a limited efficacy towards its target. This is because as the number of snake species in the immunogen mixture increase, the antigen-specific antibody against each species reduces and this becomes obvious particularly in an IgG format. Nevertheless, it should be noted that antivenom of high venom binding capacity does not infer an equal neutralisation efficacy, but

weak binding activity strongly suggests neutralisation inefficacy. Likewise, even excellent *in vivo* results (Ramos-Cerrillo et al. 2008) could fail to reflect such efficacies in clinical settings (Baldé et al. 2013). Therefore, the ELISA binding assay is one of the suitable tests that can contribute to the assessment of antivenom quality.

6.1.3 Safety assessment for antivenom

In addition to demonstration of efficacy, antivenom must demonstrate an excellent safety profile, which may be affected by its physicochemical properties, e.g., purity, stability and quantity (Burnouf et al. 2004). From a manufacturing perspective, consistent quality, efficacy and safety are achieved through effective removal of side effect-inducing impurities such as albumin, Fc fragments and pepsin (Kurtović et al. 2019). In this respect, the antivenom product reported in this study had no measurable trace of Fc, albumin and pepsin impurities. In fact, this product has achieved a superior purity to that required by the current WHO guidance for commercial antivenom quality (World Health Organization 2016). This was confirmed by SEC-HPLC, Coomassie stained SDS-PAGE and Western blot analysis. Additionally, this method offers potential viral reduction by incorporating approved viral removal steps (Mpandi et al. 2007; Caricati et al. 2013) whilst circumventing expensive procedures such as nanofiltration and Gamma Irradiation viral clearance strategies. To minimise process-related antibody damage, the process uses an adaption of a process shown to preserve antibody activity following pepsin digestion (Morais and Massaldi 2005). In addition to exhibiting excellent titration values and safety-related profiles, the method has offered enhanced yield of antivenom product as well as excellent potency titres and purity.

This confirms that the optimum operating parameters were confirmed by negligible process-related variations. This is a crucial step in transferring technology across different laboratories because altering critical process parameters (CPP) has a profound impact on the critical quality attributes (CQA). This confirmed not only the robustness of the operating parameters defined for this study but also their impact on product quality was accurately and reliably predicted.

6.2 Characterisation of equine IgG subclasses

Despite demonstrating excellent physicochemical properties (i.e., purity and stability) and neutralisation efficacy, administration of large quantities of antivenom may still trigger adverse reactions. This is because antivenoms are heterologous proteins where the neutralisation-relevant (also referred to as antigen-specific) antibodies represent only 10-40% of the total antivenom protein (Segura et al. 2013; Al-Abdulla et al. 2014; Pla et al. 2017). Several studies have suggested that the neutralising activity of equine-derived antivenom is afforded by the IgG(T) subclass (Fernandes et al. 1991; Fernandes et al. 1997; Fernandes et al. 2000b). This encourages the removal of 60-90% irrelevant proteins as a measure to improve safety and efficacy of antivenom. IgG(T) is a key component of equine IgG, and it comprises two IgG subclasses (IgG_3 and IgG_5) of the seven IgG subclasses recently identified (Lewis et al. 2008). Indeed, some of the high quality antivenoms (Boels et al. 2012; Bourke et al. 2021) are reported as IgG(T)-based products (Grandgeorge et al. 1996; Pepin-Covatta et al. 1997). Despite reporting improved efficacy and safety, the IgG(T)-enrichment technology is not considered for producing antivenom for SSA. Besides using a very expensive technology, IgG(T) antivenoms demonstrate variations in neutralising capacity (Fernandes et al. 2000a; Toro et al. 2006).

To explore this variation, we investigated the binding activity of different equine IgG subclasses in antivenoms against snake venoms from SSA. The IgG subclasses were separated chromatographically and quantified by ELISA where the isolation of IgG(T) was confirmed by western blot analysis. In parallel to published data (Fernandes et al. 2000a; Fernandes et al. 2000b), our results demonstrated that IgG(T) was the major constituent, but combined IgGa and IgGb represents a significant quantity (~24%) of total IgG content of HHP. However, contrary to published data (Fernandes et al. 1991; Fernandes et al. 1997; Fernandes et al. 2000b), the results obtained from this study demonstrated that the binding activity of antivenom is not entirely encapsulated within the IgG(T) subclass. In fact, our data demonstrated that the venom binding capacity within the IgG(T)-depleted samples was greater than 2.4 times (group *Echis*) and 1.5 times (group *Naja*) that of IgG(T)-

enriched samples when assessed against individual venoms. Similar binding trends were observed when these antivenoms were assessed against venom mixtures that used in the immunising protocol for the antivenom in test.

This is supported by published results that showed both IgGa and IgG(T) antivenoms have comparable titration values and neutralisation efficacies (Toro et al. 2006). This may suggest that the venom neutralising activity of equine IgG subclasses is affected by antigen variability and immunisation strategies, thus different antivenoms present different neutralisation activity profiles. This hypothesis is supported by the findings that the neutralisation activity of IgG(T) was three times and seven times more potent than IgGa in anti-bothropic and anti-crotalic antivenoms, respectively (Fernandes et al. 1997).

Furthermore, the western blot analysis indicated that the IgG(T)-enriched and IgG(T)-depleted samples provided a different toxin recognition pattern, which may indicate different neutralisation strengths of each subclass. Accordingly, the IgG(T)-depleted sample showed more intense staining of a venom component which corresponded to the molecular weight of svPLA$_2$. Interestingly, the binding capacity of the IgG(T)-depleted antivenom appears to correlate with the PLA$_2$ content within the viper and elapid venoms. This suggests that the inclusion of the IgG(T)-depleted fraction in antivenom formulation is critically important to provide adequate protection against svPLA$_2$, the effects of which include tissue necrosis and extensive haemolysis (Warrell et al. 1976b). This observation is supported by studies which showed that AV with ineffective IgGa offered a significantly poorer neutralisation of svPLA$_2$ (Fernandes et al. 2000a). Thus, based on the data presented here, manufacture of antivenom by IgG(T)-enrichment may not necessarily lead to a universally improved efficacy. Nevertheless, this warrants further investigation which includes murine studies and advanced venomics, in order to provide detailed characterisation of the different equine IgG subclasses raised against snake species from SSA region.

6.3 Development of Invertebrate and Cell based assays

Although *in vitro* QC assays improve the quality and safety of antivenoms, the *in* vivo murine assay is still regarded as the gold standard means of determining the ED_{50} for a newly developed and/or newly manufactured antivenom batch (World Health Organization 2016; Gutiérrez et al. 2021). However, its use is restricted by technical, biological, logistical, and ethical challenges. Furthermore, there is an unprecedented effort to implement the 3Rs in the study of snake venom toxicity and antivenom efficacy. In this study, we investigated the suitability of a novel invertebrate model to assess 1) the snake venom toxicity and 2) the efficacy of antivenoms at neutralising the toxic activities of these venoms. In addition to offering technical advantages, the similarity of the innate immunity between *G. mellonella* and mammals makes it an excellent model as a potential replacement for the murine test.

However, despite expressing similarities with mammals e.g., innate immunity, gastrointestinal tract, expression of coagulation proteins and Na_v (Cordero et al. 2016; Maguire 2017; Ménard et al. 2021), there are some basic anatomical and physiological dissimilarities between *G. mellonella* and mammals. Indeed, the phylogenetic (evolutionary) divergence between mammals and insects occurred about 555 million years ago and this makes comparison between the two species challenging (Smith and Casadevall 2021). Similarly, the lack of adaptive immune response in *G. mellonella* is another key limitation for the model (Smith and Casadevall 2021). With the exception of Na_v (Cordero et al. 2016), it is unclear if the model expresses L-type voltage gated ion channels such as K_v & Ca_v which are important targets for snake venom toxins such as 3FTXs, KTT and PLA_2 (Ranawaka et al. 2013; Ferraz et al. 2019). More importantly, further studies are required to unravel if the model expresses neuromuscular junction system; a key target for snake venoms, particularly from the elapid species, predominated by neurotoxins such as 3FTXs, KTT and PLA_2 (Petras et al. 2011; Laustsen et al. 2015; Ainsworth et al. 2018). Until then, the use of *G. mellonella* as a model for snake venom toxicity should be assessed on case-by-case basis.

Nevertheless, to make comparison impartial, the protocol was adjusted to reflect the current murine test protocols. The study provided fascinating

characteristic results based on the activity of these snake venom toxins. To provide a rational use of the model, snake venoms with known proteomic and pathophysiological profiles were used. In this respect, the snake venoms used in this study include venoms dominated by the haemorrhagic and coagulopathic activity of *Echis* and *Bitis* species, snake venoms with necrotic activity of *N. nigricollis* venom toxins and venom toxins dominated with neurotoxic activities of *N. haje* and *N. melanoleuca* species.

The larvae displayed distinct signs in response to venom, possibly correlated to their proteomic "toxicological" profile. Immediate discolouration (melanisation) and leakage of dark-coloured fluids from the entire surface of the body were observed following injection with venoms from *Viperidae* species (*B. arietans, B. gabonica, E. leucogaster* and *E. ocellatus*). However, severity varied greatly between venom species tested, with *B. arietans* having a particularly marked effect, with immediate extensive discoloration, and *B. gabonica* causing the fewest toxicity signs of viper venoms.

In humans, bites by *B. arietans* are characterised by systemic effects such as haemorrhage and dysregulated cardiac and haemostasis systems, and local effects including blistering, necrosis, and significant lymphoedema (Megale et al. 2019). Similar symptoms, including local tissue necrosis, oedema, local swelling and haemorrhage were observed in patients envenomed by *B. gabonica* (Marsh et al. 2007). These signs and symptoms are typically related to SVSPs and SVMPs which are the abundant toxins in these genera (Calvete et al. 2007; Casewell et al. 2009; Casewell et al. 2014b). The SVMPs make up approximately 38.5% (*B. arietans*), 22.9% (*B. gabonica*) and 72 % (*Echis ocellatus*) of the total venom proteins (Calvete et al. 2007; Casewell et al. 2009). Whereas SVSPs make up around 19.5% (*B. arietans*), 26.4% (*B. gabonica*) and <2% (*Echis* species) of the total venom proteins (Tasoulis and Isbister 2017). Furthermore, snake venom toxins C-type Lectin, disintegrin and $svPLA_2$ were characterised, albeit in distinct relative abundances, from venoms of *Bitis* (Calvete et al. 2007) and *Echis* (Casewell et al. 2009) genera. These venom toxins are also known for their amplification of envenoming by initiating key cellular and systemic functions (Megale et al. 2019).

In addition to melanisation, administration of *E. leucogaster* and *E. ocellatus* venoms caused extensive fluid exudation. Consistent with this, in patients,

envenoming by these snakes, particularly *E. ocellatus,* is characterised by spontaneous bleeding, coagulopathy, local tissue swelling and local necrosis (Warrell et al. 1974). In most cases, cerebral haemorrhage is the main cause of death (Warrell et al. 1974).

The model exhibited distinct signs of toxicity in response to administration of *Naja* venoms, where flaccidity, loss of righting reflex, immediate reduction in movement, paralysis and death were commonly observed. Clinically, envenomings by *Naja* spp., particularly *N. haje* and *N. melanoleuca* present with drowsiness, ptosis, loss of consciousness, paralysis, respiratory paralysis and cardiac arrest (Warrell et al. 1976a; Warrell et al. 1976b; Baldé et al. 2013). There is strong evidence linking these clinical manifestations to the venom toxins revealed by their proteomes, which are predominated by α-neurotoxin of the 3FTX family (Lauridsen et al. 2017). The 3FTXs comprise 57.1% to 73.3% of the total venom proteins of the *Naja* venoms, whereas svPLA$_2$ only account for 4% to 21.9 % (Tasoulis and Isbister 2017). Alongside the neurotoxic signs, the larvae treated with *N. nigricollis* venom displayed increased discolouration with minimal fluid exudation compared to larvae treated with viper venoms. This may reflect the clinical manifestations associated with bites by *N. nigricollis,* which include extensive local necrosis, haemorrhage, oedema and neurotoxic signs (Warrell et al. 1976b; Baldé et al. 2013).

6.3.1 Quantification of snake venom toxicity using *G. mellonella* complemented by Vero cell cytotoxicity

Beside exhibiting signs and symptoms of toxicity comparable to human envenoming, the *G. mellonella* model appears as a strong tool for estimating the Median Lethal Dose (LD$_{50}$) for each snake species tested. In this respect, the data generated from this study reflects the *in vivo* results. Furthermore, statistically significant differences in toxicity effects (i.e., LD$_{50}$ values) were observed within the *Bitis* and *Naja* genera. In parallel to the *in vivo* results (Casasola et al. 2009; Segura et al. 2010), venom of *B. gabonica* was the least toxic (LD$_{50}$ =45.9µg/ larvae) but the *N. melanoleuca* (LD$_{50}$ =3.2 µg/ larvae) was the second most toxic snake species to the larvae. Unexpectedly, venom of *N. nigricollis* was extremely toxic (LD$_{50}$ =1.6 µg/larvae) to the larvae. This is a

contradictory result, which does not reflect the murine test (Casasola et al. 2009) that suggested *N. melanoleuca* venom is much more toxic than *N. nigricollis* venom. Although prey-specific toxicity was observed in snake venoms (Barlow et al. 2009; Richards et al. 2012), there is no evidence that for *N. nigricollis, G. mellonella* (or phylogenetically related species) forms part of its diet.

Nevertheless, the model offered a good comparison of snake venom LD_{50}s between mammalian and insect larvae tests, and, in many cases the venom toxicity was comparable between larvae and mice when mg venom/ mouse or /larva was considered. However, when the toxicity was compared on the basis of mg venom/ kg body weight, all the tested snake venoms were greater than ten times more toxic to the larvae than to mice. However, such differences in lethality should not discredit this model because variations in LD_{50} are commonly observed in murine tests carried out at different laboratories, which also, among many other factors, is affected by venom origin (Sánchez et al. 2015a; Ainsworth et al. 2020). Furthermore, toxicity variations were observed between different mammalian species, the dog being as twice sensitive as the mouse to snake venoms (Marsh and Whaler 1984). However, given the consistency of the toxicity trends and the credible toxicity index observations, it appears that the model could be standardised where its sensitivity is increased so that it can be used as self-sufficient test or as a surrogate assay.

In addition to the *G. mellonella* assay*,* this study has explored the use of a Vero cell cytotoxicity assay as another tool (or platform) to assess snake venom toxicity. Almost all snake venoms contain proteolytic proteins which interfere with cell attachment to the plate; which is a key requirement for cells to maintain growth and/or proliferation. This has been one of the main challenges that hinders the application of cell assays in snake venom research. Herein, we showed that the Vero cell cytotoxicity assay can be optimised using CellTiter-Blue, where rapid screening and high sensitivity can be achieved. The cytotoxicity assay results, utilising CellTitre-Blue, demonstrated a dose-dependent inhibition of cell growth in response to treatment with snake venom.

6.3.2 Antivenom Potency measurement using the *G. mellonella* complemented by Vero cell assays

In addition to the venom toxicity, the invertebrate model has been able to correctly predict species-specific antivenom ED_{50}. The Polyvalent $F(ab')_2$ antivenom demonstrated the highest efficacy against *E. ocellatus* (~2 mg/mL) and lowest (0.2 mg/mL) against *B. arietans*. Although this is contrary to published *in vivo* data, which showed that Fav-Afrique™ antivenom has its highest potency against *B. arietans,* such differences are common even in murine result from different laboratory groups (Ainsworth et al. 2020).

Furthermore, the Polyvalent $F(ab')_2$ offered a full protection against toxicity effects induced by *B. gabonica* but the antivenom was ineffective to protect the larvae against the *B. arietans* toxicity signs. There is no *in vivo* data are available for Fav-Afrique potency against *B. gabonica* to draw a direct comparison between the two adder species. However, from a clinical standpoint, envenomings by *B. gabonica* have shown a good response to antivenom treatment with a relatively uncomplicated recovery (Marsh et al. 2007).

Nevertheless, the *G. mellonella* model estimated the efficacy of the Polyvalent $F(ab')_2$ against the *Echis* genus and exhibited that potency against *E. ocellatus* was approximately twice that of *E. leucogaster.* This is corroborated by published *in vivo* studies in which Fav-Afrique™ demonstrated similar potency trend against the two *Echis* species (Ainsworth et al. 2020). Indeed, *E. ocellatus* is a deadly snake found throughout SSA (World Health Organization 2016), and its venom is responsible for systemic bleeding, coagulopathy and intracranial haemorrhage (Warrell et al. 1977; Habib et al. 2008; Habib and Abubakar 2011; Habib 2015). In our study, the *E. ocellatus* venom-treated group of larvae were fully protected without any signs of toxicity, following antivenom treatment. This suggests that the key toxins in *E. ocellatus* venom are readily neutralised by target antivenoms. This hypothesis is supported by published *in vivo* results (Ainsworth et al. 2020) and clinical data (Potet et al. 2019) which demonstrated that most antivenoms available in SSA that target *E. ocellatus* have been efficacious on successfully treating the underlaying envenoming. Interestingly, even the SAIMR Polyvalent antivenom (Table 1.4),

which does not include *E. ocellatus* in the immunogen mixture, showed a good efficacy against this venom (Ainsworth et al. 2020). This could be due to the fact that SVMPs,- the main venom toxin proteins responsible for the symptoms attributed to *E. ocellatus* venom (Gutierrez et al. 2005b; Wagstaff et al. 2009), are ubiquitously found in almost all venomous snakes, albeit in different proportions (Tasoulis and Isbister 2017). This may increase the production of specific antibodies against the SVMPs family following immunisation of donor animals, which will cross react with those in the venoms of other species.

Interestingly, the larval model demonstrated that the Polyvalent $F(ab')_2$ antivenom had a significantly poorer neutralisation efficacy (0.3 mg/mL) against *N. nigricollis* venom. The literature does not contain data on Fav-Afrique™ against *N. nigricollis* for us to make comparisons but its potency against *N. melanoleuca* is reported and it was ~0.2 mg/mL (Ainsworth et al. 2020). Thus, this is a milestone finding showing that the model was able to correctly identify the lower efficacy of polyvalent antivenoms commonly observed against elapid venoms. In this respect, most, if not all, of the major polyvalent antivenoms struggle to provide a balanced efficacy against elapid and viper venoms, both at preclinical (Ainsworth et al. 2020) and clinical (Baldé et al. 2013) levels. For example, EchiTab Plus ICP had an average potency of ~0.6 mg/mL neutralisation efficacy against *N. nigricollis* which is around 6 and 5-fold weaker than the potency reported for *B. arietans* and *E. ocellatus*, respectively. Similarly, Antivipmyn®Africa has a potency of ~0.5 mg/mL against *N. nigricollis* which is 4.5 and around 3-fold weaker than the potency reported against *B. arietans* and *E. ocellatus*, respectively (Ramos-Cerrillo et al. 2008). Antivipmyn®Africa is a polyvalent $F(ab')_2$ lyophilised antivenom against 11 snake species (from *Bitis, Dendroaspis, Echis* and *Naja* genera) endemic to SSA (Ramos-Cerrillo et al. 2008).

However, it is not expected that polyspecific antivenom will provide universal efficacy against all target snake venoms. This is because several clinical (Baldé et al. 2013; Chippaux et al. 2015a; Potet et al. 2019) and preclinical (Harrison et al. 2017) studies have shown that most polyvalent antivenoms only offer full protection against bites by *Echis* and *Bitis* species but only limited protection against envenoming by *Elapidae* species. This has been the focus

of many scientific hubs, globally, where research has been directed at solving these challenges.

6.4 Strengths and Weaknesses of the study

Excellent results were obtained from this project suggesting that a workable ELISA, an *in vitro* cytotoxicity assay and a *G. mellonella* larval model are potentially suitable means of measuring antivenom efficacy. The results obtained from these models appeared to complement each other and, therefore, may suggest the use of these assays as ideal candidates to expand the quality control assessment of antivenom efficacy. This potentially saves the lives of numerous test animals, improves the quality of antivenoms by establishing rigorous quality control measurements, and reduces production cost by minimising the use of *in vivo* testing. Additionally, the study projected that good quality antivenom can be produced inexpensively thus reducing its market cost.

However, the study highlighted some limitations. Firstly, the study should have focused on only one snake venom from each of the *Viperidae* and *Elapidae* families. This would have led to more realistically controllable experiments, although screening across all the target species enables us to better understand the interactions between venom and the *G. mellonella* model and Vero cell cytotoxicity assays. Secondly, the $F(ab')_2$ based product should have been directly compared to Fav-Afrique™ on the *G. mellonella* model and the cell-based assay. However, it was difficult to obtain Fav-Afrique™ beyond a 10 mL ampoule, kindly provided by Professor Nick Casewell. Additionally, the *G. mellonella* model should have been used to assess the toxicity of *Dendroaspis* venoms and antivenom potency against these venoms. Unfortunately, we ran out of time, mainly due to the COVID 19 pandemic, which coincided with the major part of the project. The CellTiter-Blue immunocytotoxicity assays should have been optimised and run concurrently with the *G. mellonella* larval study, which would have helped to make definitive conclusions on assay suitability. However, both plans (*Dendroaspis* study on *G. mellonella* and optimisation of Vero cells) were severely disrupted by the pandemic that is estimated for ~12 months, which is occurred during the prime time of the project.

Although it is believed that the IgG(T)-depleted sample was mainly IgGa, the study lacks the specificity to differentiate between IgGa and IgGb and the fractions were, therefore, identified as 'IgG(T)-depleted' and 'IgG(T)-enriched' samples. This is another key deficiency in this study. Finally, to further maximise the quality of the antivenom product, the study should have included additional physicochemical and immunological assays. This would include quantification of antigen-specific antibodies using optimised Small-Scale Affinity Chromatography (SSAC) and comparison of antivenoms' avidity to the snake venoms using a chaotropic ELISA assay as described by Harrison and colleagues (2017).

6.5 Future work

Observations from this study have provided a strong base for further exploration of different aspects. Firstly, it would be interesting to achieve complete separation of IgGa and IgGb in order to investigate the affinity of IgGa and IgG(T) to snake venoms. This could be complemented by the *G. mellonella* larval assay to determine their efficacy against whole venom as well as purified venom components such as PLA_2. The use of *in vivo* murine studies could also have been performed to ratify the results. Towards that end, snake venom toxins with known toxicity scores (form *in vivo* studies) will be isolated and their toxicity ranks will be assessed in the *G. mellonella* model. This will provide valuable insights into the actions of snake venom toxins within the invertebrate model. Also, this will assess whether the model is reflecting the mechanism of snake venom toxicity in mammals, e.g., murine and human, maximising the likelihood of impartial correlations with mammalian models. Once correlations with *in vivo* model (e.g., murine) are established, the *G. mellonella* could be used as validated model for extrapolating toxicity information to murine and human envenomings.

Secondly, the efficacy of the polyvalent $F(ab')_2$ based antivenom against elapid venoms could be improved. Although it is challenging to achieve a universally equivalent neutralisation against all target species, increasing the HHP volume of anti-elapid plasma in the blending of the active pharmaceutical ingredients (API) may improve the antivenom potency against these species. Another option is to pool the final purified antivenom products (that are

prepared separately) based on their binding determined by ELISA and/or ED_{50} determined by the *G. mellonella* larval assay. Alternatively, four batches of antivenom could be prepared based on genus, i.e., Anti-*Bitis*, Anti-*Naja*, Anti-*Echis* and Anti-*Dendroaspis*.

Thirdly, findings from the *G. mellonella* study have shown some inconsistent results particularly against the *Dendroaspis* species. This may suggest that the test requires further optimisation and standardisation to provide consistent data. This could be achieved by controlling factors associated with data variations (for e.g., age and sex of larvae), for example by using pharmaceutical grade larvae. To minimise the higher cost incurred with these assays, however, high-street larvae could be used for all the initial assessments and then the pharmaceutical grade larvae will subsequently be used for final development and optimisation. This would be followed by assessing the capability of the model to distinguish the inter/intraspecies toxicity variation and also neutralisation efficacy of antivenoms against snake species from different geographical origins. Various antivenoms including whole IgG (e.g., EchiTab Plus ICP), $F(ab')_2$ (e.g., Fav-Afrique™) and Fab (e.g., ViperaTAb®) would be recruited to further inspect its suitability to assess antivenom potency. Further to this, a larval survival study which records the death at different time points, preferably every hour could be included in the protocol of this model.

Preliminary observations from the CellTiter-Blue cytotoxicity assay would suggest that the Vero cell is a suitable cell line for assessing antivenom neutralisation of venom cytotoxicity. Future work might involve standardising the assay so that it can be applied to all target snake venoms. It is also important that assay suitability is tested using various antivenom products and formats including whole IgG (e.g., EchiTab Plus ICP), $F(ab')_2$ (e.g., Fav-Afrique™) and Fab (e.g., ViperaTAb®).

6.6 Concluding remarks

In conclusion this project provides a unique look into several facets of toxicological, immunological and biological research as well as the antivenom manufacturing process. Advances in laboratory techniques will continue to unravel the mechanisms controlling the synthesis of the different equine IgG

subclasses and their role in venom toxin neutralisation. Eventually, this will lead to developing innovative strategies to enable enriching the relevant IgG subclass during immunisations periods and manufacturing processes. Until then, preparation of antivenom on the basis of a single IgG subclass does not appear an ideal approach and may lead to ineffective antivenom, particularly against the snake species reported in this study. It is projected that antivenom can be manufactured at a significantly reduced cost and this being achieved by avoiding and/or replacing expensive manufacturing stages and processes, including implementation of caprylic acid precipitation, heat inactivation and/or pasteurisation and replacement and/or reduction of *in vivo* testing.

Finally, the rapid and inexpensive *G. mellonella* larval model appears to be a promising tool with the potential to replace and/or reduce the use of *in vivo* murine tests in the field of antivenom efficacy testing. Complementing the invertebrate model with a cytotoxicity assay provides a potential expansion of antivenom quality assessment. However, both assays need to be standardised prior to implementation as universal tools for assessing snake venom toxicity and antivenom efficacy. Once validated, it would represent a successful application of the 3Rs, and a significant tool for improving the design and development of effective antivenoms.

Chapter 7: Appendices

Appendix I: Buffer recipes and stock concentrations

A. Buffers used for small scale affinity purification

All buffers used for small scale affinity purification were prepared according to the protocols established by MicroPharm Ltd.

Preparation of swelling solution: 1 mM HCl

Chemical name	Molecular Weight (g/mol)	Quantity/ volume	Molarity / %
37% Hydrochloric acid	36.46	83 µL	1 mM
Water for Irrigation (WFI)	-	Up to 1 L	-

Preparation of coupling buffer: 100 mM sodium carbonate, 500 mM sodium chloride; pH 8.3 ± 0.2

Chemical name	Molecular Weight (g/mol)	Quantity/ volume	Molarity / %
Sodium bicarbonate	84.01	8.2 g	97.61 mM
Sodium carbonate	105.99	0.3 g	2.36 mM
Sodium chloride	58.44	29.2 g	500 mM
Water for Irrigation (WFI)	-	Up to 1 L	-

Preparation of Blocking solution: 1 M ethanolamine, pH 8.0±0.2 (pH was adjusted with 2 M Hydrochloric acid)

Chemical name	Molecular Weight (g/mol)	Quantity/ volume	Molarity / %
Ethanolamine	61.1	61.1 g	1000 mM
Water for Irrigation (WFI)	-	Up to 1 L	-

Preparation of washing buffer: 100 mM sodium acetate, 500 mM sodium chloride (pH 4.0 ± 0.2)

Chemical name	Molecular Weight (g/mol)	Quantity/ volume	Molarity / %
Sodium acetate	82.03	1.3 g	16.2 mM
Acetic acid	60.05	5.1 g	83.3 mM
Sodium chloride	58.44	29.2 g	500 mM
Water for Irrigation (WFI)	-	Up to 1 L	-

Preparation of 100 mM phosphate containing 500 mM sodium chloride; pH 7.4 ± 0.2

Chemical name	Molecular Weight (g/mol)	Quantity/ volume	Molarity / %
Di-sodium phosphate anhydrous	141.96	12.07 g	85 mM
Sodium phosphate dihydrogen	156.01	2.34 g	15 mM
Sodium chloride	58.44	29.44 g	500 mM
Water for Irrigation (WFI)	-	Up to 1 L	-

Preparation of elute buffer: 100 mM glycine, pH 1.5 ± 0.2 (pH was adjusted with 2 M Hydrochloric acid)

Chemical name	Molecular Weight (g/mol)	Quantity/ volume	Molarity / %
Glycine	75.07	7.51 g	1000 mM
Water for Irrigation (WFI)	-	Up to 1 L	-

B. Buffers used for Western blot analysis

Buffers such as running and washing buffers were prepared from 10x Ready-made Bio-Rad buffers

10x Tris/Glycine/SDS (product number 1610732)

1x Running buffer was prepared by diluting 10x Tris/Glycine/SDS. The 1x running buffer contains 25 mM Tris, 192 mM glycine, 0.1% SDS, pH 8.3.

10x Tris Buffered Saline (TBS) (product number 1706435)

Following diluting with WFI (1:10), the TBST washing buffer was prepared by adding Tween-20 at 0.1% (v/v).

Blocking buffer (TBST +milk) was prepared by adding skimmed milk at 5% (w/v) to the TBST buffer. If required, pH was adjusted to pH7.4±0.2

C. Buffers used for ELISA method

Coating buffer: Phosphate-buffered saline (PBS), pH 7.4±0.2

Chemical name	Molecular Weight (g/mol)	Quantity/ volume	Molarity / %
Di-sodium phosphate anhydrous	141.96	12.07 g	85 mM
Sodium phosphate dihydrogen	156.01	2.34 g	15 mM
Sodium chloride	58.44	8.76 g	150 mM
Water for Irrigation (WFI)	-	Up to 1 L	-

ELISA washing/ diluting buffer: PBST - 0.1% (v/v) + Tween-20

Chemical name	Molecular Weight (g/mol)	Quantity/ volume	Molarity / %
Di-sodium phosphate anhydrous	141.96	12.07 g	85 mM
Sodium phosphate dihydrogen	156.01	2.34 g	15 mM
Sodium chloride	58.44	8.76 g	150 mM
Tween-20	58.44	1 mL	0.1%
Water for Irrigation (WFI)	-	Up to 1 L	-

D. Pepsin dissolving solution

20 mM citrate buffered saline, pH 6.0±0.2

Chemical name	Molecular Weight (g/mol)	Quantity/ volume	Molarity / %
Tri-sodium citrate dihydrate	294.10	5.40 g	18.36 mM
Citric acid monohydrate	210.14	0.35 g	1.66 mM
Sodium chloride	58.44	8.76 g	150 mM
Water for Irrigation (WFI)	-	Up to 1 L	-

E. SEC-HPLC solution

Preparation of 1L 20 mM Phosphate, pH 6.0±0.2

Chemical name	Molecular Weight (g/mol)	Quantity/ volume	Molarity / %
Di-sodium hydrogen phosphate anhydrous	141.96	0.39 g	2.74 mM
Sodium phosphate monobasic dihydrate	156.01	2.69 g	17.26 mM
Sodium chloride	58.44	7.59 g	130 mM
Sodium Azide	65.01	0.2 g	0.02 %
Water for Irrigation (WFI)	-	Up to 1 L	-

F. Buffers and solutions used for Anion exchange chromatography (AEX)

Preparation of washing buffer: 10 mM phosphate buffered low saline (PBL), pH7.0±0.1

Chemical name	Molecular Weight (g/mol)	Quantity/ volume	Molarity / %
Di-sodium phosphate anhydrous	141.96	0.85 g	5.99 mM
Sodium phosphate dihydrogen	156.01	0.63 g	4.03 mM
Sodium chloride	58.44	0.58 g	10 mM
Water for Irrigation (WFI)	-	Up to 1 L	-

Preparation of eluting buffer: 10 mM phosphate buffered high saline (PBH), pH 7.0±0.1

Chemical name	Molecular Weight (g/mol)	Quantity/ volume	Molarity / %
Di-sodium phosphate anhydrous	141.96	0.85 g	5.99 mM
Sodium phosphate dihydrogen	156.01	0.63 g	4.03 mM
Sodium chloride	58.44	58.44 g	1000 mM
Water for Irrigation (WFI)	-	Up to 1 L	-

Appendix II: Manufacturing process maps, AV stability data and AV binding activity

Appendix II(A): Process map for manufacturing whole IgG Antivenom

PROCESS		Activities
Pool Hyperimmune Plasma		
↓		
Warm to 25 to 30°C		
↓		
Heat to 56°C±1°C		0.5 M HCl
↓		
Cool to room temperature	←	Add 0.5x HHP WFI volume
↓		
Add caprylic acid 3% (v/v): mix vigorously for 1 h at room temperature	←	Adjust pH to 4.88±0.05
↓		
Centrifuge at 4500 RCF, 45 minutes, 22°C	→	Pellets to waste
↓		
Filter through GF (0.65µm) + 0.2µm followed by Millistak+® CR40		
↓		
Concentration and diafiltration using 100 kDa nMWCO PESU (7xvolumes)	←	0.9% NaCl
↓		
Filter through 0.2µL and add Tween-80 at 0.05 (v/v)		
Add Excipients (e.g., PS80) and adjust concentration to 50 g/L ±1 g/L	←	Under sterilisation conditions

Appendix II(B): Process map for manufacturing F(ab')$_2$ antivenom

PROCESS		Activities
Caprylic acid Purified IgG	←	Filtered through Activated Carbon and 0.2µm filters
↓		
Warm to 30°C ±1°C		
↓		
Adjust pH 3.00 (3.00 to 3.10)	←	0.5 M HCl
↓		
Add pepsin at a final concentration of 2% (w/w) and process the digestion for 1h		
↓		
Terminate digest to pH 4.8 to 5.0	←	1 M NaOH
↓		
Depth filtration		
↓		
Concentration and diafiltration 50 kDa nMWCO PESU (7 volumes)	←	20mM piperazine, 65mM NaCl, pH5.0, conductivity 9-10mS/m
↓		
Filter through 0.2µm Filter		
↓		
Load into Q-AEX column	→	Bound fraction to waste
↓		
Concentration and diafiltration 30 kDa nMWCO	←	Formulating buffer (0.9%NaCl)

Appendix II(C): Stability data for liquid formulated antivenoms

Visual inspection was conducted under Apollo II system. Stability results were confirmed by two independent qualified individuals from MicroPharm Ltd. ELE, MD, RD, MA and NM are initials for Quality Assurance (QA) records retained by MicroPharm Ltd.

EXP240820-IgG - All Groups (LBN: 098 pg 199 -206)			
Formulation - pH 7.4 - 7.6			
Formulation content	**0.9g/L NaCl + 0.05% PS80 (v/v)**		
Volume	10 mL		
Concentration (A280)	50 (±1) g/L		
Protein content (total)	500 (±10mg) mg		
Purity (HPSEC) %	96.2		
Appearance	slightly creamy (slightly obelasant under dark background)		
Stability study *against particles, fibres and colour change*			
Time Point	37°C	RoomT	4 - 8°C
0	Clear	Clear	Clear
72 h	Clear	Clear	Clear
7 days	Clear	Clear	Clear
2 Weeks	Clear	Clear	Clear
3 Weeks	Clear	Clear	Clear
4 Weeks	Clear	Clear	Clear
5 Weeks	Clear	Clear	Clear
6 Weeks	Clear	Clear	Clear
7 Weeks	Clear	Clear	Clear
8 Weeks	Clear	Clear	Clear
9 Weeks	Clear	Clear	Clear
10 Weeks	Clear	Clear	Clear
11 Weeks	Clear	Clear	Clear
12 Weeks	Clear	Clear	Clear
13 Weeks	Clear	Clear	Clear
14 Weeks	Clear	Clear	Clear
15 Weeks	Clear	Clear	Clear
16 Weeks	Clear	Clear	Clear
17 Weeks	Clear	Clear	Clear
18 Weeks	Clear	Clear	Clear
19 Weeks	Clear	Clear	Clear
20 Weeks	Clear	Clear	Clear
21 Weeks	Clear	Clear	Clear
22 Weeks	Clear	Clear	Clear
23 Weeks: 23 Feb 2021	Co-assessed by ELE		
24 Weeks	Clear	Clear	Clear
25 Weeks	Clear	Clear	Clear
26 Weeks	Clear	Clear	Clear
27 Weeks	Clear	Clear	Clear
28 Weeks	Clear	Clear	Clear
29 Weeks	Clear	Clear	Clear
30 Weeks	Clear	Clear	Clear
31 Weeks	Clear	Clear	Clear
32 Weeks 26 Apr 2021	Clear	Clear	Clear
terminated @ 8 months - Co-assessed by MA			

EXP150421-F(ab')2- All Groups (LBN: 127 pg 112-130)		
FormulationPS80 - pH 7.4 - 7.6		
Formulation content	**0.9g/L NaCl + 0.05% PS80 (v/v)**	
Volume	10 mL	
Concentration (A280)	50 (±1) g/L	
Protein content (total)	500 (±10) mg	
Purity (HPSEC) %	96.8	
Appearance	slightly creamy (slightly obelasant under dark background)	
Stability study *against particles, fibres and colour change*		
Time Point	37°C	4 - 8°C
0 22 Apr 2021	Clear	Clear
72 h	Clear	Clear
7 days	Clear	Clear
2 Weeks	Clear	Clear
3 Weeks	Clear	Clear
4 Weeks	Clear	Clear
5 Weeks	Clear	Clear
6 Weeks: 03 Jun 2021	Co-assessed by NW	
7 Weeks	Clear	Clear
8 Weeks	Clear	Clear
9 Weeks	Clear	Clear
10 Weeks	Clear	Clear
11 Weeks	Clear	Clear
12 Weeks	Clear	Clear
13 Weeks	Clear	Clear
14 Weeks	Clear	Clear
15 Weeks	Clear	Clear
16 Weeks	Clear	Clear
17 Weeks	Clear	Clear
18 Weeks	Clear	Clear
19 Weeks	Clear	Clear
20 Weeks	Clear	Clear
21 Weeks	Clear	Clear
22 Weeks	Clear	Clear
23 Weeks:	Clear	Clear
24 Weeks	Clear	Clear
25 Weeks 27 Oct 2021	Co-assessed by MD	
26 Weeks	Clear	Clear
27 Weeks	Clear	Clear
28 Weeks	Clear	Clear
29 Weeks	Clear	Clear
30 Weeks	Clear	Clear
31 Weeks	Clear	Clear
32 Weeks 21 Dec 2021	Clear	Clear
terminated @ 8 months - Co-assessed by RD		

Appendix III: ELISA for quantifying binding activities of equine IgG subclasses

Appendix III(A): preparations of standards used for the ELISA binding assay

ELISA- Preparations of Standards				
	µg/mL	mg/mL	Sample(µL)	PBST(µL)
Std #1	125	0.125	62.5	3437.5
Std #2	7.813	0.007813	312.5	4687.5
Std #3	1.953	0.001953	1249.8	3750.2
Std #4	0.781	0.0007812	2000.0	3000.0
Std #5	0.312	0.00031248	2000.0	3000.0
Std #6	0.125	0.00012499	2000.0	3000.0
Std #7	0.01	0.00001	400.0	4600.0
Std #8	0.0008	0.0000008	400.0	4600.0

Appendix III(B): Standard curve used for interpolating unknown samples from ELISA binding assay

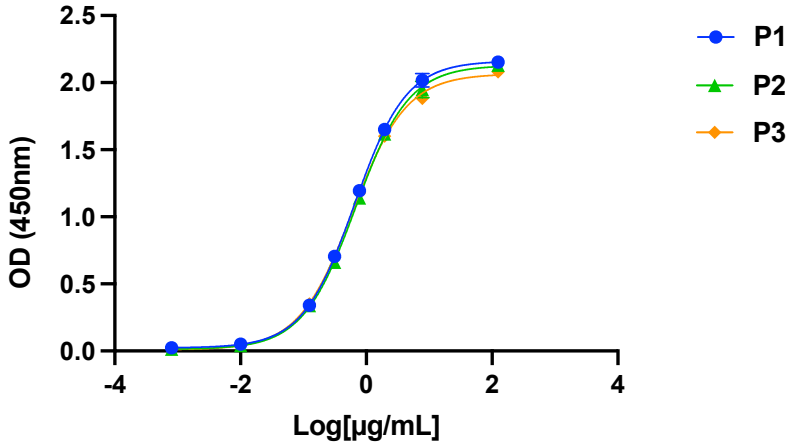

	P1	P2	P3
Goodness of Fit			
Degrees of Freedom	20	20	20
R squared	0.9990	0.9990	0.9989
Sum of Squares	0.01572	0.01567	0.01555
Sy.x	0.02804	0.02799	0.02788

Appendix III(C): relative binding activity for IgG subclasses against individual venoms

		IgG(T)-depleted Samples								
IgG(T)-depleted Samples		EXP1-181120			EXP2-191120			EXP3-241120		
		Rep1	Rep2	Rep3	Rep1	Rep2	Rep3	Rep1	Rep2	Rep3
	N. haje	47.80985	46.40372	44.64973	48.16321	41.71966	40.17595	40.5592	35.58509	36.73427
	N. melanoleuca	60.35027	57.16405	57.91419	50.77069	50.3759	46.97242	44.53068	42.6367	43.99852
	N. nigricollis	74.51029	74.93145	75.39121	64.96512	62.15969	62.04305	62.70948	53.05022	59.16557
IgG(T)-Enriched Samples		EXP1-181120			EXP2-191120			EXP3-241120		
		Rep1	Rep2	Rep3	Rep1	Rep2	Rep3	Rep1	Rep2	Rep3
	N. haje	30.75703	29.29279	26.11177	29.8309	25.24912	24.32768	31.45206	30.25357	28.75602
	N. melanoleuca	28.66067	23.25932	26.81172	25.29816	24.40695	22.19195	28.99892	24.58982	25.07734
	N. nigricollis	31.04029	30.21576	29.56399	27.60035	23.41823	25.14741	40.76062	27.31073	36.03884
Total IgG (TIgG) samples		EXP1-181120			EXP2-191120			EXP3-241120		
		Rep1	Rep2	Rep3	Rep1	Rep2	Rep3	Rep1	Rep2	Rep3
	N. haje	37.19255	37.03171	32.51746	35.89139	31.3836	30.87877	31.41931	27.44816	29.76824
	N. melanoleuca	38.63841	36.36316	38.63015	33.62482	33.89395	31.61103	29.06011	25.69666	29.10777
	N. nigricollis	47.76324	46.29401	44.69447	39.02969	37.91701	38.14772	44.44823	29.76247	39.86351
IgG(T)-depleted Samples										
		EXP1-141120			EXP2-151120			EXP3-161120		
		Rep1	Rep2	Rep3	Rep1	Rep2	Rep3	Rep1	Rep2	Rep3
	E. leucogaster	37.70329	42.06616	40.94095	63.5407	61.70601	70.87833	54.07657	53.05595	53.97362
	E. ocellatus	40.10083	42.23897	47.76419	66.07682	61.68988	60.37548	58.13462	54.79375	54.79375
IgG(T)-Enriched Samples		EXP1-141120			EXP2-151120			EXP3-161120		
		Rep1	Rep2	Rep3	Rep1	Rep2	Rep3	Rep1	Rep2	Rep3
	E. leucogaster	15.03472	17.91605	17.08226	17.99495	17.39956	20.26933	22.75018	20.84261	20.61554
	E. ocellatus	20.94759	17.93781	19.34772	27.15069	18.65709	20.04331	27.98954	26.99516	26.99516
Total IgG (TIgG) samples		EXP1-141120			EXP2-151120			EXP3-161120		
		Rep1	Rep2	Rep3	Rep1	Rep2	Rep3	Rep1	Rep2	Rep3
	E. leucogaster	17.84005	20.5781	20.80504	20.24557	20.78494	21.67362	34.1032	32.51456	33.75213
	E. ocellatus	23.19961	20.8741	21.92161	25.8196	18.15653	18.48696	42.36201	40.0761	40.0761

Appendix III(D): Data for the relative binding activity for the different antivenom samples against snake venoms from the Echis and Naja species

ELISA: average OD values from 3 biological of 3x technical assays

ELISA OD *against Echis* spp.					
AV concentration (µg/mL)		TigG AV	IgG(T)-Enriched AV	IgG(T)-depleted AV	Neg Ctrl Sample
		2.43494444	2.25416667	2.45794444	0.18083333
31.25		2.32672222	2.0655	2.37955556	0.078
7.8125		2.1505	1.83861111	2.23016667	0.042
1.953125		1.66483333	1.38788889	1.7735	0.03166667
0.48828125		0.90622222	0.73811111	1.03922222	0.02744444
0.122070313		0.34627778	0.28105556	0.42305556	0.02544444
0.030517578		0.11688889	0.09766667	0.14777778	0.02561111
0.007629395		0.05027778	0.04283333	0.05538889	0.02316667
0.001907349		0.03277778	0.02855556	0.03005556	0.02355556
0.000476837		0.0265	0.02572222	0.02477778	0.02266667
0.000119209		0.02594444	0.02544444	0.02327778	0.02238889
0.0000298		0.02422222	0.02555556	0.02366667	0.02322222

ELISA OD against *Naja* spp.					
AV concentration (µg/mL)		TigG AV	IgG(T)-Enriched AV	IgG(T)-depleted AV	Neg Ctrl Sample
		2.549444444	2.343777778	2.761166667	0.239055556
31.25		2.417388889	2.106833333	2.609277778	0.088888889
7.8125		2.1115	1.721333333	2.165277778	0.054833333
1.953125		1.409333333	1.078555556	1.326444444	0.034055556
0.48828125		0.628055556	0.456	0.577722222	0.032944444
0.122070313		0.211277778	0.154944444	0.194	0.028944444
0.030517578		0.077333333	0.061611111	0.071444444	0.028777778
0.007629395		0.040111111	0.036111111	0.038666667	0.030277778
0.001907349		0.030444444	0.029277778	0.029666667	0.029722222
0.000476837		0.028277778	0.027444444	0.028722222	0.028
0.000119209		0.028333333	0.027444444	0.026888889	0.028611111
0.0000298		0.030277778	0.032111111	0.034277778	0.029944444

Appendix IV: Data generated from the *Galleria mellonella* study

Appendix IV(A): Range-finding experiment for G. mellonella model

Waxmoth Experiment-19/05/2021-Group1 (EXP190521-G1)

EXP190521-G1 -5 insects of each subgroup

	venom conc. (µg/mL)	Dose (µg) /larvae	Time 1h	Time 24 h	Time 48 h	Time 72 h may not be needed
Control	PBS	0	Alive with less movement, pale,	All alive with excellent movement, pale	2 died (dark) 3 alive (pale)	3 died (dark), 2 alive (pale+ some movement)
B. arietnas	1	5	3 died, darkened, 2 limited movement	all died and dark	all died and dark	all died (dark)
	0.2	1	Alive with less movement, pale,	2 died (dark) and 2 alive (dark) and 1 alive (pale)	2 died (dark), 2 alive (dark) and 1 alive (pale)	3 died (dark), 2alive (1 black+1plae +some mov't
	0.04	0.2	Alive with less movement, pale,	only one died, all pale	2 died (dark), 3 alive (pale)	2 died (dark), 3 alive (pale + full movement)
D. polylepis	2	10	Alive with less movement, pale,	all alive, all pale with limited movement	1 died (dark), 4 alive (pale)	1 died + 1 dying (black), 3 alive (pale+little mov't)
	0.4	2	Alive with less movement, pale,	all alive, all pale with good movement	All alive (pale)	all alive, pale + full movement
	0.08	0.4	Alive with less movement, pale,	All alive, all pale, with excellent movement	2 died (dark), 3 alive (pale)	2 died(dark), 3 alive + pale + little movement
E. ocellatus	1	5	Alive with less movement, pale,	all died, 3 pale, 2 dark	All died (discoloured)	all died (dark)
	0.2	1	Alive with less movement, pale,	all alive, all pale with limited movement	1 died (dark) 4 alive (pale)	1 died (dark), 4 alive (pale)+ full movemnt
	0.04	0.2	Alive with less movement, pale,	All alive, all pale, with excellent movement	2 died (dark), 3 alive (pale)	2 died (dark), 3 alive (pale)+full movement
N. nigricollis	1	5	Alive with slow movement, pale,	all dead, 1 dark, 4 pale	All died (dark)	all died (dark)
	0.2	1	Alive with less movement, pale,	all dead, discoulring	All died (discoloured)	all died (dark)
	0.04	0.2	Alive with less movement, pale,	1 died, 4 with no or very limited movement (pale)	3 died (dark), 2 alive (pale)	4 died (dark), 1 alive (pale)+little movement

Appendix IV(B): Mortality of G. mellonella larvae injected with snake venoms

	Mortality in group *Bitis arietans*				**Average**
Venom toxins		Number of larvae died (n=10)			
µg/µL	µg/ larvae	EXP020721	EXP170721	EXP090721	
0.8	40	9	10	10	10
0.6	30	7	8	9	8
0.5	25	8	7	8	8
0.4	20	6	6	7	6
0.3	15	2	5	5	4
0.2	10	2	4	2	3
0.1	5	1	0	1	1
0.05	2.5	1	0	0	0
DPBS	0	0	0	0	0

	Mortality in group *Bitis gabonica*				**Average**
Venom toxins		Number of larvae died (n=10)			
µg/µL	µg/ larvae	EXP090721	EXP140721	EXP160721	
2.5	125	10	10	10	10
2	100	10	8	10	9
1.5	75	4	9	7	7
1	50	3	3	4	3
0.5	25	1	4	1	2
0.2	10	0	2	2	1
0.1	5	0	0	1	0
DPBS	0	0	0	0	0

	Mortality in group *E. leucogaster*				**Average**
Venom toxins		Number of larvae died (n=10)			
µg/µL	µg/ larvae	EXP090721	EXP140721	EXP160721	
1	50	10	10	10	10
0.5	25	10	10	10	10
0.4	20	9	10	9	9
0.3	15	9	8	4	7
0.2	10	2	7	4	4
0.1	5	1	6	3	3
0.05	2.5	0	2	1	1
DPBS	0	0	0	0	0

	Mortality in group *E. ocellatus*				**Average**
Venom toxins		Number of larvae died (n=10)			
µg/µL	µg/ larvae	EXP090721	EXP140721	EXP160721	
1	50	10	9	10	10
0.5	25	8	6	10	8
0.4	20	10	6	9	8
0.3	15	4	3	3	3
0.2	10	3	2	5	3
0.1	5	0	1	6	2
0.05	2.5	0	1	1	1
DPBS	0	0	0	0	0

	Mortality in group for *N. haje*				**Average**
Venom toxins		Number of larvae died (n=10)			
µg/µL	µg/ larvae	EXP020921	EXP030921	EXP080921	
1	50	10	10	10	10
0.6	30	10	10	10	10
0.5	25	8	10	10	9
0.4	20	5	8	10	8
0.3	15	3	7	9	6
0.2	10	4	1	3	3
0.1	5	6	0	1	2
DPBS	0	0	0	0	0

	Mortality in group *N. melanoleuca*				**Average**
Venom toxins		Number of larvae died (n=10)			
µg/µL	µg/ larvae	EXP020921	EXP030921	EXP080921	
0.5	25	10	10	10	10
0.2	10	6	10	10	9
0.15	7.5	2	10	10	7
0.1	5	6	3	8	6
0.05	2.5	1	0	6	2
0.02	1	0	0	3	1
0.002	0.1	2	0	0	1
DPBS	0	0	0	0	0

	Mortality in group *N. nigricollis*				**Average**
Venom toxins		Number of larvae died (n=10)			
µg/µL	µg/larvae	EXP020721	EXP070721	EXP090721	
0.1	5	10	10	10	10
0.08	4	8	9	10	9
0.06	3	7	10	10	9
0.04	2	5	5	5	5
0.02	1	1	0	5	2
0.01	0.5	1	0	3	1
DPBS	0	0	0	0	0

Summary of LD_{50} which determined for each replicate (individually) is shown on the following table

Snake species	**Lethality of snake venoms on Larvae**		
B. arietans	EXP020721	EXP170721	EXP090721
LD_{50}	16.84	15.358	14.284
B. gabonica	EXP090721	EXP140721	EXP160721
LD_{50}	60.009	35.767	36.402
E. leucogaster	EXP090721	EXP140721	EXP160721
LD_{50}	10.818	5.012	9.58
E. ocellatus	EXP090721	EXP140721	EXP160721
LD_{50}	13.9	18.319	7.861
N. haje	EXP020921	EXP030921	EXP080921
LD_{50}	9.409	13.96	9.964
N. melanoleuca	EXP020921	EXP030921	EXP080921
LD_{50}	7.262	5.098	1.79
N. nigricollis	EXP020721	EXP070721	EXP090721
LD_{50}	1.903	2.009	0.992

Appendix IV(C): Survival of G. mellonella larvae treated with antivenoms

Number of larvae survived after treating with V: AV mixtures (against *Bitis arietans* at a challenge does of 30.1 µg/ Larvae)				
Quantity of AV (mixed with 30.1 µg venom)	EXP210921	EXP240921	EXP250921	**Average**
1000 µg	7	6	5	**6**
250 µg	5	4	2	**4**
62.5 µg	0	7	1	**3**
15.6 µg	3	2	1	**2**
3.9 µg	1	1	0	**1**
1.0 µg	0	2	0	**1**
Venom only (30.1 ug)	1	2	0	**1**
AV only (1000µg)	10	9	10	**10**

Number of larvae survived after treating with V: AV mixtures (against *Echis leucogaster* at a challenge does of 33.7 µg/ Larvae)				
Quantity of AV (mixed with 33.7 µg venom)	EXP020921	EXP170921	EXP220921	**Average**
1000 µg	10	10	9	10
250 µg	9	9	6	8
62.5 µg	2	4	2	3
15.6 µg	4	4	1	3
3.9 µg	1	1	0	1
1.0 µg	0	0	0	**0**
Venom only (33.7 µg)	0	1	0	**0**
AV only (1000 µg)	10	10	9	**10**

Number of larvae survived after treating with V: AV mixtures (against *Echis ocellatus* at a challenge does of 38.1 µg/ Larvae)				
Quantity of AV (mixed with 38.1 µg venom)	EXP170921	EXP220921	EXP250921	**Average**
1000 µg	10	9	9	**9**
250 µg	9	9	9	**9**
62.5 µg	3	6	2	**4**
15.6 µg	4	4	3	**4**
3.9 µg	2	3	2	**2**
1.0 µg	0	2	0	**1**
Venom only (38.1 µg)	1	0	0	**0**
AV only (1000 µg)	10	9	10	**10**

Number of larvae survived after treating with V: AV mixtures (against *Naja nigricollis* at a challenge does of 1.6 µg/ Larvae)				
Quantity of AV (mixed with 4.8 µg venom)	EXP170921	EXP220921	EXP250921	**Average**
1000 µg	10	6	9	8
250 µg	6	2	8	5
62.5 µg	1	0	3	1
15.6 µg	1	0	1	1
3.9 µg	0	0	1	0
1.0 µg	0	0	0	0
Venom only (4.8 µg)	0	0	0	**0**
AV only (1000µg)	10	9	10	**10**

Number of larvae survived after treating with V: AV mixtures (against *B. gabonica* at a challenge does of 137.7 µg/ Larvae)	
Quantity of AV (mixed with 137.7 µg venom)	EXP210921
1000 µg	10
250 µg	7
62.5 µg	4
15.6 µg	2
3.9 µg	1
1.0 µg	1
Venom only (137.7 µg)	**0**
AV only (1000µg)	**10**

Number of larvae survived after treating with V: AV mixtures (against *Naja melanoleuca* at a challenge does of 8 µg/ Larvae)	
Quantity of AV (mixed with 8 µg venom)	EXP220921
1000 µg	10
250 µg	8
62.5 µg	2
15.6 µg	1
3.9 µg	0
1.0 µg	2
Venom only (8 µg)	0
AV only (1000µg)	9

Appendix IV(D): Estimations of ED_{50} and Potency for the $F(ab')_2$ AV against the different snake species

The following data shows calculations for ED_{50} in units of µL per larvae (µL /larvae) with confidence interval, ED_{50} in mg of venom per mL of antivenom (mg/mL), µL of antivenom per mg of venom and "Potency" mg of venom completely neutralised by 1 mL of antivenom (mg/mL). Challenge doses are in µg per larvae. ED_{50} was obtained from Probits using SPSS software.

Snake species	LD_{50} (µg/ larvae)	LD_{50}s used (n)	n-1	Challenge dose (µg)	ED_{50} (µL/ larvae; 95% CI)	ED_{50} (mg/mL)	ED_{50} (µL/mg)	Potency (mg/mL)
B. arietans	15.0	2.0	1.0	30.1	10.4 (2.13 - 2613.4)	2.9	347.1	0.2
E. leucogaster	8.4	4.0	3.0	33.7	1.2 (0.6 - 2.8)	27.9	35.8	1.1
E. ocellatus	12.7	3.0	2.0	38.1	0.7 (0.3 - 2.1)	53.4	18.7	2.1
N. nigricollis	1.6	3.0	2.0	4.8	5.4 (2.5 - 16.4)	0.9	1121.5	0.3

The neutralisation efficacies presented here are derived from the average of the number of larvae survived in the triplicates.

$$\text{Conversion to mg /mL} = \frac{\text{challenge dose } (\mu g)}{\text{ED}_{50}(\frac{\mu L}{mouse})}$$

$$\text{Conversion to µL /larvae} = [\frac{1}{\text{ED}_{50}(\frac{mg}{mL})}]x1000$$

$$\text{Potency (P)} = \frac{(\text{n} - 1)x\text{LD}_{50}}{\text{ED}_{50}(\frac{\text{mg}}{\text{mL}})}$$

The concentration of the Polyvalent $F(ab')_2$ antivenom is 50 g/L

Potency (mg/mL) for each repeat was determined separately as follows:

Snake species	Experiment Replicates	LD_{50} (µg)	Challenge dose (µg)	n-1	(n-1)xLD_{50} (µg)	ED_{50} (µL/ larvae)	LD_{50} (µg)	LD_{50} (µg)
B. arietans	EXP210921	15.0	30.1	1.0	15.0	6.9	4.3	0.3
B. arietans	EXP240921	15.0	30.1	1.0	15.0	4.2	7.1	0.5
B. arietans	EXP250921	15.0	30.1	1.0	15.0	26.3	1.1	0.1
E. leucogaster	EXP170921	8.4	33.7	3.0	25.3	0.8	41.9	1.7
E. leucogaster	EXP220921	8.4	33.7	3.0	25.3	3.3	10.1	0.4
E. leucogaster	EXP020921	8.4	33.7	3.0	25.3	1.0	32.5	1.3
E. ocellatus	EXP170921	12.7	38.1	2.0	25.4	0.8	48.0	1.9
E. ocellatus	EXP220921	12.7	38.1	2.0	25.4	0.4	101.6	4.0
E. ocellatus	EXP250921	12.7	38.1	2.0	25.4	0.4	101.6	4.0
N. nigricollis	EXP170921	1.6	4.8	2.0	3.2	3.1	1.5	0.5
N. nigricollis	EXP220921	1.6	4.8	2.0	3.2	14.4	0.3	0.1
N. nigricollis	EXP250921	1.6	4.8	2.0	3.2	1.9	2.5	0.8

Appendix IV(E): Potency for B. gabonica & N. melanoleuca (determined from single experiment)

Snake species	LD_{50} (µg/ larvae)	LD_{50}s used (n)	n-1	Challenge dose (µg)	ED_{50} (µL/ larvae; 95% CI)	ED_{50} (mg/mL)	ED_{50} (µL/mg)	Potency (mg/mL)
B. gabonica	45.9	3.0	2.0	137.7	2.3 (0.5 - 3.5)	59.9	16.7	1.5
N. melanoleuca	3.2	2.5	1.5	8.0	2.1 *	5.1	195.0	0.9

*The test for *N. melanoleuca* failed to generate 95% CI. This is just a preliminary data collected from single experiment

Appendix V: Data from cells viability assay

Appendix V(A): Venom concentrations and pre-normalise Cytotoxicity data

		2.5-Folds dilution-Non-normalised data										
	Venom [µg/mL]	500	200	80	32	12.8	5.12	2.048	0.8192	0.32768	0.13107	0.13107
B. arietans		1.58303	2.52216	2.77265	4.17007	28.5818	81.77	94.1466	95.9243	90.7561	89.9495	86.9892
		0.95731	1.67677	1.69467	1.92781	4.40098	80.2896	107.382	113.153	102.078	109.774	96.4421
		1.6412	4.2843	3.94716	5.4714	34.2194	87.5557	101.846	108.316	95.0573	98.9939	96.7061
	Average	**1.39385**	**2.82774**	**2.80483**	**3.85643**	**22.4007**	**83.2051**	**101.125**	**105.798**	**95.9637**	**99.5726**	**93.3791**
B. gabonica		-0.92681	-0.85928	-1.33108	-1.29487	21.495	57.2898	69.2111	80.11	86.3371	96.1223	86.707
		5.44938	6.32493	9.08819	17.0665	46.1011	65.7583	76.0635	82.7977	90.5643	94.5296	98.528
		-6.50779	-4.37093	-1.53585	5.76004	39.2908	54.1604	67.9477	67.8692	71.1213	82.0484	84.0013
	Average	**-0.66174**	**0.36491**	**2.07375**	**7.17723**	**35.6289**	**59.0695**	**71.0741**	**76.9256**	**82.6742**	**90.9001**	**89.7454**
		2.5-Folds dilution-Non-normalised data										
	Venom [µg/mL]	**250**	**100**	**40**	**16**	**6.4**	**2.56**	**1.024**	**0.4096**	**0.16384**	**0.065536**	**0.0262144**
E. leucogaster	EXP170321	-7.82171	-0.25764	3.16551	11.1121	25.9195	44.9127	69.0568	74.8553	75.7476	80.373	81.5147
	EXP010421	10.4203	14.8357	14.9814	18.2814	68.1059	78.3022	81.5816	86.3665	81.101	86.5798	86.0689
	EXP1504321	-2.92619	0.72205	5.90451	15.212	29.8439	58.2928	88.7748	96.9337	89.182	95.5223	89.9034
	Average	**-0.109191**	**5.100021**	**8.017129**	**14.8685**	**41.28976**	**60.50259**	**79.80441**	**86.05184**	**82.0102**	**87.49169**	**85.829**
E. ocellatus	EXP170321	-7.33864	-4.4192	-2.94729	4.29947	34.0003	52.2964	57.1831	67.7584	71.2492	83.2888	84.1064
	EXP010421	5.12515	8.22096	7.99082	7.66472	51.4456	68.9638	80.6982	60.56	62.4885	72.8755	72.0002
	EXP1504321	-3.76869	0.73317	4.15662	14.0564	33.13	43.6733	50.8962	84.6128	84.5239	95.4784	92.5191
	Average	**-1.99406**	**1.511642**	**3.066717**	**8.673513**	**39.52533**	**54.97783**	**62.92586**	**70.97703**	**72.75386**	**83.88089**	**82.87521**

	2-Folds dilution-non-normalised data									
	venom [µg/mL]	125	62.5	31.25	15.625	7.8125	3.9063	1.9531	0.9766	0.9766
N. haje	EXP070821	9.394741	11.00857	23.45565	60.24868	135.6481	156.3549	171.4877	173.6344	140.2086
	EXP150821	10.3837	11.30149	9.925727	10.36762	50.22705	144.2272	177.2864	169.914	93.48049
	EXP280721	17.34413	17.89993	26.29212	61.98314	149.9206	154.1559	161.9203	140.4231	127.382
	Average	**12.37419**	**13.40333**	**19.89116**	**44.19981**	**111.9319**	**151.5793**	**170.2315**	**161.3238**	**120.357**
N. melanoleuca	EXP070821	8.906247	10.05957	19.04735	46.32784	127.7394	186.5065	177.3647	173.6132	142.4585
	EXP150821	10.21007	10.97926	10.48759	10.06639	16.15028	135.7013	180.8169	168.7425	101.37
	EXP280721	14.10303	14.25985	19.47685	41.90821	126.6935	148.6256	153.9389	153.1414	155.4031
	Average	**11.07312**	**11.76622**	**16.33726**	**32.76748**	**90.1944**	**156.9445**	**170.7068**	**165.1657**	**133.0772**
	venom [µg/mL]	125	62.5	31.25	15.625	7.8125	3.9063	1.9531	0.9766	0.9766	**0.4883**
N. nigricollis	EXP070821	19.5269	25.09553	29.74117	55.1126	104.8815	125.5594	126.1065	151.2817	106.1246	78.1279
	EXP150821	10.39151	10.93323	16.90132	29.82367	66.657	114.7578	126.5199	121.3427	96.80688	69.9829
	EXP280721	20.32455	23.45222	23.39909	31.99635	70.95983	95.62048	114.4355	120.8135	127.3934	96.7198
	Average	**16.74765**	**19.82699**	**23.34719**	**38.97754**	**80.83277**	**111.9792**	**122.354**	**131.146**	**110.1083**	**81.61016**

The following data show dose-dependent inhibition of Vero cells treated with different snake venom concentrations. Data was derived from mean of three technical, 3 biological experiments (N=3& n=3).

Snake species	Cytotoxicity of snake venoms on Larvae		
B. arietans	EXP050621	EXP290521	EXP150521
IC_{50}	9.648	9.779	15.2
B. gabonica	EXP050621	EXP290521	EXP150521
IC_{50}	6.714	9.721	12.06
E. leucogaster	EXP170321	EXP080421	EXP150421
IC_{50}	3.887	8.715	3.911
E. ocellatus	EXP170321	EXP080421	EXP150421
IC_{50}	4.708	7.44	2.217
N. haje	EXP0708421	EXP150821	EXP280821
IC_{50}	12.74	6.924	15
N. melanoleuca	EXP0708421	EXP150821	EXP280821
IC_{50}	10.86	5.166	11.03
N. nigricollis	EXP0108421	EXP150821	EXP280821
IC_{50}	12.52	8.415	6.934

Appendix V(B): Neutralisation efficacy of antivenom against cytotoxicity by Echis species.

The efficacy of a polyspecific F(ab')$_2$ AV on inhibiting the toxic activities of *E. leucogaster* & *E. ocellatus* to Vero cells. Different AV concentrations (1000 µg/mL – 7.8 µg/mL) were used against a challenge dose of 26.5 and 26 µg/mL of *E. leucogaster* & *E. ocellatus,* respectively.

Averages from two biologically independent experiments, composing 3 technichal replicates								
F(ab')2 AV [µg/mL]	1000	500	250	125	62.5	31.25	15.625	7.8125
E. ocellatus	86.37184283	80.09385457	67.0005282	31.399813	14.9709469	8.64678294	5.25369729	2.307756719
	88.67409591	57.48394665	27.3974726	12.2624939	13.6720452	8.59992448	7.31264751	0.430615504
E. leucogaster	106.2457225	92.6654859	90.6760422	65.7052382	13.2000743	8.50661726	5.99165494	-2.4906587
	114.5991294	97.76137062	77.1643645	63.7667203	26.5735921	19.1061095	7.98430591	-1.00583884
Averages								
Echis leucogaster	87.52296937	68.78890061	47.1990004	21.8311534	14.3214961	8.62335371	6.2831724	1.369186111
Echis ocellatus	97.45990921	75.07471628	59.0367574	38.983866	13.4360598	8.55327087	6.65215122	-1.0300216
	Challenge dose	*E. leucogaster*	5xLD$_{50}$	26.5 µg/mL				
		E. ocellatus	5xLD$_{50}$	26 µg/mL				
Apart from the controls, cells were treated with snake venom (at the specified challenge dose) and AV (at the stated concentration)								
Negative control - challenge dose (28.5 and 16.5 µg/mL for *Echis leucogaster & Echis ocellatus, respectively*)								
Positive control-AV only (1000 µg/mL)								

Appendix VI: Assessment of antivenom potency using Vero cells

An immunocytotoxicity assay using a Vero cell line was used to determine the venom neutralising capacity of antivenom. This is expressed as EC_{50} of antivenom which requires to inhibit 50% of the cytotoxicity induced by each snake venom. Considering the murine assay, $5xIC_{50}$ of venom was used as a 'challenge dose' and preincubated with differing amounts of antivenom [see Appendix V(B) above]. The antivenom demonstrated a better neutralisation of cytotoxicity induced by *E. ocellatus* venom compared to that by *E. leucogaster* venom, the difference was not statistically significant (Figure VI). However, these observations lack the support of biologically independent replicates. Morphological analysis of cells demonstrated that the antivenom effectively prevented disruption of venom-induced monolayer integrity (images not shown).

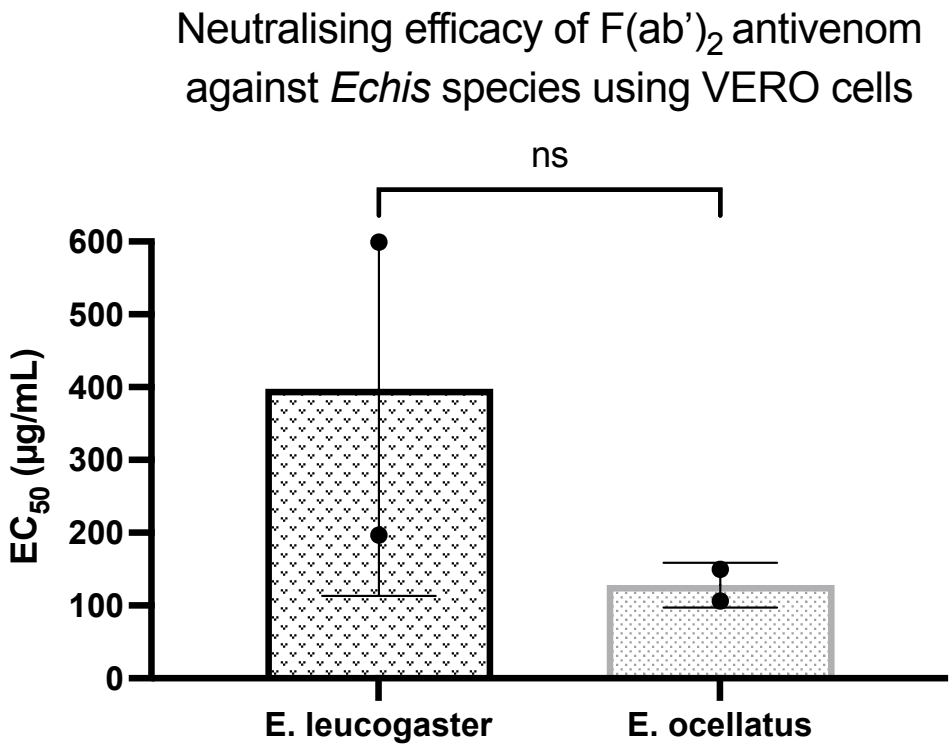

Figure VII. Neutralising efficacy of AV against cytotoxicity caused by Echis species.

Unpaired *t-test* with Welch's correction was used to determine statistical significance and pairwise statistical comparisons are shown by asterisks. Error bars represent mean ±SD of two biologically independent experiments composing 3 technical replicates. Cell viability was determined by CellTiter-Blue assay and normalised to the cells treated only with venom (considered 100% of cytotoxicity).

Abbreviations: EC_{50}, half-maximal effective concentration; AV, antivenom; ns, not significant.

Appendix VII: Details of published manuscript

Mender, M. M., Bolton, F., Berry, C. and Young, M. 2021. Antivenom: An immunotherapy for the treatment of snakebite envenoming in sub-Saharan Africa. *Advances in protein chemistry and structural biology* 129, pp. 435-477.

Chapter 8: References

Abubakar, I. S. et al. 2010a. Randomised controlled double-blind non-inferiority trial of two antivenoms for saw-scaled or carpet viper (Echis ocellatus) envenoming in Nigeria. *PLoS Neglected Tropical Diseases* 4(7), p. e767. doi: 10.1371/journal.pntd.0000767

Abubakar, S. et al. 2010b. Pre-clinical and preliminary dose-finding and safety studies to identify candidate antivenoms for treatment of envenoming by saw-scaled or carpet vipers (Echis ocellatus) in northern Nigeria. *Toxicon* 55(4), pp. 719-723. doi: 10.1016/j.toxicon.2009.10.024.

Ainsworth, S., Menzies, S. K., Casewell, N. R. and Harrison, R. A. 2020. An analysis of preclinical efficacy testing of antivenoms for sub-Saharan Africa: Inadequate independent scrutiny and poor-quality reporting are barriers to improving snakebite treatment and management. *PLoS Neglected Tropical Diseases* 14(8), p. e0008579. doi: 10.1371/journal.pntd.0008579

Ainsworth, S. et al. 2018. The medical threat of mamba envenoming in sub-Saharan Africa revealed by genus-wide analysis of venom composition, toxicity and antivenomics profiling of available antivenoms. *Journal of Proteomics* 172, pp. 173-189. doi: 10.1016/j.jprot.2017.08.016

Aird, S. D. 2002. Ophidian envenomation strategies and the role of purines. *Toxicon* 40(4), pp. 335-393. doi: 10.1016/s0041-0101(01)00232-x

Al-Abdulla, I., Casewell, N. R. and Landon, J. 2013. Long-term physicochemical and immunological stability of a liquid formulated intact ovine immunoglobulin-based antivenom. *Toxicon* 64, pp. 38-42. doi: 10.1016/j.toxicon.2012.12.022

Al-Abdulla, I., Casewell, N. R. and Landon, J. 2014. Single-reagent one-step procedures for the purification of ovine IgG, F (ab′) 2 and Fab antivenoms by caprylic acid. *Journal of Immunological Methods* 402(1-2), pp. 15-22. doi: 10.1016/j.jim.2013.11.001

Alape-Girón, A., Miranda-Arrieta, K. and Stiles, B. G. 1997. A comparison of in vitro methods for assessing the potency of therapeutic antisera against the venom of the coral snake Micrurus nigrocinctus. *Toxicon* 35(4), pp. 573-581.

Albulescu, L.-O. et al. 2020. Preclinical validation of a repurposed metal chelator as an early-intervention therapeutic for hemotoxic snakebite. *Science Translational Medicine* 12(542), p. eaay8314.

Alirol, E., Lechevalier, P., Zamatto, F., Chappuis, F., Alcoba, G. and Potet, J. 2015. Antivenoms for snakebite envenoming: what is in the research pipeline?

PLoS Neglected Tropical Diseases 9(9), p. e0003896. doi: 10.1371/journal.pntd.0003896

Alirol, E., Sharma, S. K., Bawaskar, H. S., Kuch, U. and Chappuis, F. 2010. Snake bite in South Asia: a review. *PLoS Neglected Tropical Diseases* 4(1), doi: 10.1371/journal.pntd.0000603

Alshammari, T. M. 2016. Drug safety: the concept, inception and its importance in patients' health. *Saudi Pharmaceutical Journal* 24(4), pp. 405-412. doi: 10.1016/j.jsps.2014.04.008

Alvarenga, L. M., Zahid, M., di Tommaso, A., Juste, M. O., Aubrey, N., Billiald, P. and Muzard, J. 2014. Engineering venom's toxin-neutralizing antibody fragments and its therapeutic potential. *Toxins* 6(8), pp. 2541-2567. doi: 10.3390/toxins6082541

Arlinghaus, F. T. and Eble, J. A. 2012. C-type lectin-like proteins from snake venoms. *Toxicon* 60(4), pp. 512-519. doi: 10.1016/j.toxicon.2012.03.001

Awate, S., Babiuk, L. A. B. and Mutwiri, G. 2013. Mechanisms of action of adjuvants. *Frontiers in Immunology* 4, p. 114. doi: 10.3389/fimmu.2013.00114

Baldé, M., Chippaux, J.-P., Boiro, M., Stock, R. and Massougbodji, A. 2012. Étude clinique de la tolérance et de l'efficacité d'un sérum anti-ophidien polyvalent F (ab′) 2 pour l' Afrique à Kindia, Guinée. *Bulletin de la Société de Pathologie Exotique* 105(3), pp. 157-161.

Baldé, M. C., Chippaux, J.-P., Boiro, M. Y., Stock, R. P. and Massougbodji, A. 2013. Use of antivenoms for the treatment of envenomation by Elapidae snakes in Guinea, Sub-Saharan Africa. *Journal of Venomous Animals and Toxins Including Tropical Diseases* 19, pp. 1-6.

Barbosa, C., Rodrigues, R., Olortegui, C., Sanchez, E. and Heneine, L. 1995. Determination of the neutralizing potency of horse antivenom against bothropic and crotalic venoms by indirect enzyme immunoassay. *Brazilian Journal of Medical and Biological Research= Revista Brasileira de Pesquisas Medicas e Biologicas* 28(10), pp. 1077-1080.

Barlow, A., Pook, C. E., Harrison, R. A. and Wuster, W. 2009. Coevolution of diet and prey-specific venom activity supports the role of selection in snake venom evolution. *Proceedings: Biological Sciences* 276(1666), pp. 2443-2449. doi: 10.1098/rspb.2009.0048

Benjamin, J. M., Chippaux, J.-P., Sambo, B. T. and Massougbodji, A. 2018. Delayed double reading of whole blood clotting test (WBCT) results at 20 and 30 minutes enhances diagnosis and treatment of viper evenomation. *Journal of Venomous Animals and Toxins Including Tropical Diseases* 24, doi: 10.1186/s40409-018-0151-1

Bocian, A. et al. 2020. Comparison of Methods for Measuring Protein Concentration in Venom Samples. *Animals* 10(3), p. 448. doi: 10.3390/ani10030448

Boels, D., Hamel, J. F., Deguigne, M. B. and Harry, P. 2012. European viper envenomings: Assessment of Viperfav™ and other symptomatic treatments. *Clinical Toxicology* 50(3), pp. 189-196. doi: 10.3109/15563650.2012.660695

Bolton, F. 2017. *Incorporating the 3Rs (Refinement, Replacement and Reduction of animals in research) into the preclinical assessment of snake venom toxicity and antivenom efficacy.* PhD, University of Liverpool.

Bourke, L. A. et al. 2021. Pan-American lancehead Pit-vipers: Coagulotoxic venom effects and antivenom neutralisation of Bothrops Asper and B. atrox geographical variants. *Toxins* 13(2), p. 78. doi: 10.3390/toxins13020078

Boushaba, R., Kumpalume, P. and Slater, N. K. 2003. Kinetics of whole serum and prepurified IgG digestion by pepsin for F (ab') 2 manufacture. *Biotechnology Progress* 19(4), pp. 1176-1182. doi: 10.1021/bp034037+

Bowen, A. and Casadevall, A. 2018. The role of the constant region in antibody-antigen interactions: Redefining the modular model of immunoglobulin structure. In: Chaim Putterman, D.C., Steven Almo ed. *Structural Biology in Immunology*. [no place]: Academic Press, pp. 145-170.

Boyer, L. V., Seifert, S. A. and Cain, J. S. 2001. Recurrence phenomena after immunoglobulin therapy for snake envenomations: Part 2. Guidelines for clinical management with crotaline Fab antivenom. *Annals of Emergency Medicine* 37(2), pp. 196-201. doi: 10.1067/mem.2001.113134

Brezski, R. J. and Jordan, R. E. 2010. Cleavage of IgGs by proteases associated with invasive diseases: an evasion tactic against host immunity? *MAbs* 2(3), pp. 212-220. doi: 10.4161/mabs.2.3.11780

Brown, N. I. 2012. Consequences of neglect: analysis of the sub-Saharan African snake antivenom market and the global context. *PLoS Neglected Tropical Diseases* 6(6), p. e1670. doi: 10.1371/journal.pntd.0001670

Burnouf, T., Griffiths, E., Padilla, A., Seddik, S., Stephano, M. A. and Gutierrez, J. M. 2004. Assessment of the viral safety of antivenoms fractionated from equine plasma. *Biologicals* 32(3), pp. 115-128. doi: 10.1016/j.biologicals.2004.07.001

Burtscher, J., Etter, D., Biggel, M., Schlaepfer, J. and Johler, S. 2021. Further Insights into the Toxicity of Bacillus cytotoxicus Based on Toxin Gene Profiling and Vero Cell Cytotoxicity Assays. *Toxins* 13(4), p. 234.

Bush, S. P. et al. 2015. Comparison of F(ab')2 versus Fab antivenom for pit viper envenomation: a prospective, blinded, multicenter, randomized clinical

trial. *Clinical Toxicology (Philadelphia, Pa.)* 53(1), pp. 37-45. doi: 10.3109/15563650.2014.974263

Butler, J. 1997. Immunoglobulin gene organization and the mechanism of repertoire development. *Scandinavian Journal of Immunology* 45(4), pp. 455-462.

Butler, J., Wertz, N., Deschacht, N. and Kacskovics, I. 2009. Porcine IgG: structure, genetics, and evolution. *Immunogenetics* 61(3), pp. 209-230.

Butler, J. E. 1969. Bovine immunoglobulins: A review. *Journal of Dairy Science* 52(12), pp. 1895-1909.

Calvete, J. J. 2005. Structure-function correlations of snake venom disintegrins. *Current Pharmaceutical Design* 11(7), pp. 829-835. doi: 10.2174/1381612053381783

Calvete, J. J. et al. 2016. Preclinical evaluation of three polyspecific antivenoms against the venom of Echis ocellatus: Neutralization of toxic activities and antivenomics. *Toxicon* 119, pp. 280-288. doi: 10.1016/j.toxicon.2016.06.022

Calvete, J. J. et al. 2010. Antivenomic assessment of the immunological reactivity of EchiTAb-Plus-ICP, an antivenom for the treatment of snakebite envenoming in sub-Saharan Africa. *American Journal of Tropical Medicine and Hygiene* 82(6), pp. 1194-1201. doi: 10.4269/ajtmh.2010.09-0733

Calvete, J. J., Escolano, J. and Sanz, L. 2007. Snake venomics of Bitis species reveals large intragenus venom toxin composition variation: application to taxonomy of congeneric taxa. *Journal of Proteome Research* 6(7), pp. 2732-2745. doi: 10.1021/pr0701714

Calvete, J. J., Marcinkiewicz, C., Monleon, D., Esteve, V., Celda, B., Juarez, P. and Sanz, L. 2005. Snake venom disintegrins: evolution of structure and function. *Toxicon* 45(8), pp. 1063-1074. doi: 10.1016/j.toxicon.2005.02.024

Calvete, J. J., Sanz, L., Pla, D., Lomonte, B. and Gutierrez, J. M. 2014. Omics meets biology: application to the design and preclinical assessment of antivenoms. *Toxins* 6(12), pp. 3388-3405. doi: 10.3390/toxins6123388

Cannon, R., Ruha, A.-M. and Kashani, J. 2008. Acute hypersensitivity reactions associated with administration of crotalidae polyvalent immune Fab antivenom. *Annals of Emergency Medicine* 51(4), pp. 407-411.

Caricati, C. P., Oliveira‐Nascimento, L., Yoshida, J., Stephano, M., Caricati, A. and Raw, I. 2013. Safety of snake antivenom immunoglobulins: efficacy of viral inactivation in a complete downstream process. *Biotechnology Progress* 29(4), pp. 972-979.

Carregari, V. C., Rosa-Fernandes, L., Baldasso, P., Bydlowski, S. P., Marangoni, S., Larsen, M. R. and Palmisano, G. 2018. Snake Venom Extracellular vesicles (SVEVs) reveal wide molecular and functional proteome diversity. *Scientific Reports* 8(1), p. 12067. doi: 10.1038/s41598-018-30578-4

Carrette, T. and Seymour, J. 2006. Cardiotoxic effects of venoms from Chironex fleckeri and Chiropsalmus sp. on an invertebrate model. *Journal of Venomous Animals and Toxins Including Tropical Diseases* 12, pp. 245-254.

Casasola, A., Ramos-Cerrillo, B., de Roodt, A. R., Saucedo, A. C., Chippaux, J.-P., Alagón, A. and Stock, R. P. 2009. Paraspecific neutralization of the venom of African species of cobra by an equine antiserum against Naja melanoleuca: a comparative study. *Toxicon* 53(6), pp. 602-608.

Casewell, N. R. 2012. On the ancestral recruitment of metalloproteinases into the venom of snakes. *Toxicon* 60(4), pp. 449-454. doi: 10.1016/j.toxicon.2012.02.006

Casewell, N. R., Al-Abdulla, I., Smith, D., Coxon, R. and Landon, J. 2014a. Immunological cross-reactivity and neutralisation of European viper venoms with the monospecific Vipera berus antivenom ViperaTAb. *Toxins* 6(8), pp. 2471-2482. doi: 10.3390/toxins6082471

Casewell, N. R., Cook, D. A., Wagstaff, S. C., Nasidi, A., Durfa, N., Wüster, W. and Harrison, R. A. 2010. Pre-clinical assays predict pan-African Echis viper efficacy for a species-specific antivenom. *PLoS Neglected Tropical Diseases* 4(10), p. e851. doi: 10.1371/journal.pntd.0000851

Casewell, N. R., Harrison, R. A., Wuster, W. and Wagstaff, S. C. 2009. Comparative venom gland transcriptome surveys of the saw-scaled vipers (Viperidae: Echis) reveal substantial intra-family gene diversity and novel venom transcripts. *BMC Genomics* 10, p. 564. doi: 10.1186/1471-2164-10-564

Casewell, N. R., Jackson, T. N., Laustsen, A. H. and Sunagar, K. 2020. Causes and consequences of snake venom variation. *Trends in Pharmacological Sciences* 41(8), pp. 570-581. doi: 10.1016/j.tips.2020.05.006

Casewell, N. R., Wagstaff, S. C., Harrison, R. A., Renjifo, C. and Wuster, W. 2011. Domain loss facilitates accelerated evolution and neofunctionalization of duplicate snake venom metalloproteinase toxin genes. *Molecular Biology and Evolution* 28(9), pp. 2637-2649. doi: 10.1093/molbev/msr091

Casewell, N. R. et al. 2014b. Medically important differences in snake venom composition are dictated by distinct postgenomic mechanisms. *Proceedings of the National Academy of Sciences of the United States of America* 111(25), pp. 9205-9210. doi: 10.1073/pnas.1405484111

Chakrabarty, D. a. and Chanda, C. 2017. Snake Venom Disintegrins In: Gopalakrishnakone, P., Inagaki, H., Mukherjee, A., Rahmy, T., Vogel, CW. ed. *Snake Venoms*. Dordrecht: Springer, pp. 437 - 449.

Chippaux, J., Baldé, M., Sessinou, É. and Massougbodji, A. 2015a. Evaluation of a new polyvalent antivenom against snakebite envenomation (Inoserp® Panafricain) in two different epidemiological settings: Northern Benin and Maritime Guinea. *Médecine et Santé Tropicales* 25(1), pp. 56-64. doi: 10.1684/mst.2014.0413

Chippaux, J., Stock, R. and Massougbodji, A. 2015b. Antivenom safety and tolerance for the strategy of snake envenomations management. In: Gopalakrishnakone, P., Inagaki, H., Mukherjee, A., Rahmy, T., Vogel, CW. ed. *Snake Venoms*. Dordrecht: Springer pp. 1-16.

Chippaux, J.-P. 1998. The development and use of immunotherapy in Africa. *Toxicon* 36(11), pp. 1503-1506. doi: 10.1016/s0041-0101(98)00140-8

Chippaux, J.-P. and Goyffon, M. 1998. Venoms, antivenoms and immunotherapy. *Toxicon* 36(6), pp. 823-846.

Chippaux, J.-P. and Habib, A. G. 2015. Antivenom shortage is not circumstantial but structural. *Transactions of the Royal Society of Tropical Medicine and Hygiene* 109(12), pp. 747-748. doi: 10.1093/trstmh/trv088.

Chippaux, J.-P., Massougbodji, A., Stock, R. and Alagon, A. 2007. Clinical trial of an F (ab') 2 polyvalent equine antivenom for African snake bites in Benin. *The American journal of tropical medicine and hygiene* 77(3), pp. 538-546.

Chippaux, J.-P., Stock, R. P. and Massougbodji, A. 2010. Methodology of clinical studies dealing with the treatment of envenomation. *Toxicon* 55(7), pp. 1195-1212.

Chippaux, J. P. 2011. Estimate of the burden of snakebites in sub-Saharan Africa: a meta-analytic approach. *Toxicon* 57(4), pp. 586-599. doi: 10.1016/j.toxicon.2010.12.022

Chippaux, J. P. 2017. Snakebite envenomation turns again into a neglected tropical disease! *Journal of Venomous Animals and Toxins Including Tropical Diseases* 23, p. 38. doi: 10.1186/s40409-017-0127-6

Chippaux, J. P., Williams, V. and White, J. 1991. Snake venom variability: methods of study, results and interpretation. *Toxicon* 29(11), pp. 1279-1303.

Chong, H. P., Tan, K. Y. and Tan, C. H. 2020. Cytotoxicity of Snake Venoms and Cytotoxins From Two Southeast Asian Cobras (Naja sumatrana, Naja kaouthia): Exploration of Anticancer Potential, Selectivity, and Cell Death Mechanism. *Frontiers in molecular biosciences* 7, doi: 0.3389/fmolb.2020.583587

Clark, J. M. 2018. The 3Rs in research: a contemporary approach to replacement, reduction and refinement. *British Journal of Nutrition* 120(s1), pp. S1-S7. doi: 10.1017/S0007114517002227

Clement, H., Corrales-García, L. L., Bolaños, D., Corzo, G. and Villegas, E. 2019. Immunogenic Properties of Recombinant Enzymes from Bothrops ammodytoides towards the Generation of Neutralizing Antibodies against Its Own Venom. *Toxins* 11(12), p. 702.

Conlon, J. M., Attoub, S., Arafat, H., Mechkarska, M., Casewell, N. R., Harrison, R. A. and Calvete, J. J. 2013. Cytotoxic activities of [Ser(4)(9)]phospholipase A(2) from the venom of the saw-scaled vipers Echis ocellatus, Echis pyramidum leakeyi, Echis carinatus sochureki, and Echis coloratus. *Toxicon* 71, pp. 96-104. doi: 10.1016/j.toxicon.2013.05.017

Cook, D. A., Owen, T., Wagstaff, S. C., Kinne, J., Wernery, U. and Harrison, R. A. 2010. Analysis of camelid antibodies for antivenom development: Neutralisation of venom-induced pathology. *Toxicon* 56(3), pp. 373-380.

Cordero, M. et al. 2016. Identifying Insect Protein Receptors Using an Insecticidal Spider Toxin. in: P. Gopalakrishnakone, Gerardo Corzo; Maria Elena de Lima; Elia Diego-García (eds.) Spider venoms, Toxicology. *Springer Science+Business Media, Dordrecht.*, pp. 405-418. doi: 0.1007/978-94-007-6389-0_22

Costa, T. R., Burin, S. M., Menaldo, D. L., de Castro, F. A. and Sampaio, S. V. 2014. Snake venom L-amino acid oxidases: an overview on their antitumor effects. *Journal of Venomous Animals and Toxins Including Tropical Diseases* 20, p. 23. doi: 10.1186/1678-9199-20-23

Cresswell, C., Newcombe, A. R., Davies, S., Macpherson, I., Nelson, P., O'Donovan, K. and Francis, R. 2005. Optimal conditions for the papain digestion of polyclonal ovine IgG for the production of biotherapeutic Fab fragments. *Biotechnology and Applied Biochemistry* 42(2), pp. 163-168.

Cunha, C. W., McGuire, T. C., Kappmeyer, L. S., Hines, S. A., Lopez, A. M., Dellagostin, O. A. and Knowles, D. P. 2006. Development of specific immunoglobulin Ga (IgGa) and IgGb antibodies correlates with control of parasitemia in Babesia equi infection. *Clinical and Vaccine Immunology* 13(2), pp. 297-300.

Currier, R. B., Calvete, J. J., Sanz, L., Harrison, R. A., Rowley, P. D. and Wagstaff, S. C. 2012. Unusual stability of messenger RNA in snake venom reveals gene expression dynamics of venom replenishment. *PloS One* 7(8), p. e41888. doi: 10.1371/journal.pone.0041888

Currier, R. B., Harrison, R. A., Rowley, P. D., Laing, G. D. and Wagstaff, S. C. 2010. Intra-specific variation in venom of the African Puff Adder (Bitis arietans): Differential expression and activity of snake venom

metalloproteinases (SVMPs). *Toxicon* 55(4), pp. 864-873. doi: 10.1016/j.toxicon.2009.12.009

da Silva Jr, N. J. and Aird, S. D. 2001. Prey specificity, comparative lethality and compositional differences of coral snake venoms. *Comparative Biochemistry and Physiology Part C: Toxicology & Pharmacology* 128(3), pp. 425-456.

Dalhat, M. M. 2015. Socioeconomic Aspects of Snakebite in Africa and the Tropics. In: Gopalakrishnakone, P., Faiz, A., Fernando, R., Gnanathasan, C., Habib, A., Yang, CC. ed. *Clinical Toxinology in Asia Pacific and Africa*. Vol. 2. Dordrecht.: Springer, pp. 300-308.

Dalton, J. P., Uy, B., Swift, S. and Wiles, S. 2017. A novel restraint device for injection of Galleria mellonella larvae that minimizes the risk of accidental operator needle stick injury. *Frontiers in Cellular and Infection Microbiology* 7, p. 99.

Daltry, J. C., Wüster, W. and Thorpe, R. S. 1996. Diet and snake venom evolution. *Nature* 379(6565), pp. 537-540.

Dart, R. C. and McNally, J. 2001. Efficacy, safety, and use of snake antivenoms in the United States. *Annals of Emergency Medicine* 37(2), pp. 181-188.

Dart, R. C. et al. 1997. Affinity-purified, mixed monospecific crotalid antivenom ovine Fab for the treatment of crotalid venom poisoning. *Annals of Emergency Medicine* 30(1), pp. 33-39.

De Gregorio, E. et al. 2002. An immune-responsive Serpin regulates the melanization cascade in Drosophila. *Developmental Cell* 3(4), pp. 581-592.

de la Rosa, G., Corrales-García, L. L., Rodriguez-Ruiz, X., López-Vera, E. and Corzo, G. 2018. Short-chain consensus alpha-neurotoxin: a synthetic 60-mer peptide with generic traits and enhanced immunogenic properties. *Amino Acids* 50(7), pp. 885-895.

De la Rosa, G., Olvera, F., Archundia, I. G., Lomonte, B., Alagón, A. and Corzo, G. 2019. Horse immunization with short-chain consensus α-neurotoxin generates antibodies against broad spectrum of elapid venomous species. *Nature communications* 10(1), pp. 1-8.

de Silva, H. A. et al. 2011. Low-dose adrenaline, promethazine, and hydrocortisone in the prevention of acute adverse reactions to antivenom following snakebite: a randomised, double-blind, placebo-controlled trial. *PLoS Medicine* 8(5), p. e1000435.

de Silva, H. A., Ryan, N. M. and de Silva, H. J. 2016. Adverse reactions to snake antivenom, and their prevention and treatment. *British Journal of Clinical Pharmacology* 81(3), pp. 446-452. doi: 10.1111/bcp.12739

de Souza, L. L., Stransky, S., Guerra-Duarte, C., Flor-Sa, A., Schneider, F. S., Kalapothakis, E. and Chávez-Olórtegui, C. 2015. Determination of toxic activities in Bothrops spp. snake venoms using animal-free approaches: correlation between in vitro versus in vivo assays. *Toxicological Sciences* 147(2), pp. 458-465.

Dennis, E. A., Cao, J., Hsu, Y. H., Magrioti, V. and Kokotos, G. 2011. Phospholipase A2 enzymes: physical structure, biological function, disease implication, chemical inhibition, and therapeutic intervention. *Chemical Reviews* 111(10), pp. 6130-6185. doi: 10.1021/cr200085w

Deshmukh, V., Motghare, V., Gajbhiye, D., Sv, B., Deshpande, R. and Pise, H. 2014. Study on acute adverse drug reactions of antisnake venom in a rural tertiary care hospital. *Asian journal of pharmaceutical and clinical research* 7(5), pp. 13-15.

Dhananjaya, B. L., Menon, J. C., Joseph, J. K., Raveendran, D. K. and Oommen, O. V. 2015. Snake venom detection kit (svdk): Update on current aspects and challenges. *Clinical Toxinology in Asia Pacific and Africa*, pp. 379-400.

Dias da Silva, W. and V Tambourgi, D. 2011. The humoral immune response induced by snake venom toxins. *Inflammation & Allergy-Drug Targets (Formerly Current Drug Targets-Inflammation & Allergy)* 10(5), pp. 343-357.

Doley, R. and Kini, R. 2009. Protein complexes in snake venom. *Cellular and Molecular Life Sciences* 66(17), pp. 2851-2871.

Du, X. Y. and Clemetson, K. J. 2002. Snake venom L-amino acid oxidases. *Toxicon* 40(6), pp. 659-665.

Duong-Ly, K. C. and Gabelli, S. B. 2014. Salting out of proteins using ammonium sulfate precipitation. *Methods in Enzymology* 541, pp. 85-94. doi: 10.1016/b978-0-12-420119-4.00007-0

Ediriweera, D. S. et al. 2016. Mapping the Risk of Snakebite in Sri Lanka - A National Survey with Geospatial Analysis. *PLoS Neglected Tropical Diseases* 10(7), p. e0004813. doi: 10.1371/journal.pntd.0004813

Egli, A. et al. 2014. Vaccine adjuvants–understanding molecular mechanisms to improve vaccines. *Swiss Medical Weekly* 144(2122),

Erhirhie, E. O., Ihekwereme, C. P. and Ilodigwe, E. E. 2018. Advances in acute toxicity testing: strengths, weaknesses and regulatory acceptance. *Interdisciplinary Toxicology* 11(1), pp. 5-12.

Escoriza, D., Metallinou, M., Donaire-Barroso, D., Amat, F. and Carranza, S. 2009. Biogeography of the White-Bellied Carpet Viper Echis leucogaster

Roman, 1972 in Morocco, a study combining mitochondrial DNA data and ecological niche modeling. *Butll. Soc. Cat. Herp.* 18, pp. 55-68.

Escoubas, P., Palma, M. and Nakajima, T. 1995. A microinjection technique using Drosophila melanogaster for bioassay-guided isolation of neurotoxins in arthropod venoms. *Toxicon* 33(12), pp. 1549-1555.

European Medicines Agency. 2003. *ICH Topic Q 1 A (R2): Stability Testing of new Drug Substances and Products, Step 5.* London: Available at: https://www.ema.europa.eu/en/documents/scientific-guideline/ich-q-1-r2-stability-testing-new-drug-substances-products-step-5_en.pdf [Accessed: 08 May 2022].

Fedhila, S. et al. 2010. Comparative analysis of the virulence of invertebrate and mammalian pathogenic bacteria in the oral insect infection model Galleria mellonella. *Journal of Invertebrate Pathology* 103(1), pp. 24-29.

Fernandes, I., Lima, E. X., Takehara, H. A., Moura-da-Silva, A. M., Tanjoni, I. and Gutierrez, J. M. 2000a. Horse IgG isotypes and cross-neutralization of two snake antivenoms produced in Brazil and Costa Rica. *Toxicon* 38(5), pp. 633-644.

Fernandes, I., Takehara, H. A. and Mota, I. 1991. Isolation of IgGT from hyperimmune horse anti-snake venom serum: its protective ability. *Toxicon* 29(11), pp. 1373-1379.

Fernandes, I., Takehara, H. A., Santos, A. C., Cormont, F., Latinne, D., Bazin, H. and Mota, I. 1997. Neutralization of bothropic and crotalic venom toxic activities by IgG(T) and IgGa subclasses isolated from immune horse serum. *Toxicon* 35(6), pp. 931-936.

Fernandes, I., Tavares, F. L., Sano-Martins, I. S. and Takehara, H. A. 2000b. Efficacy of bothropic antivenom and its IgG(T) fraction in restoring fibrinogen levels of Bothrops jararaca envenomed mice. *Toxicon* 38(7), pp. 995-998.

Ferraz, C. R., Arrahman, A., Xie, C., Casewell, N. R., Lewis, R. J., Kool, J. and C.;, C. F. 2019. Multifunctional Toxins in Snake Venoms and Therapeutic Implications: From Pain to Hemorrhage and Necrosis. *Front. Ecol. Evol. 7:218.*, doi: doi: 10.3389/fevo.2019.00218

Fox, J. W. and Serrano, S. M. 2005. Structural considerations of the snake venom metalloproteinases, key members of the M12 reprolysin family of metalloproteinases. *Toxicon* 45(8), pp. 969-985. doi: 10.1016/j.toxicon.2005.02.012

Fox, J. W. and Serrano, S. M. 2008. Insights into and speculations about snake venom metalloproteinase (SVMP) synthesis, folding and disulfide bond formation and their contribution to venom complexity. *Febs j* 275(12), pp. 3016-3030. doi: 10.1111/j.1742-4658.2008.06466.x

Frangieh, J., Rima, M., Fajloun, Z., Henrion, D., Sabatier, J.-M., Legros, C. and Mattei, C. 2021. Snake venom components: Tools and cures to target cardiovascular diseases. *Molecules* 26(8), p. 2223.

Freire, P. F., Labrador, V., Martín, J. P. and Hazen, M. 2005. Cytotoxic effects in mammalian Vero cells exposed to pentachlorophenol. *Toxicology* 210(1), pp. 37-44.

Fry, B. G. 2005. From genome to "venome": molecular origin and evolution of the snake venom proteome inferred from phylogenetic analysis of toxin sequences and related body proteins. *Genome Research* 15(3), pp. 403-420. doi: 10.1101/gr.3228405

Fry, B. G. et al. 2008. Evolution of an arsenal: structural and functional diversification of the venom system in the advanced snakes (Caenophidia). *Molecular & Cellular Proteomics* 7(2), pp. 215-246. doi: 10.1074/mcp.M700094-MCP200

Fry, B. G. et al. 2006. Early evolution of the venom system in lizards and snakes. *Nature* 439(7076), pp. 584-588. doi: 10.1038/nature04328

Fry, B. G., Vidal, N., van der Weerd, L., Kochva, E. and Renjifo, C. 2009. Evolution and diversification of the Toxicofera reptile venom system. *Journal of Proteomics* 72(2), pp. 127-136. doi: 10.1016/j.jprot.2009.01.009

Fry, B. G., Wickramaratana, J. C., Lemme, S., Beuve, A., Garbers, D., Hodgson, W. C. and Alewood, P. 2005. Novel natriuretic peptides from the venom of the inland taipan (Oxyuranus microlepidotus): isolation, chemical and biological characterisation. *Biochemical and Biophysical Research Communications* 327(4), pp. 1011-1015. doi: 10.1016/j.bbrc.2004.11.171

García-Arredondo, A., Martínez, M., Calderón, A., Saldívar, A. and Soria, R. 2019. Preclinical assessment of a new polyvalent antivenom (Inoserp europe) against several species of the subfamily viperinae. *Toxins* 11(3), p. 149.

Ghose, A. and White, J. 2016. Asian Snakes. In: Brent J., B.K., Dargan P., Hatten B., Megarbane B., Palmer R ed. *Critical Care Toxicology*. Springer, Cham.

Girish, V. M., Kumar, S., Joseph, L., Jobichen, C., Kini, R. M. and Sivaraman, J. 2012. Identification and structural characterization of a new three-finger toxin hemachatoxin from Hemachatus haemachatus venom. *PloS One* 7(10), p. e48112. doi: 10.1371/journal.pone.0048112

Goding, J. 1996. *Monoclonal antibodies*. London: Academic Press.

Gorr, S.-U., Flory, C. M. and Schumacher, R. J. 2019. In vivo activity and low toxicity of the second-generation antimicrobial peptide DGL13K. *PloS One* 14(5), p. e0216669.

Grandgeorge, M., Véron, J., Lutsch, C., Makula, M., Riffard, P., Pépin, S. and Scherrmann, J. 1996. Preparation of improved F (ab) 2 antivenoms. An example: new polyvalent anti-European vipers (equine). *Toxicon* 2(34), p. 148.

Guidolin, F. R., Caricati, C. P., Marcelino, J. R. and da Silva, W. D. 2016. Development of Equine IgG Antivenoms against Major Snake Groups in Mozambique. *PLoS Neglected Tropical Diseases* 10(1), p. e0004325. doi: 10.1371/journal.pntd.0004325

Gutiérrez, J., Gené, J., Rojas, G. and Cerdas, L. 1985. Neutralization of proteolytic and hemorrhagic activities of Costa Rican snake venoms by a polyvalent antivenom. *Toxicon* 23(6), pp. 887-893.

Gutierrez, J. M., Calvete, J. J., Habib, A. G., Harrison, R. A., Williams, D. J. and Warrell, D. A. 2017a. Snakebite envenoming. *Nat Rev Dis Primers* 3, p. 17079. doi: 10.1038/nrdp.2017.79

Gutierrez, J. M., Guillermo, L., Bruno, L. and Yamileth, A. 2011. Antivenoms for snakebite envenomings. *Inflammation & Allergy-Drug Targets (Formerly Current Drug Targets-Inflammation & Allergy)* 10(5), pp. 369-380.

Gutiérrez, J. M., Higashi, H. G., Wen, F. H. and Burnouf, T. 2007. Strengthening antivenom production in Central and South American public laboratories: report of a workshop. *Toxicon* 49(1), pp. 30-35.

Gutiérrez, J. M., León, G. and Lomonte, B. 2003. Pharmacokinetic-pharmacodynamic relationships of immunoglobulin therapy for envenomation. *Clinical Pharmacokinetics* 42(8), pp. 721-741.

Gutiérrez, J. M. et al. 2009. Snake venomics and antivenomics: Proteomic tools in the design and control of antivenoms for the treatment of snakebite envenoming. *Journal of Proteomics* 72(2), pp. 165-182.

Gutierrez, J. M., Lomonte, B., Sanz, L., Calvete, J. J. and Pla, D. 2014. Immunological profile of antivenoms: preclinical analysis of the efficacy of a polyspecific antivenom through antivenomics and neutralization assays. *Journal of Proteomics* 105, pp. 340-350. doi: 10.1016/j.jprot.2014.02.021

Gutierrez, J. M. et al. 2005a. Pan-African polyspecific antivenom produced by caprylic acid purification of horse IgG: an alternative to the antivenom crisis in Africa. *Transactions of the Royal Society of Tropical Medicine and Hygiene* 99(6), pp. 468-475. doi: 10.1016/j.trstmh.2004.09.014

Gutierrez, J. M., Rucavado, A., Escalante, T. and Diaz, C. 2005b. Hemorrhage induced by snake venom metalloproteinases: biochemical and biophysical mechanisms involved in microvessel damage. *Toxicon* 45(8), pp. 997-1011. doi: 10.1016/j.toxicon.2005.02.029

Gutierrez, J. M. et al. 2017b. Preclinical Evaluation of the Efficacy of Antivenoms for Snakebite Envenoming: State-of-the-Art and Challenges Ahead. *Toxins* 9(5), doi: 10.3390/toxins9050163

Gutiérrez, J. M. et al. 2013. Assessing the preclinical efficacy of antivenoms: From the lethality neutralization assay to antivenomics. *Toxicon* 69, pp. 168-179.

Gutiérrez, J. M. et al. 2021. In vitro tests for assessing the neutralizing ability of snake antivenoms: toward the 3Rs principles. *Frontiers in Immunology* 11, p. 617429.

Habib, A. and Abubakar, S. 2011. Factors affecting snakebite mortality in north-eastern Nigeria. *International Health* 3(1), pp. 50-55.

Habib, A. G. 2015. Venomous Snakes and Snake Envenomation in Nigeria. In: Gopalakrishnakone, P., Faiz, S.M.A., Gnanathasan, C. A., Habib, A. G., Fernando, R., Yang, C-C., Vogel, C-W., Tambourgi, D.V., Seifert, S. A. ed. *Clinical Toxinology*. Vol. 2. Dordrecht: Springer pp. 275 - 295.

Habib, A. G. et al. 2008. Envenoming after carpet viper (Echis ocellatus) bite during pregnancy: timely use of effective antivenom improves maternal and foetal outcomes. *Tropical Medicine and International Health* 13(9), pp. 1172–1175. doi: 10.1111/j.1365-3156.2008.02122.x

Habib, A. G., Kuznik, A., Hamza, M., Abdullahi, M. I., Chedi, B. A., Chippaux, J. P. and Warrell, D. A. 2015a. Snakebite is Under Appreciated: Appraisal of Burden from West Africa. *PLoS Neglected Tropical Diseases* 9(9), p. e0004088. doi: 10.1371/journal.pntd.0004088

Habib, A. G., Lamorde, M., Dalhat, M. M., Habib, Z. G. and Kuznik, A. 2015b. Cost-effectiveness of antivenoms for snakebite envenoming in Nigeria. *PLoS Neglected Tropical Diseases* 9(1), p. e3381.

Habib, A. G., Musa, B. M., Iliyasu, G., Hamza, M., Kuznik, A. and Chippaux, J.-P. 2020. Challenges and prospects of snake antivenom supply in sub-Saharan Africa. *PLoS Neglected Tropical Diseases* 14(8), p. e0008374.

Habib, A. G. and Warrell, D. A. 2013. Antivenom therapy of carpet viper (Echis ocellatus) envenoming: effectiveness and strategies for delivery in West Africa. *Toxicon* 69, pp. 82-89.

Halassy, B., Kurtovic, T., Lang Balija, M., Brgles, M., Tunjic, M. and Sviben, D. 2019. Concept of sample-specific correction of immunoassay results for precise and accurate IgG quantification in horse plasma. *Journal of Pharmaceutical and Biomedical Analysis* 164, pp. 276-282. doi: 10.1016/j.jpba.2018.10.020

Halilu, S., Iliyasu, G., Hamza, M., Chippaux, J. P., Kuznik, A. and Habib, A. G. 2019. Snakebite burden in Sub-Saharan Africa: estimates from 41 countries. *Toxicon* 159, pp. 1-4. doi: 10.1016/j.toxicon.2018.12.002

Hamza, M. et al. 2016. Cost-Effectiveness of Antivenoms for Snakebite Envenoming in 16 Countries in West Africa. *PLoS Neglected Tropical Diseases* 10(3), p. e0004568. doi: 10.1371/journal.pntd.0004568

Han, J. et al. 2020. Relative Quantitation of Subclass-Specific Murine IgG Fc N-Glycoforms by Multiple Reaction Monitoring. *ACS omega* 5(15), pp. 8564-8571.

Harris, J. B. and Scott-Davey, T. 2013. Secreted phospholipases A2 of snake venoms: effects on the peripheral neuromuscular system with comments on the role of phospholipases A2 in disorders of the CNS and their uses in industry. *Toxins* 5(12), pp. 2533-2571. doi: 10.3390/toxins5122533

Harrison, R. A. et al. 2017. Preclinical antivenom-efficacy testing reveals potentially disturbing deficiencies of snakebite treatment capability in East Africa. *PLoS Neglected Tropical Diseases* 11(10), p. e0005969. doi: 10.1371/journal.pntd.0005969

Harvey, A. L. and Robertson, B. 2004. Dendrotoxins: structure-activity relationships and effects on potassium ion channels. *Current Medicinal Chemistry* 11(23), pp. 3065-3072.

Hasan, S. M., Basher, A., Molla, A. A., Sultana, N. K. and Faiz, M. A. 2012. The impact of snake bite on household economy in Bangladesh. *Tropical Doctor* 42(1), pp. 41-43. doi: 10.1258/td.2011.110137

Herrera, M. et al. 2014. Antivenomic characterization of two antivenoms against the venom of the taipan, Oxyuranus scutellatus, from Papua New Guinea and Australia. *The American Journal of Tropical Medicine and Hygiene* 91(5), p. 887.

Hjelholt, A., Christiansen, G., Sørensen, U. S. and Birkelund, S. 2013. IgG subclass profiles in normal human sera of antibodies specific to five kinds of microbial antigens. *Pathogens and Disease* 67(3), pp. 206-213.

Hooper-McGrevy, K. E., Wilkie, B. N. and Prescott, J. F. 2003. Immunoglobulin G subisotype responses of pneumonic and healthy, exposed foals and adult horses to Rhodococcus equi virulence-associated proteins. *Clinical and Diagnostic Laboratory Immunology* 10(3), pp. 345-351.

Inagaki, H. 2017. Snake Venom Protease Inhibitors: Enhanced Identification, Expanding Biological Function, and Promising Future. In: Gopalakrishnakone, P., Inagaki, H., Mukherjee, A., Rahmy, T., Vogel, CW. ed. *Snake Venoms*. Dordrecht: Springer, pp. 1-26.

Ionova, Y. and Wilson, L. 2020. Biologic excipients: Importance of clinical awareness of inactive ingredients. *PloS One* 15(6), p. e0235076.

Irani, V., Guy, A. J., Andrew, D., Beeson, J. G., Ramsland, P. A. and Richards, J. S. 2015. Molecular properties of human IgG subclasses and their implications for designing therapeutic monoclonal antibodies against infectious diseases. *Molecular Immunology* 67(2), pp. 171-182.

Isbister, G. K. 2010. Antivenom efficacy or effectiveness: the Australian experience. *Toxicology* 268(3), pp. 148-154.

Isbister, G. K., Brown, S. G., MacDonald, E., White, J. and Currie, B. J. 2008. Current use of Australian snake antivenoms and frequency of immediate‐type hypersensitivity reactions and anaphylaxis. *Medical Journal of Australia* 188(8), pp. 473-476.

Janeway, J., Charles A, Travers, P., Walport, M. and Shlomchik, M. J. 2001. *The structure of a typical antibody molecule*. New York: Garland Science.

Junqueira, J. C. 2012. Galleria mellonella as a model host for human pathogens: recent studies and new perspectives. *Virulence* 3(6), doi: 10.4161/viru.22493

Kamiguti, A. S., Zuzel, M. and Theakston, R. D. 1998. Snake venom metalloproteinases and disintegrins: interactions with cells. *Brazilian Journal of Medical and Biological Research* 31(7), pp. 853-862. doi: 10.1590/s0100-879x1998000700001

Kang, T. S. et al. 2011. Enzymatic toxins from snake venom: structural characterization and mechanism of catalysis. *Febs Journal* 278(23), pp. 4544-4576. doi: 10.1111/j.1742-4658.2011.08115.x

Kao, D., Lux, A., Schaffert, A., Lang, R., Altmann, F. and Nimmerjahn, F. 2017. IgG subclass and vaccination stimulus determine changes in antigen specific antibody glycosylation in mice. *European Journal of Immunology* 47(12), pp. 2070-2079.

Kasturiratne, A. et al. 2017. The socio-economic burden of snakebite in Sri Lanka. *PLoS Neglected Tropical Diseases* 11(7), p. e0005647. doi: 10.1371/journal.pntd.0005647

Kasturiratne, A. et al. 2008. The global burden of snakebite: a literature analysis and modelling based on regional estimates of envenoming and deaths. *PLoS Medicine* 5(11), p. e218. doi: 10.1371/journal.pmed.0050218

Kay, S., Edwards, J., Brown, J. and Dixon, R. 2019. Galleria mellonella infection model identifies both high and low lethality of Clostridium perfringens toxigenic strains and their response to antimicrobials. *Frontiers in Microbiology* 10, p. 1281.

Keggan, A., Freer, H., Rollins, A. and Wagner, B. 2013. Production of seven monoclonal equine immunoglobulins isotyped by multiplex analysis. *Veterinary Immunology and Immunopathology* 153(3-4), pp. 187-193.

Kessler, P., Marchot, P., Silva, M. and Servent, D. 2017. The three-finger toxin fold: a multifunctional structural scaffold able to modulate cholinergic functions. *Journal of Neurochemistry* 142 Suppl 2, pp. 7-18. doi: 10.1111/jnc.13975

Khaing, E. M. et al. 2018. Development of an ELISA assay to determine neutralising capacity of horse serum following immunisation with Daboia siamensis venom in Myanmar. *Toxicon* 151, pp. 163-168.

Kini, R. M. and Doley, R. 2010. Structure, function and evolution of three-finger toxins: mini proteins with multiple targets. *Toxicon* 56(6), pp. 855-867. doi: 10.1016/j.toxicon.2010.07.010

Kinman, A. W. and Pompano, R. R. 2019. Optimization of Enzymatic Antibody Fragmentation for Yield, Efficiency, and Binding Affinity. *Bioconjugate Chemistry* 30(3), pp. 800-807.

Kipanyula, M. and Kimaro, W. 2015. Snakes and snakebite envenoming in Northern Tanzania: a neglected tropical health problem. *Journal of Venomous Animals and Toxins Including Tropical Diseases* 21(1), p. 32.

Klinman, N. R., Rockey, J. H. and Karush, F. 1965. Equine antihapten antibody II. The γG (7Sγ) components and their specific interaction. *Immunochemistry* 2(1), pp. 51-60.

Kriegel, C., Festag, M., Kishore, R. S., Roethlisberger, D. and Schmitt, G. 2019. Pediatric safety of polysorbates in drug formulations. *Children (Basel)* 7(1), p. 1. doi: 10.3390/children7010001

Krifi, M., El Ayeb, M. and Dellagi, K. 1999. The improvement and standardization of antivenom production in developing countries: comparing antivenom quality, therapeutical efficiency, and cost. *Journal of Venomous Animals and Toxins* 5(2), pp. 128-141.

Kuo, Y. J., Chung, C. H. and Huang, T. F. 2019. From Discovery of Snake Venom Disintegrins to A Safer Therapeutic Antithrombotic Agent. *Toxins* 11(7), doi: 10.3390/toxins11070372

Kurtovic, T., Brvar, M., Grenc, D., Lang Balija, M., Krizaj, I. and Halassy, B. 2016. A Single Dose of Viperfav(TM) May Be Inadequate for Vipera ammodytes Snake Bite: A Case Report and Pharmacokinetic Evaluation. *Toxins* 8(8), doi: 10.3390/toxins8080244

Kurtović, T. et al. 2019. Refinement strategy for antivenom preparation of high yield and quality. *PLoS Neglected Tropical Diseases* 13(6), p. e0007431.

Kwadha, C. A., Ong'amo, G. O., Ndegwa, P. N., Raina, S. K. and Fombong, A. T. 2017. The biology and control of the greater wax moth, Galleria mellonella. *Insects* 8(2), p. 61.

Laemmli, U. K. 1970. Cleavage of structural proteins during the assembly of the head of bacteriophage T4. *Nature* 227(5259), pp. 680-685.

Laing, G. D. et al. 2003. A new Pan African polyspecific antivenom developed in response to the antivenom crisis in Africa. *Toxicon* 42(1), pp. 35-41.

Lalloo, D. G. and Theakston, R. D. G. 2003. Snake antivenoms: antivenoms. *Journal of Toxicology: Clinical Toxicology* 41(3), pp. 277-290.

Landon, J. and Smith, D. S. 2003. Merits of sheep antisera for antivenom manufacture. *Journal of Toxicology: Toxin Reviews* 22(1), pp. 15-22.

Lange, A., Schäfer, A., Bender, A., Steimle, A., Beier, S., Parusel, R. and Frick, J.-S. 2018. Galleria mellonella: a novel invertebrate model to distinguish intestinal symbionts from pathobionts. *Frontiers in Immunology* 9, p. 2114.

Lauridsen, L. P., Laustsen, A. H., Lomonte, B. and Gutierrez, J. M. 2016. Toxicovenomics and antivenom profiling of the Eastern green mamba snake (Dendroaspis angusticeps). *Journal of Proteomics* 136, pp. 248-261. doi: 10.1016/j.jprot.2016.02.003

Lauridsen, L. P., Laustsen, A. H., Lomonte, B. and Gutierrez, J. M. 2017. Exploring the venom of the forest cobra snake: Toxicovenomics and antivenom profiling of Naja melanoleuca. *Journal of Proteomics* 150, pp. 98-108. doi: 10.1016/j.jprot.2016.08.024

Laustsen, A. H., Lomonte, B., Lohse, B., Fernandez, J. and Gutierrez, J. M. 2015. Unveiling the nature of black mamba (Dendroaspis polylepis) venom through venomics and antivenom immunoprofiling: Identification of key toxin targets for antivenom development. *Journal of Proteomics* 119, pp. 126-142. doi: 10.1016/j.jprot.2015.02.002

Laustsen, A. H. et al. 2018. Pros and cons of different therapeutic antibody formats for recombinant antivenom development. *Toxicon* 146, pp. 151-175. doi: 10.1016/j.toxicon.2018.03.004

Ledsgaard, L. et al. 2018. Antibody cross-reactivity in antivenom research. *Toxins* 10(10), p. 393.

Lee, H.-J., Woo, Y., Hahn, T.-W., Jung, Y. M. and Jung, Y.-J. 2020. Formation and maturation of the phagosome: a key mechanism in innate immunity against intracellular bacterial infection. *Microorganisms* 8(9), p. 1298.

Leiva, C. L. et al. 2019. IgY-based antivenom against Bothrops alternatus: Production and neutralization efficacy. *Toxicon* 163, pp. 84-92.

Leon, G., Herrera, M., Segura, A., Villalta, M., Vargas, M. and Gutierrez, J. M. 2013. Pathogenic mechanisms underlying adverse reactions induced by intravenous administration of snake antivenoms. *Toxicon* 76, pp. 63-76. doi: 10.1016/j.toxicon.2013.09.010

Leon, G., Monge, M., Rojas, E., Lomonte, B. and Gutierrez, J. M. 2001. Comparison between IgG and F(ab')(2) polyvalent antivenoms: neutralization of systemic effects induced by Bothrops asper venom in mice, extravasation to muscle tissue, and potential for induction of adverse reactions. *Toxicon* 39(6), pp. 793-801.

León, G. et al. 2011. Immune response towards snake venoms. *Inflammation & Allergy-Drug Targets (Formerly Current Drug Targets-Inflammation & Allergy)(Discontinued)* 10(5), pp. 381-398.

Leon, G., Stiles, B., Alape, A., Rojas, G. and Gutierrez, J. M. 1999. Comparative study on the ability of IgG and F(ab')2 antivenoms to neutralize lethal and myotoxic effects induced by Micrurus nigrocinctus (coral snake) venom. *American Journal of Tropical Medicine and Hygiene* 61(2), pp. 266-271.

León, G., Valverde, J. M., Rojas, G., Lomonte, B. and Gutiérrez, J. M. a. 2000. Comparative study on the ability of IgG and Fab sheep antivenoms to neutralize local hemorrhage, edema and myonecrosis induced by Bothrops asper (terciopelo) snake venom. *Toxicon* 38(2), pp. 233-244.

Lewis, M. J., Wagner, B. and Woof, J. M. 2008. The different effector function capabilities of the seven equine IgG subclasses have implications for vaccine strategies. *Molecular Immunology* 45(3), pp. 818-827. doi: 10.1016/j.molimm.2007.06.158

Link, C. 2005. Invertebrate models of Alzheimer's disease. *Genes, Brain and Behavior* 4(3), pp. 147-156.

Loh, J. M., Adenwalla, N., Wiles, S. and Proft, T. 2013. Galleria mellonella larvae as an infection model for group A streptococcus. *Virulence* 4(5), pp. 419-428.

Longbottom, J. et al. 2018. Vulnerability to snakebite envenoming: a global mapping of hotspots. *Lancet* 392(10148), pp. 673-684. doi: 10.1016/s0140-6736(18)31224-8

Lopes-de-Souza, L., Costal-Oliveira, F., Stransky, S., de Freitas, C. F., Guerra-Duarte, C., Braga, V. M. and Chávez-Olórtegui, C. 2019. Development of a cell-based in vitro assay as a possible alternative for determining bothropic antivenom potency. *Toxicon* 170, pp. 68-76.

Lopez, A. M., Hines, M. T., Palmer, G. H., Alperin, D. C. and Hines, S. A. 2002. Identification of pulmonary T-lymphocyte and serum antibody isotype

responses associated with protection against Rhodococcus equi. *Clinical and Diagnostic Laboratory Immunology* 9(6), pp. 1270-1276.

Lopez, E., Scott, N. E., Wines, B. D., Hogarth, P., Wheatley, A. K., Kent, S. and Chung, A. W. 2019. Low pH exposure during Immunoglobulin G purification methods results in aggregates that avidly bind Fcγ Receptors: Implications for measuring Fc dependent antibody functions. *Frontiers in Immunology* 10, p. 2415.

LoVecchio, F., Klemens, J., Roundy, E. B. and Klemens, A. 2003. Serum sickness following administration of Antivenin (Crotalidae) Polyvalent in 181 cases of presumed rattlesnake envenomation. *Wilderness and Environmental Medicine* 14(4), pp. 220-221.

Luiselli, L., Angelici, F. M. and Akani, G. C. 2002. Comparative feeding strategies and dietary plasticity of the sympatric cobras Naja melanoleuca and Naja nigricollis in three diverging Afrotropical habitats. *Canadian Journal of Zoology* 80(1), pp. 55-63.

Luna, M. S., Valente, R. H., Perales, J., Vieira, M. L. and Yamanouye, N. 2013. Activation of Bothrops jararaca snake venom gland and venom production: a proteomic approach. *Journal of Proteomics* 94, pp. 460-472. doi: 10.1016/j.jprot.2013.10.026

Lyons, K., Dugon, M. M. and Healy, K. 2020. Diet breadth mediates the prey specificity of venom potency in snakes. *Toxins* 12(2), p. 74.

Mackessy, S. 2010. *Handbook of Venoms and Toxins of Reptiles*. Boca Raton, London, New York: Taylor & Francis

Mackessy, S. P. 2009. *Handbook of Venoms and Toxins of Reptiles.* Boca Raton: CRC Press.

Mackessy, S. P. and Baxter, L. M. 2006. Bioweapons synthesis and storage: The venom gland of front-fanged snakes. *European Journal of Pharmaceutics and Biopharmaceutics* 245(3-4), pp. 147 -159.

Mackessy, S. P. and Saviola, A. J. 2016. Understanding Biological Roles of Venoms Among the Caenophidia: The Importance of Rear-Fanged Snakes. *Integrative and Comparative Biology* 56(5), pp. 1004-1021. doi: 10.1093/icb/icw110

Maguire, R. C. 2017. *The development of Galleria mellonella as a model to test the toxicity of food additives.* PhD, National University of Ireland Maynooth.

Malasit, P., Warrell, D. A., Chanthavanich, P., Viravan, C., Mongkolsapaya, J., Singhthong, B. and Supich, C. 1986. Prediction, prevention, and mechanism of early (anaphylactic) antivenom reactions in victims of snake bites. *British Medical Journal (Clinical Research Ed.)* 292(6512), pp. 17-20.

Malih, I., Ahmad rusmili, M. R., Tee, T. Y., Saile, R., Ghalim, N. and Othman, I. 2014. Proteomic analysis of Moroccan cobra Naja haje legionis venom using tandem mass spectrometry. *Journal of Proteomics* 96, pp. 240-252. doi: 10.1016/j.jprot.2013.11.012

Malmquist, J. A., Rogan, M. R. and McGillivray, S. M. 2019. Galleria mellonella as an infection model for Bacillus anthracis Sterne. *Frontiers in Cellular and Infection Microbiology* 9, p. 360.

Manning, M. C., Chou, D. K., Murphy, B. M., Payne, R. W. and Katayama, D. S. 2010. Stability of protein pharmaceuticals: an update. *Pharmaceutical Research* 27(4), pp. 544-575. doi: 10.1007/s11095-009-0045-6

Manzoli-Palma, M., Gobbi, N. and Palma, M. 2003. Insects as biological models to assay spider and scorpion venom toxicity. *Journal of Venomous Animals and Toxins Including Tropical Diseases* 9(2), pp. 174-185.

Maria, W. S., Pacheco, B. G., Barbosa, C. F., Velarde, D. T. and Chávez-Olórtegui, C. 2001. Determination of the neutralizing potency of horse antibothropic and anticrotalic antivenoms in blood samples collected on filter paper. *Toxicon* 39(10), pp. 1607-1609.

Marsh, N., DeRoos, F. and Touger, M. 2007. Gaboon viper (Bitis gabonica) envenomation resulting from captive specimens–a review of five cases. *Clinical Toxicology* 45(1), pp. 60-64.

Marsh, N. A. and Whaler, B. C. 1984. The Gaboon viper (Bitis gabonica): its biology, venom components and toxinology. *Toxicon* 22(5), pp. 669-694.

Mateljak Lukačević, S., Kurtović, T., Lang Balija, M., Brgles, M., Steinberger, S., Marchetti-Deschmann, M. and Halassy, B. 2020. Quality-Related Properties of Equine Immunoglobulins Purified by Different Approaches. *Toxins* 12(12), p. 798.

McGuire, T., Crawford, T. and Henson, J. eds. 1972. *The Isolation, Characterisation and Functional Properties of Equine Immunoglobulin Classes and Subclasses*. *Equine Infectious Diseases.* Paris, Basel: Karger

McKenzie, E., Esser, M. and Payton, E. 2014. Serum Immunoglobulin Concentrations in Racing Endurance Horses. *Equine Veterinary Journal* 46, pp. 18-18.

Megale, Â. A. A., Magnoli, F. C., Kuniyoshi, A. K., Iwai, L. K., Tambourgi, D. V., Portaro, F. C. and Silva, W. D. d. 2019. Kn-Ba: a novel serine protease isolated from Bitis arietans snake venom with fibrinogenolytic and kinin-releasing activities. *Journal of Venomous Animals and Toxins Including Tropical Diseases* 24,

Ménard, G., Rouillon, A., Cattoir, V. and Donnio, P.-Y. 2021. Galleria mellonella as a suitable model of bacterial infection: past, present and future. *Frontiers in Cellular and Infection Microbiology* 11, p. 782733.

Mender, M. M., Bolton, F., Berry, C. and Young, M. 2021. Antivenom: An immunotherapy for the treatment of snakebite envenoming in sub-Saharan Africa. *Advances in Protein Chemistry and Structural Biology* 129, pp. 435-477. doi: https://doi.org/10.1016/bs.apcsb.2021.11.004

Meyer, W. et al. 1997. First clinical experiences with a new ovine Fab Echis ocellatus snake bite antivenom in Nigeria: randomized comparative trial with Institute Pasteur Serum (Ipser) Africa antivenom. *The American journal of tropical medicine and hygiene* 56(3), pp. 291-300.

Mitra, A. K. and Mawson, A. R. 2017. Neglected Tropical Diseases: Epidemiology and Global Burden. *Trop Med Infect Dis* 2(3), doi: 10.3390/tropicalmed2030036

Modahl, C. M. and Mackessy, S. P. 2019. Venoms of rear-fanged snakes: New proteins and novel activities. *Frontiers in Ecology and Evolution* 7, p. 279.

Mohapatra, B. et al. 2011. Snakebite mortality in India: a nationally representative mortality survey. *PLoS Neglected Tropical Diseases* 5(4), p. e1018. doi: 10.1371/journal.pntd.0001018

Morais, V. 2018. Antivenom therapy: efficacy of premedication for the prevention of adverse reactions. *Journal of Venomous Animals and Toxins Including Tropical Diseases* 24,

Morais, V., Ifran, S., Berasain, P. and Massaldi, H. 2010. Antivenoms: potency or median effective dose, which to use? *Journal of Venomous Animals and Toxins Including Tropical Diseases* 16, pp. 191-193.

Morais, V. and Massaldi, H. 2005. Effect of pepsin digestion on the antivenom activity of equine immunoglobulins. *Toxicon* 46(8), pp. 876-882.

Morais, V. and Massaldi, H. 2006. Economic evaluation of snake antivenom production in the public system. *Journal of Venomous Animals and Toxins Including Tropical Diseases* 12(3), pp. 497-511.

Morais, V. and Massaldi, H. 2012. A model mechanism for protein precipitation by caprylic acid: application to plasma purification. *Biotechnology and Applied Biochemistry* 59(1), pp. 50-54. doi: 10.1002/bab.68

Morita, T. 2005. Structures and functions of snake venom CLPs (C-type lectin-like proteins) with anticoagulant-, procoagulant-, and platelet-modulating activities. *Toxicon* 45(8), pp. 1099-1114. doi: 10.1016/j.toxicon.2005.02.021

Mpandi, M. et al. 2007. Partitioning and inactivation of viruses by the caprylic acid precipitation followed by a terminal pasteurization in the manufacturing process of horse immunoglobulins. *Biologicals* 35(4), pp. 335-341.

Munawar, A., Ali, S. A., Akrem, A. and Betzel, C. 2018. Snake Venom Peptides: Tools of Biodiscovery. *Toxins* 10(11), doi: 10.3390/toxins10110474

Munawar, A. et al. 2014. Elapid snake venom analyses show the specificity of the peptide composition at the level of genera Naja and Notechis. *Toxins* 6(3), pp. 850-868. doi: 10.3390/toxins6030850

Nalbantsoy, A., Karabay-Yavasoglu, N., Sayim, F., Deliloglu-Gurhan, I., Gocmen, B., Arikan, H. and Yildiz, M. 2012. Determination of in vivo toxicity and in vitro cytotoxicity of venom from the Cypriot blunt-nosed viper Macrovipera lebetina lebetina and antivenom production. *Journal of Venomous Animals and Toxins Including Tropical Diseases* 18(2), pp. 208-216.

Nikapitiya, B. and Maduwage, K. 2018. Pharmacodynamics and pharmacokinetics of snake antivenom. *Sri Lanka Journal of Medicine* 27(1), pp. 54–65. doi: http://doi.org/10.4038/sljm.v27i1.79

Nudel, B. C., Perdomenico, C., Iacono, R. and Cascone, O. 2012. Optimization by factorial analysis of caprylic acid precipitation of non-immunoglobulins from hyperimmune equine plasma for antivenom preparation. *Toxicon* 59(1), pp. 68-73. doi: 10.1016/j.toxicon.2011.10.014

O'brien, J., Wilson, I., Orton, T. and Pognan, F. 2000. Investigation of the Alamar Blue (resazurin) fluorescent dye for the assessment of mammalian cell cytotoxicity. *European Journal of Biochemistry* 267(17), pp. 5421-5426.

Ogawa, T., Chijiwa, T., Oda-Ueda, N. and Ohno, M. 2005. Molecular diversity and accelerated evolution of C-type lectin-like proteins from snake venom. *Toxicon* 45(1), pp. 1-14. doi: 10.1016/j.toxicon.2004.07.028

Okuda, D., Nozaki, C., Sekiya, F. and Morita, T. 2001. Comparative biochemistry of disintegrins isolated from snake venom: consideration of the taxonomy and geographical distribution of snakes in the genus Echis. *The Journal of Biochemistry* 129(4), pp. 615-620.

Oliveira, J., De Oca, H. M., Duarte, M., Diniz, C. and Fortes-Dias, C. 2002. Toxicity of South American snake venoms measured by an in vitro cell culture assay. *Toxicon* 40(3), pp. 321-325.

Oron, U. and Bdolah, A. 1973. Regulation of protein synthesis in the venom gland of viperid snakes. *Journal of Cell Biology* 56(1), pp. 177-190. doi: 10.1083/jcb.56.1.177

Otero, R. et al. 1999. A randomized blinded clinical trial of two antivenoms, prepared by caprylic acid or ammonium sulphate fractionation of IgG, in

Bothrops and Porthidium snake bites in Colombia: correlation between safety and biochemical characteristics of antivenoms. *Toxicon* 37(6), pp. 895-908.

Otero, R. et al. 2006. Efficacy and safety of two whole IgG polyvalent antivenoms, refined by caprylic acid fractionation with or without β-propiolactone, in the treatment of Bothrops asper bites in Colombia. *Transactions of the Royal Society of Tropical Medicine and Hygiene* 100(12), pp. 1173-1182.

Otero-Patino, R. et al. 1998. A randomized, blinded, comparative trial of one pepsin-digested and two whole IgG antivenoms for Bothrops snake bites in Uraba, Colombia. The Regional Group on Antivenom Therapy Research (REGATHER). *American Journal of Tropical Medicine and Hygiene* 58(2), pp. 183-189.

Otero-Patiño, R. et al. 2012. Comparative study of the efficacy and safety of two polyvalent, caprylic acid fractionated [IgG and F (ab′) 2] antivenoms, in Bothrops asper bites in Colombia. *Toxicon* 59(2), pp. 344-355.

Oyama, E. and Takahashi, H. 2017. Structures and Functions of Snake Venom Metalloproteinases (SVMP) from Protobothrops venom Collected in Japan. *Molecules* 22(8), doi: 10.3390/molecules22081305

Ozverel, C. S., Damm, M., Hempel, B.-F., Göçmen, B., Sroka, R., Süssmuth, R. D. and Nalbantsoy, A. 2019. Investigating the cytotoxic effects of the venom proteome of two species of the Viperidae family (Cerastes cerastes and Cryptelytrops purpureomaculatus) from various habitats. *Comparative Biochemistry and Physiology Part C: Toxicology & Pharmacology* 220, pp. 20-30.

Paixão-Cavalcante, D., Kuniyoshi, A. K., Portaro, F. C., da Silva, W. D. and Tambourgi, D. V. 2015. African adders: partial characterization of snake venoms from three Bitis species of medical importance and their neutralization by experimental equine antivenoms. *PLoS Neglected Tropical Diseases* 9(2),

Paniagua, D., Vergara, I., Boyer, L. and Alagón, A. 2015. Role of lymphatic system on snake venom absorption. In: Gopalakrishnakone, P., Inagaki, H., Mukherjee, A., Rahmy, T., Vogel, CW. ed. *Snake Venoms* Dordrecht: Springer, pp. 1-19.

Parasuraman, S. 2011. Toxicological screening. *Journal of Pharmacology & Pharmacotherapeutics* 2(2), pp. 74-79. doi: 10.4103/0976-500X.81895

Patra, A., Kalita, B., Chanda, A. and Mukherjee, A. K. 2017. Proteomics and antivenomics of Echis carinatus carinatus venom: Correlation with pharmacological properties and pathophysiology of envenomation. *Scientific Reports* 7(1), doi: 10.1038/s41598-017-17227-y

Patra, A., Kalita, B. and Mukherjee, A. K. 2018. Assessment of quality, safety, and pre-clinical toxicity of an equine polyvalent anti-snake venom (Pan Africa):

Determination of immunological cross-reactivity of antivenom against venom samples of Elapidae and Viperidae snakes of Africa. *Toxicon*, doi: 10.1016/j.toxicon.2018.08.018

Pepin-Covatta, S., Lutsch, C., Grandgeorge, M. and Scherrmann, J. M. 1997. Immunoreactivity of a new generation of horse F(ab')2 preparations against European viper venoms and the tetanus toxin. *Toxicon* 35(3), pp. 411-422.

Pereira, T. C. et al. 2018. Recent advances in the use of Galleria mellonella model to study immune responses against human pathogens. *Journal of Fungi* 4(4), p. 128.

Petras, D., Heiss, P., Harrison, R. A., Sussmuth, R. D. and Calvete, J. J. 2016. Top-down venomics of the East African green mamba, Dendroaspis angusticeps, and the black mamba, Dendroaspis polylepis, highlight the complexity of their toxin arsenals. *Journal of Proteomics* 146, pp. 148-164. doi: 10.1016/j.jprot.2016.06.018

Petras, D. et al. 2011. Snake venomics of African spitting cobras: toxin composition and assessment of congeneric cross-reactivity of the pan-African EchiTAb-Plus-ICP antivenom by antivenomics and neutralization approaches. *Journal of Proteome Research* 10(3), pp. 1266-1280. doi: 10.1021/pr101040f

Pla, D., Rodríguez, Y. and Calvete, J. J. 2017. Third generation antivenomics: Pushing the limits of the in vitro preclinical assessment of antivenoms. *Toxins* 9(5), p. 158. doi: 10.3390/toxins9050158

Pook, C. E., Joger, U., Stümpel, N. and Wüster, W. 2009. When continents collide: phylogeny, historical biogeography and systematics of the medically important viper genus Echis (Squamata: Serpentes: Viperidae). *Molecular Phylogenetics and Evolution* 53(3), pp. 792-807.

Pope, C. 1939a. The action of proteolytic enzymes on the antitoxins and proteins in immune sera: I. True digestion of the proteins. *British Journal of Experimental Pathology* 20(2), pp. 132-149.

Pope, C. 1939b. The action of proteolytic enzymes on the antitoxins and proteins in immune sera: II. Heat denaturation after partial enzyme action. *British Journal of Experimental Pathology* 20(3), pp. 201-212.

Portes-Junior, J. A. et al. 2014. Unraveling the processing and activation of snake venom metalloproteinases. *Journal of Proteome Research* 13(7), pp. 3338-3348. doi: 10.1021/pr500185a

Postnikova, E. et al. 2018. Testing therapeutics in cell-based assays: Factors that influence the apparent potency of drugs. *PloS One* 13(3), p. e0194880. doi: 10.1371/journal.pone.0194880

Potet, J., Smith, J. and McIver, L. 2019. Reviewing evidence of the clinical effectiveness of commercially available antivenoms in sub-Saharan Africa

identifies the need for a multi-centre, multi-antivenom clinical trial. *PLoS Neglected Tropical Diseases* 13(6), p. e0007551.

Potter, L. R., Yoder, A. R., Flora, D. R., Antos, L. K. and Dickey, D. M. 2009. Natriuretic peptides: their structures, receptors, physiologic functions and therapeutic applications. *Handbook of Experimental Pharmacology* (191), pp. 341-366. doi: 10.1007/978-3-540-68964-5_15

Pucca, M. B., Cerni, F. A., Janke, R., Bermúdez-Méndez, E., Ledsgaard, L., Barbosa, J. E. and Laustsen, A. H. 2019. History of envenoming therapy and current perspectives. *Frontiers in Immunology* 10, p. 1598.

Rahman, R. et al. 2010. Annual incidence of snake bite in rural bangladesh. *PLoS Neglected Tropical Diseases* 4(10), p. e860. doi: 10.1371/journal.pntd.0000860

Ramarao, N., Nielsen-Leroux, C. and Lereclus, D. 2012. The insect Galleria mellonella as a powerful infection model to investigate bacterial pathogenesis. *Journal of visualized experiments: JoVE* (70),

Ramos-Cerrillo, B. et al. 2008. Characterization of a new polyvalent antivenom (Antivipmyn® Africa) against African vipers and elapids. *Toxicon* 52(8), pp. 881-888.

Ranawaka, U. K., Lalloo, D. G. and de Silva, H. J. 2013. Neurotoxicity in snakebite—the limits of our knowledge. *PLoS Neglected Tropical Diseases* 7(10), p. e2302.

Ratanabanangkoon, K., Simsiriwong, P., Pruksaphon, K., Tan, K. Y., Chantrathonkul, B., Eursakun, S. and Tan, C. H. 2018. An in vitro potency assay using nicotinic acetylcholine receptor binding works well with antivenoms against Bungarus candidus and Naja naja. *Scientific Reports* 8(1), p. 9716. doi: 10.1038/s41598-018-27794-3

Ratanabanangkoon, K. et al. 2017. A novel in vitro potency assay of antisera against Thai Naja kaouthia based on nicotinic acetylcholine receptor binding. *Scientific Reports* 7(1), p. 8545. doi: 10.1038/s41598-017-08962-3

Repetto, G., Del Peso, A. and Zurita, J. L. 2008. Neutral red uptake assay for the estimation of cell viability/cytotoxicity. *Nature Protocols* 3(7), pp. 1125-1131.

Rial, A., Morais, V., Rossi, S. and Massaldi, H. 2006. A new ELISA for determination of potency in snake antivenoms. *Toxicon* 48(4), pp. 462-466.

Richards, D. P., Barlow, A. and Wüster, W. 2012. Venom lethality and diet: differential responses of natural prey and model organisms to the venom of the saw-scaled vipers (Echis). *Toxicon* 59(1), pp. 110-116.

Rocha, J. N. et al. 2019. PNAG-specific equine IgG1 mediates significantly greater opsonization and killing of Prescottella equi (formerly Rhodococcus equi) than does IgG4/7. *Vaccine* 37(9), pp. 1142-1150.

Rogalski, A. et al. 2017. Differential procoagulant effects of saw-scaled viper (Serpentes: Viperidae: Echis) snake venoms on human plasma and the narrow taxonomic ranges of antivenom efficacies. *Toxicology Letters* 280, pp. 159-170. doi: 10.1016/j.toxlet.2017.08.020

Rojas, A. et al. 2013. Role of the animal model on the pharmacokinetics of equine-derived antivenoms. *Toxicon* 70, pp. 9-14.

Rojas, G., Jiménez, J. and Gutiérrez, J. 1994. Caprylic acid fractionation of hyperimmune horse plasma: description of a simple procedure for antivenom production. *Toxicon* 32(3), pp. 351-363.

Ruha, A.-M. et al. 2002. Initial postmarketing experience with crotalidae polyvalent immune Fab for treatment of rattlesnake envenomation. *Annals of Emergency Medicine* 39(6), pp. 609-615.

Ryan, N. M., Downes, M. A. and Isbister, G. K. 2015. Clinical features of serum sickness after Australian snake antivenom. *Toxicon* 108, pp. 181-183.

Ryan, N. M., Kearney, R. T., Brown, S. G. and Isbister, G. K. 2016. Incidence of serum sickness after the administration of Australian snake antivenom (ASP-22). *Clinical Toxicology* 54(1), pp. 27-33.

Saganuwan, S. A. 2016. The new algorithm for calculation of median lethal dose (LD50) and effective dose fifty (ED50) of Micrarus fulvius venom and anti-venom in mice. *International Journal of Veterinary Science and Medicine* 4(1), pp. 1-4.

Sakai, F., Carneiro, S. M. and Yamanouye, N. 2012. Morphological study of accessory gland of Bothrops jararaca and its secretory cycle. *Toxicon* 59(3), pp. 393-401. doi: 10.1016/j.toxicon.2011.12.012

Sánchez, A. et al. 2015a. Effect of geographical variation of Echis ocellatus, Naja nigricollis and Bitis arietans venoms on their neutralization by homologous and heterologous antivenoms. *Toxicon* 108, pp. 80-83.

Sanchez, A. et al. 2017. Expanding the neutralization scope of the EchiTAb-plus-ICP antivenom to include venoms of elapids from Southern Africa. *Toxicon* 125, pp. 59-64. doi: 10.1016/j.toxicon.2016.11.259

Sánchez, E. E., Migl, C., Suntravat, M., Rodriguez-Acosta, A., Galan, J. A. and Salazar, E. 2019. The neutralization efficacy of expired polyvalent antivenoms: An alternative option. *Toxicon* 168, pp. 32-39.

Sánchez, L. V., Pla, D., Herrera, M., Chippaux, J. P., Calvete, J. J. and Gutiérrez, J. M. 2015b. Evaluation of the preclinical efficacy of four

antivenoms, distributed in sub-Saharan Africa, to neutralize the venom of the carpet viper, Echis ocellatus, from Mali, Cameroon, and Nigeria. *Toxicon* 106, pp. 97-107.

Schaloske, R. H. and Dennis, E. A. 2006. The phospholipase A2 superfamily and its group numbering system. *Biochimica et Biophysica Acta* 1761(11), pp. 1246-1259. doi: 10.1016/j.bbalip.2006.07.011

Schwartzberg, L. S. and Navari, R. M. 2018. Safety of polysorbate 80 in the oncology setting. *Advances in Therapy* 35(6), pp. 754-767.

Sciani, J. M. and Pimenta, D. C. 2017. The modular nature of bradykinin-potentiating peptides isolated from snake venoms. *Journal of Venomous Animals and Toxins Including Tropical Diseases* 23, p. 45. doi: 10.1186/s40409-017-0134-7

Ségalat, L. 2007. Invertebrate animal models of diseases as screening tools in drug discovery. *ACS Chemical Biology* 2(4), pp. 231-236.

Segura, A., Herrera, M., Gonzalez, E., Vargas, M., Solano, G., Gutierrez, J. M. and Leon, G. 2009. Stability of equine IgG antivenoms obtained by caprylic acid precipitation: towards a liquid formulation stable at tropical room temperature. *Toxicon* 53(6), pp. 609-615. doi: 10.1016/j.toxicon.2009.01.012

Segura, Á., Herrera, M., Villalta, M., Vargas, M., Gutiérrez, J. M. and León, G. 2013. Assessment of snake antivenom purity by comparing physicochemical and immunochemical methods. *Biologicals* 41(2), pp. 93-97.

Segura, Á. et al. 2010. Preclinical assessment of the efficacy of a new antivenom (EchiTAb-Plus-ICP®) for the treatment of viper envenoming in sub-Saharan Africa. *Toxicon* 55(2-3), pp. 369-374.

Seifert, S. A. and Boyer, L. V. 2001. Recurrence phenomena after immunoglobulin therapy for snake envenomations: Part 1. Pharmacokinetics and pharmacodynamics of immunoglobulin antivenoms and related antibodies. *Annals of Emergency Medicine* 37(2), pp. 189-195.

Selistre-de-Araujo, H. S., Pontes, C. L., Montenegro, C. F. and Martin, A. C. 2010. Snake venom disintegrins and cell migration. *Toxins* 2(11), pp. 2606-2621. doi: 10.3390/toxins2112606

Sells, P., Ioannou, P. and Theakston, R. 1998. A humane alternative to the measurement of the lethal effects (LD50) of non-neurotoxic venoms using hens' eggs. *Toxicon* 36(7), pp. 985-991.

Sells, P., Laing, G. and Theakston, R. 2001. An in vivo but insensate model for the evaluation of antivenoms (ED50) using fertile hens' eggs. *Toxicon* 39(5), pp. 665-668.

Sells, P., Richards, A., Laing, G. and Theakston, R. 1997. The use of hens' eggs as an alternative to the conventional in vivo rodent assay for antidotes to haemorrhagic venoms. *Toxicon* 35(9), pp. 1413-1421.

Sells, P. G. 2003. Animal experimentation in snake venom research and in vitro alternatives. *Toxicon* 42(2), pp. 115-133.

Serrano, S. M. 2013. The long road of research on snake venom serine proteinases. *Toxicon* 62, pp. 19-26. doi: 10.1016/j.toxicon.2012.09.003

Serrano, S. M. and Maroun, R. C. 2005. Snake venom serine proteinases: sequence homology vs. substrate specificity, a paradox to be solved. *Toxicon* 45(8), pp. 1115-1132. doi: 10.1016/j.toxicon.2005.02.020

Sheoran, A. S. and Holmes, M. A. 1996. Separation of equine IgG subclasses (IgGa, IgGb and IgG(T)) using their differential binding characteristics for staphylococcal protein A and streptococcal protein G. *Veterinary Immunology and Immunopathology* 55(1-3), pp. 33-43.

Sheoran, A. S., Timoney, J. F., Holmes, M. A., Karzenski, S. S. and Crisman, M. V. 2000. Immunoglobulin isotypes in sera and nasal mucosal secretions and their neonatal transfer and distribution in horses. *American Journal of Veterinary Research* 61(9), pp. 1099-1105.

Silva, A., Cristofori-Armstrong, B., Rash, L. D., Hodgson, W. C. and Isbister, G. K. 2018. Defining the role of post-synaptic α-neurotoxins in paralysis due to snake envenoming in humans. *Cellular and Molecular Life Sciences* 75(23), pp. 4465-4478.

Silva, A. and Isbister, G. K. 2020. Current research into snake antivenoms, their mechanisms of action and applications. *Biochemical Society Transactions* 48(2), pp. 537-546.

Skaper, S. D. 2012. The neurotrophin family of neurotrophic factors: an overview. *Methods in Molecular Biology* 846, pp. 1-12. doi: 10.1007/978-1-61779-536-7_1

Smith, D. C., Reddi, K. R., Laing, G., Theakston, R. D. and Landon, J. 1992. An affinity purified ovine antivenom for the treatment of Vipera berus envenoming. *Toxicon* 30(8), pp. 865-871.

Smith, F. D. and Casadevall, A. 2021. Fungal immunity and pathogenesis in mammals versus the invertebrate model organism Galleria mellonella. *Pathogens and Disease* 79(3), p. ftab013. doi: doi.org/10.1093/femspd/ftab013

Squaiella-Baptistao, C. C., Marcelino, J. R., Ribeiro da Cunha, L. E., Gutierrez, J. M. and Tambourgi, D. V. 2014. Anticomplementary activity of horse IgG and F(ab')2 antivenoms. *American Journal of Tropical Medicine and Hygiene* 90(3), pp. 574-584. doi: 10.4269/ajtmh.13-0591

Squaiella-Baptistao, C. C., Sant'Anna, O. A., Marcelino, J. R. and Tambourgi, D. V. 2018. The history of antivenoms development: Beyond Calmette and Vital Brazil. *Toxicon* 150, pp. 86-95. doi: 10.1016/j.toxicon.2018.05.008

Stock, R. P., Massougbodji, A., Alagón, A. and Chippaux, J.-P. 2007. Bringing antivenoms to sub-Saharan Africa. *Nature Biotechnology* 25(2), pp. 173-177.

Stone, S. F. et al. 2013. Immune response to snake envenoming and treatment with antivenom; complement activation, cytokine production and mast cell degranulation. *PLoS Neglected Tropical Diseases* 7(7), p. e2326.

Stransky, S., Costal-Oliveira, F., Lopes-de-Souza, L., Guerra-Duarte, C., Chávez-Olórtegui, C. and Braga, V. M. M. 2018. In vitro assessment of cytotoxic activities of Lachesis muta muta snake venom. *PLoS Neglected Tropical Diseases* 12(4), p. e0006427.

Sugiura, T., Imagawa, H. and Kondo, T. 2000. Purification of horse immunoglobulin isotypes based on differential elution properties of isotypes from protein A and protein G columns. *Journal of Chromatography B: Biomedical Sciences and Applications* 742(2), pp. 327-334.

Sunagar, K., Jackson, T. N., Undheim, E. A., Ali, S. A., Antunes, A. and Fry, B. G. 2013. Three-fingered RAVERs: Rapid Accumulation of Variations in Exposed Residues of snake venom toxins. *Toxins* 5(11), pp. 2172-2208. doi: 10.3390/toxins5112172

Sunagar, K., Johnson, W. E., O'Brien, S. J., Vasconcelos, V. and Antunes, A. 2012. Evolution of CRISPs associated with toxicoferan-reptilian venom and mammalian reproduction. *Molecular Biology and Evolution* 29(7), pp. 1807-1822. doi: 10.1093/molbev/mss058

Takeda, S., Takeya, H. and Iwanaga, S. 2012. Snake venom metalloproteinases: structure, function and relevance to the mammalian ADAM/ADAMTS family proteins. *Biochimica et Biophysica Acta* 1824(1), pp. 164-176. doi: 10.1016/j.bbapap.2011.04.009

Tasoulis, T. and Isbister, G. K. 2017. A Review and Database of Snake Venom Proteomes. *Toxins* 9(9), doi: 10.3390/toxins9090290

Theakston, R., Lloyd-Jones, M. J. and Reid, H. 1977. Micro-ELISA for detecting and assaying snake venom and venom-antibody. *The Lancet* 310(8039), pp. 639-641.

Theakston, R. and Reid, H. 1979. Enzyme-linked immunosorbent assay (ELISA) in assessing antivenom potency. *Toxicon* 17(5), pp. 511-515.

Theakston, R. and Reid, H. 1983. Development of simple standard assay procedures for the characterization of snake venoms. *Bulletin of the World Health Organization* 61(6), p. 949.

Theakston, R. D. G., Warrell, D. and Griffiths, E. 2003. Report of a WHO workshop on the standardization and control of antivenoms. *Toxicon* 41(5), pp. 541-557.

To, C. Z. and Bhunia, A. K. 2019. Three dimensional Vero cell-platform for rapid and sensitive screening of Shiga-toxin producing Escherichia coli. *Frontiers in Microbiology* 10, p. 949.

Tonello, F. and Rigoni, M. 2017. Cellular Mechanisms of Action of Snake Phospholipase A2 Toxins. In: Gopalakrishnakone, P., Inagaki, H., Mukherjee, A., Rahmy, T., Vogel, CW. ed. *Snake Venoms*. Dordrecht.: Springer pp. 49 - 63.

Toro, A. F. et al. 2006. Role of IgG(T) and IgGa isotypes obtained from arachnidic antivenom to neutralize toxic activities of Loxosceles gaucho, Phoneutria nigriventer and Tityus serrulatus venoms. *Toxicon* 48(6), pp. 649-661. doi: 10.1016/j.toxicon.2006.07.029

Tothova, C., Nagy, O. and Kovac, G. 2016. Serum proteins and their diagnostic utility in veterinary medicine: a review. *Veterinarni Medicina* 61(9), pp. 475-496.

Tsai, C. J.-Y., Loh, J. M. S. and Proft, T. 2016. Galleria mellonella infection models for the study of bacterial diseases and for antimicrobial drug testing. *Virulence* 7(3), pp. 214-229.

Ulfman, L. H., Leusen, J. H., Savelkoul, H. F., Warner, J. O. and Van Neerven, R. 2018. Effects of bovine immunoglobulins on immune function, allergy, and infection. *Frontiers in nutrition* 5, p. 52.

Valenza, L., Allavena, R., Haworth, M., Cochrane, J. and Henning, J. 2021. Diagnosis and Treatment of Snake Envenomation in Dogs in Queensland, Australia. *Veterinary sciences* 8(2), p. 14.

Viala, V. L. et al. 2015. Proteomic analysis of the rare Uracoan rattlesnake Crotalus vegrandis venom: Evidence of a broad arsenal of toxins. *Toxicon* 107(Pt B), pp. 234-251. doi: 10.1016/j.toxicon.2015.09.023

Vidal, N. 2002. Colubroid systematics: evidence for an early appearance of the venom apparatus followed by extensive evolutionary tinkering. *Journal of Toxicology: Toxin Reviews* 21(1-2), pp. 21-41. doi: 10.1081/TXR-120004740

Vidal, N., Delmas, A. S., David, P., Cruaud, C., Couloux, A. and Hedges, S. B. 2007. The phylogeny and classification of caenophidian snakes inferred from seven nuclear protein-coding genes. *C R Biol* 330(2), pp. 182-187. doi: 10.1016/j.crvi.2006.10.001

Vilmos, P. and Kurucz, E. 1998. Insect immunity: evolutionary roots of the mammalian innate immune system. *Immunology Letters* 62(2), pp. 59-66.

Vink, S., Jin, A. H., Poth, K. J., Head, G. A. and Alewood, P. F. 2012. Natriuretic peptide drug leads from snake venom. *Toxicon* 59(4), pp. 434-445. doi: 10.1016/j.toxicon.2010.12.001

Visser, L., Kyei-Faried, S., Belcher, D., Geelhoed, D., van Leeuwen, J. S. and Van Roosmalen, J. 2008. Failure of a new antivenom to treat Echis ocellatus snake bite in rural Ghana: the importance of quality surveillance. *Transactions of the Royal Society of Tropical Medicine and Hygiene* 102(5), pp. 445-450.

Wagner, B. 2006. Immunoglobulins and immunoglobulin genes of the horse. *Developmental and Comparative Immunology* 30(1-2), pp. 155-164.

Wagner, B., Greiser-Wilke, I., Wege, A. K., Radbruch, A. and Leibold, W. 2002. Evolution of the six horse IGHG genes and corresponding immunoglobulin gamma heavy chains. *Immunogenetics* 54(5), pp. 353-364.

Wagner, B., Miller, D. C., Lear, T. L. and Antczak, D. F. 2004. The complete map of the Ig heavy chain constant gene region reveals evidence for seven IgG isotypes and for IgD in the horse. *Journal of Immunology* 173(5), pp. 3230-3242.

Wagstaff, S. C. and Harrison, R. A. 2006. Venom gland EST analysis of the saw-scaled viper, Echis ocellatus, reveals novel alpha9beta1 integrin-binding motifs in venom metalloproteinases and a new group of putative toxins, renin-like aspartic proteases. *Gene* 377, pp. 21-32. doi: 10.1016/j.gene.2006.03.008

Wagstaff, S. C., Sanz, L., Juarez, P., Harrison, R. A. and Calvete, J. J. 2009. Combined snake venomics and venom gland transcriptomic analysis of the ocellated carpet viper, Echis ocellatus. *Journal of Proteomics* 71(6), pp. 609-623. doi: 10.1016/j.jprot.2008.10.003

Walther, S., Rusitzka, T. V., Diesterbeck, U. S. and Czerny, C. P. 2015. Equine immunoglobulins and organization of immunoglobulin genes. *Developmental and Comparative Immunology* 53(2), pp. 303-319. doi: 10.1016/j.dci.2015.07.017

Wang, Y. L. et al. 2010. Cobra CRISP functions as an inflammatory modulator via a novel Zn2+- and heparan sulfate-dependent transcriptional regulation of endothelial cell adhesion molecules. *Journal of Biological Chemistry* 285(48), pp. 37872-37883. doi: 10.1074/jbc.M110.146290

Warrell, D. 2009. Commissioned article: management of exotic snakebites. *QJM: An International Journal of Medicine* 102(9), pp. 593-601.

Warrell, D., Barnes, H. and Piburn, M. 1976a. Neurotoxic effects of bites by the Egyptian cobra (Naja haje) in Nigeria. *Transactions of the Royal Society of Tropical Medicine and Hygiene* 70(1), pp. 78-79.

Warrell, D., Davidson, N. M., Greenwood, B., Ormerod, L., Pope, H. M., Watkins, B. J. and Prentice, C. 1977. Poisoning by bites of the saw-scaled or carpet viper (Echis carinatus) in Nigeria. *QJM: An International Journal of Medicine* 46(1), pp. 33-62.

Warrell, D., Davidson, N. M., Omerod, L., Pope, H. M., Watkins, B. J., Greenwood, B. and Ried, H. 1974. Bites by the saw-scaled or carpet viper (Echis carinatus): trial of two specific antivenoms. *British Medical Journal* 4(5942), pp. 437-440.

Warrell, D., Greenwood, B., Davidson, N. M., Ormerod, L. and Prentice, C. 1976b. Necrosis, haemorrhage and complement depletion following bites by the spitting cobra (Naja nigricollis). *QJM: An International Journal of Medicine* 45(1), pp. 1-22.

Warrell, D., Ormerod, L. and Davidson, N. M. 1975. Bites by puff-adder (Bitis arietans) in Nigeria, and value of antivenom. *British Medical Journal* 4(5998), pp. 697-700.

Warrell, D. A. 2008. Unscrupulous marketing of snake bite antivenoms in Africa and Papua New Guinea: choosing the right product--'what's in a name? ‘. *Transactions of the Royal Society of Tropical Medicine and Hygiene* 102(5), pp. 397–399. doi: doi:10.1016/j.trstmh.2007.12.005

Weber, J., Peng, H. and Rader, C. 2017. From rabbit antibody repertoires to rabbit monoclonal antibodies. *Experimental and Molecular Medicine* 49(3), pp. e305-e305.

Weber, S. S., Ducry, J. and Oxenius, A. 2014. Dissecting the contribution of IgG subclasses in restricting airway infection with Legionella pneumophila. *The Journal of Immunology* 193(8), pp. 4053-4059.

Widders, P. R., Stokes, C. R. and Bourne, F. J. 1986. Investigation of the antigenic relationship between equine IgG and IgGT. *Veterinary Immunology and Immunopathology* 13(3), pp. 255-259.

Wijesinghe, C. A. et al. 2015. A randomized controlled trial of a brief intervention for delayed psychological effects in snakebite victims. *PLoS Neglected Tropical Diseases* 9(8), p. e0003989.

Williams, D., Gutierrez, J. M., Harrison, R., Warrell, D. A., White, J., Winkel, K. D. and Gopalakrishnakone, P. 2010. The Global Snake Bite Initiative: an antidote for snake bite. *Lancet* 375(9708), pp. 89-91. doi: 10.1016/s0140-6736(09)61159-4

Williams, D. J. et al. 2019a. Strategy for a globally coordinated response to a priority neglected tropical disease: Snakebite envenoming. *PLoS Neglected Tropical Diseases* 13(2), p. e0007059.

Williams, D. J., Habib, A. G. and Warrell, D. A. 2018. Clinical studies of the effectiveness and safety of antivenoms. *Toxicon* 150, pp. 1-10. doi: 10.1016/j.toxicon.2018.05.001

Williams, H. F., Layfield, H. J., Vallance, T., Patel, K., Bicknell, A. B., Trim, S. A. and Vaiyapuri, S. 2019b. The urgent need to develop novel strategies for the diagnosis and treatment of snakebites. *Toxins* 11(6), p. 363.

World Health Organization. 2010. *Guidelines for the prevention and clinical management of snakebite in Africa*. Brazzaville: Available at: https://apps.who.int/iris/handle/10665/204458 [Accessed: 25 May 2022].

World Health Organization. 2016. *Expert Committee on Biological Standardization World Health Organization. WHO Expert Committee on Biological Standardization: Sixty-sixth Report*. Geneva: Available at: https://apps.who.int/iris/handle/10665/208900 [Accessed: 21 April 2020].

Xiao, H., Pan, H., Liao, K., Yang, M. and Huang, C. 2017. Snake Venom PLA2, a Promising Target for Broad-Spectrum Antivenom Drug Development. *Biomed Res Int* 2017, p. 6592820. doi: 10.1155/2017/6592820

Yamazaki, Y., Hyodo, F. and Morita, T. 2003. Wide distribution of cysteine-rich secretory proteins in snake venoms: isolation and cloning of novel snake venom cysteine-rich secretory proteins. *Archives of Biochemistry and Biophysics* 412(1), pp. 133-141. doi: 10.1016/s0003-9861(03)00028-6

Yamazaki, Y., Matsunaga, Y., Tokunaga, Y., Obayashi, S., Saito, M. and Morita, T. 2009. Snake venom Vascular Endothelial Growth Factors (VEGF-Fs) exclusively vary their structures and functions among species. *Journal of Biological Chemistry* 284(15), pp. 9885-9891. doi: 10.1074/jbc.M809071200

Yamazaki, Y. and Morita, T. 2004. Structure and function of snake venom cysteine-rich secretory proteins. *Toxicon* 44(3), pp. 227-231. doi: 10.1016/j.toxicon.2004.05.023

Yamazaki, Y. and Morita, T. 2006. Molecular and functional diversity of vascular endothelial growth factors. *Molecular Diversity* 10(4), pp. 515-527. doi: 10.1007/s11030-006-9027-3

Yates, V., Lebas, E., Orpiay, R. and Bale, B. 2010. Management of snakebites by the staff of a rural clinic: the impact of providing free antivenom in a nurse-led clinic in Meserani, Tanzania. *Annals of Tropical Medicine and Parasitology* 104(5), pp. 439-448.

Young, B. A. and Zahn, K. 2001. Venom flow in rattlesnakes: mechanics and metering. *Journal of Experimental Biology* 204(Pt 24), pp. 4345-4351.

Yuan, C. H., He, Q. Y., Peng, K., Diao, J. B., Jiang, L. P., Tang, X. and Liang, S. P. 2008. Discovery of a distinct superfamily of Kunitz-type toxin (KTT) from tarantulas. *PloS One* 3(10), p. e3414. doi: 10.1371/journal.pone.0003414

Zupunski, V., Kordis, D. and Gubensek, F. 2003. Adaptive evolution in the snake venom Kunitz/BPTI protein family. *FEBS Letters* 547(1-3), pp. 131-136. doi: 10.1016/s0014-5793(03)00693-8